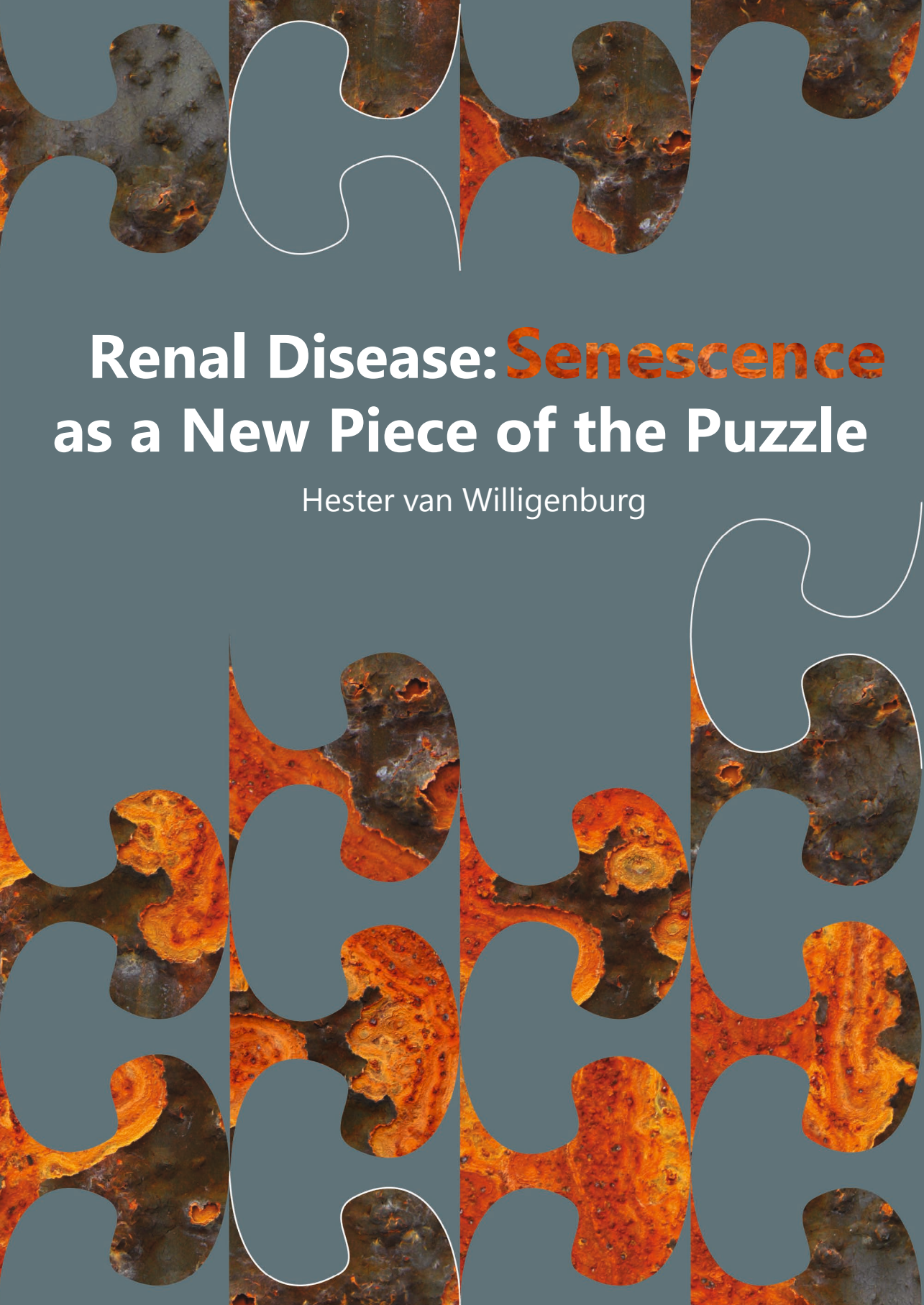

Renal Disease: Senescence as a New Piece of the Puzzle

Hester van Willigenburg

Renal disease:

senescence as a new piece of the puzzle

Hester van Willigenburg

COLOPHON

Renal Disease: Senescence as a new piece of the puzzle

Provided by thesis specialist Ridderprint, ridderprint.nl

Author:	Hester van Willigenburg
Cover and internal artwork:	Hester van Willigenburg
Cover photo:	Jana Scott
Layout and design:	Anke Muijsers | persoonlijkproefschrift.nl
Printing:	Ridderprint | ridderprint.nl

Printing of this thesis was very kindly financially supported by the Erasmus MC University Medical Center Rotterdam and Chiesi Pharmaceuticals B.V.

Renal Disease: Senescence as a new piece of the puzzle

Nierziekten: senescence als een nieuw stukje van de puzzel

Proefschrift

ter verkrijging van de graad van doctor aan de

Erasmus Universiteit Rotterdam op gezag van de rector magnificus

Prof. dr. A.L. Bredenoord

en volgens besluit van het College voor Promoties.

De openbare verdediging zal plaatsvinden op

donderdag 9 juni 2022 om 15.30 uur

door

Hester van Willigenburg

geboren te Haarlem

Erasmus University Rotterdam

Erasmus

Promotiecommissie:

Promotor:	Dr. ing. R.W.F. de Bruin
Overige leden:	Prof. dr. J.H.J. Hoeijmakers Prof. dr. J. Campisi Prof. dr. F.U.S. Mattace Raso
Copromotor:	Dr. P.L.J. de Keizer

TABLE OF CONTENTS

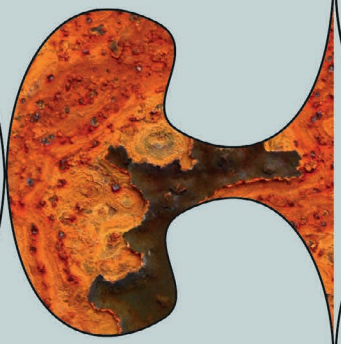

Chapter 1

General Introduction

Causes and consequences of renal aging

Life expectancy has been increasing for decades, from a global average life expectancy of 29 years for those born in 1850 to an average of 73 years in 2019[1,2]. Consequently, there is a substantial increase in the proportion of elderly people, so that by 2050 1 in 6 people will be aged over 65 years old, as compared to 1 in 11 in 2019[3]. Unfortunately, the expected average health span – years lived in good health – does not keep up with the increase in average lifespan[2]. These prospects implicate that although we can expect to live a longer life than our ancestors, many of the extra years lived will be years lived with age-related diseases. These future outlooks present a serious challenge for the provision of health care of our elderly.

Biological aging is a multifactorial process that affects all organs of the human body. This thesis focusses specifically on the age-related decline of the kidney. The kidney is an essential vertebrate organ that functions as a blood filtering system. A human has two fist-sized kidneys, located on either side of the spine at the lowest level of the rib cage. They participate in the regulation of the body's fluid volume, electrolyte and acid/base concentration, and the removal of toxins[4]. Each kidney is composed of, on average, 1.000.000 functional units – called nephrons – that together filter roughly 180 liters of blood per day[5,6]. Arterial blood arrives in these nephrons at the glomeruli, which are small clusters of capillaries that are embraced by a sphere-shaped cell layer, also known as the Bowman's capsule[4]. Here, blood is filtered based on particle size and the filtrated fluid flows from the Bowman's capsule into a lengthy winding tubular system. In the renal tubule, most of the water and solutes are recovered and returned to the blood circulation[4]. The remaining waste product is urine, of which approximately 1.4 liters is produced and excreted every day[6].

With increasing age, the number of nephrons in a human kidney decreases, and correspondingly kidney function decreases with age as well[7,8]. Other structural changes in the aging kidney include sclerosis (the abnormal thickening or hardening of structures such as the glomeruli) and fibrosis (the excessive deposition of extracellular matrix)[9]. Together, these changes to the kidney reduce kidney function and impair its recovery from injury[9]. The gradual loss of kidney function can eventually result in chronic kidney disease (CKD). CKD is the collective classification for all long-term, non-curable kidney conditions that are marked by deficient kidney function. Besides an age-related decline in kidney function, CKD can be caused and accelerated by diabetes[10,11], hypertension[12,13], cardiovascular diseases[14,15] and inflammation[16,17], pathologies that have a high incidence in the elderly population. CKD can also be the result of kidney diseases, including renal inflammation and polycystic kidney disease[18]. With a prevalence of 9.1% in 2017 globally[19] and a prevalence of approximately 50% in those aged 70 years or older[20,21], CKD is a considerable age-related condition. CKD is divided in five stages, based on the estimated glomerular filtration rate (eGFR)— which is a measurement of kidney function[22]. Patients reaching stage five CKD, also known as end stage renal disease (ESRD), have lost kidney

function to a fatal extent. These patients need to be treated with renal replacement therapy (RRT), such as dialysis or kidney transplantation[23]. It is estimated that by 2030, 5.4 million people worldwide will be in need of RRT yearly. Unfortunately, a substantial number of these people will not be able to receive it in time[24]. The high incidence of death due to untreated ESRD, caused by poor access to treatment and a shortage of donor kidneys[25,26], sets a demanding task for nephrology and geriatric research. To meet this task, it is of essence to understand what aging is and how it affects the kidney, so that we can explore measures to counteract renal aging and disease.

Unresolved damage leads to aging

There are many theories on the causes of aging. One theory is that we are genetically programmed to age. If we consider aging to be an unintended part of life, however, aging could simply be the result of declined natural selection after reproductive age. True as these may be, there is a lot of evidence for the chronic accumulation of damage in our cells during aging[27]. Despite their differences, together these theories conclude that aging can be defined as an accumulation of unresolved damage that unbalances homeostasis and results in gradual loss of function[27,28]. As DNA lies at the centre of organismal functioning, one powerful hypothesis is that aging of our body is a direct cause of DNA damage accumulation[27,29].

Deoxyribonucleic acid (DNA), serves as the archive of all information to build and maintain an organism. Most human cells have just two distinct copies of DNA per cell. One copy inherited from the mother, and one from the father. Unlike other cellular components as proteins, mRNA, lipids, and metabolites, DNA cannot be regenerated. This means our cells can only rely on repair of the molecule once it is damaged. And DNA is continuously exposed to damage from endogenous and exogenous sources[30]. Intrinsic damage can be caused by the attrition of telomeres – protective DNA-end structures – after excessive cell cycle division during aging. Intrinsic damage can also originate from reactive oxygen species formed during extreme cell metabolism[28,31,32]. Furthermore, DNA itself is unstable and prone to spontaneous chemical alterations[33]. Cells can also be damaged by exogenous agents, such as UV radiation from sunlight, inhaled toxins from smoking or ingested toxins from our diet or from therapeutics[32]. Maintaining DNA integrity is therefore essential to life, and as such, all living organisms are equipped with mechanisms to repair DNA damage[34]. In fact, somatic mutations in DNA damage repair pathways can be embryonic lethal or can cause progeroid syndromes, which are characterized by premature death and phenotypes of accelerated aging[35], emphasizing the importance of DNA damage repair to maintain life and longevity. Still, not all DNA lesions can be repaired and DNA damage repair itself is not perfect. These imperfections can lead to permanent mutations in the genetic code[36]. As a result, DNA damage and mutations can alter gene and protein function or protein abundance, which can have a harmful effect on cellular function. Therefore, DNA damage and mutations increase the probability of developing disease, cancer and aging[33] (Figure 1).

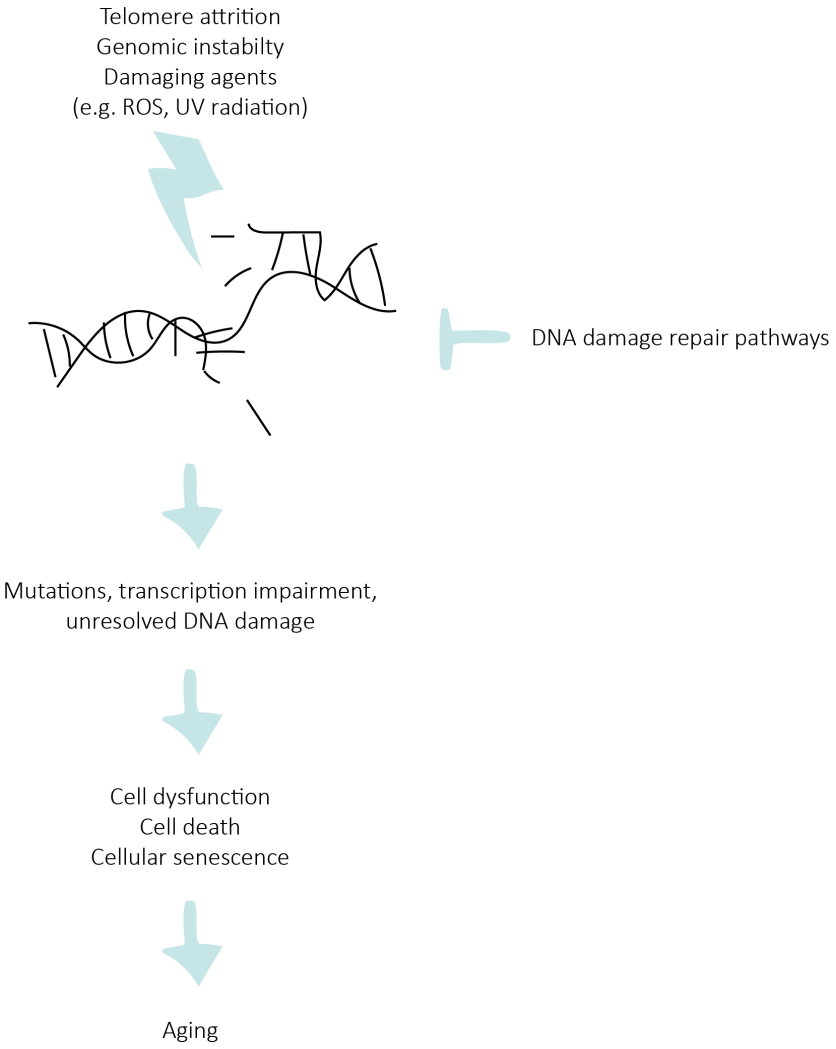

Figure 1. The central role of DNA damage in cellular aging

Enforcing the cellular senescent arrest

A damaged cell can reduce the function of a tissue and thereby reduce homeostasis. Furthermore, unresolved damage can result into the DNA becoming mutated. Over time, these mutations can cause damaged cells to progress into cancer. Both threaten the chances of survival of the organism. Fortunately, cells are equipped with two major coping mechanisms when damaged DNA is beyond repair, or when the damage load surpasses repair capacity: apoptosis (programmed cell death) and cellular senescence (permanently suppressed cell division)[37]. The choice for either of these pathways depends on the cell type, the type of damage and on the severity of damage[38]. Interestingly, apoptosis pathways are often upregulated in senescent cells, however, these cells are able to resist

apoptosis by upregulating anti-apoptosis pathways[38–40]. The persistent activation of two major pathways initiates the cellular senescence cell fate: the p53-p21^{Cip1} and the p16^{INK4A} pathways[41,42]. These pathways enforce a permanent cell cycle arrest, rendering the cell unresponsive to proliferative signals[41]. As a direct result of p53 or p16^{ink4a} upregulation, the expression of proteins that ensure nuclear integrity, such as Lamin B1, is lost[43]. This has several important consequences. First of all, Lamin B1 is a nuclear structural protein that serves as a DNA scaffold, ensuring accurate chromatin organization[44]. Loss of Lamin B1 causes chromatin to reorganize[45], promoting the formation of senescence-associated heterochromatin foci (SAHF)[44]. These regions of tightly packed DNA contribute to the silencing of genes that promote cell proliferation[46], enforcing the senescent cell cycle arrest. Together with SAHF, DNA segments with chromatin alterations reinforcing senescence (DNA-SCARS) are prominent nuclear morphological markers of senescence[63]. DNA-SCARS derive from persistent DNA lesions that sustain the senescence cell cycle arrest[63]. The loss in nuclear integrity caused by Lamin B1 loss, results in nuclear enlargement and an abnormal nuclear shape[47]. Thus LaminB1 loss results in some distinguishing morphological hallmarks of senescence[48]. Lastly, the loss of nuclear integrity leads to leakage of nuclear chromatin into the cytoplasm[49], triggering the cGAS-STING mediated immune defence mechanism that is normally activated by cytoplasmic viral or bacterial DNA. As a consequence, these cytosolic chromatin fragments play a key role in the activation of an important characteristic of senescent cells[50,51]: the senescence associated secretory phenotype (SASP)[48].

Impaired DNA damage repair drives a senescence associated secretory phenotype during aging

Senescent cells can exhibit a hyper secretory phenotype, and can secrete a plethora of pro-inflammatory chemokines, cytokines but also growth factors, alarmins, extracellular matrix, and matrix metalloproteinases (MMPs)[52,53]. Besides the manifestation of cytoplasmic DNA, multiple cascades, including the DNA damage response[54], are involved in inducing and maintaining the SASP. Most of these cascades rely on the activation of transcription factors nuclear factor κB (NF-κB) and CEBP-β[54–56]. Together, NF-κB and CEBP-β control the transcription of inflammatory SASP factors, such as interleukins IL-1α, IL-6 and IL-8[42,52,56]. In turn, the expression of these key SASP factors stimulates NF-κB and CEBP-β activation, enforcing SASP signalling[55,57]. Not only can SASP factors reinforce senescence, the transfer of SASP factors to surrounding healthy cells can enforce senescence in these cells as well[58–60], emphasizing the essence of SASP in enforcing the senescent state. Together these transformations to the senescent cell implement and enforce the important hallmarks of senescent cells, including the permanent growth arrest and its secretory phenotype.

Distinguishing characteristics of senescent cells

Persistent DNA damage signaling
Persistent DNA damage is a characteristic of senescent cells. This damage accumulates in DNA segments with chromatin alterations reinforcing senescence (DNA-SCARS), forming nuclear foci characterized by an abundance of DDR proteins (p-p53, FOXO4, 53BP1, γ-H2AX[40,63,64])

Apoptosis resistance
Both pro-apoptotic and anti-apoptotic pathways are upregulated in senescent cells[65]. So far, six different anti-apoptotic pathways have been identified in senescent cells, which are influenced by senescent cell-type origin and the mode of senescence induction[66]. Anti-apoptosis markers that can be detected in senescent cells comprise Bcl-2, Bcl-w, Bcl-xL and FOXO4[38,40].

Cell cycle arrest
The cell cycle arrest is set in motion by the upregulation of cyclin-dependent kinase (CDK) inhibitors (e.g. $p16^{INK4A}$, $p21^{Cip1}$ [42,65]). As a consequence, an absence of proliferation markers can be measured (e.g. ki67), accompanied by a loss of DNA replication, which can be assessed via e.g. an EdU incorporation assay[67].

Altered morphology
Senescent cells can, especially *in vitro,* be recognized by an enlarged and flattened cellular morphology. Additionally, the nuclear loss of Lamin B1[43] can be assessed, as well as the resulting nuclear enlargement, cytoplasmic chromatin fragments (CCFs)[49], as well as senescence-associated heterochromatin foci (SAHF), regions that stain densely by a nuclear staining, and can be enriched in e.g. HPA proteins[67,68].

Senescence associated secretory phenotype
Out of the wide range of SASP factors the following factors are commonly measured to detect SASP: pro-inflammatory chemokines (e.g. IL-8, CCL-2[53,60]), cytokines (e.g. IL-1α, IL-6[53]), alarmins (e.g. release of HMGB1 from nucleus[69]) and matrix metalloproteinases (e.g. MMP1, MMP10[42]).

Increases in mitochondrial and lysosomal numbers
Lysosomes and mitochondria in senescent cells progressively deteriorate in function, but increase in numbers[48,65,70]. The detection of increased lysosomal content in senescent cells by measuring SA-βgal activity is one of the oldest assays of senescence detection[71]. However, constitutive expression of SA-beta-gal has been identified in non-senescent cells[67,72]. Some studies have measured mitochondrial membrane potential to characterize senescent cells [73,74].

Box 1 Here several characteristics of senescent cells are described. Due to the heterogeneity of senescent cells, a universal marker for senescence has yet to be identified. Therefore it is encouraged to combine multiple of the mentioned markers to confirm the presence of senescent cells *in vitro* and *in vivo*.

The expression and secretion of SASP factors by senescent cells is heterogeneous and dynamic and its composition is dependent on the cell type affected, the senescence inducing trigger and the activated senescence pathways[52,61,62]. Furthermore, SASP changes over time[53], which all together has two major implications. First, not one senescent cell is the same. How to distinguish senescent cells from healthy cells is summarized in **Box 1**. Secondly, the effects of a senescent cell on its surrounding are diverse.

Consequences of senescent cells and the senescence associated secretory phenotype

In addition to serving as a tumour-suppressive mechanism, senescent cells have been found to exert some other beneficial effects. For example, senescent cells that arise at sites of injury have been found to accelerate wound repair and limit fibrosis through the secretion of various components of the SASP[75–77]. The senescence program can also aid in embryonic development, where the induction and later clearance of senescent cells by macrophages contributes to tissue remodelling[78]. However, recent research has shed a new light on the senescent cell, as a culprit for many age-related diseases. It was in the late end of the 20th century that researchers discovered that the number of senescent cells increases with age[79,80]. This was followed by the first realization that besides their positive characteristics, senescent cells can have a negative impact on homeostasis as well. It was found that the altered secretory profile of senescent cells creates a tumour-promoting environment, driving the age-related increase in cancer incidence[53,81,82]. A decade later, the systemic removal of senescent cells in mice revealed that senescent cells drive several age-related diseases and shorten healthy lifespan[83,84]. Since then, numerous studies have been published that causatively link senescence to age-related diseases, including cancer[41,53,85–87], cardiovascular disease[88,89], diabetes[48,90,91], and important for kidney pathology: in glomerulosclerosis[84], diabetic nephropathy[92,93], acute kidney injury- to chronic kidney disease progression[94], chronic kidney disease [95–97] and age related decline in kidney function[40]. Notably, senescent cells seem to exert beneficial functions early in life as they aid in tumour suppression, wound healing and embryonic development, but are attributed a negative role with increasing age as they are causatively linked to age-related diseases. The cause for these age-dependent effects of senescence can be largely attributed to the interaction between senescent cells and the immune system.

Impaired immune cell-mediated senescence clearance leads to aging

The secretion of pro-inflammatory chemokines and cytokines by senescent cells attract and activate several members of the immune system[98]. On top of that, senescent cells express several immune ligands, such as NKG2D ligands, marking themselves for immune cell-mediated senescence clearance[99]. Although senescence clearing behaviour has been attributed to macrophages[100,101], neutrophils[101] and T-cells[102,103], it is mainly the NK-cell that is responsible for the removal of senescent cells[76,103–106]. Activation of the NK-cell by stimulatory NKG2D ligands triggers NK-cells to release cytotoxic vesicles that induce

cell death in its target cell[99]. However, impairment of immune cell function can impair the removal of senescent cells[103,105]. Impaired immune function happens for example as a result of aging or as a result of a genetic defect in cytotoxic vesicle production in NK-cells[103,105]. Furthermore, senescent cells have been found to upregulate immune-cell inhibitory ligands and shed immune cell stimulatory ligands over time, resulting in immune evasion of senescent cells[107,108].

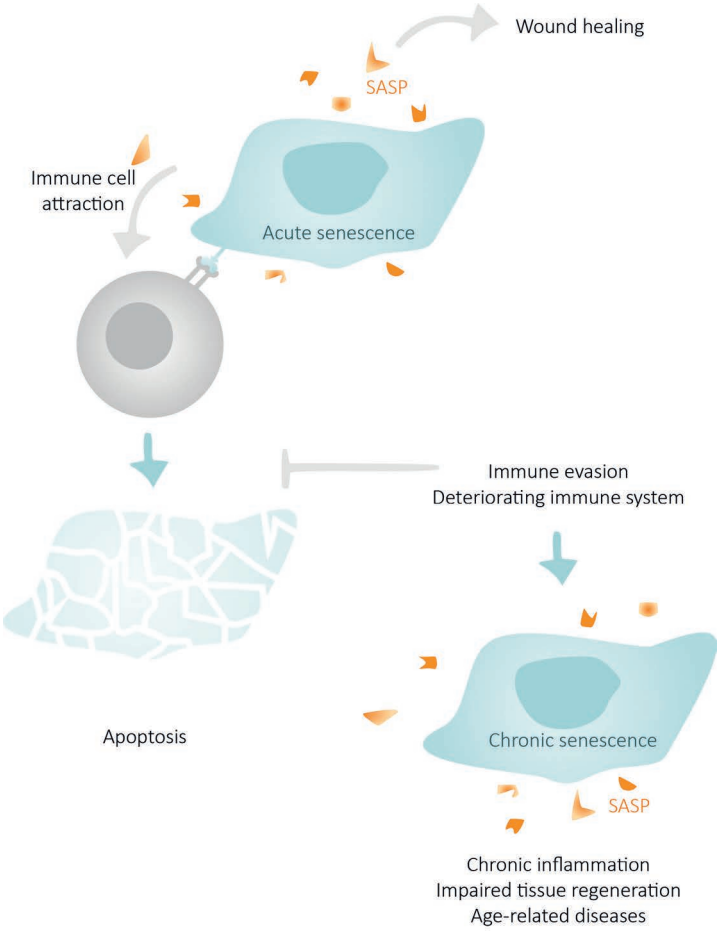

Figure 2 Acute vs chronic senescence
Immune-cell ligands and SASP factors mark senescent cells for immune-cell mediated cell death (apoptosis). Repression of this system by immune evasion of senescent cells, or an impaired immune system, results in chronically present senescent cells. An accumulation of senescent cells contributes to chronic inflammation, impaired tissue regeneration and age-related diseases. SASP: senescence associated secretory phenotype.

Together, senescence immune evasion and the age-related deteriorating function of the immune system result in increases in the number of senescent cells with increasing age[103,105,107,108]. The failure to remove senescent cells leads to persistently present senescent cells that have outstayed their primary function. As a result, a senescent cell that might have aided in wound repair, resides after wound healing. Its secretion of inflammatory factors and growth factors that contributed to wound healing will have a completely new influence on its surrounding. Therefore, a distinction is made between acute and persistent or chronic senescent cells. Acute senescence is thought to benefit our chances of survival, whereas the lack of senescent cell clearance of these acute senescent cells results in chronic senescence, which is an important driver of ageing[109] (Figure 2). These findings have inspired researchers to find methods to remove chronic senescent cells by other means than the immune system.

Senolytics: a class of drugs that remove senescent cells to counteract aging

Senolytics are the therapeutic group of compounds that selectively induce cell death in senescent cells[66]. These compounds have the goal to delay, prevent or even reverse age-related diseases by removing senescent cells. To be able to specifically target senescent cells, most senolytics target the apoptosis-resistant nature of senescent cells[39,66]. Tipping the balance between the upregulated anti-apoptotic and pro-apoptotic pathways towards apoptosis results in cell death in senescent cells[66]. After the discovery of the senolytic potential of the drugs quercetin and dasatinib in 2015[110], multiple other senolytics were discovered and designed, including navitoclax[111], HSP-90 inhibitors[112] and the FOXO4-DRI peptide[40]. These compounds are thoroughly described in chapter 5 of this thesis. Senolytics have been found to alleviate various age-related diseases in animals[40,110,111,113–115] and have encouraged the use of senolytics to counter human disease. Currently, two clinical trials test the senolytic effects of the senolytic cocktail of quercetin and dasatinib on patients with idiopathic pulmonary fibrosis or diabetes mellitus and CKD[116,117]. Preliminary results demonstrate that the treatment with quercetin and dasatinib decreases senescence markers and report good tolerance for the senolytic treatment[116,117]. The use of senolytics spark the imagination to counteract renal aging and disease and improve health span of humans.

Scope of this thesis

Hundreds of millions people worldwide are affected by renal aging and disease. Only limited treatment options for kidney diseases are available, which often have high costs or poor outcome. Consequently, renal aging and disease have a high clinical and economic burden. The emerging role for senescence as a driver of aging and age-related diseases urges for a better understanding of its role in kidney disease. Therefore, the aim of this thesis was to identify the causes and consequences of senescent cells in several kidney diseases.

Outline of this thesis

In **chapter 2** we explore the presence of senescent cells in autosomal dominant polycystic kidney disease (ADPKD). Thereby contributing to our understanding of the mechanisms driving this incurable progressive hereditary disease. ADPKD accounts for up to 9% of all end stage renal disease (ESRD) cases and most ESRD patients will need to undergo renal replacement therapy such as kidney transplantation. Due to the increasing age of kidney donors, we investigate in **chapter 3 and 4** the role of senescent cells in aged kidneys on the recovery from acute kidney injury (AKI), which is a transplantation associated injury. In these chapters, we show that senescent cells impair recovery from AKI and that the use of the senolytic FOXO4-DRI can counteract this, offering a rationale for the use of senolytics to optimize aged kidneys and increase the donor pool. **Chapter 5 and 6** provide literature overviews of senescence and senolytics, with a focus on kidney transplantation (chapter 5). To prevent immune-cell mediated rejection of transplanted kidneys, transplant patients adhere to a lifelong treatment of immunosuppressive therapy. We wondered whether these therapeutics would, as a side effect, impair immune-mediated senescence clearance. Therefore we investigate the effect of immunosuppressive compounds on immune-mediated senescence clearance. To be able to do so, we present a new method to analyse the blood concentration of the immunosuppressive drug tacrolimus in mouse blood in **chapter 7**. Subsequently, we show in **chapter 8** the inhibitory effect of tacrolimus on the senescence clearance by NK-cells *in vitro*. Lastly, in **chapter 9**, we present a novel tool to tightly down regulate gene expression levels using a controllable U6 promoter. This tool will enable us to mimic decreased gene expression as observed in disease, broadening our toolbox for gene function analyses. Finally, in **chapter 10** we discuss the general findings of this thesis and provide future perspectives.

Overall, this thesis provides novel insights into the role of senescent cells in kidney disease, from those patients with ADPKD, to those undergoing transplantation and receiving immunosuppressive therapy. These findings contribute to the general understanding of renal aging and provide a starting point for the exploration of senolytic treatment in ADPKD, AKI and immunosuppressive therapy. Furthermore, two new methods are presented that will aid in the future research on immunosuppressive studies in mice and the study of gene function.

REFERENCES

1. Life Expectancy at Birth (Total) | Clio Infra | Reconstructing Global Inequality. https://clio-infra.eu/Indicators/LifeExpectancyatBirthTotal.html.
2. World Health Organization, Department of Data and Analytics, Division of Data, A. and D. for I. & WHO, G. WHO methods and data sources for life tables 1990-2019. (2020).
3. World Population Prospects - Population Division - United Nations. https://population.un.org/wpp/.
4. Hansel, D. E., Kane, C. J., Paner, G. P. & Chang, S. S. The Kidney. (2016) doi:10.1007/978-1-4939-3286-3.
5. Bertram, J. F., Douglas-Denton, R. N., Diouf, B., Hughson, M. D. & Hoy, W. E. Human nephron number: implications for health and disease. Pediatric Nephrology 2011 26:9 26, 1529–1533 (2011).
6. Kaufman, D. P., Basit, H. & Knohl, S. J. Physiology, Glomerular Filtration Rate. StatPearls (2020).
7. Nyengaard, J. R. & Bendtsen, T. F. Glomerular Number and Size in Relation to Age, Kidney Weight, and Body Surface in Normal Man. 232194–201 (1992).
8. Lindeman, R. D., Tobin, J. & Shock, N. W. Longitudinal Studies on the Rate of Decline in Renal Function with Age tutes of Aging, Baltimore City Hospitals. Gerontology Research Center doi:10.1111/j.1532-5415.1985.tb07117.x.
9. O'Sullivan, E. D., Hughes, J. & Ferenbach, D. A. Renal Aging: Causes and Consequences. Journal of the American Society of Nephrology : JASN 28, 407 (2017).
10. Foster, M. C. et al. Overweight, Obesity, and the Development of Stage 3 CKD: The Framingham Heart Study. American Journal of Kidney Diseases 52, 39–48 (2008).
11. Boer, I. H. de et al. Obesity and Change in Estimated GFR Among Older Adults. American journal of kidney diseases : the official journal of the National Kidney Foundation 54, 1043 (2009).
12. Lindeman, R. D., Tobin, J. D. & Shock, N. W. Association between blood pressure and the rate of decline in renal function with age. Kidney International 26, 861–868 (1984).
13. Bleyer, A. J., Shemanski, L. R., Burke, G. L., Hansen, K. J. & Appel, R. G. CLINICAL NEPHROLOGY-EPIDEMIOLOGY-CLINICAL TRIALS Tobacco, hypertension, and vascular disease: Risk factors for renal functional decline in an older population. Kidney International 57, 2072–2079 (2000).
14. Fox, C. S. et al. Predictors of New-Onset Kidney Disease in a Community-Based Population. JAMA 291, 844–850 (2004).
15. Bleyer, A. J., Shemanski, L. R., Burke, G. L., Hansen, K. J. & Appel, R. G. CLINICAL NEPHROLOGY-EPIDEMIOLOGY-CLINICAL TRIALS Tobacco, hypertension, and vascular disease: Risk factors for renal functional decline in an older population. Kidney International 57, 2072–2079 (2000).
16. Fried, L. et al. Inflammatory and Prothrombotic Markers and the Progression of Renal Disease in Elderly Individuals. Journal of the American Society of Nephrology 15, 3184–3191 (2004).
17. Vlassara, H. et al. Role of oxidants/inflammation in declining renal function in chronic kidney disease and normal aging. Kidney International 76, S3–S11 (2009).
18. Webster, A. C., Nagler, E. V., Morton, R. L. & Masson, P. Chronic Kidney Disease. The Lancet 389, 1238–1252 (2017).
19. Bikbov, B. et al. Global, regional, and national burden of chronic kidney disease, 1990–2017: a systematic analysis for the Global Burden of Disease Study 2017. The Lancet 395, 709–733 (2020).
20. Stevens, L. A., Viswanathan, G. & Weiner, D. E. Chronic kidney disease and end-stage renal disease in the elderly population: current prevalence, future projections, and clinical significance. Advances in chronic kidney disease 17, 293–301 (2010).
21. Hallan, S. I. et al. Age and the Association of Kidney Measures with Mortality and End-Stage Renal Disease. JAMA : the journal of the American Medical Association 308, 2349 (2012).
22. Levey, A. S. et al. Definition and classification of chronic kidney disease: A position statement from Kidney Disease: Improving Global Outcomes (KDIGO). Kidney International 67, 2089–2100 (2005).

23. Agarwal, R. Defining end-stage renal disease in clinical trials: a framework for adjudication: Table 1. Nephrology Dialysis Transplantation 31, 864–867 (2016).
24. Liyanage, T. et al. Worldwide access to treatment for end-stage kidney disease: a systematic review. The Lancet 385, 1975–1982 (2015).
25. McCormick, F., Held, P. J. & Chertow, G. M. The Terrible Toll of the Kidney Shortage. Journal of the American Society of Nephrology 29, 2775–2776 (2018).
26. Liyanage, T. et al. Worldwide access to treatment for end-stage kidney disease: a systematic review. The Lancet 385, 1975–1982 (2015).
27. Maynard, S., Fang, E. F., Scheibye-Knudsen, M., Croteau, D. L. & Bohr, V. A. DNA Damage, DNA Repair, Aging, and Neurodegeneration. Cold Spring Harbor Perspectives in Medicine 5, (2015).
28. López-Otín, C., Blasco, M. A., Partridge, L., Serrano, M. & Kroemer, G. The hallmarks of aging. Cell vol. 153 (2013).
29. Schumacher, B., Pothof, J., Vijg, J. & Hoeijmakers, J. H. J. The central role of DNA damage in the ageing process. Nature 2021 592:7856 592, 695–703 (2021).
30. Hakem, R. DNA-damage repair; the good, the bad, and the ugly. The EMBO Journal 27, 589 (2008).
31. Boonstra, J. & Post, J. A. Molecular events associated with reactive oxygen species and cell cycle progression in mammalian cells. Gene 337, 1–13 (2004).
32. Hakem, R. DNA-damage repair; the good, the bad, and the ugly. The EMBO Journal 27, 589 (2008).
33. Hoeijmakers, J. H. J. DNA Damage, Aging, and Cancer. New England Journal of Medicine 361, 1475–1485 (2009).
34. Huang, R. & Zhou, P.-K. DNA damage repair: historical perspectives, mechanistic pathways and clinical translation for targeted cancer therapy. Signal Transduction and Targeted Therapy 2021 6:1 6, 1–35 (2021).
35. Carrero, D., Soria-Valles, C. & López-Otín, C. Hallmarks of progeroid syndromes: lessons from mice and reprogrammed cells. Disease Models & Mechanisms 9, 719–735 (2016).
36. Huang, R. & Zhou, P.-K. DNA damage repair: historical perspectives, mechanistic pathways and clinical translation for targeted cancer therapy. Signal Transduction and Targeted Therapy 2021 6:1 6, 1–35 (2021).
37. Campisi, J. & d'Adda di Fagagna, F. Cellular senescence: when bad things happen to good cells. Nature Reviews Molecular Cell Biology 8, 729–740 (2007).
38. Childs, B. G., Baker, D. J., Kirkland, J. L., Campisi, J. & Deursen, J. M. van. Senescence and apoptosis: dueling or complementary cell fates? EMBO reports 15, 1139–1153 (2014).
39. Wang, E. Senescent Human Fibroblasts Resist Programmed Cell Death, and Failure to Suppress bcl2 Is Involved. Cancer Research 55, (1995).
40. Baar, M. P. et al. Targeted Apoptosis of Senescent Cells Restores Tissue Homeostasis in Response to Chemotoxicity and Aging. Cell 169, (2017).
41. Campisi, J. Aging, Cellular Senescence, and Cancer. Annual Review of Physiology 75, 685–705 (2013).
42. Kumari, R. & Jat, P. Mechanisms of Cellular Senescence: Cell Cycle Arrest and Senescence Associated Secretory Phenotype. Frontiers in Cell and Developmental Biology 0, 485 (2021).
43. Freund, A., Laberge, R.-M., Demaria, M. & Campisi, J. Lamin B1 loss is a senescence-associated biomarker. Molecular Biology of the Cell 23, 2066–2075 (2012).
44. Sadaie, M. et al. Redistribution of the Lamin B1 genomic binding profile affects rearrangement of heterochromatic domains and SAHF formation during senescence. Genes & Development 27, 1800 (2013).
45. Shah, P. P. et al. Lamin B1 depletion in senescent cells triggers large-scale changes in gene expression and the chromatin landscape. Genes and Development 27, 1787–1799 (2013).
46. Narita, M. et al. Rb-Mediated Heterochromatin Formation and Silencing of E2F Target Genes during Cellular Senescence. Cell 113, 703–716 (2003).

47. Pathak, R. U., Soujanya, M. & Mishra, R. K. Deterioration of nuclear morphology and architecture: A hallmark of senescence and aging. Ageing Research Reviews vol. 67 101264 (2021).
48. Hernandez-Segura, A., Nehme, J. & Demaria, M. Hallmarks of Cellular Senescence. Trends in Cell Biology 28, 436–453 (2018).
49. Ivanov, A. et al. Lysosome-mediated processing of chromatin in senescence. Journal of Cell Biology 202, 129–143 (2013).
50. Takahashi, A. et al. Downregulation of cytoplasmic DNases is implicated in cytoplasmic DNA accumulation and SASP in senescent cells. Nature Communications 9, 1–12 (2018).
51. Yang, H., Wang, H., Ren, J., Chen, Q. & Chen, Z. J. cGAS is essential for cellular senescence. Proceedings of the National Academy of Sciences 114, E4612–E4620 (2017).
52. Coppé, J.-P., Desprez, P.-Y., Krtolica, A. & Campisi, J. The senescence-associated secretory phenotype: the dark side of tumor suppression. Annual review of pathology 5, 99–118 (2010).
53. Coppé, J.-P. et al. Senescence-Associated Secretory Phenotypes Reveal Cell-Nonautonomous Functions of Oncogenic RAS and the p53 Tumor Suppressor. PLoS Biology 6, e301 (2008).
54. A, F., CK, P. & J, C. p38MAPK is a novel DNA damage response-independent regulator of the senescence-associated secretory phenotype. The EMBO journal 30, 1536–1548 (2011).
55. Acosta, J. C. et al. Chemokine Signaling via the CXCR2 Receptor Reinforces Senescence. Cell 133, 1006–1018 (2008).
56. T, K. et al. Oncogene-induced senescence relayed by an interleukin-dependent inflammatory network. Cell 133, 1019–1031 (2008).
57. Orjalo, A. V., Bhaumik, D., Gengler, B. K., Scott, G. K. & Campisi, J. Cell surface-bound IL-1 is an upstream regulator of the senescence-associated IL-6/IL-8 cytokine network. Proceedings of the National Academy of Sciences 106, 17031–17036 (2009).
58. Nelson, G. et al. A senescent cell bystander effect: senescence-induced senescence. Aging Cell 11, 345–349 (2012).
59. Nelson, G., Kucheryavenko, O., Wordsworth, J. & von Zglinicki, T. The senescent bystander effect is caused by ROS-activated NF-κB signalling. Mechanisms of Ageing and Development 170, 30–36 (2018).
60. Acosta, J. C. et al. A complex secretory program orchestrated by the inflammasome controls paracrine senescence. Nature Cell Biology 2013 15:8 15, 978–990 (2013).
61. Kirschner, K., Rattanavirotkul, N., Quince, M. F. & Chandra, T. Functional heterogeneity in senescence. Biochemical Society Transactions vol. 48 765–773 (2020).
62. Basisty, N. et al. A proteomic atlas of senescence-associated secretomes for aging biomarker development. PLoS biology 18, e3000599 (2020).
63. Rodier, F. et al. DNA-SCARS: distinct nuclear structures that sustain damage-induced senescence growth arrest and inflammatory cytokine secretion. Journal of Cell Science 124, 68–81 (2011).
64. Minieri, V. et al. Persistent DNA damage-induced premature senescence alters the functional features of human bone marrow mesenchymal stem cells. Journal of Cellular and Molecular Medicine 19, 734 (2015).
65. Sharpless, N. E. & Sherr, C. J. Forging a signature of in vivo senescence. Nature Reviews Cancer 2015 15:7 15, 397–408 (2015).
66. Kirkland, J. L., Tchkonia, T., Zhu, Y., Niedernhofer, L. J. & Robbins, P. D. The Clinical Potential of Senolytic Drugs. Journal of the American Geriatrics Society 65, 2297–2301 (2017).
67. Crowe, E. P. et al. Detecting Senescence: Methods and Approaches. Methods in Molecular Biology 1170, 425–445 (2014).
68. R, Z., W, C. & PD, A. Molecular dissection of formation of senescence-associated heterochromatin foci. Molecular and cellular biology 27, 2343–2358 (2007).
69. Davalos, A. R. et al. p53-dependent release of Alarmin HMGB1 is a central mediator of senescent phenotypes. The Journal of cell biology 201, 613–29 (2013).

70. JT, P., YS, L., KA, C. & SC, P. Adjustment of the lysosomal-mitochondrial axis for control of cellular senescence. Ageing research reviews 47, 176–182 (2018).
71. K, I., J, C. & GP, D. Methods to detect biomarkers of cellular senescence: the senescence-associated beta-galactosidase assay. Methods in molecular biology (Clifton, N.J.) 371, 21–31 (2007).
72. Kopp, H.-G., Hooper, A. T., Shmelkov, S. V. & Rafii, S. ß-Galactosidase staining on bone marrow. The osteoclast pitfall. Histology and Histopathology 22, 971–976 (2007).
73. Passos, J. F. et al. Mitochondrial Dysfunction Accounts for the Stochastic Heterogeneity in Telomere-Dependent Senescence. PLOS Biology 5, e110 (2007).
74. Passos, J. F. et al. Feedback between p21 and reactive oxygen production is necessary for cell senescence. Molecular Systems Biology 6, 347 (2010).
75. Demaria, M. et al. An essential role for senescent cells in optimal wound healing through secretion of PDGF-AA. Developmental cell 31, 722–33 (2014).
76. Krizhanovsky, V. et al. Senescence of Activated Stellate Cells Limits Liver Fibrosis. Cell 134, 657–667 (2008).
77. Jun, J.-I. & Lau, L. F. Cellular senescence controls fibrosis in wound healing. Aging 2, 627–31 (2010).
78. Muñoz-Espín, D. et al. Programmed Cell Senescence during Mammalian Embryonic Development. Cell 155, (2013).
79. Mishima, K. et al. Senescence-associated beta-galactosidase histochemistry for the primate eye. Investigative Ophthalmology & Visual Science June, 1590–1593 (1999).
80. Dimri, G. P. et al. A biomarker that identifies senescent human cells in culture and in aging skin in vivo. Proceedings of the National Academy of Sciences of the United States of America 92, 9363 (1995).
81. Rinehart, C. A. & Torti, V. R. Aging and Cancer: The Role of Stromal Interactions With Epithelial Cells. MOLECULAR CARCINOGENESIS 18, 187–192 (1997).
82. Krtolica, A., Parrinello, S., Lockett, S., Desprez, P.-Y. & Campisi, J. Senescent fibroblasts promote epithelial cell growth and tumorigenesis: A link between cancer and aging. Proceedings of the National Academy of Sciences 98, 12072–12077 (2001).
83. Baker, D. J. et al. Clearance of p16Ink4a-positive senescent cells delays ageing-associated disorders. Nature 479, 232–236 (2011).
84. Baker, D. J. et al. Naturally occurring p16Ink4a-positive cells shorten healthy lifespan. Nature 530, 184–189 (2016).
85. Laberge, R.-M. et al. MTOR regulates the pro-tumorigenic senescence-associated secretory phenotype by promoting IL1A translation. Nature Cell Biology 17, (2015).
86. Pribluda, A. et al. A senescence-inflammatory switch from cancer-inhibitory to cancer-promoting mechanism. Cancer cell 24, 242–56 (2013).
87. Jurk, D. et al. Chronic inflammation induces telomere dysfunction and accelerates ageing in mice. Nature Communications 2, (2014).
88. Gorenne, I., Kavurma, M., Scott, S. & Bennett, M. Vascular smooth muscle cell senescence in atherosclerosis. Cardiovascular Research vol. 72 9–17 (2006).
89. Shakeri, H., Lemmens, K., Gevaert, A. B., De Meyer, G. R. Y. & Segers, V. F. M. Cellular senescence links aging and diabetes in cardiovascular disease. American Journal of Physiology - Heart and Circulatory Physiology vol. 315 H448–H462 (2018).
90. Palmer, A. K. et al. Cellular senescence in type 2 diabetes: A therapeutic opportunity. Diabetes 64, 2289–2298 (2015).
91. Khosla, S., Farr, J. N., Tchkonia, T. & Kirkland, J. L. The role of cellular senescence in ageing and endocrine disease. Nature Reviews Endocrinology vol. 16 263–275 (2020).
92. G, W., A, S., RA, S., SJ, S. & K, A. p27(Kip1) Knockout mice are protected from diabetic nephropathy: evidence for p27(Kip1) haplotype insufficiency. Kidney international 68, 1583–1589 (2005).
93. M, A.-D. et al. The cyclin kinase inhibitor p21WAF1/CIP1 is required for glomerular hypertrophy in experimental diabetic nephropathy. Kidney international 56, 1691–1699 (1999).

94. Cippà, P. E. et al. Transcriptional trajectories of human kidney injury progression. JCI insight 3, (2018).
95. Stenvinkel, P. et al. CDKN2A/p16INK4a expression is associated with vascular progeria in chronic kidney disease. Aging 9, 494–507 (2017).
96. Quimby, J. M. et al. Feline chronic kidney disease is associated with shortened telomeres and increased cellular senescence. American Journal of Physiology-Renal Physiology 305, F295–F303 (2013).
97. Hickson, L. T. J. et al. Senolytics decrease senescent cells in humans: Preliminary report from a clinical trial of Dasatinib plus Quercetin in individuals with diabetic kidney disease. EBioMedicine 47, 446–456 (2019).
98. Sagiv, A. & Krizhanovsky, V. Immunosurveillance of senescent cells: the bright side of the senescence program. Biogerontology 14, 617–628 (2013).
99. A, S. et al. NKG2D ligands mediate immunosurveillance of senescent cells. Aging 8, 328–344 (2016).
100. Lujambio, A. et al. Non-cell-autonomous tumor suppression by p53. Cell 153, 449–460 (2013).
101. W, X. et al. Senescence and tumour clearance is triggered by p53 restoration in murine liver carcinomas. Nature 445, 656–660 (2007).
102. Kang, T. W. et al. Senescence surveillance of pre-malignant hepatocytes limits liver cancer development. Nature 479, 547–551 (2011).
103. Ovadya, Y. et al. Impaired immune surveillance accelerates accumulation of senescent cells and aging. Nature Communications 9, 1–15 (2018).
104. Soriani, A. et al. ATM-ATR-dependent up-regulation of DNAM-1 and NKG2D ligands on multiple myeloma cells by therapeutic agents results in enhanced NK-cell susceptibility and is associated with a senescent phenotype. Blood 113, 3503–3511 (2009).
105. Sagiv, A. et al. Granule exocytosis mediates immune surveillance of senescent cells. Oncogene 32, 1971–1977 (2013).
106. Antonangeli, F. et al. Natural killer cell recognition of in vivo drug-induced senescent multiple myeloma cells. OncoImmunology 5, (2016).
107. Pereira, B. I. et al. Senescent cells evade immune clearance via HLA-E-mediated NK and CD8+ T cell inhibition. Nature Communications 10, 1–13 (2019).
108. DP, M. et al. Targetable mechanisms driving immunoevasion of persistent senescent cells link chemotherapy-resistant cancer to aging. JCI insight 5, (2019).
109. van Deursen, J. M. The role of senescent cells in ageing. Nature 509, 439–446 (2014).
110. Zhu, Y. et al. The Achilles' heel of senescent cells: from transcriptome to senolytic drugs. Aging Cell 14, 644–658 (2015).
111. Zhu, Y. et al. Identification of a novel senolytic agent, navitoclax, targeting the Bcl-2 family of anti-apoptotic factors. Aging Cell 15, (2016).
112. Fuhrmann-Stroissnigg, H. et al. Identification of HSP90 inhibitors as a novel class of senolytics. Nature Communications 8, 422 (2017).
113. Roos, C. M. et al. Chronic senolytic treatment alleviates established vasomotor dysfunction in aged or atherosclerotic mice. Aging Cell 15, 973–977 (2016).
114. Schafer, M. J. et al. Cellular senescence mediates fibrotic pulmonary disease. Nature Communications 8, 14532 (2017).
115. Iske, J. et al. Senolytics prevent mt-DNA-induced inflammation and promote the survival of aged organs following transplantation. Nature Communications 11, (2020).
116. Hickson, L. T. J. et al. Senolytics decrease senescent cells in humans: Preliminary report from a clinical trial of Dasatinib plus Quercetin in individuals with diabetic kidney disease. EBioMedicine 47, 446–456 (2019).
117. Justice, J. N. et al. Senolytics in idiopathic pulmonary fibrosis: Results from a first-in-human, open-label, pilot study. EBioMedicine 40, 554–563 (2019).

Chapter 2

Senescence is a hallmark of polycystic kidney disease

Hester van Willigenburg[1,2]*, Annegien T. Kenter[3,4,5,]*, Frans Schutgens[6,7,]*, Eveline Rentmeester[3], Job van Riet[8,9], Beatrice Tan[3,], Harmen J.G. van de Werken[8,9], Anusha S. Shankar[5], Martin J. Hoogduijn[5], Geert J.L.H. van Leenders[10], Paul C.M.S. Verhagen[9], Ron W.F. de Bruin[1], Peter L.J. de Keizer[11], Wilfred F.J. van IJcken[12] Jeroen A.A. Demmers[13], Marianne C. Verhaar[7], Gert Jansen[4], Robert Zietse[5], Maarten B. Rookmaaker[7], Dorien J.M. Peters[14], Ewout J. Hoorn[5#], Joost H. Gribnau[3#]

[1]Department of Surgery, Erasmus MC, University Medical Center Rotterdam, Rotterdam, The Netherlands, [2] Department of Molecular Genetics, Erasmus MC, University Medical Center Rotterdam, Rotterdam, The Netherlands, [3] Department of Developmental Biology, Erasmus MC, University Medical Center Rotterdam, Oncode Institute, Rotterdam, The Netherlands, [4] Department of Cell Biology, Erasmus MC, University Medical Center Rotterdam, Rotterdam, The Netherlands, [5] Department of Internal Medicine, Division of Nephrology and Transplantation, Erasmus MC, University Medical Center Rotterdam, Rotterdam, The Netherlands, [6] Hubrecht Institute–Royal Netherlands Academy of Arts and Sciences, Utrecht, the Netherlands, [7] Department of Nephrology and Hypertension, University Medical Center Utrecht, the Netherlands, [8]Cancer Computational Biology Center, Erasmus MC, University Medical Center Rotterdam, Rotterdam, The Netherlands, [9]Department of Urology, Erasmus MC, University Medical Center Rotterdam, Rotterdam, The Netherlands, [10]Department of Pathology, Erasmus MC, University Medical Center Rotterdam, Rotterdam, The Netherlands, [11] Department of Molecular Cancer Research, Center for Molecular Medicine, University Medical Center Utrecht, (UMCU), the Netherlands, [12]Erasmus Center for Biomics, Erasmus MC, University Medical Center Rotterdam, Rotterdam, The Netherlands, [13] Proteomics Center, Erasmus MC, University Medical Center Rotterdam, Rotterdam, The Netherlands, [14]Department of Human Genetics, Leiden University Medical Center (LUMC). The Netherlands

* these authors contributed equaly

Submitted for publication

ABSTRACT

Autosomal Dominant Polycystic Kidney Disease (ADPKD) is the most common inherited kidney disease. So far, the exact molecular mechanism of cyst formation has not yet been elucidated. Here we generated kidney tubuloid model systems to study ADPKD using adult stem cells derived from cyst lining epithelium of ADPKD patients and control material. Patient derived tubuloids harboured a germline mutation in *PKD1* and additional somatic mutations in various genes unique for each cyst-derived organoid line. Comparative transcriptome analysis indicated that PKD organoids displayed various hallmarks of cellular senescence, including reduced expression of Lamin B1 and cell cycle genes, as well as upregulation of genes involved in the senescence associated secretory phenotype (SASP). A role for senescence in ADPKD was further supported by the characteristic expression of senescence markers in polycystic kidney tissue from ADPKD mice and patients. In addition, SASP factors were detected in cyst fluid and exposure to cyst fluid and SASP factors increased proliferation of tubular epithelial cells. The identification of senescence as hallmark of ADPKD and the link between senescence and cyst formation provides new insight into the pathophysiology and opens new treatment possibilities owing to the recent discovery of senolytic compounds.

INTRODUCTION

Polycystic Kidney Disease (PKD) is a heterogeneous group of diseases that can be inherited or acquired. The most common genetic form is Autosomal Dominant Polycystic Kidney Disease (ADPKD) with an estimated prevalence of 4-10:10.000 people [1,2]. ADPKD patients gradually develop numerous cysts resulting in massive enlargement of the kidneys. Around 70% of the patients develop end-stage kidney disease between the fourth and seventh decade of life [3]. Although Tolvaptan – a vasopressin receptor antagonist – has recently become available for patients with rapidly progressive ADPKD, a definitive curative treatment that prevents kidney failure is currently unavailable.

ADPKD is caused by a heterozygous germline mutation in *PKD1* or *PKD2* in ~80% and ~15% of the patients, respectively [4]. The two *PKD* genes encode for polycystin-1 and -2, transmembrane proteins, which form a ligand-gated non selective cation channel complex [5–9]. Polycystin-1 acts in a dose dependent fashion with low levels or overexpression of functional polycystin-1 resulting in a polycystic phenotype [10,11]. In the kidney epithelial cell, a second genetic hit in either *PKD1* or other genes involved in PKD-signaling have been proposed to precede cyst formation [12–16]. The precise cellular function of polycystin-1 remains to be elucidated, but it plays an important role during kidney development and kidney injury response, when *PKD1* expression levels are upregulated [17–19]. Moreover, while *Pkd1* deletion in adult mice leads to the formation of only a few cysts, a massive polycystic phenotype rapidly develops when *Pkd1* deletion is followed by kidney injury [20–24]. In addition, following kidney injury, non-cystic *Pkd1*$^{+/-}$ mice exhibit increased kidney damage, apoptosis, and infiltration of inflammatory cells as compared to wild type controls, showing that *Pkd1* heterozygosity is haploinsufficient and impairs the injury response [25]. Interestingly, in kidneys without a *PKD* mutation, kidney injury, chronic kidney disease, or physiological ageing can also induce cystogenesis, and this phenomenon is referred to as acquired cystic kidney disease [26–35]. How kidney injury and ageing trigger cystogenesis also remains to be elucidated.

Cellular senescence plays an important role in injury repair and aging [36]. Senescence is an irreversible cell cycle arrest, controlled through either p53-p21 or p16-pRb signaling and induced in response to severe cell stress, for example caused by excessive DNA-damage, telomere shortening, or oncogene activation [37,38]. Besides a permanent growth arrest, another characteristic of senescent cells is the development of a chronic pro-inflammatory state called the senescence associated secretory phenotype (SASP) [37,39]. Important SASP factors are inflammatory proteins, such as IL-6 and IL-8 and several growth factors, but also matrix remodeling enzymes [37,39]. SASP expression can vary between senescent cells can vary over time depending on cell type, environmental cues, and mode of senescence induction [39,40]. Therefore, SASP factors can exert various effects on the microenvironment, including extracellular matrix remodeling and local inflammation by attraction of immune cells [38,39,41]. Furthermore, SASP factors can induce

senescence or, paradoxically, proliferation of neighboring cells in a paracrine manner [36,39,40]. Through these processes, senescent cells were shown to aid in tumor suppression, embryonic development and wound healing or injury repair [42–44]. However during aging or repetitive injury, immune clearance of senescent cells can be suppressed [45]. SASP factors can have negative effects when senescent cells are not cleared from tissues over time, resulting in chronic senescence which leads to persistent inflammation and fibrosis [38,41,46–48] In the kidney, senescence is found to have a beneficial effect during the early phase of acute kidney injury, however, once senescent cells are not cleared and chronically reside in kidney tissue, their presence in repetitive and chronic kidney injury is detrimental [49,50]. Eliminating senescent cells from aged or injured animals using anti-senescence ("senolytic") drugs reduces age-related kidney damage and preserves renal function [42,51,52].

Given the link between *PKD* and injury repair, we hypothesized that cellular senescence plays a role in PKD. We found that cellular senescence is an important feature of polycystic kidney disease *in vitro* and *in vivo*. First, we established a novel human adult stem cells (ASC) kidney tuboloid 3D model, derived from ADPKD kidney explants and control kidney tissue. ASC organoids are a powerful tool to study human diseases and have been established from multiple organs without immortalization, which is crucial when investigating cell cycle regulation [53,54]. Kidney ASC tubuloids consist of polarized epithelium from proximal and distal tubular segments which can be passaged long term while maintaining genetic stability [54]. We found that ADPKD ASC tubuloids exhibit a cellular senescence phenotype. In addition, our results show that ADPKD kidneys display accelerated senescence. Moreover, we show that cyst fluid contains several SASP factors that promote proliferation of kidney epithelial cells and can therefore contribute to cystogenesis. The fact that senescence is a hallmark of ADPKD provides new mechanistic insights in cystogenesis and implicates that senolytics might be used as therapeutic strategy to halt disease progression in ADPKD.

RESULTS

ADPKD derived kidney tubuloids

Recently, we established adult stem cell kidney tubuloid cultures from healthy mice and humans to study infectious, malignant and hereditary kidney disease [54]. Here we applied this approach to generate ADPKD patient derived ASC kidney tubuloids. These tubuloids represent a powerful model system to study healthy and diseased epithelial kidney epithelial cell types and tissue. We collected polycystic kidney explants from patients clinically diagnosed with ADPKD. From each explant, we established tubuloid cultures from cysts lining epithelium of three individual cysts. In parallel, control kidney tubuloid lines were isolated from unaffected regions of excised kidneys with renal cell carcinoma. In total, six ADPKD and six control (wild type) kidney tubuloid lines were included in this study (**Table 1 and Figure 1a**). For both ADPKD and normal kidney tubuloid cultures,

tubuloid growth was observed from day 3 after seeding and could be continuously propagated for > 4 months, with a 1:3 weekly split ratio. However, ADPKD tubuloid lines exhibited notably slower growth as compared to the normal controls. Morphologically, patient derived tubuloids resembled the normal kidney tubuloids forming round spheres, consisting of a monolayer of cuboid epithelium with occasionally regions with thickening, branching and folding of the sphere wall (**Figure 1b, c and Supplemental Figure 1**). We did not find significant differential *PKD1* and *PKHD1* mRNA expression levels between ADPKD and normal tubuloid lines (**Figure 1d**).

Patient nr	Phenotype	Gender	Age	Germ line mutation	Organoids clones	Reasons for nephrectomy	Size & weight explant
1	ADPKD	male	47	PKD1 c.9377G>C / p.Thr3126Arg & PKHD1 c.10858C>T / p.Arg3620Cys	1a / 1b / 1c	Infection	23.5 x 12 x 5 cm / 1018 gr
2	ADPKD	female	73	PKD1 c.4969delA / p.Arg1657fs	2a / 2b / 2c	Space for transplant	24 x 17 x 8 cm / 1900 gr
3	WT	female	51	n.a.	3a / 3b / 3c	Tumor	n.a.
4	WT	male	72	n.a.	4a / 4b / 4c	Tumor	n.a.

Table 1. Patient characteristics

PKD1 germline and somatic mutations in ADPKD tubuloids

Whole exosome sequencing was performed on all PKD tubuloid lines and a control kidney fragment from the same patient as reference genome to identify germline and somatic mutations. We verified that both patients had a pathogenic mutation in *PKD1*, present in all three tubuloid lines from three different cysts and in the reference sample, indicating that these were germ line mutations **(Table 1 and Figure 2a**). In patient 1 we found a missense mutation in *PKD1* exon 26 resulting in a nonsynonymous amino acid change, categorized as pathogenic in the PKD mutation database [55]. Surprisingly, patient 1 was also carrier of a heterozygous pathogenic missense mutation in *PKHD1*, a gene implicated in the recessive form of PKD (ARPKD). In patient 2 a frame shift mutation was observed in *PKD1* exon 15 resulting in a protein truncation. Since a second genetic hit in kidney epithelial cells is proposed to be the initiating event in cystogenesis, we assessed whether we could detect somatic mutations that are cyst/tubuloid line specific. We found various mutations exome wide, which were unique to tubuloid lines from individual cysts. In total 141 mutations (SNV/indels) were detected in various genes (**Figure 2b**). No somatic mutations in *PKD1*, *PKD2* or *PKHD1* could be observed (**Figure 2**), nor could we detect somatic copy number alterations of these genes (data not shown).

Transcriptome analysis of ADPKD tubuloids indicates cellular senescence

To gain insight in the molecular pathways affected in ADPKD tubuloids we performed RNA sequencing of six ADPKD and six normal kidney tubuloids. All tubuloids displayed high expression of EPCAM, PAX8 and other epithelial markers as well as the ASC markers PROM1 and SOX9 (**Supplemental Figure 1b**). We detected expression of proximal tubule markers (ABCC1, ABCC3, ABCC4, SLC22A3, SLC40A1), and comparison of our RNA-seq data with single-cell RNA-seq data showed clear correlation in expression with our previous established tubuloids, and confirmed the tubular epithelial nature of control and ADPKD tubuloids (**Supplemental Figure 1c-d**) [54, 107].

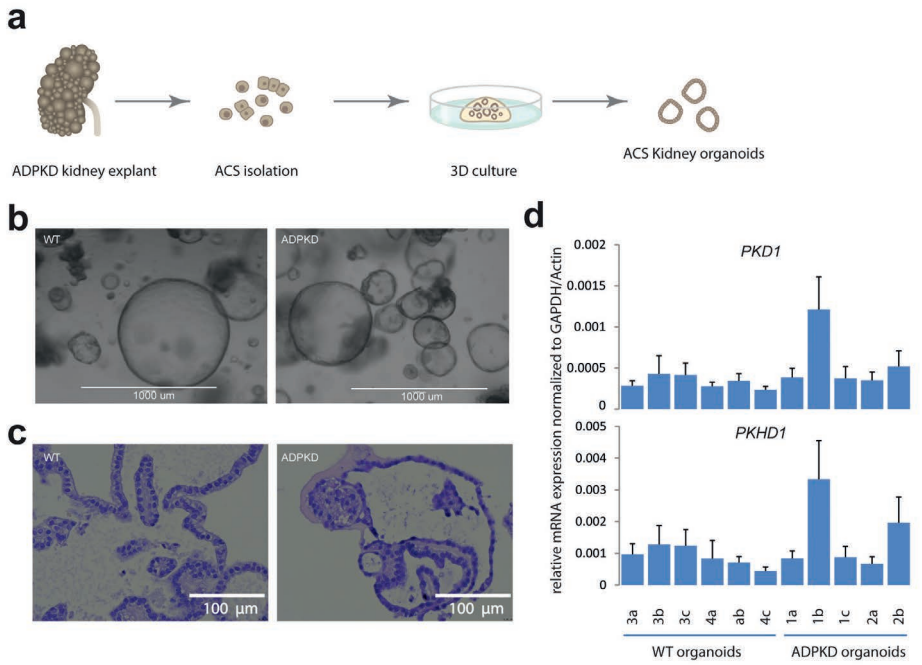

Figure 1. PKD patient-derived kidney tubuloid lines
(a) Schematic overview of experimental setup. From each ADPKD kidney explant tubuloid cultures were established from three individual cysts. **(b)** PKD patient derived and normal tubuloid lines (brightfield). **(c)** Hematoxylin and Eosin (H&E) staining of kidney tubuloids. **(d)** PKD1 gene expression was analysed by qRT-PCR, Ct values are normalized using GAPDH. qRT-PCR was performed in duplicate twice, error bars represent SD of both experiments.

Nevertheless, proximal tubule markers appeared slightly increased in ADPKD tubuloids, and t-SNE analysis of the transcriptomes demonstrated that ADPKD and normal kidney tubuloids clustered separately (**Figure 3a**). Comparative analysis of ADPKD and normal tubuloids expression profiles yielded 2,803 genes that were differentially expressed (adjusted P-value < 0.01) (**Figure 3b**). Gene Ontology (GO) term and KEGG pathway analyses both revealed that genes upregulated in ADPKD tubuloids are involved in a variety of biological processes and molecular functions, including immunity, extracellular matrix organisation, cytokine and chemokine signaling, whereas genes downregulated in ADPKD tubuloids are linked to cell cycle, DNA replication and repair (**Figure 3c and Supplemental Figure 2a**). Interestingly, senescence markers *Lamin B1* (*LMNB1*) and *Ki67* (*MKI67*) that are downregulated in senescence cells were also significantly downregulated in ADPKD tubuloids (adjusted P-value < 0.01, **Figure 3d**). In addition, various SASP factors were significantly upregulated in ADPKD tubuloids, including *IL-6, IL-8* (*CXCL8*) and *CCN1* (*Cyr61*) (**Figure 3d and Supplemental Figure 2b**).

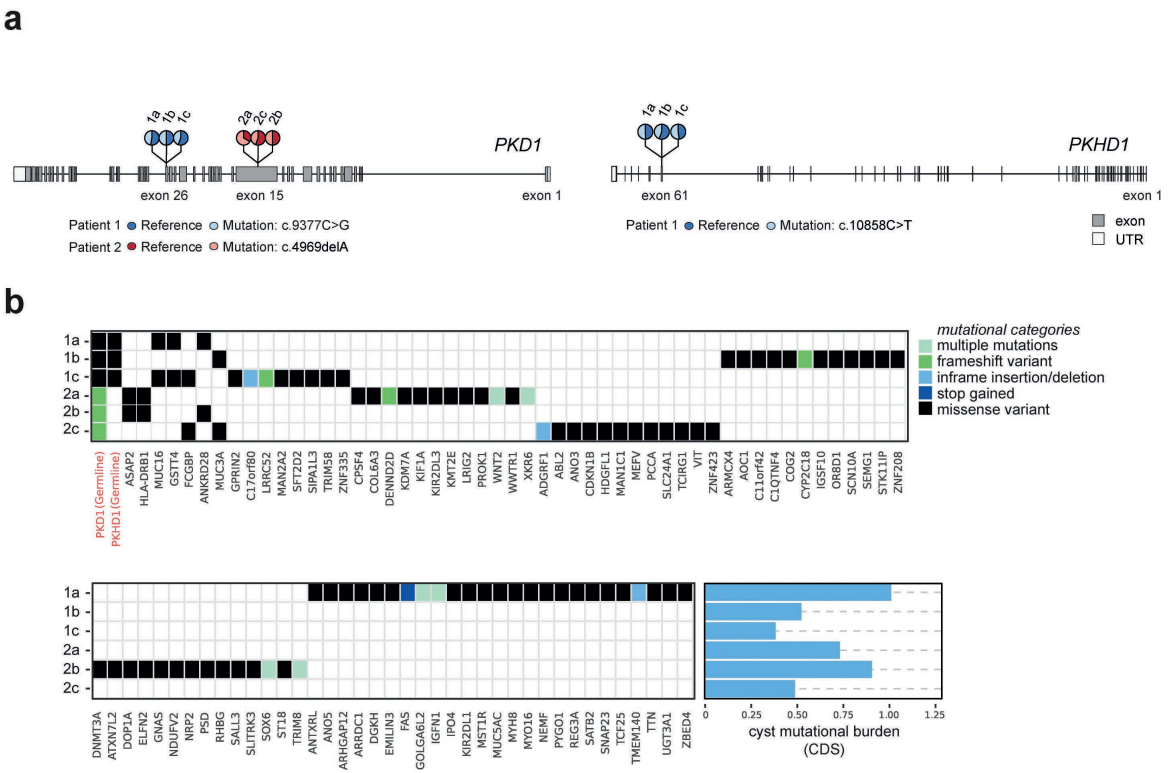

Figure 2 Mutational landscape of PKD patient-derived tubuloid lines

(a) Whole Exome Sequencing was performed on ADPKD tubuloids and unaffected kidney fragments as reference genome identifying heterozygous pathogenic germ line mutation in *PKD1* for patient 1 and patient 2. Patient 1 also harbours a heterozygous germ line mutation in *PKHD1* that is marked as pathogenic in the COSMIC database. **(b)** Comparative analysis of variants in tubuloid line (top) versus unaffected kidney (bottom), showing somatic mutations unique for each cyst derived tubuloid.

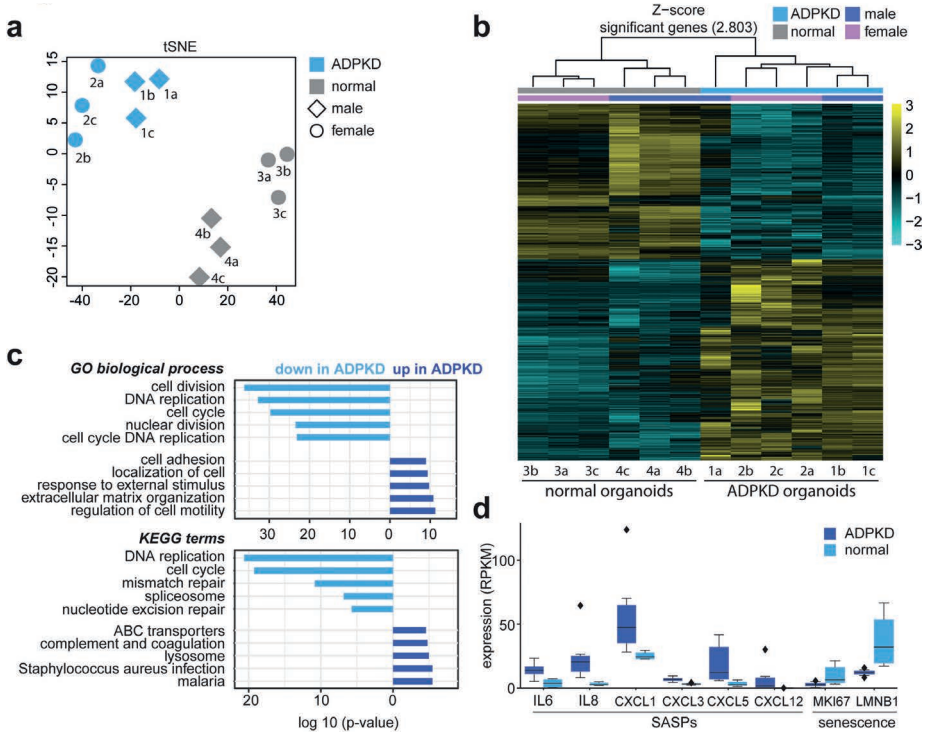

Figure 3 Transcriptome analysis of ADPKD tubuloids reveals expression changes implying cellular senescence

(a) tSNE analysis of gene expression data showing the first two dimensions. **(b)** Heatmap showing differentially expressed genes (adjusted p-value < 0.01) in tubuloids. **(c)** Gene Set Enrichment analysis of GO and KEGG Pathways of differentially expressed genes. **(d)** RNA-seq data indicates that *LMNB1* (*Lamin B1*) and *MKI67* (*Ki67)* expression (RPKM) is reduced in ADPKD tubuloids (right), whereas SASP factors are significantly upregulated in ADPKD tubuloids (left) (adjusted *p-value* < 0.01).

Senescence in mice with polycystic kidneys

Our findings indicate a senescence phenotype in ADPKD tubuloids. To verify whether these *in vitro* findings could be confirmed *in vivo*, we tested whether senescence is present in kidney tissue of three PKD mouse models. The PKD mouse models included one with a hypomorphic *Pkd1* allele (*Pkd1*^{nl,nl}, resulting in reduced *Pkd1* expression and leading to cyst formation from around birth onwards [56]), and two in which a kidney-specific *Pkd1* knockout was induced on postnatal day 10 or 18 (resulting in a severe or mild phenotype, respectively [57]). Immunofluorescence staining of cystic kidney tissue from these three mouse models was performed and analysed for nuclear loss of the senescence markers Lamin B1 and HMGB1 [58,59] (**Figure 4**). *Pkd1*^{nl,nl} mice have significantly more cells with reduced nuclear staining of both Lamin B1 and HMGB1 (10- and 3-fold change, respectively), indicating elevated levels of senescence in these cystic kidneys (**Figure 4c and 4d**). Similarly, in *Pkd1* P10 and P18 conditional knock out mice, we found

a significant decrease in cells positive for Lamin B1 and/or HMGB1 (**Figure 4c and 4d**). Furthermore, in *Pkd1*^{nl,nl} mice, cyst size correlated with the presence of senescent cells in the cyst epithelium (**Figure 4e**).

Senescence in human polycystic kidneys

Subsequently, we verified whether cellular senescence is also present in human polycystic kidney disease. Similar to the studies in mice, immunofluorescence staining revealed reduced levels of LaminB1 and HMGB1 positive cells in human ADPKD snap-frozen kidney tissues, compared to healthy age-matched controls (**Fig 5a-b**). Analyses of immunofluorescent images for nuclear loss of the senescence markers LaminB1 and HMGB1 showed that ADPKD kidneys have significantly more senescent cells compared to healthy age matched controls (**Figure 5c-d**). Furthermore, increased mRNA expression of the senescence inducing gene *CDKN2A*, (coding for p16^{INK4A}) was found in ADPKD kidney samples of patients compared to healthy age-matched control kidney samples (**Figure 5e**). Notably, no difference in gene expression of the other major senescence inducer *CDKN1A* (coding for P21^{CIP1}) was detected between these tissues (**Figure 5e**). Confirming previous studies, expression of the major ADPKD driving gene *MYC* was also upregulated in ADPKD kidney samples. In addition to senescence observed in the cells of the cystic epithelium, senescent cells were also present in stroma cells of the cyst micro environment (**Supplemental figure 3**). Together, these results show an increase in the amount of senescent cells in human ADPKD kidney tissues, both in the cyst epithelium and in the interstitial cells.

SASP factors promote renal epithelial cell proliferation *in vitro*

Considering that SASP factors are expressed in ADPKD tubuloids and cystic kidney tissue, we hypothesized that these factors might be secreted into the cyst fluid. We collected three kidney cyst fluid samples from ADPKD kidney explants. We used mass spectrometry to test if SASP factors were present in kidney cyst fluid and detected a total of 15 SASP factors (**Figure 6a**). Because cytokines are biologically highly active and therefore usually present at low concentrations, they may be missed with mass spectrometry. To specifically analyse whether cytokines are present in cyst fluid, we used a cytokine multiplex assay, and detected the inflammatory SASP factors IL-6 and IL-8 and, at lower concentrations, CXCL5 and CXCL1 (**Figure 6b**).Next, we tested whether cyst fluid has the potential to induce proliferation in tubular epithelial cells (RPTEC/hTERT1) in a proliferation assay [60]. We found that tubular epithelial cells cultured in medium supplemented with kidney cyst fluid exhibited a higher proliferation rate as compared to controls, demonstrating that cyst fluid contains factors that induce proliferation of tubular epithelial cells (**Figure 6c**).Given the presence of SASP factors in cystic fluid and ADPKD tubuloids, we analyzed whether SASP factors by themselves could promote proliferation in tubular epithelial cells by treating tubular epithelial cells with various recombinant human SASP proteins. We found that treatment with low doses of several of these SASP factors, such as IL-6 and IL-8, could promote proliferation in these cells

as compared to controls (**Figure 6d**). Together, these results show that SASP factors are present in human cysts and cystic fluid, and that single SASP factors can promote cell growth of tubular epithelial cells.

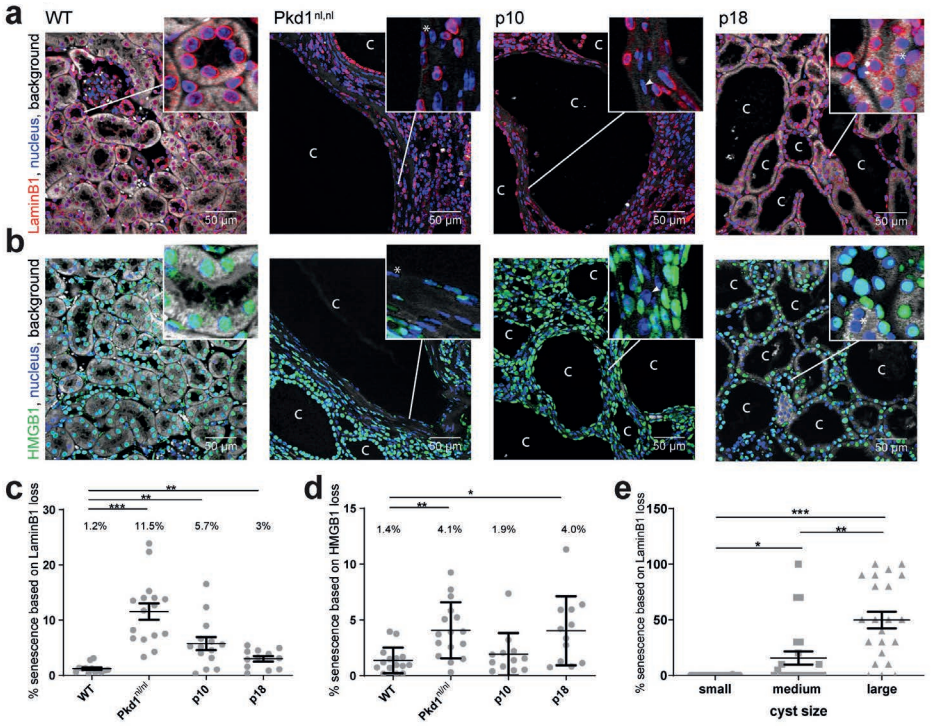

Figure 4 Cellular senescence in vivo (IF) on cystic tissue from ADPKD mouse kidneys
(a-b) Representative images of kidneys from 26-week WT, *Pkd1*^{nl,nl} mice, and *Pkd1* conditional knockout mice postnatally induced on day 18 (P18) or day 10 (P10), stained for Lamin B1 **(a)** and HMGB1 **(b)** (n=4). "C" indicates cyst with diameter>50um, arrows and asterisks indicate senescent interstitial and epithelial cells respectively. Quantified are the average % of nuclei per kidney negative for Lamin B1 and HMGB1 **(c and d resp.)**. Averages of 4 random images per mouse (at least 400 nuclei per mouse), 4 mice per group. **(e)** Quantification of % Lamin B1 loss in epithelial cells lining cysts with increasing cyst diameter. Sixty-six random cysts were divided over 3 equal groups: small (20-130 µm), medium (130-500 µm) or large cysts (500-1500 µm). p values were calculated using one-way ANOVA with Bonferroni post-test correction, * $p < 0.05$, ** $p < 0.01$, *** $p<0.001$, error bars represent the SEM.

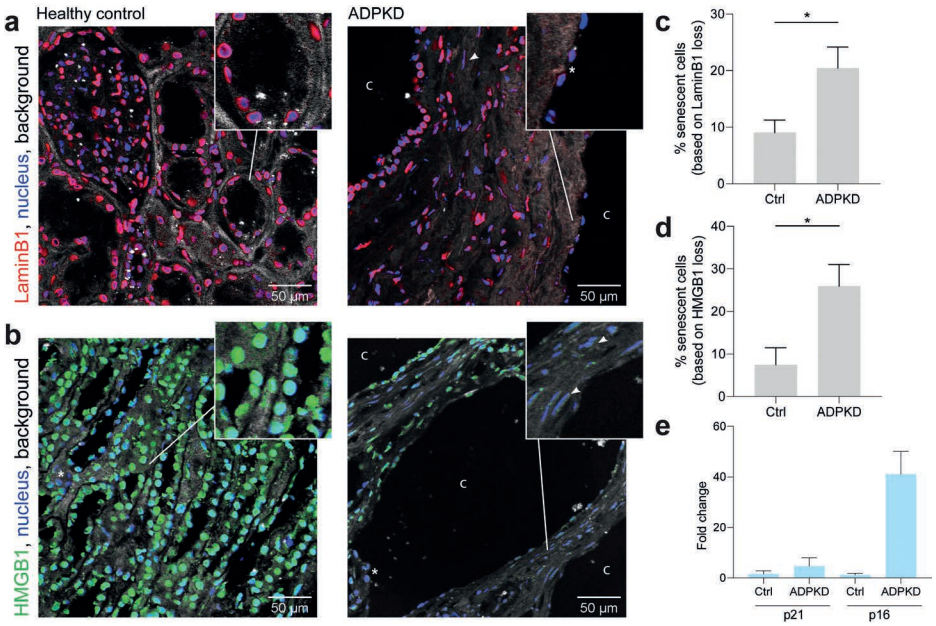

Figure 5 Markers of cellular senescence are elevated in kidneys from ADPKD patients
(a) Representative images of kidneys from healthy control and ADPKD human snap-frozen kidney tissue stained for Lamin B1 **(a)** (healthy control n=5, ADPKD n=4) and HMGB1 **(b)** (healthy control n=4, ADPKD n=6). "C" indicates cyst with diameter>50um, arrows indicate senescent interstitial and asterisks senescent epithelial cells. Quantified are the average % of nuclei per kidney negative for Lamin B1 **(c)** and HMGB1 **(d)**. Averages of 5 random images per sample (at least 400 nuclei per kidney sample). **(e)** Real-Time PCR measurements of $P21^{CIP1}$(*CDKN1A*) expression, $p16^{INK4A}$ (*CDKN2A*) expression and c-Myc (*MYC*) in ADPKD and healthy kidney tissues (ADPKD n=3, Healthy control n=6). P-values were calculated using unpaired students t-test, *p<0.05 error bars represent the SEM.

DISCUSSION

The exact molecular mechanism of ADPKD remains to be elucidated. Here, we found cellular senescence as a hallmark of ADPKD pathogenesis. Using an ASC kidney tubuloid model we find that ADPKD tubuloids display a senescent phenotype. Accordingly, we show that in ADPKD senescent cells accumulate in the kidney. Moreover, our findings suggest that senescent cells might contribute to the formation and growth of cysts through the secretion of SASP factors. Cystogenesis is triggered by kidney injury in ADPKD as well as genetically normal kidneys [24–35,61]. Kidney injury leads to a complex physiologic repair response process in the kidney in which cellular senescence plays a crucial role [50,62,63]. Shortly after injury occurs, p53 and p21 are upregulated massively in the tubular epithelium [64–68]. Next, senescent cells aid in the wound healing process, by stimulating proliferation in neighboring cells and by attracting immune cells via SASP factor secretion [36,43,50,63]. In turn, these immune cells ensure clearance of senescent cells [36,41,50,63].

a

Protein names	Gene names	iBAQ	Peptides
Angiogenin	ANG	29822000	4
C-C motif chemokine 15, 14, 3,23	CCL15/14/3/23	6279300	2
Cathepsin B	CTSB	44694000	7
Stromal cell-derived factor 1	CXCL12	2952300	1
Epidermal growth factor receptor	EGFR	1884700	6
Fibronectin	FN1	782150000	84
Insulin-like growth factor-binding protein 1	IGFBP1	2822000	2
Insulin-like growth factor-binding protein 2	IGFBP2	73480000	11
Insulin-like growth factor-binding protein 3	IGFBP3	13598000	6
Insulin-like growth factor-binding protein 5	IGFBP5	14365000	3
Insulin-like growth factor-binding protein 6	IGFBP6	144240000	6
Insulin-like growth factor-binding protein 7	IGFBP7	269150000	9
Macrophage migration inhibitory factor	MIF	325790000	4
Metalloproteinase inhibitor 1	TIMP1	1074800000	8
Metalloproteinase inhibitor 2	TIMP2	127970000	3

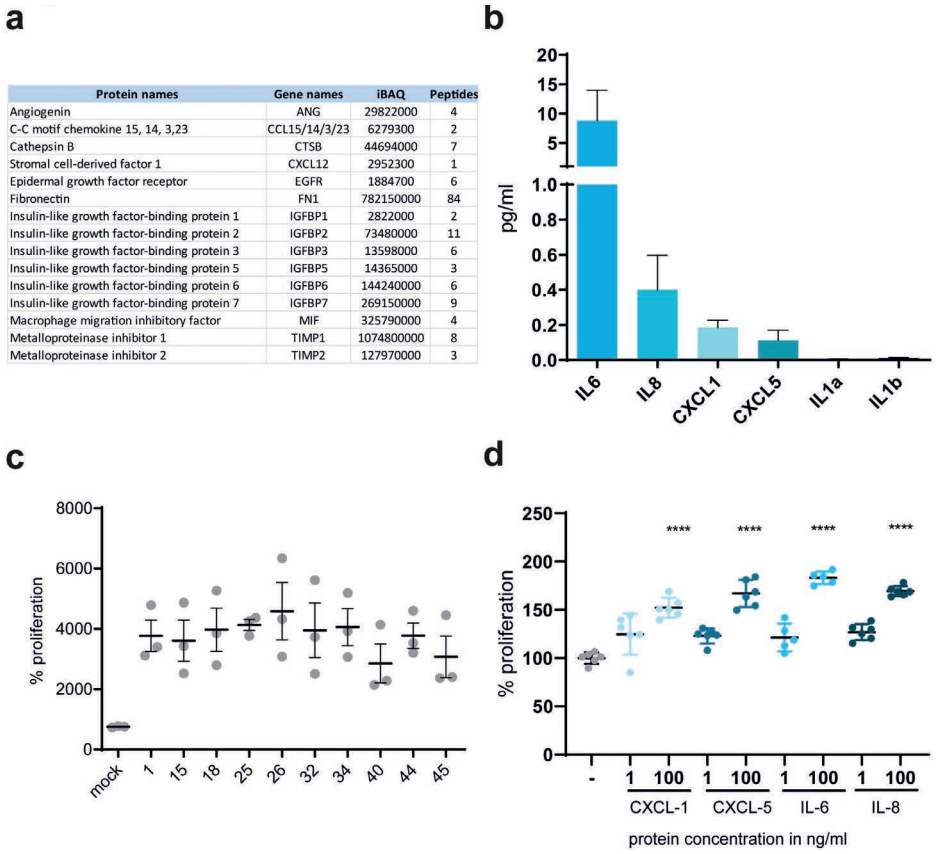

Figure 6 SASP factors are present in cyst fluid and induce proliferation *in vitro*
(a) SASP factors detected by mass spectrometry in cyst fluid. **(b)** ELISA/Cytokine multiplex assay detecting SASP factors in cyst fluid. **(c)** RPTEC/hTERT cells cultured with 10% cyst fluid supplemented to the medium for 4 days. Four biological replicates were used, error bars represent the SEM. **(d)** RPTEC/hTERT cells cultured with recombinant human SASP factors supplemented to the medium for 7 days. Three biological replicates in duplicate were used, p values were calculated using one-way ANOVA with Bonferroni post-test correction, * $p < 0.05$, ** $p < 0.01$, *** $p<0.001$, error bars represent the SEM.

Although senescence has a beneficial effect during the early phase of acute kidney injury, during aging and in repetitive and chronic kidney injury, senescent cells can evade immune clearance and chronically reside in kidney tissue [45]. Their presence is detrimental, leading to chronic inflammation, fibrosis and loss of kidney function [47-51].

In ADPKD, the acute kidney injury response is impaired. In *Pkd1*$^{+/-}$ and *Pkd2*$^{+/-}$ mice immediate upregulation of p21 and p53 in response to injury is abrogated [25,61,69]. Accordingly, in our study *p21* activation was found to be absent in ADPKD mice and human tissue, an observation that has been reported for human tissue previously [70]. The

incapability of p21 upregulation could be explained by the elevated expression of c-MYC in ADPKD [71], an inhibitor of *p21* promotor activation [72]. Interestingly, *Pkd1*$^{+/-}$, *Pkd2*$^{+/-}$, *p53*$^{-/-}$, *p21* conditional knock out mice and *c-Myc* overexpressing mice are sensitive to renal injury. Injury in these mice leads to more severe histological changes compared to wild type controls; including increased proliferation, persistent inflammation, fibrosis, and tubular dilatations, followed by cyst formation and decline in renal function [23–25,61,66,67,73]. Interestingly, inflammation and fibrosis was found to precede cyst formation, implying that this is a direct consequence of polycystin dysfunction instead of a secondary consequence of cyst growth [61]. Here, we show that ADPKD kidneys also display an increase in accumulation of senescent cells compared to control tissue. Whilst *p21* upregulation is abrogated in ADPKD, we found increased *p16* expression in cystic tissue, implying that in ADPKD senescence is induced in a p16/Rb dependent manner.

Thus, upregulation of polycystin-1, in response to kidney injury, plays an important role in tissue repair. Our results suggest a model in which, the polycystin-1 mediated p21/p53 senescence response is impaired in ADPKD and leads to accumulation of senescent cells, resulting in fibrosis, inflammation and cystogenesis (**Figure 7**).

The question remains whether senescence itself can trigger cystogenesis. Previous studies showed that in close proximity of a cyst, novel cysts arise, suggesting local paracrine signaling initiates cyst formation [74]. SASP factors have previously been shown to induce proliferation of neighboring cells [36,39,40], and our findings therefore suggest that focal secretion of SASP factors by senescent cells, promotes cystogenesis in a paracrine manner. We found that ADPKD ASC tubuloids express several SASP factors, including CCN1 (Cyr61), an important regulator of senescence during injury repair [75]. Furthermore, we detected known inflammatory factors present in cyst fluid that can be classified as SASP factors [76–80]. Interestingly, a recent study showed expression of these same SASP factors (CTGF, CXCL1, CXCL5, IL-8) after *in vitro* deletion of *PKHD1* using CRISPR/Cas9 [81]. This suggests that secretion of these SASP factors is a direct result of loss of *PKD1* or *PKHD1*, rather than a secondary consequence of micro-environmental effects such as immune cell infiltration or mechanical pressure from cysts. These are factors that are known chemo attractants, recruiting immune cells and inducing inflammation in cystic tissues [41,47]. We also demonstrated that culturing tubular epithelial cells with either cystic fluid or single SASP factors, such as IL-6, IL-8 or CXCL1 and CXCL5 promotes cell growth in tubular epithelial cells *in vitro*. We found IL-8 – one of the major SASP components involved in injury repair [82] – as one of the SASP factors differentially expressed in our ADPKD ASC kidney tubuloid model, present in cyst fluid from ADPKD patients and displaying a proliferative effect on tubular epithelial cells *in vitro*. Accordingly, IL-8 expression was found to induce cell proliferation in *PKHD1* mutant cells and is a central player in pathogenesis of the recessive form of PKD [81]. Moreover, IL-8 inhibition reduces cyst growth *in vitro* [83], implying that IL-8 might be one of the SASP factors responsible for promoting cystogenesis in ADPKD.

Senescence as a trigger for cystogenesis could explain variability in disease severity within ADPKD families, since exposure to renal injury inducing factors will differ between these family members.

Also in line with the fact that physiological aging of the human kidney– which is characterized by chronic accumulation of senescent cells – is associated with increased prevalence of kidney cysts [35].

Our findings highlight the potential of tubuloids to study disease. Nevertheless, our cystic derived tubuloids did not reveal a second hit in *PKD1* – a somatic mutation rendering these cells null for *PKD1* - as has been described before. Although other studies reported the absence of a second mutation, our findings with ADPKD tubuloids could be explained by *in vitro* cell selection against cells with a second mutation, a hypothesis that could be tested through knocking out the unaffected copy of P*KD1* in our patient tubuloids. Finally, our tubuloids represent the end stage of ADPKD where senescence plays an important role in the disease, but do not allow us to study the early disease stages, for which different models might be more suitable

In conclusion, we show that senescence is a hallmark of ADPKD. We propose that in ADPKD the injury response is impaired resulting in accumulation of senescent cells that chronically reside in the kidney. In addition, our results suggest that senescence and associated SASP factor secretion might even trigger cystogenesis. Eliminating senescent cells using anti-senescence ("senolytic") drugs therefore offers a potential therapeutic strategy in ADPKD.

METHODS

Patient Material collection

Kidney explants were obtained from patients undergoing elective nephrectomy. ADPKD was diagnosed based on established criteria, including positive family history and ultrasound criteria. Material collection was approved by the Medical Ethics Committee of the Erasmus Medical Center, Rotterdam the Netherlands (MEC20130-188). Cyst fluid was isolated from cysts of various sizes by needle aspiration. Aspirates with a turbid aspect due to bleeding or infection were not used. Samples were placed on ice immediately, passed through a 0.22 µm filter and stored at -80˚C until further processing. For immunostaining on ADPKD and ARPKD, kidney and liver and the age/gender matched normal controls, we obtained tissue slides from the Erasmus pathology biobank.

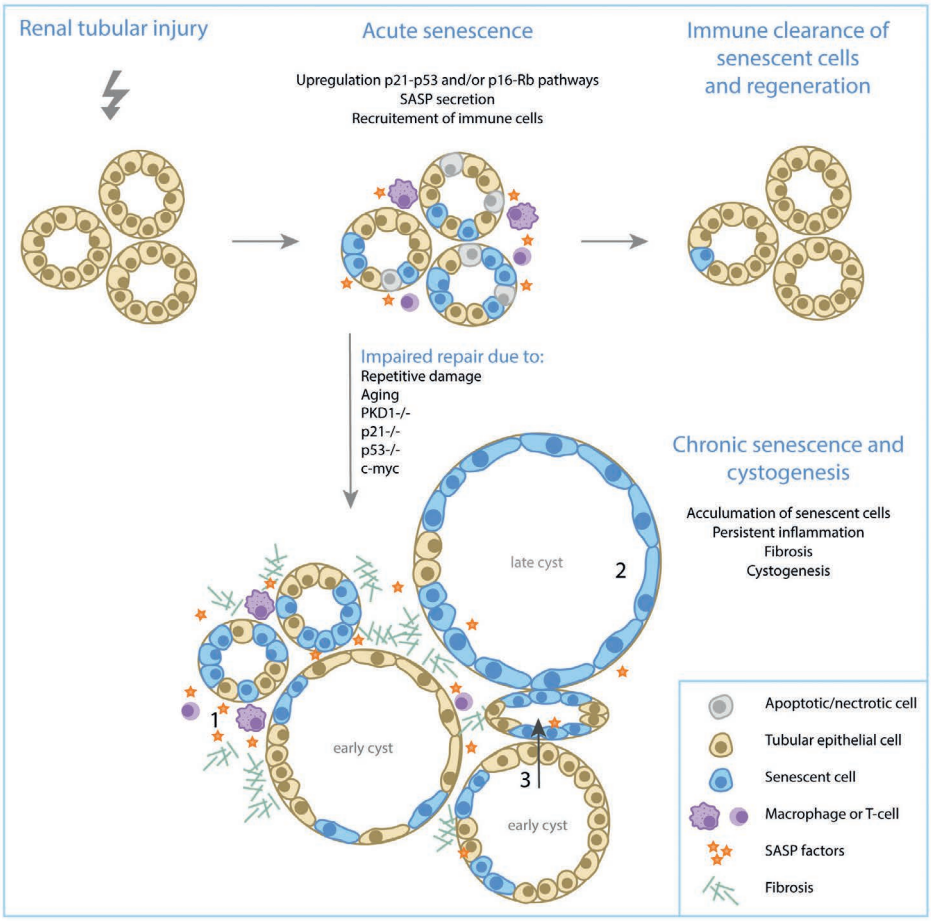

Figure 7 Model for causes & consequences of senescence in ADPKD
Schematic representation of hypothetical model on senescence in cystogenesis. 1) Persistent senescent cells promote cyst growth through SASP and attracts immune cells. 2) Cyst growth is inhibited with increasing cyst size due to replicative senescence. 3) Physical pressure of growing cysts induces senescence in neighboring stromal cells.

Human Adult Stem Cell Kidney Tubuloid Culture

ASC kidney tubuloids were cultured as described previously [54]. In short, cyst lining epithelial cells and control tubular fragments were isolated by collagenase digestion (C9407, Sigma) for 45 minutes at 1 mg/ml and seeded in growth factor-reduced Matrigel (Corning). Tubuloids were cultured in Advanced DMEM:F12, supplemented with 1% penicillin / streptomycin, HEPES, Glutamax, N-acetylcysteine (1 mM, Sigma) and 1.5% B27 supplement (Gibco)), supplemented with 10% Rspo1-conditioned medium[48] or 1% Rspo3-conditioned medium, the latter produced via the r-PEX protein expression platform (U-Protein Express), EGF (50 ng/ml, Peprotech), FGF-10 (100 ng/ml, Preprotech),

Rho-kinase inhibitor Y-27632 (10 µM, Abmole) A8301 (5 µM, Tocris Bioscience) and primocine (0.1 mg/ml, Invivogen).

Whole Exome Sequencing

After alignment and quality control, sequence reads originating from multiple lanes were merged using GATK PrintReads (v3.6.0) prior to further analysis. Sequence duplicates were marked using PicardTools (v1.129). Somatic variant calling was performed by Strelka2 (v2.8.3) using a matched-normal design with default exome settings. Variants were annotated with GENCODE annotations using ANNOVAR . Heuristic filtering removed variants which did not pass all standard Strelka2 post-calling filters, had fewer than 6 total reads or had an allelic frequency above 0,02% in the ExAC population . CONTROL-FREEC (v11.0) was used to detect somatic copy-number aberrations using the same matched normal scheme as previously described with default exome settings on SureSelect v5 target regions . Structural variants (>50bp) were detected by Illumina Manta (v1.1.0) using a tumour-only design with default exome settings and post-calling filters. Genomic data was visualized with the R statistical platform .

Analysis of Whole Exome Sequencing

After alignment and quality control, sequence reads originating from multiple lanes were merged using GATK PrintReads (v3.6.0) prior to further analysis [85.] Sequence duplicates were marked using PicardTools (v1.129).[86] Somatic variant calling was performed by Strelka2 (v2.8.3) using a matched-normal design with default exome settings [87]. Variants were annotated with GENCODE annotations using ANNOVAR [88,89]. Heuristic filtering removed variants which did not pass all standard Strelka2 post-calling filters, had fewer than 6 total reads or had an allelic frequency above 0,02% in the ExAC population [90]. CONTROL-FREEC (v11.0) was used to detect somatic copy-number aberrations using the same matched normal scheme as previously described with default exome settings on SureSelect v5 target regions [91]. Structural variants (>50bp) were detected by Illumina Manta (v1.1.0) using a tumor-only design with default exome settings and post-calling filters [92]. Genomic data was visualized with the R statistical platform .

RNA-sequencing

A strand-specific mRNA sequencing library was prepared for analysis according to the Illumina TruSeq stranded mRNA-seq protocol (www.illumina.com). Briefly, 200 ng of total RNA was purified using poly-T oligo-attached magnetic beads to end up with poly-A containing mRNA. This was fragmented and cDNA was synthesized using SuperScript II. cDNA fragments were A-tailed and paired-end adapters with dual indexes were ligated to the A-tailed cDNA fragments and purified using AMPure XP beads. The resulting adapter-modified cDNA fragments were enriched by 15 cycles of PCR. One microliter of library was assessed for concentration and quality on an Agilent Technologies 2100 Bioanalyzer using a DNA 1000 assay. The libraries were sequenced for single reads 50bp in length, on an Illumina HiSeq2500 system, using TruSeq Rapid v2 chemistry. At least 20M reads have

been generated per sample. Reads were aligned against the human reference genome (GRCh38) with hisat2 version 2.0.4.[95]. For scRNA-seq comparisons only genes were used with a minimum of 10 reads in the bulk RNA-seq and across all cells in the sc-RNA-seq experiments. The UMAP was generated in Seurat.

Analysis RNA-sequencing

IIllumina single-end reads of 51 bases were trimmed by removing the TrueSeq adapter sequences using Trimmomatic (v.0.33)[97]. Subsequently, the reads were mapped to the human reference genome build hg38 with the RNA-seq aligner STAR (v2.5.3a)[98] and the Homo sapiens GENCODE v26 annotation[89] and, in parallel, to build mm10 with GENCODE v25 annotation. Raw counts were summed with the summarizeOverlaps function with union mode from the Bioconductor Genomic Alignments package (v1.14.0). Samples are visualized using t-Distributed Stochastic Neighbor Embedding (t-SNE)[101] with a perplexity of 3 and a theta of 0.5. Genes were called differentially expressed with a generalized linear model using a negative binomial distribution and correcting for gender. DESeq2 (v1.16.1)[102] was used to perform these calculations. We applied a Wald-test to identify statistical significant differentially expressed genes. *P*-values were adjusted using Benjamini- Hochberg[103] correction and a threshold value was set to < 0.05. Counts were normalized with blind variance stabilizing log2 transformation function of DESeq2, and the differentially expressed genes were selected to calculate scaled gene-wise values (Z-score). The scaled values were clustered hierarchically with complete linkage using Euclidean distances and plotted in a heatmap with pheatmap package (v1.0.8). Gene Ontology (GO) and Kyoto Encyclopedia of Genes and Genomes (KEGG) gene enrichment analyses were carried out as described previously[104]. We used R(v 3.4.2)[93] for statistics and visualization of the data.

Quantitative Real Time PCR

Cells were lysed in Tri reagent (Sigma) for 5 minutes. After chloroform extraction, RNA was precipitated using isopropanol and washed with 75% ethanol. RNA was dissolved in 20 µl DepC treated H_20 and stored at -80^{o}C. To remove DNA, RNA samples were incubated with 1U DNase (Thermo Fisher Scientific) for 30 minutes at 37^{o}C. DNAse was stopped by incubating with EDTA (25 mM) at 65^{o}C for 10 minutes. random hexamers (stock 50 µM, final 5 µM, Thermo Fisher Scientific) and dNTPs (10 mM) were added and incubated 65^{o}C for 5 minutes. After denaturation, samples were placed on ice and RT-mix was added containing 5x first strand buffer, DTT (0.1 M) and RNase out (Thermo Fisher Scientific). Samples were incubated at 25^{o}C for 2 minutes. Next 200 U Superscript II was added (Thermo Fisher Scientific) and incubated for 10 minutes at 25^{o}C and 15 minutes at 70^{o}C. Samples were stored at -20^{o}C. Quantitative Real Time-PCR was performed in a 10 µl final reaction volume using Platinum Taq DNA polymerase (Life Technologies) and Sybr Green (Sigma Aldrich) in a CFX 384 Real Time system (BioRad). Expression levels were normalize to Actin/GAPDH. Primer sequences are listed in Supplemental methods Table 1.

Proliferation assay

RPTEC/hTERT1 cells were obtained from the American Type Culture Collection (ATCC), and cultured in DMEM:Ham'sF12 (1:1) media (Gibco life), supplemented with 100 U/ml penicillin-streptomycin, 100x Insulin-Transferrin-Selenium (ITS) (Thermo Fisher Scientific), 5 pM triiodo-L-thyronine (Sigma), 3.5 µg/ml ascorbic acid (Sigma), 10 ng/ml Recombinant human EGF (Peprotech), 25 ng/ml Prostaglandin E1 (Sigma), 25 ng/ml hydrocortisone (Sigma), 100 µg/ml G418 (Thermo Fisher Scientific). Medium was refreshed 2-3 times a week and cells were passaged by trypsinization when near confluence, inactivation of trypsin with Soybean Trypsin inhibitor (Sigma-Aldrich 10109886001). For the proliferation assay: RPTEC/hTERT1 cells were plated (500 cells/well) in an opaque-walled 96 wells plate (Greiner Bio-one 655088). Medium was supplemented with a final concentration of 10% cyst fluid or recombinant human protein (Sigma) of IL-6 , CXCL8 (IL-8), CXCL-1, or CXCL-5. Proliferation was measured indirectly by measuring ATP-levels on day 4 or 7 (for cyst fluid or SASP factors respectively) using a CellTiter-Glo assay (Promega). In brief, medium was replaced for fresh medium and plates were equilibrated to room temperature. Subsequently CellTiter-Glo-buffer (1:1) was added to the cells and plates were shaken for 2 minutes to ensure cell lysis. Plates were incubated for another 10 minutes on room temperature, after which luminescent signals were recorded. Mean and standard deviation were calculated from four biological replicates.

Immunofluorescence on human and mice tissue slides

Three ADPKD mouse models we used; *Pkd1*^{nl,nl} mice, with a hypomorphic *Pkd1* allele resulting in reduced *Pkd1* expression leading to cyst formation around birth onwards [56], a kidney specific inducible *Pkd1* knock out mouse with tamoxifen induction postnatally on day 18 (P18) or day 10 (P10), resulting in a mild or more severe progressive phenotype respectively [57]. Paraffin sections of 5 µm mouse kidney specimens were deparaffinized in Xylene, rehydrated in decreasing concentrations of ethanol and heated to 100^{o}C for 30 min in 10 mM sodium citrate buffer, pH 6, for antigen retrieval. After heating, the solution containing the slides was allowed to cool down at RT to 37^{o}C and the slides were subsequently processed as described below. Snapfrozen fresh human tissues were cryosectioned in 5 µm slices and air-dried at RT for 5 min after which the tissue sections were surrounded with a hydrophobic barrier using a barrier pen. The cryo or paraffin tissues were fixed with formalin for 30 min, subsequently, tissues were washed in Tris Buffered Saline (TBS) and permeabilized for 5 min in 0.2% Triton X-100 in TBS. To reduce background staining, the cells were blocked for 30min with 5% Normal Horse Serum (NHS) in a 50nM glycine and 0.2% gelatin-TBS solution. Subsequently, 50-300µl droplets (depending on size of tissue slice) containing primary antibody dilutions were spread over the tissues, which were placed in a dark moisture chamber and incubated overnight at 4^{o}C (primary antibodies: Lamin B1, 1:1000 (ab16048 Abcam); HMGB1, 1:500 (ab18256 Abcam)). The next day, slides were washed 3x 20min with 0,2% gelatin-TBS. Secondary antibody (1:1000 A-11034, A-21202 Invitrogen) incubation occurred as described for the primary antibody including a nuclear staining with Hoechst 1:1000 (565877 BD

Pharmingen) and the slides were incubated for one hour at room temperature. Following 2x 10min washes with 0,2% TBS-Gelatin, 1 wash with regular TBS and 1 dip in dH2O, the slides were mounted using soft set mounting medium (Vectashield) and sealed with nail polish. Spectral Imaging on paraffin sections was performed using lambda mode on a Zeiss LSM510 confocal microscope, within an emission spectrum of 460-560 nm. The spectral stack was linearly unmixed and assigned pseudocolors which allowed us to distinguish senescence markers from background signal. Fluorescently stained cryostat sections were imaged with a LSM510 confocal microscope. All images were processed and analysed with FIJI software. Lamin B1 or HMGB1 protein levels were quantified per nucleus in these tissues. When comparisons were made between images of the same experiment, all levels were adjusted equally and the ratio between the levels was not altered. To quantify this observation, we measured cyst diameter of 66 random cysts and related this to the percentage of Lamin B1 loss. By dividing all measured cysts in 3 equal groups containing small, medium or large cysts, we found an increase in percentage of senescent cells with increasing cyst size. To quantify the correlation between cyst size and the occurrence of senescent cells in the cyst epithelium this observation, we measured cyst diameter of 66 random cysts and related this to the percentage of Lamin B1 loss. By dividing all measured cysts in 3 equal groups containing small, medium or large cysts.

Mass spectrometry cyst fluid

Proteins were subjected to reduction with dithiothreitol, alkylation with iodoaceta¬mide and then in-solution digested with trypsin (sequencing grade; Promega). Proteolytic peptides were collected, washed and subsequently fractionated by HILIC chromatography into six fractions per sample and each fraction was analyzed by liquid chromatography tandem mass spectrometry (nLC-MS/MS) performed on an EASY-nLC coupled to an Orbitrap Fusion Lumos Tribid mass spectrometer (Thermo) oper¬ating in positive mode. Peptides were separated on a ReproSil-C18 reversed-phase column (Dr Maisch; 15 cm × 50 µm) using a linear gradient of 0–80% acetonitrile (in 0.1% formic acid) during 90 min at a rate of 200 nl/min. The elution was directly sprayed into the electrospray ionization (ESI) source of the mass spectrometer. Spectra were acquired in continuum mode; fragmentation of the peptides was performed in data-dependent mode by HCD. Raw mass spectrometry data were analyzed with the MaxQuant software suite [105] version 1.6.2.6 with the additional options 'LFQ' and 'iBAQ' selected. The Andromeda search engine was used to search the MS/MS spectra against the Uniprot database (taxonomy: Homo sapiens, release: May 2018) concatenated with the reversed versions of all sequences. A maximum of two missed cleavages was allowed. The peptide tolerance was set to 10 ppm and the fragment ion tolerance was set to 0.6 Da for HCD spectra. The enzyme specificity was set to trypsin and cysteine carbamidomethylation was set as a fixed modification. Both the PSM and protein FDR were set to 0.01. In case the identified peptides of two proteins were the same or the identified peptides of one protein included all peptides of another protein, these proteins were combined by

MaxQuant and reported as one protein group. Before further statistical analysis, known contaminants and reverse hits were removed.

Cytokine multiplex assay/ ELISA

A Milliplex cytokine/chemokine immunoassay (Merck Millipore, Billerica, MA, United States) was used for the measurement of interferon-γ (IFN-γ), interleukin-6 (IL-6), chemokine (C-C motif) ligand 5 (CCL5), and tumor necrosis factor-α (TNF-α).

Data accessibility

The RNA-sequencing data from this study have been submitted to the Gene Expression Omnibus (GEO)[106] database under the accession number PRJNA636003, reviewer link: https://dataview.ncbi.nlm.nih.gov/object/PRJNA636003?reviewer=ravv58lrfcupf15ijtipii6u53.

Acknowledgements

We thank S.P. Arshad and PHJ Riegman for their help on obtaining tissue samples from the pathology biobank. Adriaan Houtsmuller and Gert-Jan Kremers of the Erasmus MC optical imaging centre (OIC) for their valuable technical and tutorial support on confocal imaging and spectral unmixing. A.K. is supported by grants from the Netherlands Organisation for Scientific Research (NWO 022.004.002.) and the Dutch Kidney Foundation (KBAO1205). H.v.W. is supported by a grant from the Dutch Kidney Foundation (15OP11). R.W.F.d.B., P.L.J.d.K, M.C.V., R.Z., M.B.R., and E.J.H. are also supported by the Dutch Kidney Foundation (CP1805).

Disclosures

None.

REFERENCES

1. Willey, C. J. et al. Prevalence of autosomal dominant polycystic kidney disease in the European Union. Nephrol Dial Transpl. 1356–1363 (2017). doi:10.1093/ndt/gfw240
2. Lanktree, M. B. et al. Prevalence Estimates of Polycystic Kidney and Liver Disease by Population Sequencing. JASN 1–8 (2018). doi:10.1681/ASN.2018050493
3. Spithoven, E. M. et al. Renal replacement therapy for autosomal dominant polycystic kidney disease (ADPKD) in Europe: prevalence and survival--an analysis of data from the ERA-EDTA Registry. Nephrol. Dial. Transplant. 29, iv15-iv25 (2014).
4. Cornec-Le Gall, E., Torres, V. E. & Harris, P. C. Genetic complexity of autosomal dominant polycystic kidney and liver diseases. J. Am. Soc. Nephrol. 29, 13–23 (2018).
5. Consortium, T. E. P. K. D. The polycystic kidney disease 1 gene encodes a 14 kb transcript and lies within a duplicated region on chromosome 16. The European Polycystic Kidney Disease Consortium. Cell 77, 881–94 (1994).
6. Mochizuki, T. et al. PKD2, a gene for polycystic kidney disease that encodes an integral membrane protein. Science 272, 1339–1342 (1996).
7. Chapin, H. C. & Caplan, M. J. The cell biology of polycystic kidney disease. 191, 701–710 (2010).
8. Harris, P. C. & Torres, V. E. Review series Genetic mechanisms and signaling pathways in autosomal dominant polycystic kidney disease. 124, 2315–2324 (2014).
9. Ong, A. C. M. & Harris, P. C. A polycystin-centric view of cyst formation and disease : the polycystins revisited. Kidney Int. 88, 699–710 (2015).
10. Thivierge, C. et al. Overexpression of PKD1 Causes Polycystic Kidney Disease Overexpression of PKD1 Causes Polycystic Kidney Disease. 26, 1538–1548 (2006).
11. Kurbegovic, A. et al. Pkd1 transgenic mice: Adult model of polycystic kidney disease with extrarenal and renal phenotypes. Hum. Mol. Genet. 19, 1174–1189 (2010).
12. Qian, F., Watnick, T. J., Onuchic, L. F. & Germino, G. G. The molecular basis of focal cyst formation in human autosomal dominant polycystic kidney disease type I. Cell 87, 979–987 (1996).
13. Brasier, J. L. & Henske, E. P. Loss of the polycystic kidney disease (PKD1) region of chromosome 16p13 in renal cyst cells supports a loss-of-function model for cyst pathogenesis. J. Clin. Invest. 99, 194–199 (1997).
14. Watnick, T. J. et al. Somatic mutation in individual liver cysts supports a two-hit model of cystogenesis in autosomal dominant polycystic kidney disease. Mol. Cell 2, 247–251 (1998).
15. Wu, G. et al. Somatic inactivation of Pkd2 results in polycystic kidney disease. Cell 93, 177–188 (1998).
16. Torra, R. et al. A loss-of-function model for cystogenesis in human autosomal dominant polycystic kidney disease type 2. Am. J. Hum. Genet. 65, 345–352 (1999).
17. Geng, L. et al. Distribution and developmentally regulated expression of murine polycystin. Am. J. Physiol. - Ren. Physiol. 272, (1997).
18. Chauvet, V. et al. Expression of PKD1 and PKD2 transcripts and proteins in human embryo and during normal kidney development. Am. J. Pathol. 160, 973–983 (2002).
19. Le Corre, S. et al. Cystic gene dosage influences kidney lesions after nephron reduction. Nephron 129, 42–51 (2015).
20. Piontek, K., Menezes, L. F., Garcia-Gonzalez, M. a, Huso, D. L. & Germino, G. G. A critical developmental switch defines the kinetics of kidney cyst formation after loss of Pkd1. Nat Med 13, 1490–1495 (2007).
21. Lantinga-van leeuwen, I. S. et al. Kidney-specific inactivation of the Pkd1 gene induces rapid cyst formation in developing kidneys and a slow onset of disease in adult mice. Hum. Mol. Genet. 16, 3188–3196 (2007).

22. Patel, V. et al. Acute kidney injury and aberrant planar cell polarity induce cyst formation in mice lacking renal cilia. Hum. Mol. Genet. 17, 1578–1590 (2008).
23. Takakura, A. et al. Renal injury is a third hit promoting rapid development of adult polycystic kidney disease. Hum. Mol. Genet. 18, 2523–2531 (2009).
24. Happé, H. et al. Toxic tubular injury in kidneys from Pkd1-deletion mice accelerates cystogenesis accompanied by dysregulated planar cell polarity and canonical Wnt signaling pathways. Hum. Mol. Genet. 18, 2532–2542 (2009).
25. Bastos, A. P. et al. Pkd1 haploinsufficiency increases renal damage and induces microcyst formation following ischemia/reperfusion. J. Am. Soc. Nephrol. 20, 2389–2402 (2009).
26. Le Corre, S. et al. Cystic gene dosage influences kidney lesions after nephron reduction. Nephron 129, 42–51 (2015).
27. Dobyan DC, Hill D, Lewis T, B. R. Cyst formation in rat kidney induced by cis-platinum administration. Lab Invest 45, 260–8 (1981).
28. Judit Kovác, Mónika Zilahy, Tamás Bányász, S. G. Evaluation of apoptosis and cell proliferation in experimentally induced renal cysts. Urol. Res. 26, 411–416 (1998).
29. Kurbegovic, A. & Trudel, M. Acute kidney injury induces hallmarks of polycystic kidney disease. Am. J. Physiol. Renal Physiol. ajprenal.00167.2016 (2016). doi:10.1152/ajprenal.00167.2016
30. Grantham, J. J. Acquired Cystic Kidney Disease. jKidney Int. 40, 143–152 (1991).
31. Ishikawa, I. Uremic Acquired Cystic Disease of the Kidney. Urology XXVI, 101–108 (1985).
32. Matson, A and Cohen, E. Acquired Cystic Kidney Disease: Occurrence, Prevalence, and Renal Cancers. Medicine (Baltimore).
33. Meola, M., Samoni, S. & Petrucci, I. Clinical Scenarios in Chronic Kidney Disease: Kidneys' Structural Changes in End-Stage Renal Disease. Contrib. Nephrol. 188, 131–143 (2016).
34. Denic, A., Glassock, R. J. & Rule, A. D. Structural and Functional Changes With the Aging Kidney. Adv. Chronic Kidney Dis. 23, 19–28 (2016).
35. Denic, A., Glassock, R. J. & Rule, A. D. Structural and functional changes with the aging kidney. Adv Chronic Kidney Dis. 23, 19–28 (2016).
36. Muñoz-Espín, D. & Serrano, M. Cellular senescence: From physiology to pathology. Nat. Rev. Mol. Cell Biol. 15, 482–496 (2014).
37. Coppé, J.-P. et al. Senescence-Associated Secretory Phenotypes Reveal Cell-Nonautonomous Functions of Oncogenic RAS and the p53 Tumor Suppressor. PLoS Biol. 6, e301 (2008).
38. Campisi, J. & Robert, L. Cell senescence: Role in aging and age-related diseases. Aging Facts Theor. 39, 45–61 (2014).
39. Coppé, J.-P., Desprez, P.-Y., Krtolica, A. & Campisi, J. The Senescence-Associated Secretory Phenotype: The Dark Side of Tumor Suppression. Annu. Rev. Pathol. Mech. Dis. 5, 99–118 (2010).
40. Campisi, J. & D'Adda Di Fagagna, F. Cellular senescence: When bad things happen to good cells. Nat. Rev. Mol. Cell Biol. 8, 729–740 (2007).
41. Sagiv, A. & Krizhanovsky, V. Immunosurveillance of senescent cells: The bright side of the senescence program. Biogerontology 14, 617–628 (2013).
42. Childs, B. G., Durik, M., Baker, D. J. & Deursen, J. M. Van. Cellular senescence in aging and age-related disease : from mechanisms to therapy. Nat. Genet. 21, 1424–1435 (2015).
43. Demaria, M. et al. Article An Essential Role for Senescent Cells in Optimal Wound Healing through Secretion of PDGF-AA. 722–733 (2014). doi:10.1016/j.devcel.2014.11.012
44. Muñoz-Espín, D. et al. Programmed cell senescence during mammalian embryonic development. Cell 155, 1104 (2013).
45. Pereira, B. I. et al. Senescent cells evade immune clearance via HLA-E-mediated NK and CD8+ T cell inhibition. Nat. Commun. 10, (2019).
46. Van Deursen, J. M. The role of senescent cells in ageing. Nature 509, 439–446 (2014).
47. Franceschi, C. & Campisi, J. Chronic inflammation (Inflammaging) and its potential contribution to age-associated diseases. Journals Gerontol. - Ser. A Biol. Sci. Med. Sci. 69, S4–S9 (2014).

48. Sturmlechner, I., Durik, M., Sieben, C. J., Baker, D. J. & van Deursen, J. M. Cellular senescence in renal ageing and disease. Nat. Rev. Nephrol. 13, 77–89 (2017).
49. van Willigenburg, H., de Keizer, P. L. J. & de Bruin, R. W. F. Cellular senescence as a therapeutic target to improve renal transplantation outcome. Pharmacol. Res. 130, 322–330 (2018).
50. Valentijn, F. A., Falke, L. L., Nguyen, T. Q. & Goldschmeding, R. Cellular senescence in the aging and diseased kidney. 69–82 (2018).
51. Darren J. Baker, Bennett G. Childs, Matej Durik, Melinde E. Wijers, Cynthia J. Sieben, Jian Zhong, Rachel Saltness, Karthik B. Jeganathan, Grace C. Versoza, Abdul- Mohammad Pezeshki, Khashayarsha Khazaie, Jordan D. Miller, and J. M. van D. Naturally occurring p16Ink4a -positive cells shorten healthy lifespan. 530, 184–189 (2016).
52. Marjolein P. Baar, Renata M.C. Brandt, Diana A. Putavet, Julian D.D. Klein, Kasper W.J. Derks, Benjamin R. M. Bourgeois, Sarah Stryeck, Yvonne Rijksen, Hester van Willigenburg, Danny A. Feijtel, Ingrid van der Pluijm, Jeroen Essers, Wiggert A. van Cappell, and P. L. J. de K. Targeted Apoptosis of Senescent Cells Restores Tissue Homeostasis in Response to Chemotoxicity and Aging Marjolein. Cell 169, 132–147 (2018).
53. Clevers, H. Modeling Development and Disease with Tubuloids. Cell 165, 1586–1597 (2016).
54. Schutgens F, Rookmaaker MB, Margaritis T, Rios A, Ammerlaan C, Jansen J, Gijzen L, Vormann M, Vonk A, Viveen M, Yengej FY, Derakhshan S, de Winter-de Groot KM, Artegiani B, van Boxtel R, Cuppen E, Hendrickx APA, van den Heuvel-Eibrink MM, Heitzer E, Lanz, C. H. Tubuloids derived from human adult kidney and urine for personalized disease modeling. Nat. Biotechnol. 303–313 (2019).
55. Autosomal Dominant Polycystic Kidney Disease Mutation Database: PKDB. http://pkdb.mayo.edu/ at <http://pkdb.mayo.edu/>
56. Happé, H. et al. Cyst expansion and regression in a mouse model of polycystic kidney disease. Kidney Int. 83, 1099–1108 (2013).
57. Leonhard, W. N., Happe, H. & Peters, D. J. M. Variable Cyst Development in Autosomal Dominant Polycystic Kidney Disease : The Biologic Context. jasn 3530–3538 (2016). doi:10.1681/ASN.2016040425
58. Dreesen, O., Chojnowski, A., Ong, P. F., Wang, A. S. & Clavel, C. Loss of lamin B1 is a biomarker to quantify cellular senescence in photoaged skin. Sci. Rep. 7, 1–8 (2017).
59. Davalos, A. R. et al. p53-dependent release of Alarmin HMGB1 is a central mediator of senescent phenotypes. J. Cell Biol. 201, 613–629 (2013).
60. Wieser, M. et al. hTERT alone immortalizes epithelial cells of renal proximal tubules without changing their functional characteristics. Am J Physiol Ren. Physiol 295, F1365-75 (2008).
61. Prasad, S., McDaid, J. P., Tam, F. W. K., Haylor, J. L. & Ong, A. C. M. Pkd2 dosage influences cellular repair responses following ischemia-reperfusion injury. Am. J. Pathol. 175, 1493–1503 (2009).
62. Jin, H. et al. Epithelial innate immunity mediates tubular cell senescence after kidney injury Find the latest version : Epithelial innate immunity mediates tubular cell senescence after kidney injury. 4, (2019).
63. Docherty, M. H., O'Sullivan, E. D., Bonventre, J. V. & Ferenbach, D. A. Cellular senescence in the kidney. J. Am. Soc. Nephrol. 30, 726–736 (2019).
64. Megyesi, J., Andrade, L., Vieira, J. M., Safirstein, R. L. & Price, P. M. Positive effect of the induction of p21WAF1/CIP1 on the course of ischemic acute renal failure. Kidney Int. 60, 2164–2172 (2001).
65. Megyesi, J. et al. Coordination of the cell cycle is an important determinant of the syndrome of acute renal failure. Am J Physiol Ren. Physiol (2002).
66. Nishioka, S. et al. The cyclin-dependent kinase inhibitor p21 is essential for the beneficial effects of renal ischemic preconditioning on renal ischemia / reperfusion injury in mice. Kidney Int. 85, 871–879 (2013).

67. Sutton, T. A. et al. p53 Is Renoprotective after Ischemic Kidney Injury by Reducing In fl amation. JASN 113–124 (2013). doi:10.1681/ASN.2012050469
68. Tang, C. et al. P53 in kidney injury and repair : Mechanism and therapeutic potentials. Pharmacol. Ther. (2018). doi:10.1016/j.pharmthera.2018.10.013
69. Bhunia, A. K. et al. PKD1 induces p21waf1 and regulation of the cell cycle via direct activation of the JAK-STAT signaling pathway in a process requiring PKD2. Cell 109, 157–168 (2002).
70. Park, J. et al. p21 is decreased in polycystic kidney disease and leads to increased epithelial cell cycle progression : roscovitine augments p21 levels. 11, 1–11 (2007).
71. Li, X. & Trudel, M. Polycystic Kidney Disease.
72. Seoane, J., Le, H. Van & Massagué, J. Myc suppression of the p21Cip1 Cdk inhibitor influences the outcome of the p53 response to DNA damage. Nature 419, 729–734 (2002).
73. Shen, Y. et al. c-Myc promotes renal fibrosis by inducing integrin αv-mediated transforming growth factor-β signaling. Kidney Int. 92, 888–899 (2017).
74. Leonhard, W. N. et al. Scattered Deletion of PKD1 in Kidneys Causes a Cystic Snowball Effect and Recapitulates Polycystic Kidney Disease. J Am Soc Nephrol 26, 1322–1333 (2015).
75. Kim, K., Won, J. H., Cheng, N. & Lau, L. F. The matricellular protein CCN1 in tissue injury repair. 273–279 (2018).
76. Gardner, K. D., Burnside, J. S., Elzinga, L. W. & Locksley, R. M. Cytokines in fluids from polycystic kidneys. 39, 718–724 (1991).
77. Nichols, M. T. et al. Secretion of cytokines and growth factors into autosomal dominant polycystic kidney disease liver cyst fluid. Hepatology 40, 836–846 (2004).
78. Lai, X. et al. Characterization of the renal cyst fluid proteome in autosomal dominant polycystic kidney disease (ADPKD) patients. Proteomics Clin Appl . 2, 1140–1152 (2008).
79. Lai, X., Blazer-Yost, B. L., Gattone, V. H., Muchatuta, M. N. & Witzmann, F. a. Protein composition of liver cyst fluid from the BALB/c-cpk/+ mouse model of autosomal recessive polycystic kidney disease. Proteomics 9, 3775–3782 (2009).
80. Mason, S. B. et al. The biomarker enriched proteome of autosomal dominant polycystic kidney disease. Proteomics Clin. Appli 3, 1247–1250 (2009).
81. Tsunoda, T. et al. Loss of Fibrocystin Promotes Interleukin-8-Dependent Proliferation and CTGF Production of Biliary Epithelium. Journal of Hepatology (European Association for the Study of the Liver, 2019). doi:10.1016/j.jhep.2019.02.024
82. Ellis, S., Lin, E. J. & Tartar, D. Immunology of Wound Healing. Curr. Dermatol. Rep. 350–358 (2018).
83. Lee, E. U. N. J. I. et al. Blockade of interleukin-8 receptor signalling inhibits cyst development in vitro , via suppression of cell proliferation in autosomal polycystic kidney disease Correspondence : ABSTRACT : Aim : Autosomal dominant polycystic kidney disease (ADPKD) is a h. Nephrology 19, 471–478 (2014).
84. Li, H. Aligning sequence reads, clone sequences and assembly contigs with BWA-MEM. 0, 1–3 (2013).
85. McKenna, A. et al. The genome analysis toolkit: A MapReduce framework for analyzing next-generation DNA sequencing data. Genome Res. 20, 1297–1303 (2010).
86. Broad Institute. Picard tools. https://broadinstitute.github.io/picard/ (2016).
87. Kim, S. et al. Strelka2: Fast and accurate variant calling for clinical sequencing applications. doi.org 192872 (2017). doi:10.1101/192872
88. Wang, K., Li, M. & Hakonarson, H. ANNOVAR: functional annotation of genetic variants from high-throughput sequencing data. Nucleic Acids Res. 38, e164 (2010).
89. Harrow, J. et al. GENCODE: The reference human genome annotation for the ENCODE project. Genome Res. 22, 1760–1774 (2012).
90. Lek, M. et al. Analysis of protein-coding genetic variation in 60,706 humans. Nature 536, 285–291 (2016).

91. Boeva, V. et al. Control-FREEC: a tool for assessing copy number and allelic content using next-generation sequencing data. Bioinformatics 28, 423–5 (2012).
92. Chen, X. et al. Manta: Rapid detection of structural variants and indels for germline and cancer sequencing applications. Bioinformatics 32, 1220–1222 (2016).
93. RCore Team. R. A language and environment for statistical computing. R Foundation for Statistical, Computing, Vienna, Austria. (The R Foundation for Statistical Computing., 2013). doi:10.1007/978-3-540-74686-7
94. Zhang, H., Meltzer, P. & Davis, S. RCircos: an R package for Circos 2D track plots. BMC Bioinformatics 14, 244 (2013).
95. Kim, D., Langmead, B. & Salzberg, S. L. HISAT: a fast spliced aligner with low memory requirements. 12, 357–360 (2016).
96. Anders, S., Pyl, P. T. & Huber, W. HTSeq-A Python framework to work with high-throughput sequencing data. Bioinformatics 31, 166–169 (2015).
97. Bolger, A. M., Lohse, M. & Usadel, B. Trimmomatic: A flexible trimmer for Illumina sequence data. Bioinformatics 30, 2114–2120 (2014).
98. Dobin, A. et al. STAR: Ultrafast universal RNA-seq aligner. Bioinformatics 29, 15–21 (2013).
99. Ahdesmäki, M. J., Gray, S. R., Johnson, J. H. & Lai, Z. Disambiguate: An open-source application for disambiguating two species in next generation sequencing data from grafted samples. F1000Research 5, 2741 (2016).
100. Liao, Y., Smyth, G. K. & Shi, W. FeatureCounts: An efficient general purpose program for assigning sequence reads to genomic features. Bioinformatics 30, 923–930 (2014).
101. Maaten, L. Van Der & Hinton, G. Visualizing Data using t-SNE. J. Mach. Learn. Res. 9, 2579–2605 (2008).
102. Love, M. I., Huber, W. & Anders, S. Moderated estimation of fold change and dispersion for RNA-seq data with DESeq2. Genome Biol. 15, 1–21 (2014).
103. Benjamini, Y. & Hochberg, Y. Controlling the False Discovery Rate : A Practical and Powerful Approach to Multiple Testing Author (s): Yoav Benjamini and Yosef Hochberg Source : Journal of the Royal Statistical Society . Series B (Methodological), Vol . 57 , No . 1 Published by : Soc. R. Stat. 57, 289–300 (1995).
104. Meinders, M., Kulu, D. I. & Werken, H. J. G. Van De. Sp1 / Sp3 transcription factors regulate hallmarks of megakaryocyte maturation , and platelet. 125, 1957–1968 (2015).
105. Cox, J. et al. PROTOCOL A practical guide to the MaxQuant computational platform for SILAC-based quantitative proteomics. Nat. Protoc. (2009). doi:10.1038/nprot.2009.36
106. Edgar, R. Gene Expression Omnibus: NCBI gene expression and hybridization array data repository. Nucleic Acids Res. 30, 207–210 (2002).
107. Liao, J et al. Single-cell RNA sequencing of human kidney. Sci Data. doi: 10.1038/s41597-019-0351-8. (2020).

SUPPLEMENTAL FIGURES

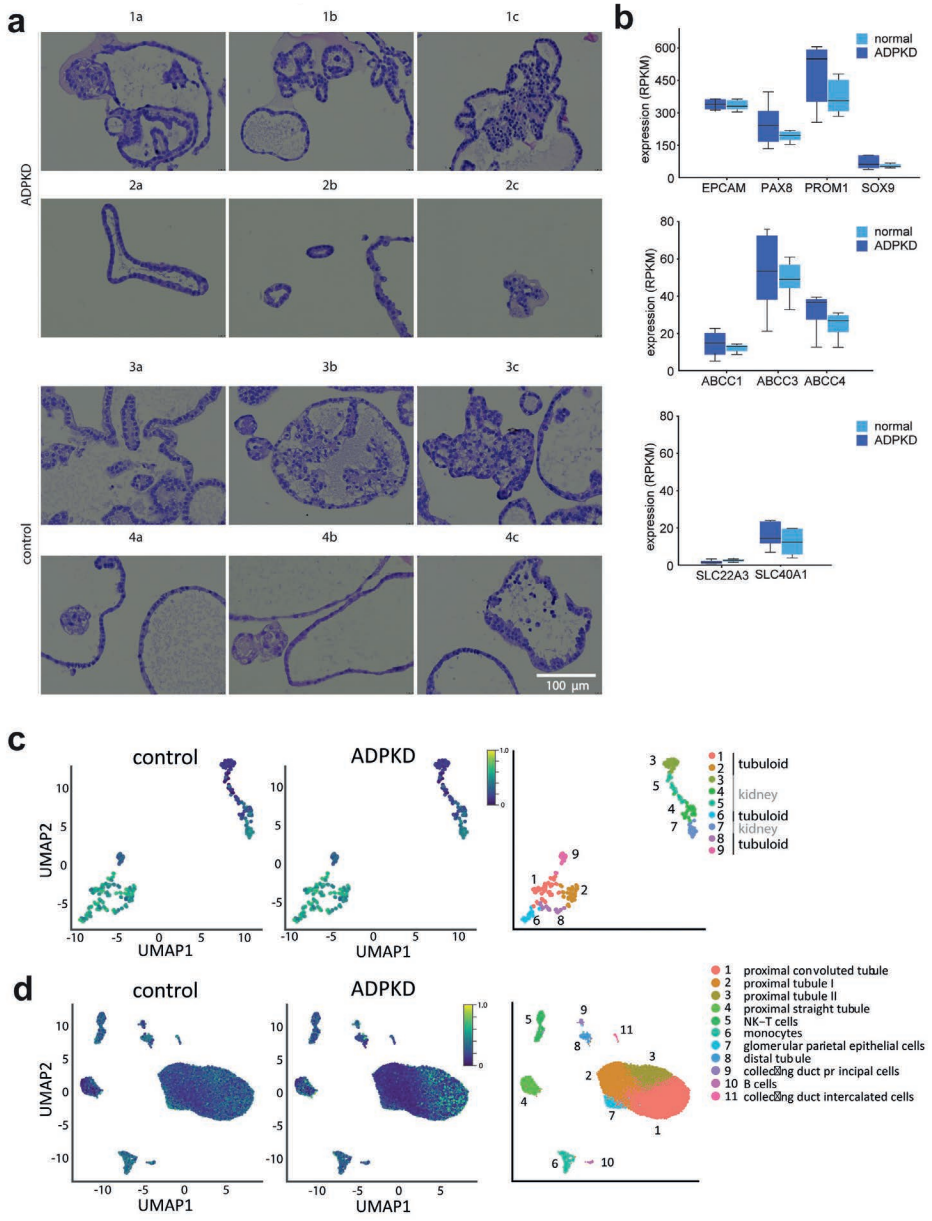

Supplemental Figure 1 Histology PKD and normal kidney tubuloids
(a) Hematoxylin and Eosin (H&E) staining of PKD and normal tubuloids. **(b)** RNA-seq expression analysis of proximal tubule markers in control and ADPKD tubuloids. **(c-d)** Correlation analysis of bulk RNA-seq data obtained from control and ADPKD tubuloids with previous published single cell sequencing data sets **(c,d)** [54, 107]. Shown is the Pearson correlation between the average bulk RNA-seq data with the RNA profile of single cells.

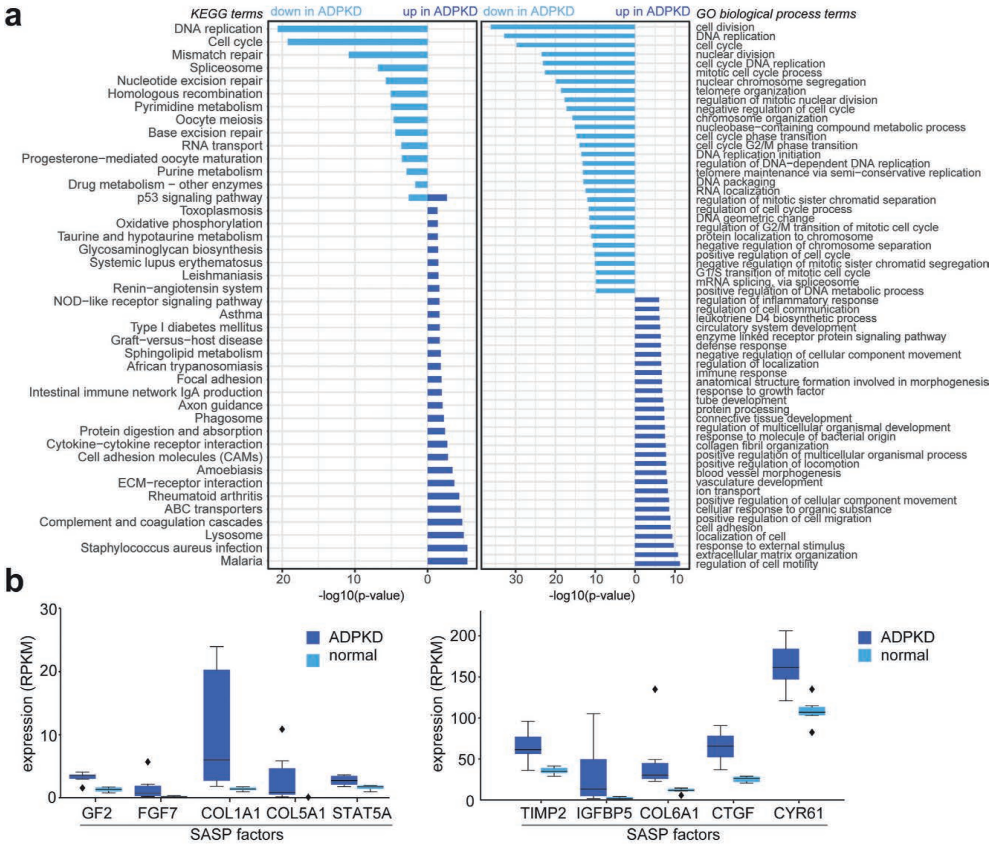

Supplemental Figure 2 Pathway analysis and differentially expressed genes in ADPKD tubuloids

(a) Gene Set Enrichment analysis of GO and KEGG Pathways of differentially expressed genes. **(b)** RNA-seq data indicates that several SASP factors are significantly upregulated in ADPKD tubuloids (adjusted *p-value* < 0.01).

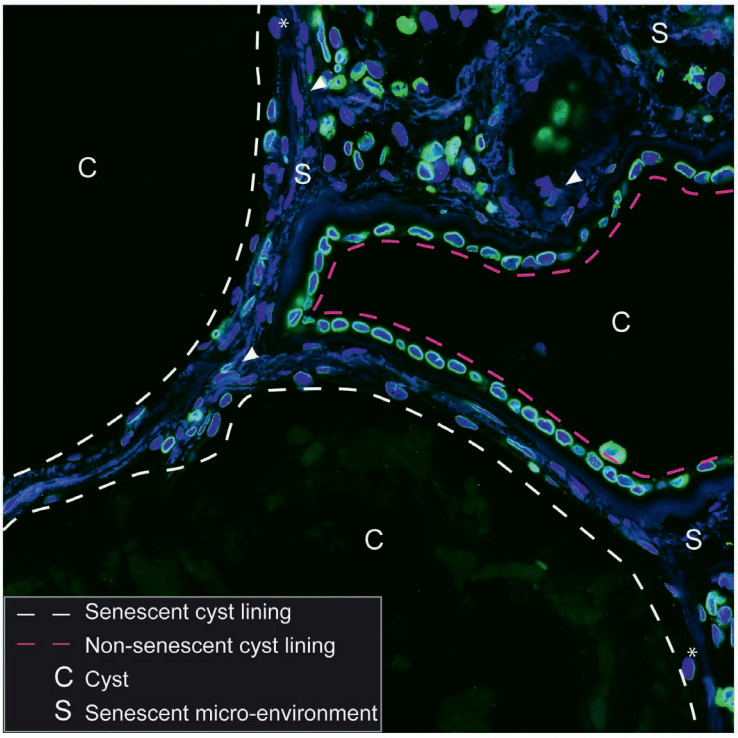

Supplemental Figure 3 Localization of senescent cells in human ADPKD tissue
Representative image of human kidney tissue from ADPKD patient stained for Lamin B1 (green) with a nuclear counterstain (blue). Loss of Lamin B1, indicating senescence, is found both in cells lining cyst epithelium (indicated with white striped lines) and in cells surrounding cysts (indicated with arrowhead).

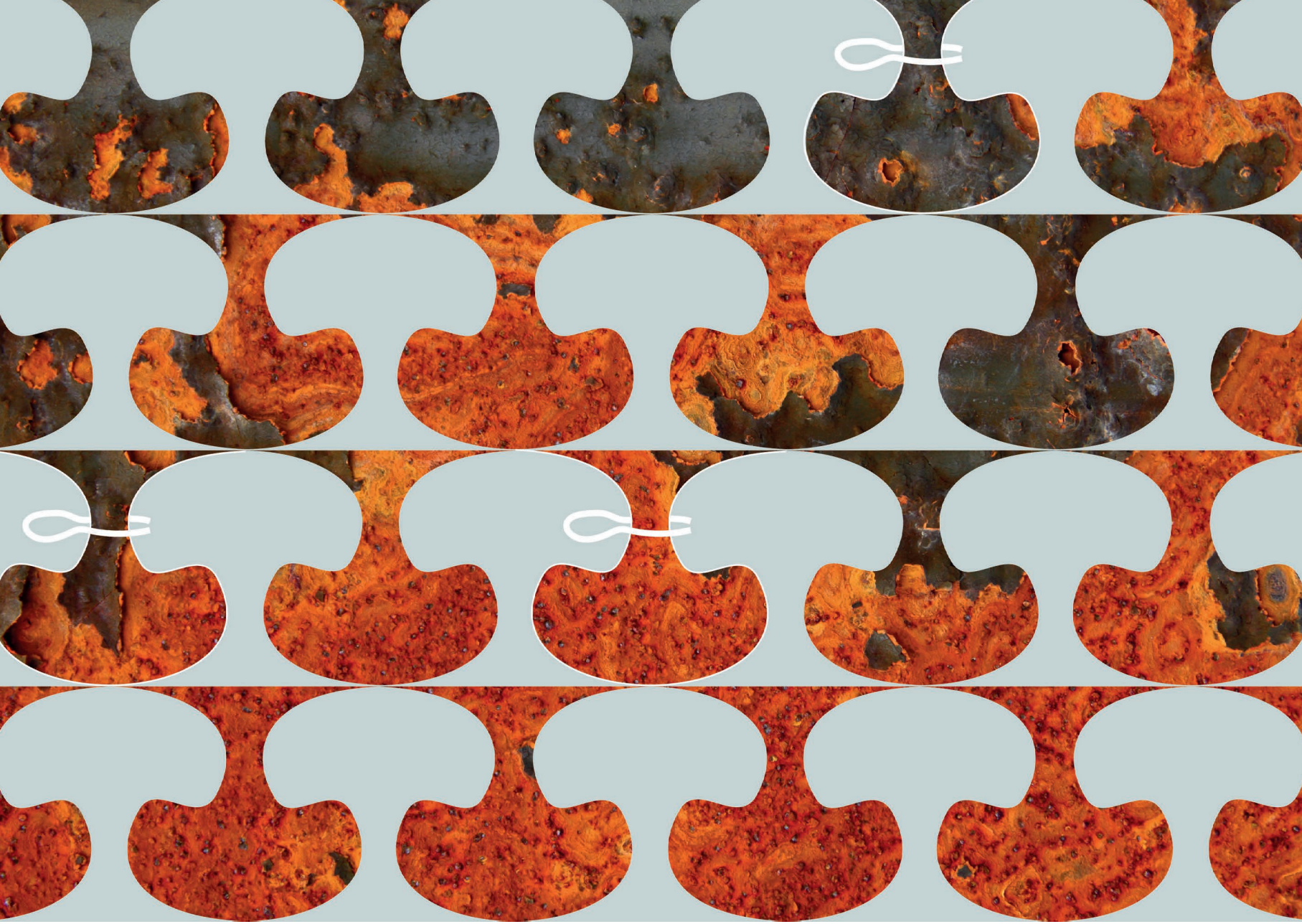

Chapter 3

Elimination of senescent cells improves the recovery of aged kidneys upon acute injury in mice

Hester van Willigenburg[1,2]* , Gisela Ambagtsheer[1], Jan N.M. IJzermans[1], Peter L.J. de Keizer[2,3], Ron W.F. de Bruin[1]

[1] Department of Surgery, Erasmus MC Transplant Institute Rotterdam, Rotterdam, The Netherlands, [2] Department of Molecular Genetics, Erasmus MC, University Medical Centre Rotterdam, Rotterdam, The Netherlands, [3] Center for Molecular Medicine, division dLAB, University Medical Center Utrecht, Utrecht, the Netherlands

Submitted for publication

Graphical Abstract

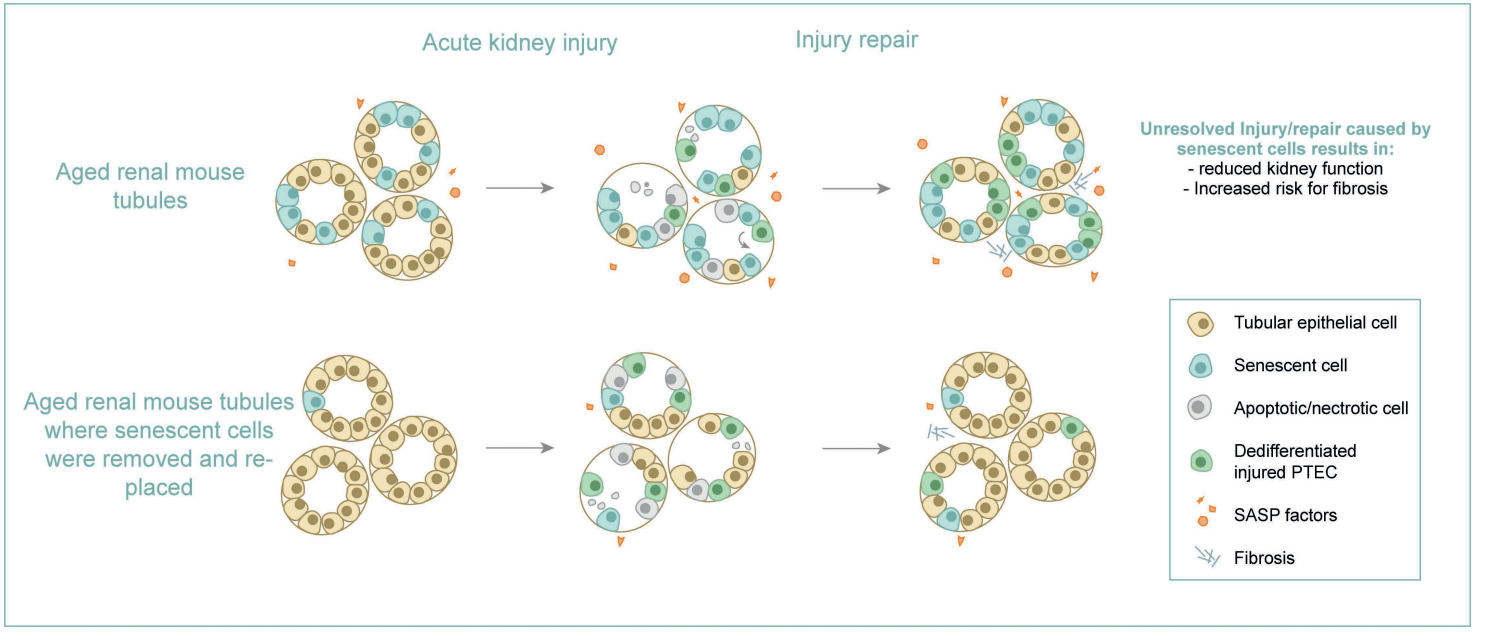

Elimination of senescent cells improves the recovery of aged kidneys upon acute injury

The presence of senescent cells impairs the tissue regeneration of the aged injured kidney, resulting in unresolved injury and reduced kidney function. The removal of senescent cells before the induction of AKI improves regeneration of the kidney, which results in improved renal function. SASP: senescence associated secretory phenotype.

ABSTRACT

Aged kidneys are more vulnerable to acute injury, which makes them less suitable for renal transplantation. However, due to the persistent shortage of donor organs, aged kidneys are increasingly being used as donor organs. This results in reduced long-term function and higher rejection rates after transplantation. Aging of the kidney is characterized by an increase in the number of senescent cells. These cells reduce renal function and promote a chronic pro-inflammatory state. Therefore, we set out to determine whether removing senescent cells in aged mice can improve resistance to acute kidney injury (AKI). To do so, senescent cells were removed 28 days before induction of bilateral renal ischemia-reperfusion injury (IRI) to induce AKI. We made use of a progeroid XpdTTD mouse model of accelerated aging and combined this genetic background with a p16::3MR transgene (encoded by the Cdkn2a promoter). Injecting these mice with ganciclovir lowered the numbers of senescent cells. In this study we show that, comparable to human aged kidneys, the XpdTTD mouse is more vulnerable to AKI. This was met with a strong trend towards improved damage repair based on NGAL and Sox9 expression and, importantly, a marked reduction in immediate and long-term (28d) renal damage as measured through plasma urea levels. Thus, ablation of senescent cells is beneficial for maintaining renal filtering capacity after IRI. These results argue that therapeutic targeting of senescence can be beneficial during clinical interventions where AKI is a common side effect, such as during kid-ney transplantation.

Keywords: Aging, senescence, SASP, acute kidney injury (AKI), ischemia reperfusion injury (IRI), p16::3MR, transplantation

INTRODUCTION

With an estimated worldwide all-age prevalence of 10%, chronic kidney disease (CKD) is a major burden on society[1,2]. Together with diabetes, hypertension and kidney diseases, acute kidney injury (AKI) is an important causal factor for the development of CKD[1,3]. Acute kidney injury is an abrupt decline in glomerular filtration rate (GFR), and includes a form of structural injury which results in reduced renal filtering capacity and elevated levels of serum creatinine and blood urea nitrogen[4]. Although complete recovery from AKI is possible, impaired repair following AKI may lead to permanent damage, including progressive fibrosis and CKD[3]. The incidence of AKI is considerably higher in the elderly (>65 years), which has been attributed to the general decline of renal capacity in the elderly and co-morbidities, such as hypertension and heart disease[5]. Additionally, there is an increased risk for progression towards CKD after AKI in aged patients[6]. With the increasing rise in age of the general population, and the increased risk of elderly towards AKI and CKD, it is meaningful to study the effect of aging on vulnerability to AKI.

At the cellular level, aging of the kidney is characterized by increases in the numbers of damaged cells that are locked in permanent cell cycle arrest – also known as senescent cells [7]. Senescence can be induced by processes that cause excessive cell damage, which activate the p53-p21 and/or the p16-Rb pathways [8–10]. A subset of senescent cells adopt a secretory phenotype known as the senescence-associated secretory phenotype (SASP), and secrete a wide variety of active compounds with which they can impair the homeostasis of neighbouring cells [11,12], and even cells in distant environments[13].

The secreted SASP factors differ per senescent cell type, mode of senescence induction and also over time[9]. Especially the latter has a great influence on the effect senescent cells assert, and therefore a distinction is made between acute and chronic senescence[14]. Acute senescence, which is the induction of senescence during injury or disease, is presumably beneficial[14]. These cells are rapidly cleared by the immune system[15] and have been found to aid in embryonic development[16,17], wound healing[18] and tissue repair[19]. The incomplete removal of senescent cells after an injury, but also the gradual accumulation of damaged senescent cells results in so called “chronic senescence”[14]. Aging is marked, amongst others, by the accumulation of these persistent dysfunctional senescent cells[7], which drive inflammaging[20,21] and reduce regeneration[22,23]. Notably, the presence of senescent cell markers in human pre-transplantation biopsies have been shown to correlate with negative outcome [24], supporting the idea that chronically present senescent cells in the kidney can negatively influence the recovery from AKI. However, it remains to be determined whether senescent cells are causative of poor recovery from AKI and not just a good biomarker.

Therefore, to test whether senescent cells impair recovery from acute kidney injury in aged kidneys, we removed senescent cells from fast-aging p16::3MR *Xpd*^{TTD} mice, before subjecting them to AKI.

MATERIALS AND METHODS

Mice

All mice used in this study were of a C57BL/6J background, either WT or *Xpd*^{TTD} mutated, expressing p16::3MR. Mice were genotyped by a standard PCR reaction using DNA isolated from tail tips as described previously [25]. The *Xpd*^{TTD} mice used in this study carry a R722W mutation at the mouse Xpd gene[26]. The resulting defect in the nucleotide excision repair pathway causes the mice to accumulate DNA damage faster than normal and already at young age exhibit many aspects of aging [26]. In the p16::3MR mice, the promoter of the senescence gene p16^{Ink4a} drives expression of Renilla luciferase (RLUC), a red fluorescent protein. Furthermore, this construct expresses a thymidine kinase (TK) from the *Herpes simplex* virus, which triggers apoptosis in p16 positive cells upon presentation of its substrate ganciclovir (GCV) [18] (Supplemental Figure 1).

All mice were bred in the Erasmus MC Rotterdam. They were brought in experiment at 26 weeks of age and were of both sexes. Animals were kept under standard laboratory conditions (12 h light/12 h dark, temperature 20-24°C, relative humidity 50-60%) with 3-4 animals per cage and allowed free access to water and standard food pellets (CRM pellets, SDS BP Nutrition Ltd.). Group compositions: the experiments presented in figure 1 were performed on groups of male mice. There were 4 mice in the TTD group, and 5 mice in the WT group. Mouse experiments as shown in figure 2 consisted of the following groups: the PBS SHAM group consisted of 2 males and 1 female, the PBS AKI group consisted of 2 males and 2 females. The GCV SHAM group consisted of 2 females and 1 male, and the GCV AKI group consisted of 3 males and 1 female.

Anti-senescence treatments

p16::3MR *Xpd*^{TTD} mice were treated 5 consecutive days either with 25mg/kg Ganciclovir (G2536 Sigma) dissolved in PBS and brought to body temperature before i.p. injection, or PBS. After the last day of anti-senescence treatment, mice were allowed to recover for 23 days before undergoing acute kidney injury by renal ischemia.

Renal Ischemia-reperfusion injury

Mice were anaesthetized by isoflurane inhalation (5% isoflurane initially and then 2–2.5% with oxygen for maintenance) (PCH 282-10-45112110, Pharmachemie). Abdominal hair was removed and skin was disinfected after which the mice were placed on heating pads to maintain body temperature until recovery from anaesthesia. Using aseptic techniques, a midline abdominal incision was made through which the left renal pedicle was localized. After the renal artery and vein were dissected, a non-traumatic clamp was

used to occlude the left kidney. The procedure was repeated immediately on the right kidney. Both kidneys were clamped for either 35 minutes (survival experiment, male WT and *Xpd*^{TTD} mice), 25 minutes (male p16::3MR *Xpd*^{TTD} mice) or 40 minutes (female p16::3MR *Xpd*^{TTD} mice). Kidneys were inspected for signs of ischemia (blue colouring), and the wound was covered with phosphate-buffered saline (PBS)-soaked gauze which was covered with an aluminium foil blanket to maintain body temperature. After release of the clamp, blood reflow was inspected by return of normal colour to the kidney. In the Sham group, all surgical procedures were performed as described before, without placement of the non-traumatic clamp. The abdominal wound was closed in two layers using Safil 5/0 sutures (B.Braun, Melsungen, Germany, C1048207). Animals were given 0.5 mL sterile PBS subcutaneously for maintenance of fluid balance and were allowed to recover under a heating lamp to maintain body temperature. All animals were observed to have regained consciousness before moving their cages from the operating room to the stable. The mice received 0.1mg/kg Buprenorphine intramuscularly (Temgesic, IND00262) as analgesic for 2 days following the surgical procedure.

Kidney sample preparations

At the end of an experiment, mice were killed by cervical dislocation. The kidneys were decapsulated and laterally sectioned. The cranial kidney halves were preserved in 4% formaldehyde buffered solution for 24 hours after which the kidneys were washed and stored in PBS before paraffin embedding. The sagittal halves were snap frozen in liquid nitrogen and preserved at -80^{o}C.

Serum urea measurements

Blood samples were collected by submandibular puncture throughout the experiments. Serum urea levels were measured using QuantiChrom assay kits (DIUR-100 BioAssay systems) according to manufacturer's protocol.

Immunofluorescence on mice tissue slides

Paraffin sections of 5 µm mouse kidney specimens were deparaffinized in Xylene, rehydrated in decreasing concentrations of ethanol and heated to 100^{o}C for 30min in 10 mM sodium citrate buffer, pH 6, for antigen retrieval. After heating, the solution containing the slides was allowed to cool down to RT. Subsequently, tissues were washed in Tris Buffered Saline (TBS) and permeabilized for 5 min in 0.2% Triton X-100 in TBS. To reduce background staining, the cells were blocked for 30min with 5% Normal Horse Serum (16050-122 Gibco) in a 50nM glycine and 0.2% gelatin-TBS solution. Slides were covered with primary antibody dilutions and placed in a dark moisture chamber and incubated overnight at 4^{o}C (primary antibodies: LaminB1, 1:1000 (ab16048 Abcam); HMGB1, 1:500 (ab18256 Abcam)). The next day, slides were washed 3x 20min with 0,2% gelatin-TBS. Secondary antibody (1:1000 A-11034, A-21202 Invitrogen) incubation occurred as described for the primary antibody including a nuclear staining with Hoechst 1:1000 (565877 BD Pharmingen) and the slides were incubated for one hour at room

temperature. Following 2x 10min washes with 0,2% TBS-Gelatin, 1 wash with regular TBS and 1 dip in dH2O, the slides were mounted using soft set mounting medium (Vectashield) and sealed with nail polish. Spectral Imaging on paraffin sections was performed using lambda mode on a Zeiss LSM510 confocal microscope, within an emission spectrum of 460-560 nm. The spectral stack was linearly unmixed and assigned pseudocolors which allowed us to distinguish the detected protein signal from background signal. All images were processed and analysed with FIJI software. When comparisons were made between or when representative images were made of images of the same experiment, all levels were adjusted equally and the ratio between the levels was not altered.

Immunohistochemistry on mice tissue slides

5 µm mouse kidney paraffin sections were deparaffinized in Xylene, rehydrated in decreasing concentrations of ethanol and heated to 100^{o}C for 30min in 10 mM sodium citrate buffer, pH 6. After the solution containing the slides was cooled down to RT, the tissues were washed in Tris Buffered Saline (TBS) with 0.05% Tween (TBS-T). Then, the cells were blocked for 30min with 5% Normal Horse Serum (16050-122 Gibco) with 1%BSA in TBS. Slides were covered with primary antibody dilutions and placed in a dark moisture chamber and incubated overnight at 4^{o}C (primary antibody: NGAL, 1:500, ab63929, Abcam). The next day, slides were washed 3x 10min with TBS-T and endogenous peroxidases were quenched for 15 minutes with 3%H2O2 solution. Biotinylated-secondary antibody (BA1000, Vector laboratories) incubation occurred as described for the primary antibody, and the slides were incubated for one hour at room temperature. Following 3x 10min washes with TBS-T, slides were incubated with ABC-solution (K3468, DAKO) for 30 minutes at RT. After two washes with dH_2O, slides were incubated with DAB substrate for 3 minutes and rinsed in dH_2O. After a counterstain in methylgreen, slides were dehydrated in butanol and xylene and mounted with pertex. Slides were scanned with a Nanozoomer and subsequently the whole cortex of the stained kidney section was analyzed with FIJI software for the levels of positive staining, and corrected for any deviations in cortex area.

Sirius red staining

5 µm mouse kidney paraffin sections were deparaffinized in Xylene and rehydrated in decreasing concentrations of ethanol. After 60 minutes of incubation in Picro Sirius Red solution, slides were rinsed in 0.05% acetic acid, dehydrated in ethanol and Xylene, and mounted with pertex. The stained tissues were scanned with a Nanozoomer and subsequently analysed with FIJI software.

RESULTS

Fast aging TTD mice have elevated levels of senescent cells and are more vulnerable to AKI

In this study we have used the progeroid *Xpd*^{TTD} mouse as a model for aging. These mice have a mutation in the *XPD* gene of nucleotide excision repair, which causes them to age faster [26]. This aging phenotype is reflected by a reduced life span[26] and poorer kidney function compared to wild type (WT) mice (Figure 1c). This is accompanied by higher levels of cellular senescence. Both LaminB1 and HMGB1 expression are reduced in senescent cells[27,28]. Figure 1a-b shows the reduced expression of nuclear proteins LaminB1 and HMGB1 in kidney tissue of 26 weeks old *Xpd*^{TTD} mice compared to kidneys of WT mice. Because ischemia reperfusion injury (IRI) is the most common cause of acute kidney injury (AKI)[29], we used renal IRI as model. Ischemia reperfusion entails the initial lack of blood flow followed by the sudden return of blood supply in a tissue, that occurs for example during kidney transplantation[30]. To examine whether *Xpd*^{TTD} mice are, comparable to aged humans, also more vulnerable to acute kidney injury, we subjected 26 weeks old male *Xpd*^{TTD} and WT mice to 35' of bilateral renal IRI (Figure 1d) and assessed survival. Within four days after the induction of acute injury, all *Xpd*^{TTD} animals had to be taken out of the experiment because of signs indicative of irreversible kidney failure, compared to 20% of the WT mice. Taken together, these data show that *Xpd*^{TTD} mice have worse kidney function and higher levels of senescent cells than WT littermates and are more vulnerable to AKI. Therefore, we have established the *Xpd*^{TTD} mouse as a model to study the effect of aging and senescence on sensitivity to AKI.

Ganciclovir treatment reduces senescence in p16::3MR-Xpd^{TTD} mice

To examine the effect of senescent cells on the recovery from acute kidney injury, we removed senescent cells in *Xpd*^{TTD} mice, before the induction of AKI. To do so, we made use of the p16::3MR senescence mouse model. In this model, the promoter of the senescence gene p16^{Ink4a} drives expression of a thymidine kinase from the *Herpes simplex* virus[18] (Supplemental Figure 1). Thymidine kinase triggers apoptosis in p16-positive senescent cells, after conversion of its nontoxic substrate ganciclovir (GCV)[18]. To ensure time for tissue regeneration after the removal of senescent cells with ganciclovir, senescent cells were removed 28 days before the induction of AKI. AKI was induced by 25 minutes bilateral clamping of the renal pedicle in males and 40 minutes in females, whom are known to be more resistant to AKI[31]. A control group was taken along that underwent sham surgery. The mice were followed for another 28 days to study the long-term effects of senescence removal in aged mice before the induction of AKI. A schematic overview of the experiment is presented in Figure 2a. First, we assessed whether ganciclovir treatment had removed senescent cells. Figure 2b-c shows that ganciclovir treatment before sham surgery reduces the expression of nuclear proteins LaminB1 and HMGB1 in kidney cortex, indicating that ganciclovir treatment had removed senescent cells in these mice.

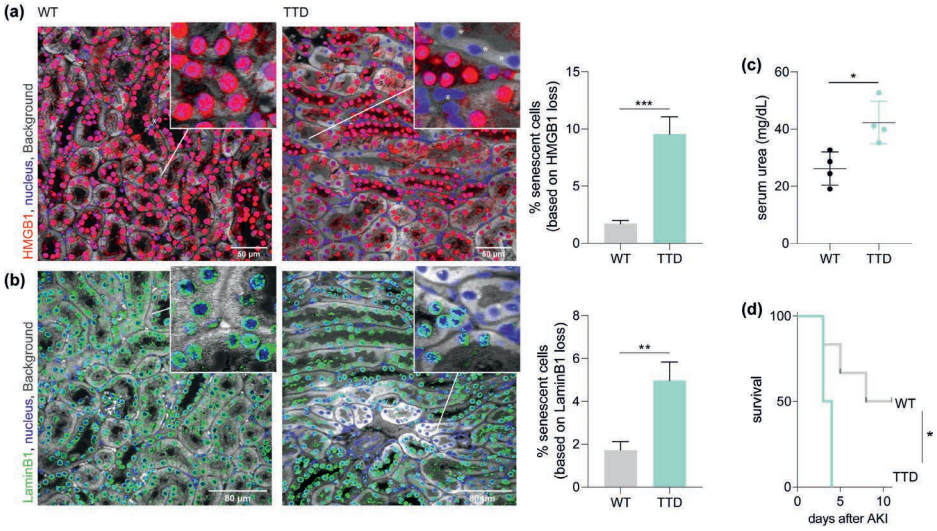

Figure 1. **Xpd^{TTD} mice show elevated numbers of senescent cells, reduced kidney function and are more vulnerable to acute kidney injury**

(a-b) Representative images of kidneys from 26-week old wild type (WT) and *Xpd^{TTD}* (TTD) mice stained for LaminB1 **(a)** and HMGB1 **(b)**. Quantified are the average % of nuclei per kidney (cortex) negative for LaminB1 and HMGB1. Averages of 5 random images per mouse (at least 1000 nuclei per mouse), 4 mice in the TTD group, 5 mice in the WT group. **(c)** Quantification of serum urea levels from 40-week old wild type (WT) and *Xpd^{TTD}* (TTD) mice. **(d)** Survival rate of 26-week old male wild type (WT) and *Xpd^{TTD}* (TTD) mice after induction of 35' ischemia reperfusion injury to induce AKI (TTD n=4, WT n=5) (p=0.019). p values were calculated using two-tailed student T-test, and the logrank test (Mantel-cox) for the Kaplan-Meier survival curve, * $p < 0.05$, ** $p < 0.01$, *** $p<0.001$, data are expressed as the mean ± SD.

Genetic removal of senescent cells in p16::3MR Xpd^{TTD} mice improves resistance to AKI

Next, we assessed the degree of long-term damage induced by AKI through IHC and measurement of plasma urea. Histologically, a Sirius red staining and a fibronectin staining suggest that tubulointerstitial fibrosis is lower in the GCV group compared to the PBS group (Figure 3a-b). Next, we looked at the effect of senescent cells on damage repair, by assessing the amount of Sox9 and NGAL. Renal injury leads to the activation of Sox9 in proximal tubules, which triggers a process of tubule self-regeneration[32]. Persistent Sox9 expression 4 weeks after AKI identifies tubules with unresolved injury-repair[33]. Again, we observe a trend towards lower levels of Sox9 positive tubular cells in the mice treated with GCV (Figure 3c). Assessment of NGAL, a commonly used biomarker for kidney injury [33,34], and recently discovered inducer of fibrosis [35], shows that NGAL expression is lower in the GCV group than in the PBS group (p=0.054) (Figure 3d). Thus, we did not find a significant difference between the GCV and PBS treated mice for these IHC-markers, although we did observe a general trend towards improved damage repair in the mice treated with ganciclovir (GCV).

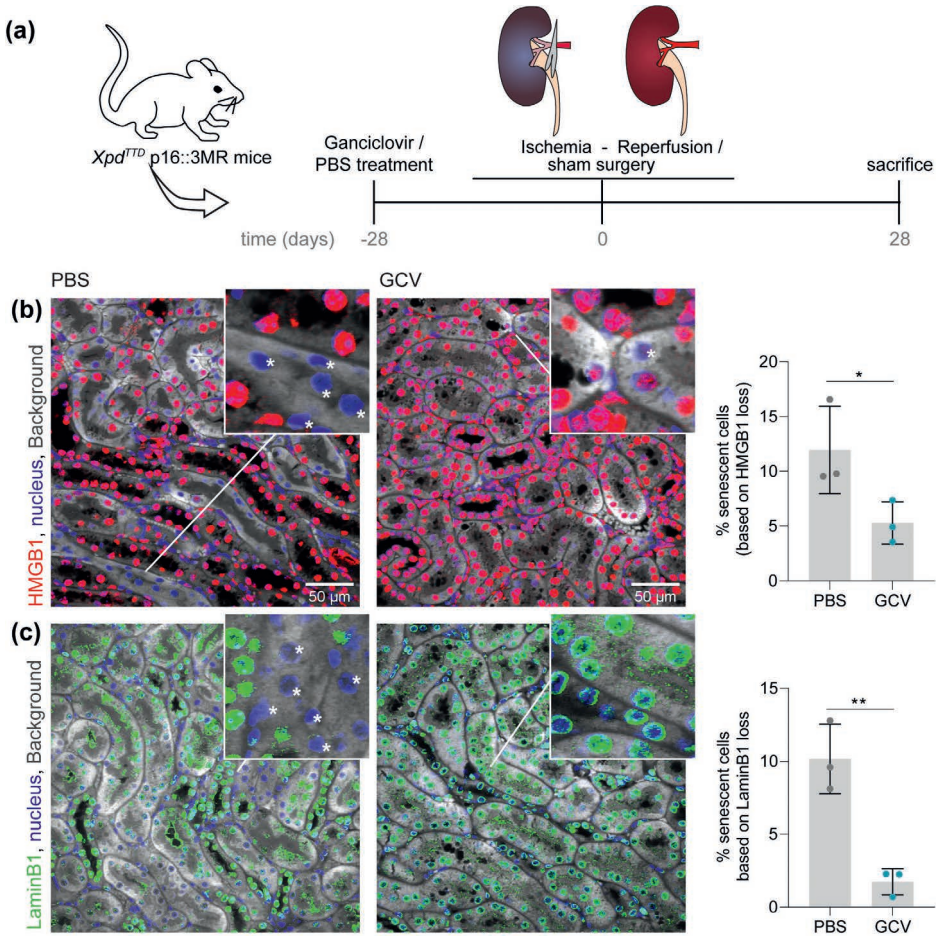

Figure 2 ***ganciclovir treatment removes senescent cells in kidney tissue of p16::3MR-Xpd^{TTD} mice***
(a) Schematic representation of experimental procedure. **(b-c)** Representative images of kidneys from p16::3MR-*Xpd^{TTD}* (TTD) mice, that received 3x every other day 5mg/kg i.p. ganciclovir (GCV), or phosphate-buffered saline (PBS), before sham surgery, were stained for HMGB1 (b) and LaminB1 **(c)**. Quantified are the average % of nuclei per kidney (cortex) negative for LaminB1 and HMGB1. Averages of 6 random images per mouse (at least 2000 nuclei per mouse), n=3. P-values were calculated using one-tailed student T-test, * $p < 0.05$, ** $p < 0.01$, *** $p<0.001$, data are expressed as the mean ± SD.

A recently published paper on the role of senescent cells in heart transplantation, underlined an important role for the attraction of dendritic cells (DCs) by senescent cells in older hearts[36]. We assessed whether the improved renal function of mice in which senescent cells were removed before AKI, could be attributed to lowered influx of DCs. IHC on DC marker cd11c showed no difference between the GCV and PBS groups that underwent IRI (Figure 3e). We also did not observe any difference in number of DCs between the animals that received sham surgery and were pretreated with GCV or PBS

(data not shown). These results indicate that the number of DCs does not play a similar role in the recovery after renal acute injury as was observed in hearts.

Since the IHC data hinted towards a potential for improved repair in the GCV mice, we assessed kidney function, by measuring serum urea levels[37]. No major changes in plasma urea were observed upon sham surgery in either PBS or GCV-pretreated p16::3MR-*Xpd*^{TTD}. In contrast, the urea levels of p16::3MR-*Xpd*^{TTD} mice spiked within 4 days after AKI (Figure 3f, left panel), confirming acute renal toxicity after AKI. This effect reduced over time, but stayed prevalent for at least 28d. Importantly, this early spike in plasma urea was strongly reduced in p16::3MR-*Xpd*^{TTD} treated with GCV. Moreover, on day 28 after AKI, there still was a significant reduction in plasma urea in GCV-pretreated mice (Figure 3f, right panel). This result provides proof-of-concept evidence that semi-genetic ablation of senescent cells prior to AKI prevents both acute and long-term (28d) reduction in renal filtering capacity.

Taken together, our data shows that the removal of senescent cells in aged mice improves renal function after AKI, and that this might be attributed to reduced injury due to IRI and an improved renal repair.

DISCUSSION

This study shows that chronic presence of senescent cells in aged kidneys sensitizes to adverse effects, including mortality, of acute kidney injury (AKI). Vice versa, senescence elimination prior to AKI dampens these deleterious effects, evident from reduced short- and long term plasma urea levels. We used the fast-aging mouse model *Xpd*^{TTD}, which suffers from higher levels of senescent cells, poorer kidney function and higher sensitivity to AKI, compared to WT mice. In this model, we had shown before that senescence clearance in aged mice could improve renal filtering capacity (Baar, 2017), but the effects on AKI had not yet been addressed. This study emphasizes the notion that aging worsens recovery from AKI, and shows that senescent cells are a culprit for this phenomenon.

Interestingly, we have observed a slight trend towards reduced fibrosis and a stronger trend in reduced NGAL expression post-AKI in those mice treated with GCV. A recent paper by Li et al. has reported that post-AKI removal of senescent cells ameliorates renal fibrosis [38], indicating that reduced levels of senescent cells post-AKI prevents renal fibrosis. Future research should point out whether therapeutic removal of senescent cells in aged humans also reduces fibrosis upon AKI.

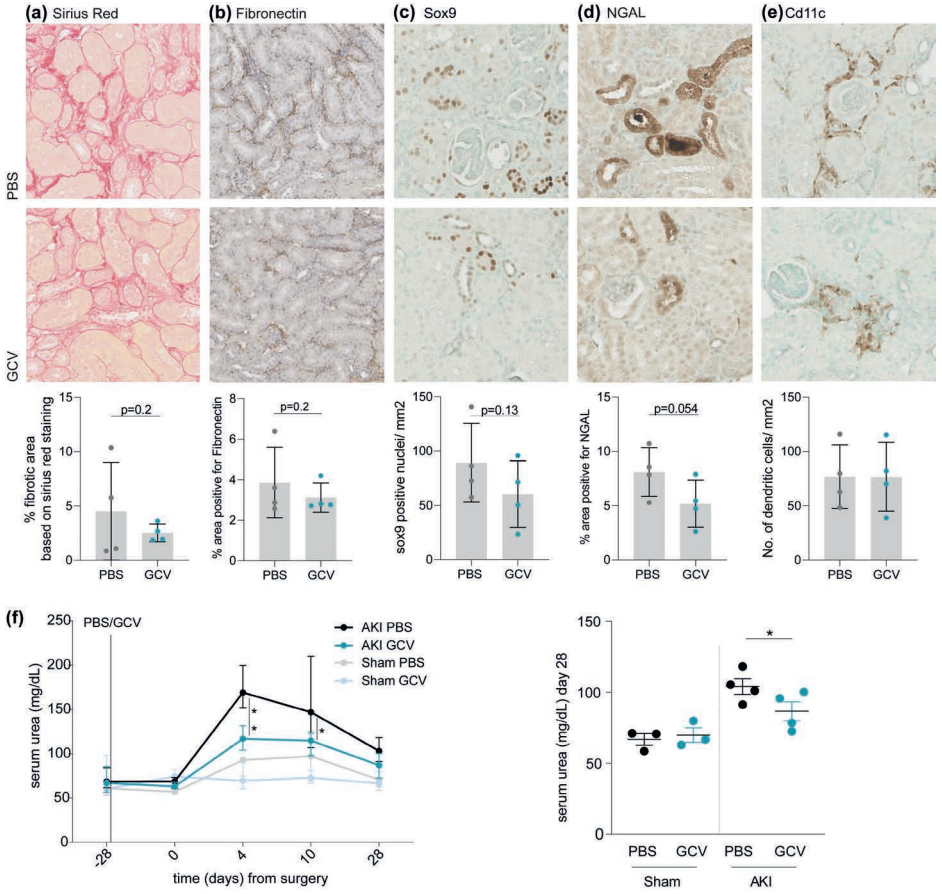

Figure 3 Removal of senescent cells in 26 weeks old p16::3MR Xpd^{TTD} mice improves recovery from acute kidney injury

P16::3MR *Xpd^{TTD}* mice received ganciclovir or PBS treatment before IRI surgery to induce AKI, tissues were collected 28 days post AKI. **(a-b)** Representative images of Sirius red staining **(a)** and fibronectin staining **(b)** for quantification of interstitial fibrosis on kidney tissues. **(c-e)** Representative images and quantification of IHC for Sox9, NGAL and Cd11c on kidney tissues. **(f)** Quantification of serum urea levels before, during and after IRI surgery, after mice received ganciclovir (GCV) or PBS treatment. The GCV group consisted of 3 males and 1 female, the PBS group of 2 males and 2 females. P-values were calculated using one-tailed student T-test, * $p < 0.05$, ** $p < 0.01$, *** $p<0.001$, data are expressed as the mean ± SD. AKI, acute kidney injury; GCV, ganciclovir; PBS phosphate-buffered saline.

Based on the stem-lock model, which proposes that senescent cells impair regeneration by blocking differentiation of dividing stem cells[39], we hypothesized that the removal of senescent cells could have a beneficial influence on the regeneration of kidney tissue after injury. The observed trend in reduced expression of stemness marker Sox9 in the

kidneys of the GCV treated mice hints towards a direct negative influence of senescent cells on renal stem-like cells, however, this has to be further elucidated.

Immune infiltration of dendritic cells was previously reported to occur during heart IRI [36]. We did not observe a lowered immune cell infiltration in mice where senescent cells were removed, suggesting this is not a conserved response to IRI per sé. The immune-modulatory effect of SASP factors advocates that the removal of senescent cells would influence the presence of immune cells. However, the role of immune cells in the recovery from AKI is predominantly in the early phase after AKI [40]. Our observations might be explained by the relatively late assessment of immune cell status (28d post-AKI), and it would be interesting to assess immune infiltration at earlier time points.

Due to the proof of concept nature of this semi-genetic senescence ablation study, there are a few limitations that should be addressed in follow-up studies. First of all, this study endured an unequal sex distribution of the groups that underwent AKI. The PBS group consisted of more females than the GCV group. This is of importance, because female mice are known to better withstand ischemia reperfusion injury, which is attributed to lower levels of testosterone[31]. Although, the females were subjected to 40 minutes of IRI, and the males to 25 minutes of IRI, the females still showed better outcomes than the males, which gave the PBS group a lower score for renal injury markers. We have observed that the males in the GCV group performed better than the males in the PBS group and the female in the GCV group scored better than the females in the PBS group for the blood urea levels, NGAL, and Sox9 measurements. These observations strengthen our hypothesis that the removal of senescent cells improves recovery from AKI, since all markers were either significantly different, or showed a trend towards improvement. Furthermore, future studies might benefit from the use of naturally aged mice to the overall understanding of senescence and aging in the recovery from AKI. Lastly, in this study senescent cells were removed 28 days before mice underwent AKI, to allow sufficient time for optimal tissue regeneration. Because senescent cells have been shown to aid in wound healing[18], we refrained from interfering with this process with ganciclovir during IRI[41]. Future research should investigate the optimal timing of senescence removal relative to the induction of AKI.

The sensitivity of aged patients to acute kidney injury has been attributed to the general decline of renal capacity[5]. Here we show that this sensitivity can also be attributed to the presence of senescent cells. The mechanism with which they exactly do so, remains to be investigated. It could be that the senescence-associated growth arrest we observed in the tubular cells is responsible for reduced tissue regeneration after AKI. Kumar et al have shown that proximal tubular injury repair is realized mainly by dedifferentiated proximal tubular epithelial cells[32], which might be impaired when a subset of those cells are senescent. Another possibility is that secreted SASP factors, with which senescent cells have been shown to alter their milieu [11], are implicated in reduced function of the

entire tubulus once senescence has occurred. If so, a potential additional mechanism to blunt the effects of senescence in AKI could be to employ antibodies, or inflammation suppressive therapeutics against such factors[42]. Irrespective of the mechanism of action, it is clear senescence is a culprit in the recovery from AKI. There are many advances in the area of therapeutic interventions against senescence, e.g. senomorphics or senolytics[43]. These therapeutics may be especially relevant for clinical situations where AKI is a common side effect, such as the use of certain types of medication[44], the use of specific contrast imaging fluids[45], and kidney transplantation[29].

Author Contributions

"Conceptualization, H.v.W., R.W.F.d.B., P.L.J.d.K.; methodology, H.v.W., G.A.; validation, H.v.W, G.A. and R.W.F.d.B.; formal analysis, H.v.W., G.A.; data curation, H.v.W., R.W.F.d.B.; writing—original draft preparation, H.v.W., R.W.F.d.B.; writing—review and editing, H.v.W, J.N.M.IJ, R.W.F.d.B. P.L.J.d.K.; visualization, H.v.W.; supervision, R.W.F.d.B., P.L.J.d.K.; project administration, R.W.F.d.B..; funding acquisition, R.W.F.d.B., P.L.J.d.K.. All authors have read and agreed to the published version of the manuscript.

Funding

H.v.W is supported by a Dutch Kidney Foundation grant (15OP11) awarded to P.L.J.d.K. and R.W.F.d.B.

Institutional Review Board Statement

Experiments were performed in accordance with the Principles of Laboratory Animal Care (National Institutes of Health publication no. 86-23) and with the guidelines approved by the Erasmus University Animal Care Committee (license code DEC105-15-01).

Acknowledgments

We thank Adriaan Houtsmuller and Gert-Jan Kremers of the Erasmus MC optical imaging centre (OIC) for their valuable technical and tutorial support on confocal imaging and spectral unmixing. Renata M.C. Brandt for the breeding of the p16::3MR TTD mice. Sandra van Damme – van den Engel for her technical support during the surgical procedures of this study. Lastly, we thank Ibrahim Maalouf for his melodic support during the performance of our surgical procedures.

Conflicts of Interest

P.L.J. de K is founder, shareholder and managing director of Cleara Biotech B.V., Utrecht, The Netherlands, a company developing anti-senescence biomarkers and therapeutics. The other authors declare no conflict of interest.

REFERENCES

1. Hill, N. R. et al. Global Prevalence of Chronic Kidney Disease - A Systematic Review and Meta-Analysis. PLoS One 11, e0158765 (2016).
2. Stevens, L. A., Viswanathan, G. & Weiner, D. E. Chronic kidney disease and end-stage renal disease in the elderly population: current prevalence, future projections, and clinical significance. Adv. Chronic Kidney Dis. 17, 293–301 (2010).
3. Belayev, L. Y. & Palevsky, P. M. The link between acute kidney injury and chronic kidney disease. Current Opinion in Nephrology and Hypertension vol. 23 149–154 (2014).
4. Makris, K. & Spanou, L. Acute Kidney Injury: Definition, Pathophysiology and Clinical Phenotypes. Clin. Biochem. Rev. 37, 85–98 (2016).
5. Yokota, L. G. et al. Acute kidney injury in elderly patients: Narrative review on incidence, risk factors, and mortality. International Journal of Nephrology and Renovascular Disease vol. 11 217–224 (2018).
6. Ishani, A. et al. Acute kidney injury increases risk of ESRD among elderly. J. Am. Soc. Nephrol. 20, 223–228 (2009).
7. López-Otín, C., Blasco, M. A., Partridge, L., Serrano, M. & Kroemer, G. The hallmarks of aging. Cell vol. 153 (2013).
8. Campisi, J. Aging, Cellular Senescence, and Cancer. Annu. Rev. Physiol. 75, 685–705 (2013).
9. Hernandez-Segura, A., Nehme, J. & Demaria, M. Hallmarks of Cellular Senescence. Trends Cell Biol. 28, 436–453 (2018).
10. Campisi, J. & d'Adda di Fagagna, F. Cellular senescence: when bad things happen to good cells. Nat. Rev. Mol. Cell Biol. 8, 729–740 (2007).
11. Coppé, J.-P., Desprez, P.-Y., Krtolica, A. & Campisi, J. The senescence-associated secretory phenotype: the dark side of tumor suppression. Annu. Rev. Pathol. 5, 99–118 (2010).
12. Sturmlechner, I., Durik, M., Sieben, C. J., Baker, D. J. & van Deursen, J. M. Cellular senescence in renal ageing and disease. Nat. Rev. Nephrol. 13, 77–89 (2016).
13. Khosla, S., Farr, J. N., Tchkonia, T. & Kirkland, J. L. The role of cellular senescence in ageing and endocrine disease. Nature Reviews Endocrinology vol. 16 263–275 (2020).
14. van Deursen, J. M. The role of senescent cells in ageing. Nature 509, 439–446 (2014).
15. Sagiv, A. & Krizhanovsky, V. Immunosurveillance of senescent cells: the bright side of the senescence program. Biogerontology 14, 617–628 (2013).
16. Rajagopalan, S. & Long, E. O. Cellular senescence induced by CD158d reprograms natural killer cells to promote vascular remodeling. Proc. Natl. Acad. Sci. U. S. A. 109, 20596–20601 (2012).
17. Muñoz-Espín, D. et al. Programmed Cell Senescence during Mammalian Embryonic Development. Cell 155, (2013).
18. Demaria, M. et al. An essential role for senescent cells in optimal wound healing through secretion of PDGF-AA. Dev. Cell 31, 722–33 (2014).
19. Krizhanovsky, V. et al. Senescence of Activated Stellate Cells Limits Liver Fibrosis. Cell 134, 657–667 (2008).
20. Franceschi, C. & Campisi, J. Chronic Inflammation (Inflammaging) and Its Potential Contribution to Age-Associated Diseases. vol. 69 4–9 (2014).
21. Kooman, J. P. et al. Inflammation and premature aging in advanced chronic kidney disease. Am. J. Physiol. Renal Physiol. 313, F938–F950 (2017).
22. Krishnamurthy, J. et al. p16INK4a induces an age-dependent decline in islet regenerative potential. Nature 443, 453–457 (2006).
23. Sousa-Victor, P. et al. Geriatric muscle stem cells switch reversible quiescence into senescence. Nature 506, 316–321 (2014).

24. McGlynn, L. M. et al. Cellular senescence in pretransplant renal biopsies predicts postoperative organ function. Aging Cell 8, 45–51 (2009).
25. Baar, M. P. et al. Targeted Apoptosis of Senescent Cells Restores Tissue Homeostasis in Response to Chemotoxicity and Aging. Cell 169, (2017).
26. De Boer, J. et al. A mouse model for the basal transcription/DNA repair syndrome trichothiodystrophy. Mol. Cell 1, 981–990 (1998).
27. Davalos, A. R. et al. p53-dependent release of Alarmin HMGB1 is a central mediator of senescent phenotypes. J. Cell Biol. 201, 613–29 (2013).
28. Freund, A., Laberge, R.-M., Demaria, M. & Campisi, J. Lamin B1 loss is a senescence-associated biomarker. Mol. Biol. Cell 23, 2066–2075 (2012).
29. Cooper, J. E. & Wiseman, A. C. Acute kidney injury in kidney transplantation. Curr. Opin. Nephrol. Hypertens. 22, 698–703 (2013).
30. Salvadori, M., Rosso, G. & Bertoni, E. Update on ischemia-reperfusion injury in kidney transplantation: Pathogenesis and treatment. World J. Transplant. 5, 52–67 (2015).
31. Park, K. M., Kim, J. I., Ahn, Y., Bonventre, A. J. & Bonventre, J. V. Testosterone is responsible for enhanced susceptibility of males to ischemic renal injury. J. Biol. Chem. 279, 52282–52292 (2004).
32. Kumar, S. et al. Sox9 Activation Highlights a Cellular Pathway of Renal Repair in the Acutely Injured Mammalian Kidney. Cell Rep. 12, 1325–1338 (2015).
33. Kumar, S. Cellular and molecular pathways of renal repair after acute kidney injury. (2018) doi:10.1016/j.kint.2017.07.030.
34. Devarajan, P. NGAL for the detection of acute kidney injury in the emergency room. Biomarkers in Medicine vol. 8 217–219 (2014).
35. Bonnard, B. et al. Antifibrotic effect of novel neutrophil gelatinase-associated lipocalin inhibitors in cardiac and renal disease models. Sci. Rep. 11, 2591 (2021).
36. Iske, J. et al. Senolytics prevent mt-DNA-induced inflammation and promote the survival of aged organs following transplantation. Nat. Commun. 11, (2020).
37. JL., L. Blood urea nitrogen and creatinine. Emerg Med Clin North Am. 4, 223–33.
38. Li, C., Shen, Y., Huang, L., Liu, C. & Wang, J. Senolytic therapy ameliorates renal fibrosis postacute kidney injury by alleviating renal senescence. FASEB J. 35, e21229 (2021).
39. de Keizer, P. L. J. The Fountain of Youth by Targeting Senescent Cells? Trends Mol. Med. 23, 6–17 (2017).
40. Lee, S. A., Noel, S., Sadasivam, M., Hamad, A. R. A. & Rabb, H. Role of Immune Cells in Acute Kidney Injury and Repair. Nephron 137, 282–286 (2017).
41. van Willigenburg, H., de Keizer, P. L. J. & de Bruin, R. W. F. Cellular senescence as a therapeutic target to improve renal transplantation outcome. Pharmacological Research vol. 130 322–330 (2018).
42. Birch, J. & Gil, J. Senescence and the SASP: Many therapeutic avenues. Genes Dev. 34, 1565–1576 (2020).
43. Amaya-Montoya, M., Pérez-Londoño, A., Guatibonza-García, V., Vargas-Villanueva, A. & Mendivil, C. O. Cellular Senescence as a Therapeutic Target for Age-Related Diseases: A Review. Advances in Therapy vol. 37 1407–1424 (2020).
44. Perazella, M. A. Drug-induced acute kidney injury. Curr. Opin. Crit. Care 25, 550–557 (2019).
45. Vandenberghe, W. & Hoste, E. Contrast-associated acute kidney injury: Does it really exist, and if so, what to do about it? [version 1; peer review: 2 approved]. F1000Research vol. 8 (2019).

Chapter 4

Targeted elimination of senescent cells with the senolytic compound FOXO4-DRI improves kidney function after renal ischemia reperfusion injury in aged mice

Hester van Willigenburg[1,2], Sarah Mitchell[3], Gisela Ambagtsheer[1], Sebastiaan Knoppert[4], Floris Valentijn[4], Jay Mitchell[3], Jan N.M. IJzermans[1], Ron W.F. de Bruin[1]

[1] Department of Surgery, Erasmus MC, University Medical Centre Rotterdam, Rotterdam, The Netherlands, [2] Department of Molecular Genetics, Erasmus MC, University Medical Centre Rotterdam, Rotterdam, The Netherlands, [3] Department of Molecular Metabolism, Harvard T H Chan School of Public Health, Boston, USA, [4] Department of Pathology, University Medical Center Utrecht (UMCU), Utrecht, Netherlands.

ABSTRACT

The worldwide shortage of donor kidneys for transplantation has led to the use of kidneys from aged donors (> 60 years). However, aged kidneys are more vulnerable to ischemia reperfusion injury (IRI), a main cause of acute kidney injury and delayed graft function after transplantation. We recently reported that the elimination of senescent cells in a fast aging mouse model improves recovery from renal ischemia reperfusion injury (IRI). Senescent cells promote a chronic pro-inflammatory state, reduce the proliferative capacity of tissues and ultimately reduce kidney function. To determine whether the therapeutic removal of senescent cells can also improve resistance to renal IRI in aged mice, we used three clinically relevant anti-senescence compounds (senolytics) to eliminate senescent cells in 19 month old wild-type mice, before induction of renal IRI. We show that treatment with the senolytic FOXO4-DRI peptide improves recovery of renal function after IRI, while treatment with navitoclax or quercetin/dasatinib did not. Surprisingly, our experiments revealed that the 19 month old mice exhibited low levels of senescent cells and barely any age-related pathologies at baseline, and therefore, these parameters were not significantly lowered in the mice treated with senolytics. Thus, while FOXO4-DRI treatment exerted moderate renoprotective effects against renal IRI, this could not be attributed to a reduction in the number of renal senescent cells.

INTRODUCTION

Kidney transplantation is the most successful treatment option for patients with end stage renal disease (ESRD)[1]. It is not a treatment without risks, however. For example, tissue in the donated kidney will become damaged due to the initial lack of blood flow followed by the sudden return of blood supply – a process known as ischemia reperfusion injury (IRI)[2]. In addition, the worldwide shortage of suitable donor kidneys has led to the use of so-called extended-donor-criteria kidneys, such as those from aged donors (>60 years)[3]. Kidneys from older donors have a higher number of complications due to IRI, such as delayed graft function and lower 5-year graft survival [1,4]. To address these adverse effects, our group has recently reported that the removal of senescent cells with a genetic construct in aged mice before the induction of IRI reduces the severity of IRI, suggesting that senescent cells contribute to the worsened outcome after IRI in aged kidney donors.

Senescence is a cellular state which comprises a permanent cell cycle arrest and apoptosis resistance[5]. It is induced upon cellular stresses such as oncogene activation, persistent DNA-damage, telomere shortening, or oxidative stress [5,6]. Senescent cells can develop a secretory profile, the so called senescence associated secretory phenotype (SASP), which is characterized by the secretion of a variety of pro-inflammatory cytokines and chemokines, alarmins, matrix metalloproteases, and growth factors, thereby affecting neighbouring cells [5,7,8]. This senescent proteome varies between senescent cells; it is cell-type specific[9,10] and is determined by the stimuli that induce senescence [7,11,12]. Therefore, senescent cells are a heterogeneous population.

Much of what is known about the effects of senescent cells on tissues and organs comes from animal studies. For example, removing senescent cells from aged mice can extend their health span and life span [13,14]. These results triggered the development of therapeutic approaches to remove senescent cells, resulting in several anti-senescence drugs, also known as senolytics. The most potent senolytics are as follows: navitoclax, a bcl-2 inhibitor that overrules the anti-apoptosis signals that are upregulated in senescent cells [15,16]; the combination of quercetin (a flavonol) and dasatinib (a pro-apoptotic tyrosine-kinase inhibitor) [17–19]; and a FOXO4-DRI peptide, which was designed to compete with the senescence-specific anti-apoptotic FOXO4-p53 interaction [20]. Since these senolytics target distinct cellular pathways, they are likely to target distinct senescent cell populations [21].

Previously, we have shown that the removal of senescent cells with a genetic construct in aged mice improves resistance to renal IRI. Here, we aim to study whether treatment with senolytics can protect aged kidneys to IRI. To test this, we treated aged mice with distinct senolytics, before subjecting the mice to renal IRI via bilateral clamping of the kidneys.

MATERIAL & METHODS

Mice

All the mice used in this study were male 19 month old WT mice of a C57BL/6J background. Mice were bred in house at the Harvard School of public health in Boston. Animals were kept under standard laboratory conditions (temperature 20–24°C, 12 h light/12 h dark, relative humidity 50–60%) mice were housed with 3–4 animals per cage and allowed unlimited access to food and water (Harvard School of Public Health, Boston, US). All experiments were performed in strict accordance with all applicable federal and institutional policies.

Anti-senescence treatments

Mice received three times (every other day) an i.v. injection of 5mg/kg FOXO4-DRI peptide (Pepscan) [20], which was freshly reconstituted in PBS. Control mice received three times (every other day) i.v. injections of PBS in injection volumes similar to peptide treatment. The combination of Quercetin (S2391 Selleckchem) and Dasatinib (S1021 Selleckchem) was administered via oral gavage at a dose of 5 an 50 mg/kg respectively for 3 days every other day. The mixture was dissolved in 2%DMSO (1029521000 Sigma), 30%PEG400 (91893 Sigma), 68% Phosal oil (368315 Lipoid). Navitoclax (A10022, Adooq) was bestowed upon the mice through oral gavage at a concentration of 50mg/kg, dissolved in 10% EtOH, 30% PEG400 and 60% Phosal oil. Navitoclax and vehicle control group were treated for 7 consecutive days. After the last day of senolytics treatment, mice could recover for 25 days before undergoing renal ischemia.

Renal Ischemia

First, mice were anaesthetized by 2.5% isoflurane inhalation (PCH 282-10-45112110, Pharmachemie). Abdominal hair was shaved and the skin was disinfected with 70% EtOH after which the mice were fastened on heating pads to maintain a stable body temperature. Then, over the abdominal midline, an incision was made. After the localization of the left renal pedicle, the renal artery and vein were dissected, and a non-traumatic clamp was used to occlude the left kidney. Immediately thereafter, the procedure was repeated on the renal artery and vein of the right kidney. Then, the wound was covered with phosphate-buffered saline (PBS)-soaked gauze which was covered with an aluminium foil covering to maintain body temperature. Both kidneys were clamped for 15 minutes. Kidneys were inspected for signs of ischemia (blue colouring). After release of the clamp, blood reflow was inspected by the recovery of normal kidney colour. Two layers of 5/0 sutures were used to close the abdominal wound. For the maintenance of fluid balance, mice received 0.5 mL PBS subcutaneously followed by a subcutaneous injection of Buprenex (buprenex hydrochloride, NDC 12496-0757-5). Then mice could recover from aneastesia under a heat lamp and their cages were moved from the operating room to the stable when they had regained consciousness. The mice received analgesics for 2 days following the surgical procedure with twice an injection of 1mg/kg slow release Buprenorfine (Rx206288 Zoopharm).

Kidney sample preparations

At the indicated timepoints, mice were killed by cervical dislocation. After decapsulation of the kidneys , they were laterally sectioned. The sagittal halves were frozen in liquid nitrogen and preserved at -80^{o}C for subsequent mRNA analyses. The cranial kidney halves were conserved in 4% formaldehyde buffered solution for 1 day and then washed with PBS before paraffin embedding.

Histology and pathology

Paraffin embedded kidneys were sliced in 3 µm sections, which underwent a hematoxylin and eosin staing, a Periodic acid–Schiff (PAS) staining or a Masson's trichrome stain. Glomerular, Tubulointerstitial, aucute tubular necrosis, and tubular dilation pathology were assessed by 2 pathologists and classified between 0 (absent) to 4 (severe) damage. No differences were found for Glomerular capillary pathology, and therefore these data were not shown in this manuscript.

Serum urea measurements

All blood samples were collected by submandibular cheek puncture. QuantiChrom assay kits (DIUR-100 BioAssay systems) were used to measure serum urea levels according to manufacturer's protocol. Whole blood cell composition was analysed with Hemavet 950 (Drew scientific).

Quantitative Real Time PCR

Kidney tissues were disintegrated and lysed in Tri reagent (Sigma) for at least 5 minutes. After chloroform extraction, RNA was precipitated using isopropanol and washed with 75% ethanol. RNA was dissolved in 20 ul DepC treated H_20 and stored at -80^{o}C. To remove DNA, RNA samples were incubated with 1U DNase (Thermo Fisher Scientific) for 30 minutes at 37^{o}C. DNAse was stopped by incubating with EDTA (25 mM) at 65^{o}C for 10 minutes. random hexamers (stock 50 uM, final 5 uM, Thermo Fisher Scientific) and dNTPs (10 mM) were added and incubated 65^{o}C for 5 minutes. After denaturation, samples were placed on ice and RT-mix was added containing 5x first strand buffer, DTT (0.1 M) and RNase out (Thermo Fisher Scientific). Samples were incubated at 25^{o}C for 2 minutes. Next 200 U Superscript II was added (Thermo Fisher Scientific) and incubated for 10 minutes at 25^{o}C and 15 minutes at 70^{o}C. Samples were stored at -20^{o}C. Quantitative Real Time-PCR was performed in a 10 µl final reaction volume using Platinum Taq DNA polymerase (Life Technologies) and Sybr Green (Sigma Aldrich) in a CFX 384 Real Time system (BioRad). Expression levels were normalize to Actin/GAPDH. Primer sequences are listed in supplementary methods Table 1.

Immunofluorescence on mice tissue slides

5 µm Paraffin sections of mouse kidney specimens were deparaffinized with Xylene and rehydrated in decreasing concentrations of ethanol. Then, sections were boiled for 30min in a pH 6, 10 mM sodium citrate buffer, for antigen retrieval. Slides were

cooled down in their buffer at RT to ~37°C and washed in Tris Buffered Saline (TBS). For 5 minutes, the slides were permeabilized in 0.2% Triton X-100 in TBS and then washed again in TBS. Tissues were blocked for 30min with 5% Normal Horse Serum (NHS) in a 0,2% gelatin-TBS solution constituted with 50nM glycine. TBS-gel containing primary antibody dilutions were spread over the tissues, which were incubated overnight at 4°C in a dark moisture chamber (primary antibodies: HMGB1, 1:500 (ab18256 Abcam), LaminB1, 1:1000 (ab16048 Abcam)). The next day, the tissues were washed with TBS-gel and then incubated with a secondary antibody (1:1000 A-11034, Invitrogen) and a nuclear staining with Hoechst 1:1000 (565877 BD Pharmingen) in TBS-gel for one hour at room temperature. Following washes with TBS-gel and dH2O, the slides were covered with soft set mounting medium (Vectashield), which was topped with a cover glass and sealed with nail polish. The stainings were imaged with a Zeiss LSM510 confocal microscope in lambda mode with subsequent spectral unmixing. Then all images were analysed with FIJI software.

Statistical analyses

All statistical analyses were performed with GraphPad Prism 8. Data are presented as mean ± SD . All p-values <0.05 were considered significant.

RESULTS

To test the effect of the senolytic removal of senescent cells in aged mice on IRI severity, we treated 19 month old WT C57BL/6J male mice with either FOXO4-DRI, navitoclax, quercetin and dasatinib (Q&D). PBS was used as a control for the FOXO4-DRI group and vehicle was used as control for the navitoclax and Q&D groups. 28 days after the start of the senolytic therapy, mice received 15' of bilateral IRI, after which they were sacrificed at 4 days and 28 days post-IRI (**figure 1a**).

Treatment with senolytics did not influence the probability of survival after IRI (**figure 1b, left and right panel**), and we did not observe any differences in overall haematological composition between treatment and control groups during the full length of the experiment (data not shown). Next, general renal function was assessed by measuring urea levels in mouse serum[22]. The urea levels of all mice peaked 4 days after IRI (**figure 1c and 1d, left panels**), confirming that IRI caused acute renal toxicity. This effect reduced over time, but stayed prevalent for at least 28 days. Importantly, on day 28 after IRI, serum urea concentrations were still significantly increased in control mice, whereas they had returned to baseline in animals treated with FOXO4-DRI peptide (**figure 1c, right panel**). No difference in urea levels were observed between the navitoclax or Q&D groups and their vehicle control on any of the measured time points (**figure 1d)**. These data provide evidence that the treatment with FOXO4-DRI peptide prior to IRI improves recovery of general renal function post IRI, while Navitoclax and Q&D did not.

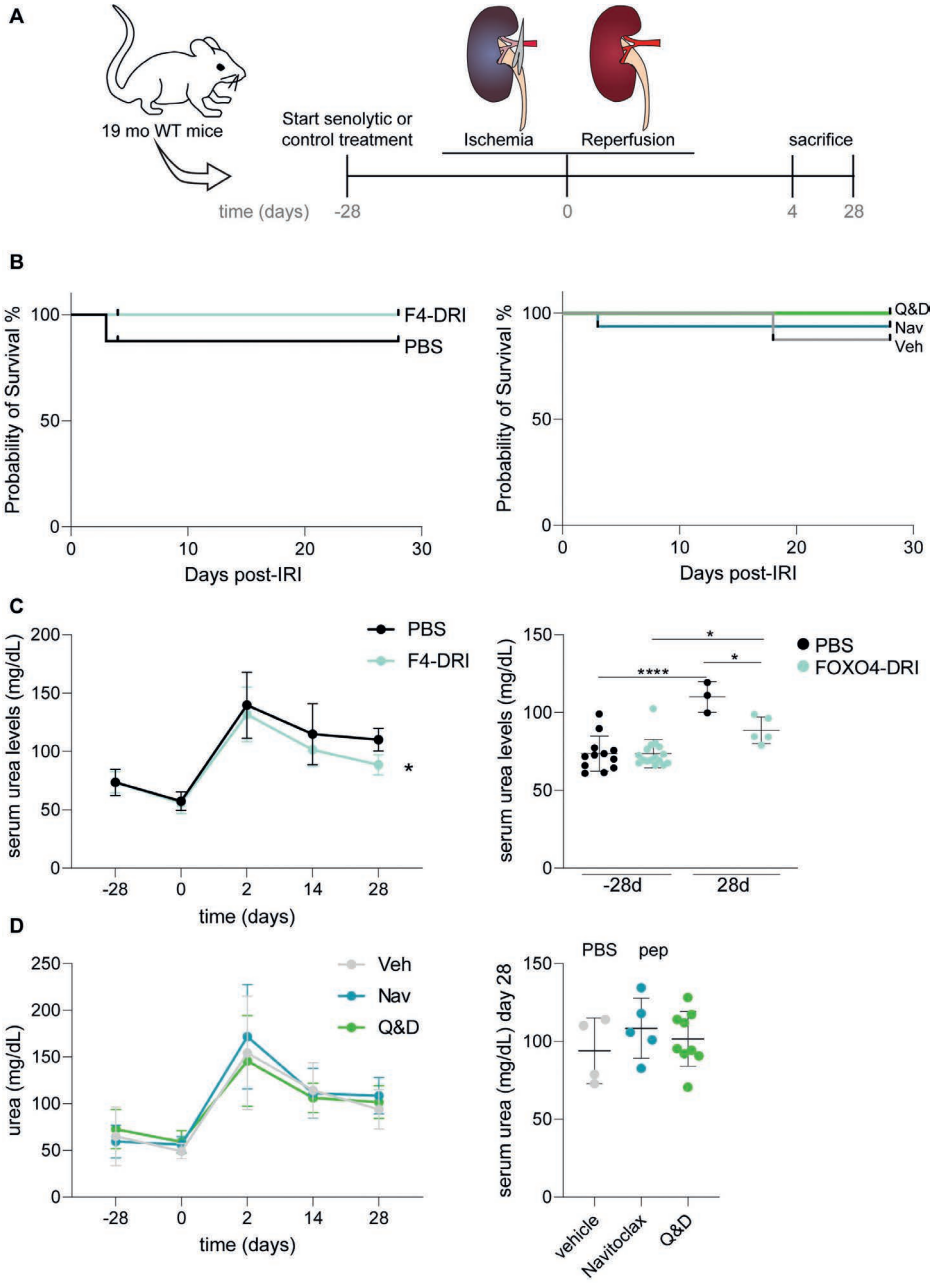

Figure 1. Removal of senescent cells in 19 month old WT C57BL/6J mice with a FOXO4-DRI peptide improves recovery after renal IRI.

A. Schematic representation of experimental procedure. WT; wild type. **B**. Kaplan-Meier survival curve post-IRI of 19 month old WT mice that were pre-treated with PBS or FOXO4-DRI before IRI (left panel) or navitoclax, quercetin and dasatinib or vehicle (right panel). **C**. Left panel: Quantification of serum urea levels over time of mice pre-treated with PBS or FOXO4-DRI at -28

days pre-IRI, until sacrifice at 28d post-IRI. Right panel: comparison between baseline (-28d) and post-IRI (28d) serum urea levels. **D**. Left panel: Quantification of serum urea levels over time of mice pre-treated with navitoclax or quercetin and dasatinib (Q&D) groups and their vehicle control at -28 days pre-IRI, until sacrifice at 28d post-IRI. Right panel: comparison between baseline (-28d) and post-IRI (28d) serum urea levels. F4-DRI; FOXO4-DRI, IRI; ischemia reperfusion injury, Nav; navitoclax, PBS; phosphate-buffered saline, Q&D; queretin and dasatinib, Veh; vehicle. P-values were calculated with one-way Anova with post-hoc Tukey's test, and the logrank test (Mantel-cox) for the Kaplan-Meier survival curve, * p < 0.05, ** p < 0.01, *** p<0.001, data are expressed as the mean ± SD.

We next assessed renal pathology of the different groups . At first, we focussed on the acute damage response, 4 days after IRI. Both the PBS and the FOXO4-DRI groups showed an upregulation in kidney injury molecule-1 (Kim1) expression levels as compared to baseline (**Figure 2a**), however, we did not observe any differences in Kim1 expression levels between the two treatments. Furthermore, there were no differences observed in the acute tubular necrosis (ATN) score between the PBS and FOXO4-DRI group 4 days after IRI (**Figure 2b**), but the overall incidence of ATN for this experiment was very low (the average of the PBS group was 0.5 on a 4-point severity scale). We did observe a trend towards the occurrence of tubular dilation, where the mice treated with FOXO4-DRI had a lower incidence of tubular dilation than the mice in the PBS group (p=0.14) (**Figure 2c**). This indicates that a mild injury could be phenotypically observed and that this tended to be lowered in the mice pre-treated with FOXO4-DRI. Again, no differences between the navitoclax or Q&D groups and their vehicle controls were observed in ATN and tubular dilation (**supplemental figure 1A-B**).

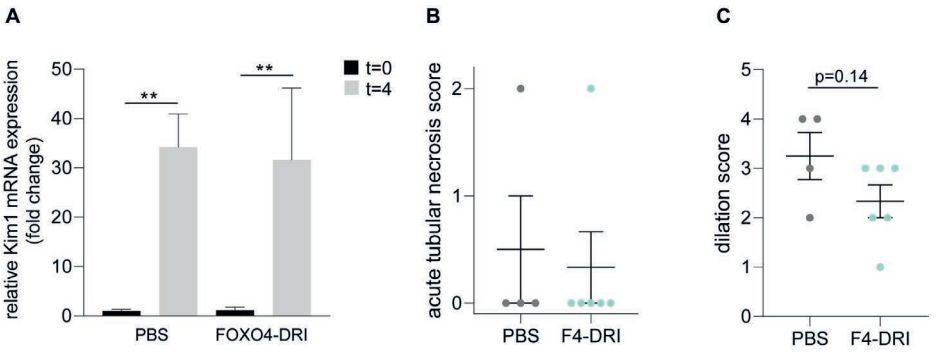

Figure 2. Renal pathology of acute injury markers in mice pre-treated with FOXO4-DRI or PBS. **A**. Relative gene expression levels of Kim1, analysed by RT-qPCR at 0 and 4 days post-IRI. **B**. Quantification of acute tubular necrosis (ATN) scores, and tubular dilation scores **(C.)** 4 days post-IRI of 19 month old WT mice that were pre-treated with PBS or FOXO4-DRI before IRI. F4-DRI; FOXO4-DRI, PBS; phosphate-buffered saline, IRI; ischemia reperfusion injury. P -values were calculated with two-tailed student T-test, * p < 0.05, ** p < 0.01, *** p<0.001, data are expressed as the mean ± SD.

Since the most pronounced effect of the FOXO4-DRI peptide on general renal function was found 28 days post-IRI, chronic kidney injury markers and markers for renal repair were assessed in the mice that were sacrificed at this time point. Kim1 mRNA expression levels were slightly lowered in the mice pre-treated with FOXO4-DRI (p=0.14) (**Figure 3a**), indicating a trend towards improved repair after injury. Next, interstitial fibrosis and tubular atrophy (IF/TA), a histological marker for expanded interstitial space that replaces healthy kidney tissue, was assessed by a renal pathologist. Again, a trend towards lowered IF/TA scores was found for the mice pre-treated with FOXO4-DRI, as compared to the PBS group (p=0.12). No differences in IF/TA scores were found between the navitoclax or Q&D groups and their vehicle control (**supplemental figure 1C**).

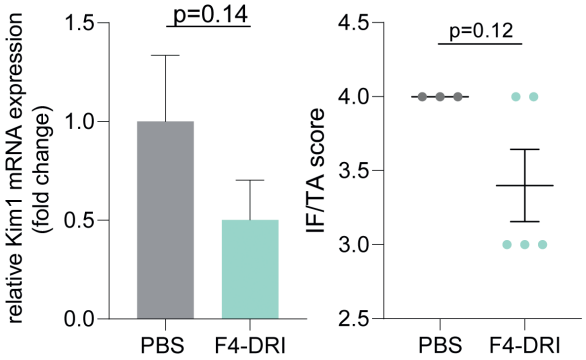

Figure 3. FOXO4-DRI pre-treated mice have slightly less renal damage 28 days after IRI compared to those pre-treated with PBS.
A. Relative gene expression levels of Kim1, analysed by RT-qPCR at 28 days post-IRI. **B**. Quantification of Interstitial fibrosis/ tubular atrophy (IF/TA) scores 28 days post-IRI of 19 month old WT mice that were pre-treated with PBS or FOXO4-DRI before IRI. F4-DRI; FOXO4-DRI, PBS; phosphate-buffered saline, IRI; ischemia reperfusion injury. P -values were calculated with two-tailed student T-test, * $p < 0.05$, ** $p < 0.01$, *** $p<0.001$, data are expressed as the mean ± SD.

Based on our unpublished data with genetic senescence removal in a mouse model, we had anticipated a more robust effect of senolytic treatment before IRI. To study this discrepancy, we checked whether the FOXO4-DRI peptide batch that was used in the mouse experiments was still functional. To do so, we used the leftover peptide in an *in vitro* experiment with senescent and proliferating IMR90 cells, as shown in the original manuscript describing the FOXO4-DRI peptide[20]. In these experiments, the FOXO4-DRI peptide induced cell death in senescent cells at low concentrations and induced cell death at high concentrations in proliferating IMR90 cells as well (data not shown). Convinced that the FOXO4-DRI peptide was capable of inducing cell death in preferentially senescent cells, we next evaluated whether FOXO4-DRI treatment in the 19 month old WT mice had removed senescent cells in the kidney. To do so, we examined senescent cell levels in mice that were sacrificed 28 days after the FOXO4-DRI of PBS treatments, without receiving renal IRI. The nuclear expression of Lamin B1 and HMGB1 both are reduced

in senescent cells[23,24]. **Figure 4A-B** shows that there is no difference in the expression of Lamin B1 and HMGB1 in kidney tissues of 19 month old WT mice treated with PBS or FOXO4-DRI. Indicating that the FOXO4-DRI treatment had not lowered the number of renal senescent cells. However, we noticed that the levels of senescent cells were already low (around 2-3%) at baseline, since the % of senescent cells in aged kidney tissues can rise to 20-30% [20]. Furthermore, the overall pathology score for these kidneys was 0.7, on a scale of 0-4, which is rather moderate for an aged mouse (**Figure 4C**). Similar results were found for the mice treated with navitoclax, Q&D and their vehicle controls (**supplemental figure 1D-E**) and in the liver (data not shown). Taken together, these data indicate that the 19 month old WT mice used in our experiment did not display any phenotype of aging. Hence, a reduction in the number of renal senescent cells could not be achieved.

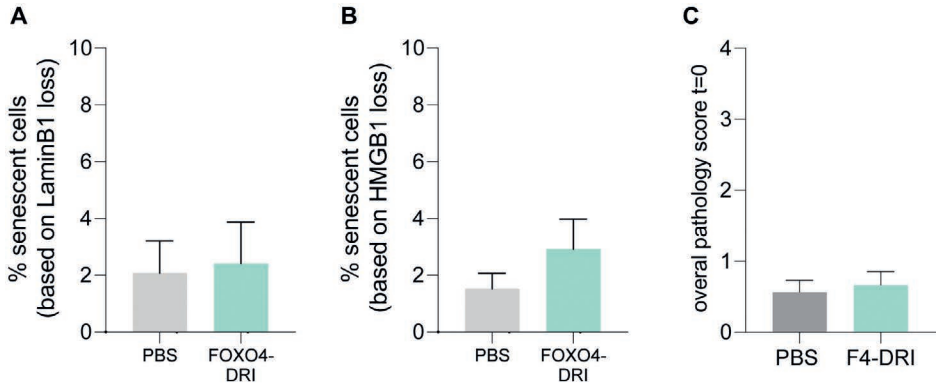

Figure 4. FOXO4-DRI does not reduce the number of senescent cells or overall pathology in 19 month old WT mice.

A-B. Quantification of % of cells positive for Lamin B1 (A) or HMGB1 (B), which was detected via immunofluorescence labelling. **C.** Quantification of overall pathology scores 28 days after start of the treatment with FOXO4-DRI or PBS in 19 month old WT mice. F4-DRI; FOXO4-DRI, PBS; phosphate-buffered saline P -values were calculated with two-tailed student T-test, * $p < 0.05$, ** $p < 0.01$, *** $p<0.001$, data are expressed as the mean ± SD.

DISCUSSION

The removal of senescent cells improves tissue integrity in various renal pathologies. Here we used several senolytics to eliminate senescent cells in 19 month old aged mice to assess whether these senolytics could improve resistance to renal ischemia reperfusion injury in aged mice. We observed that the FOXO4-DRI treatment results in better injury repair after IRI than in those mice treated with vehicle, based on improved renal function 28 days post-IRI as measured by serum urea levels, and a trend towards lowered levels of injury markers at 4 and 28 days post-IRI. No differences in injury severity after IRI was found between the navitoclax or quercetin and dasatinib groups and their vehicle control

group. However, none of the tested senolytics lowered the number of renal senescent cells that was already low at baseline.

Whether senolytics can be used to improve resistance to renal IRI in aged mice cannot be concluded from this study. Interestingly, a recent study by Mylonas et al. studying the effect of navitoclax treatment before renal IRI in aged mice, shows that this senolytic treatment is protective and improves regeneration after renal IRI. Importantly, in this study, the aged mice had high levels of senescent cells (~50% of all cells) according to LaminB1 assessment[25]. Furthermore, our previous unpublished report, wherein senescent cells had been removed with a genetic construct in aged mice before the induction of IRI, the number of senescent cells were lowered, and the severity of IRI was reduced. In this previous report, about 10 percent of all renal cells were senescent. These data support the idea that the present study cannot answer our initial research question due to the lack of senescent cells in the 19 month old mice that were used.

The fact that we could not reduce the already low number of renal senescent cells in the kidney, raises the question how the FOXO4-DRI peptide improved renal recovery after IRI. This discrepancy might be due to the limitations in detecting reductions in small numbers of cells based on LaminB1 or HMGB1intensity. Although these techniques have been demonstrated to identify a reduction or increase in the numbers of senescent cells in multiple studies before[20,23,26], it could be that these methods are not accurate enough to distinguish a difference in low levels of senescent cells.

Another possible explanation for the beneficial effects of FOXO4-DRI treatment could be that senescent cells are removed in other tissues or organs than the kidney. Senescent cells have been shown to have a deteriorating effect in cells in distant organs or tissues in mice[27]. Furthermore, the removal of senescent cells in adipose tissues of diabetic patients with the senolytic treatment quercetin and dasatinib has been shown to lower serum levels of several circulating SASP factors[28]. Suggesting that the removal of senescent cells in distant organs might have caused a better performance of the kidney after IRI in a paracrine fashion. Along with this line of reasoning, is the possibility of a senolytic effect on the cells of the immune system. Recently, Yousefzadeh et al. have reported that immunosenescence accelerates the aging of solid organs, including the kidney[29], underlining the influence of the immune system on organ function. Taken together, the FOXO4-DRI peptide might have removed senescent cells in distant organs where possibly higher levels of senescent cells were present at baseline.

Although small, FOXO4-DRI treatment had some effect, while Navitoclax and Q&D had not. The varying effects of senolytics on IRI outcome in aged mice can be attributed to their distinct targets. When senescence is induced, both pro-apoptotic and anti-apoptotic pathways are upregulated. Interfering with the anti-apoptotic response allows the pro-apoptotic pathways to induce cell death in senescent cells. So far, six different

anti-apoptotic pathways have been identified in senescent cells, which are influenced by senescent cell-type origin and the mode of senescence induction[21]. The senolytics used in this study target distinct anti-apoptotic pathways, and therefore target different senescent cells. For example, the combination of quercetin/dasatinib has been shown to strongly induce apoptosis in senescent adipose progenitor cells, but is less potent in targeting senescent renal cells[17]. In contrast, navitoclax can target senescent cells from several tissues, is lethal in fibroblast cell lines, and has no senolytic effect on senescent pre-adipocytes[30]. This likely explains the discrepancy in effect between navitoclax, quercetin and dasatinib and FOXO4-DRI treatment.

Thus, our data show that the treatment of aged mice before renal IRI with FOXO4-DRI has some beneficial effects on outcome after kidney injury induced by IRI. Due to the relatively low abundance of senescent cells in these mice, we could not demonstrate that the beneficial effects of the FOXO4-DRI peptide were caused by a reduction in the number of renal senescent cells. Follow-up research is therefore necessary to validate whether senolytics can be used to optimize aged donor kidneys for transplantation and thereby alleviate the donor kidney shortage.

Financial disclosure/Acknowledgements

HvW is supported by a grant from the Dutch Kidney Foundation (15OP11). We would like to thank dr. I. van der Pluijm for assisting us in our attempt to ship aged p16::3MR mice to Boston.

REFERENCES

1. Echterdiek F, Schwenger V, Döhler B, et al. Kidneys From Elderly Deceased Donors—Is 70 the New 60? Front Immunol. 2019;10. doi:10.3389/fimmu.2019.02701
2. Salvadori M, Rosso G, Bertoni E. Update on ischemia-reperfusion injury in kidney transplantation: Pathogenesis and treatment. World J Transplant. 2015;5(2):52-67. doi:10.5500/wjt.v5.i2.52
3. Lim WH, Clayton P, Wong G, et al. Outcomes of Kidney Transplantation From Older Living Donors. Transplant J. 2013;95(1):106-113. doi:10.1097/TP.0b013e318277b2be
4. Tasaki M, Saito K, Nakagawa Y, et al. Effect of donor–recipient age difference on long-term graft survival in living kidney transplantation. Int Urol Nephrol. 2014;46(7):1441-1446. doi:10.1007/s11255-014-0655-8
5. Hernandez-Segura A, Nehme J, Demaria M. Hallmarks of Cellular Senescence. Trends Cell Biol. 2018;28(6):436-453. doi:10.1016/J.TCB.2018.02.001
6. Campisi J. Aging, Cellular Senescence, and Cancer. Annu Rev Physiol. 2013;75(1):685-705. doi:10.1146/annurev-physiol-030212-183653
7. Coppé J-P, Desprez P-Y, Krtolica A, Campisi J. The senescence-associated secretory phenotype: the dark side of tumor suppression. Annu Rev Pathol. 2010;5:99-118. doi:10.1146/annurev-pathol-121808-102144
8. Coppé J-P, Patil CK, Rodier F, et al. Senescence-Associated Secretory Phenotypes Reveal Cell-Nonautonomous Functions of Oncogenic RAS and the p53 Tumor Suppressor. Downward J, ed. PLoS Biol. 2008;6(12):e301. doi:10.1371/journal.pbio.0060301
9. Zhang H, Pan KH, Cohen SN. Senescence-specific gene expression fingerprints reveal cell-type-dependent physical clustering of up-regulated chromosomal loci. Proc Natl Acad Sci U S A. 2003;100(6):3251-3256. doi:10.1073/pnas.2627983100
10. Shelton DN, Chang E, Whittier PS, Choi D, Funk WD. Microarray analysis of replicative senescence. Curr Biol. 1999;9(17):939-945. doi:10.1016/S0960-9822(99)80420-5
11. Aan GJ, Ahmad Hairi H, Makpol S, Abdul Rahman M. Differential Protein Expression in Senescent Human Skin Fibroblasts and Stress Induced Premature Senescence (SIPS) Fibroblasts (Perbezaan Pengekspresan Protein Dalam Fibroblas Kulit Manusia Senesen Dan Fibroblas Senesen Pramatang Teraruh Tekanan). Vol 40.; 2011.
12. Aan GJ, Hairi HA, Makpol S, Rahman MA, Karsani SA. Differences in protein changes between stress-induced premature senescence and replicative senescence states. Electrophoresis. 2013;34(15):2209-2217. doi:10.1002/elps.201300086
13. Baker DJ, Wijshake T, Tchkonia T, et al. Clearance of p16Ink4a-positive senescent cells delays ageing-associated disorders. Nature. 2011;479(7372):232-236. doi:10.1038/nature10600
14. Baker DJ, Childs BG, Durik M, et al. Naturally occurring p16Ink4a-positive cells shorten healthy lifespan. Nature. 2016;530(7589):184-189. doi:10.1038/nature16932
15. Chang J, Wang Y, Shao L, et al. Clearance of senescent cells by ABT263 rejuvenates aged hematopoietic stem cells in mice. Nat Med. 2015;22(1):78-83. doi:10.1038/nm.4010
16. Yosef R, Pilpel N, Tokarsky-Amiel R, et al. Directed elimination of senescent cells by inhibition of BCL-W and BCL-XL. Nat Commun. 2016;7:11190. doi:10.1038/ncomms11190
17. Zhu Y, Tchkonia T, Pirtskhalava T, et al. The Achilles' heel of senescent cells: from transcriptome to senolytic drugs. Aging Cell. 2015;14(4):644-658. doi:10.1111/acel.12344
18. Roos CM, Zhang B, Palmer AK, et al. Chronic senolytic treatment alleviates established vasomotor dysfunction in aged or atherosclerotic mice. Aging Cell. 2016;15(5):973-977. doi:10.1111/acel.12458

19. Hickson LTJ, Langhi Prata LGP, Bobart SA, et al. Senolytics decrease senescent cells in humans: Preliminary report from a clinical trial of Dasatinib plus Quercetin in individuals with diabetic kidney disease. EBioMedicine. 2019;47:446-456. doi:10.1016/j.ebiom.2019.08.069
20. Baar MP, Brandt RMC, Putavet DA, et al. Targeted Apoptosis of Senescent Cells Restores Tissue Homeostasis in Response to Chemotoxicity and Aging. Cell. 2017;169(1). doi:10.1016/j.cell.2017.02.031
21. Kirkland JL, Tchkonia T, Zhu Y, Niedernhofer LJ, Robbins PD. The Clinical Potential of Senolytic Drugs. J Am Geriatr Soc. 2017;65(10):2297-2301. doi:10.1111/jgs.14969
22. JL. L. Blood urea nitrogen and creatinine. Emerg Med Clin North Am. 4((2)):223-233. pmid:3516645
23. Freund A, Laberge R-M, Demaria M, Campisi J. Lamin B1 loss is a senescence-associated biomarker. Mol Biol Cell. 2012;23(11):2066-2075. doi:10.1091/mbc.E11-10-0884
24. Davalos AR, Kawahara M, Malhotra GK, et al. p53-dependent release of Alarmin HMGB1 is a central mediator of senescent phenotypes. J Cell Biol. 2013;201(4):613-629. doi:10.1083/jcb.201206006
25. Mylonas KJ, O'Sullivan ED, Humphries D, et al. Cellular senescence inhibits renal regeneration after injury in mice, with senolytic treatment promoting repair. Sci Transl Med. 2021;13(594):eabb0203. doi:10.1126/scitranslmed.abb0203
26. Wang AS, Ong PF, Chojnowski A, Clavel C, Dreesen O. Loss of lamin B1 is a biomarker to quantify cellular senescence in photoaged skin. Sci Rep. 2017;7(1):1-8. doi:10.1038/s41598-017-15901-9
27. Barinda AJ, Ikeda K, Nugroho DB, et al. Endothelial progeria induces adipose tissue senescence and impairs insulin sensitivity through senescence associated secretory phenotype. Nat Commun. 2020;11(1):1-13. doi:10.1038/s41467-020-14387-w
28. Hickson LTJ, Langhi Prata LGP, Bobart SA, et al. Senolytics decrease senescent cells in humans: Preliminary report from a clinical trial of Dasatinib plus Quercetin in individuals with diabetic kidney disease. EBioMedicine. 2019;47:446-456. doi:10.1016/j.ebiom.2019.08.069
29. Yousefzadeh MJ, Flores RR, Zhu Y, et al. An aged immune system drives senescence and ageing of solid organs. Nature. 2021;594(7861):100-105. doi:10.1038/s41586-021-03547-7
30. Zhu Y, Tchkonia T, Fuhrmann-Stroissnigg H, et al. Identification of a novel senolytic agent, navitoclax, targeting the Bcl-2 family of anti-apoptotic factors. Aging Cell. 2016;15(3). doi:10.1111/acel.12445

SUPPLEMENTAL FIGURES

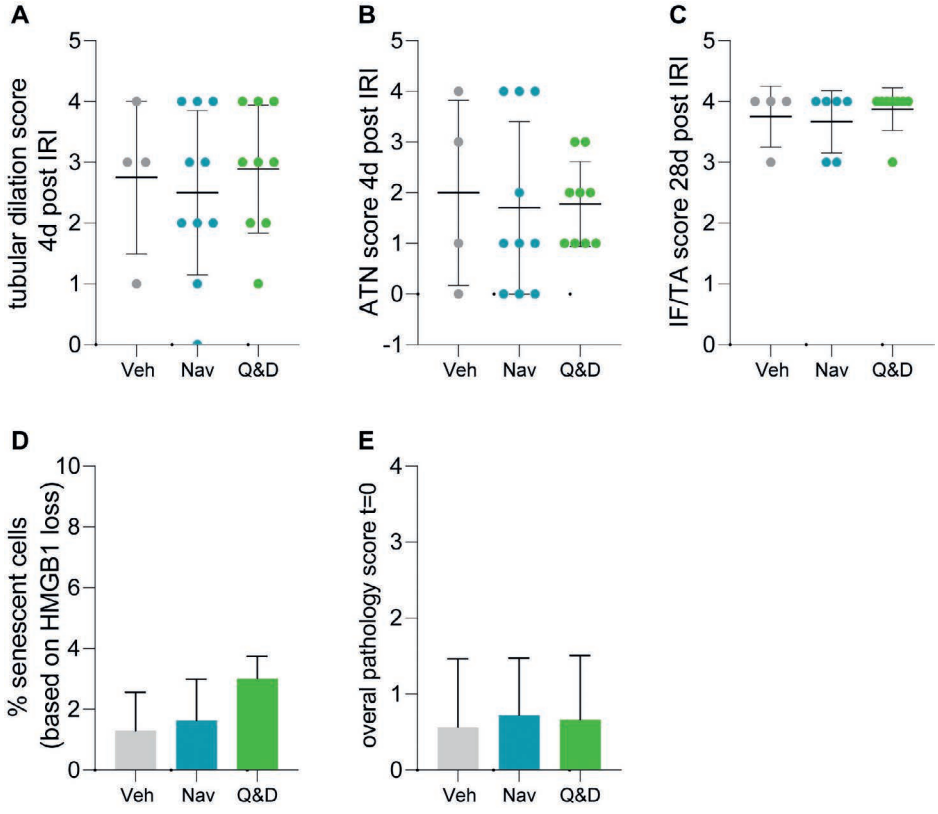

Supplemental Figure 1. Analyses of WT mice pre-treated with navitoclax or quercetin and dasatinib before renal IRI

A-B. Quantification of acute tubular necrosis (A) or tubular dilation (B) scores 4 days post renal IRI, on a scale of 0-4. **C.** Quantification of interstitial fibrosis / tubular atrophy score 28 days after renal IRI in 19 month old WT mice. **D** Quantification of % of cells positive for HMGB1, which was detected via immunofluorescence labelling, 28 days after start of the treatment with navitoclax, quercetin and dasatinib or vehicle in 19 month old WT mice. **E**. Quantification of overall pathology scores 28 days after start of the treatment with navitoclax, quercetin and dasatinib or vehicle in 19 month old WT mice. Veh; vehicle, Nav; navitoclax, Q&D; quercetin and dasatinib. P -values were calculated with two-tailed student T-test, * $p < 0.05$, ** $p < 0.01$, *** $p<0.001$, data are expressed as the mean ± SD.

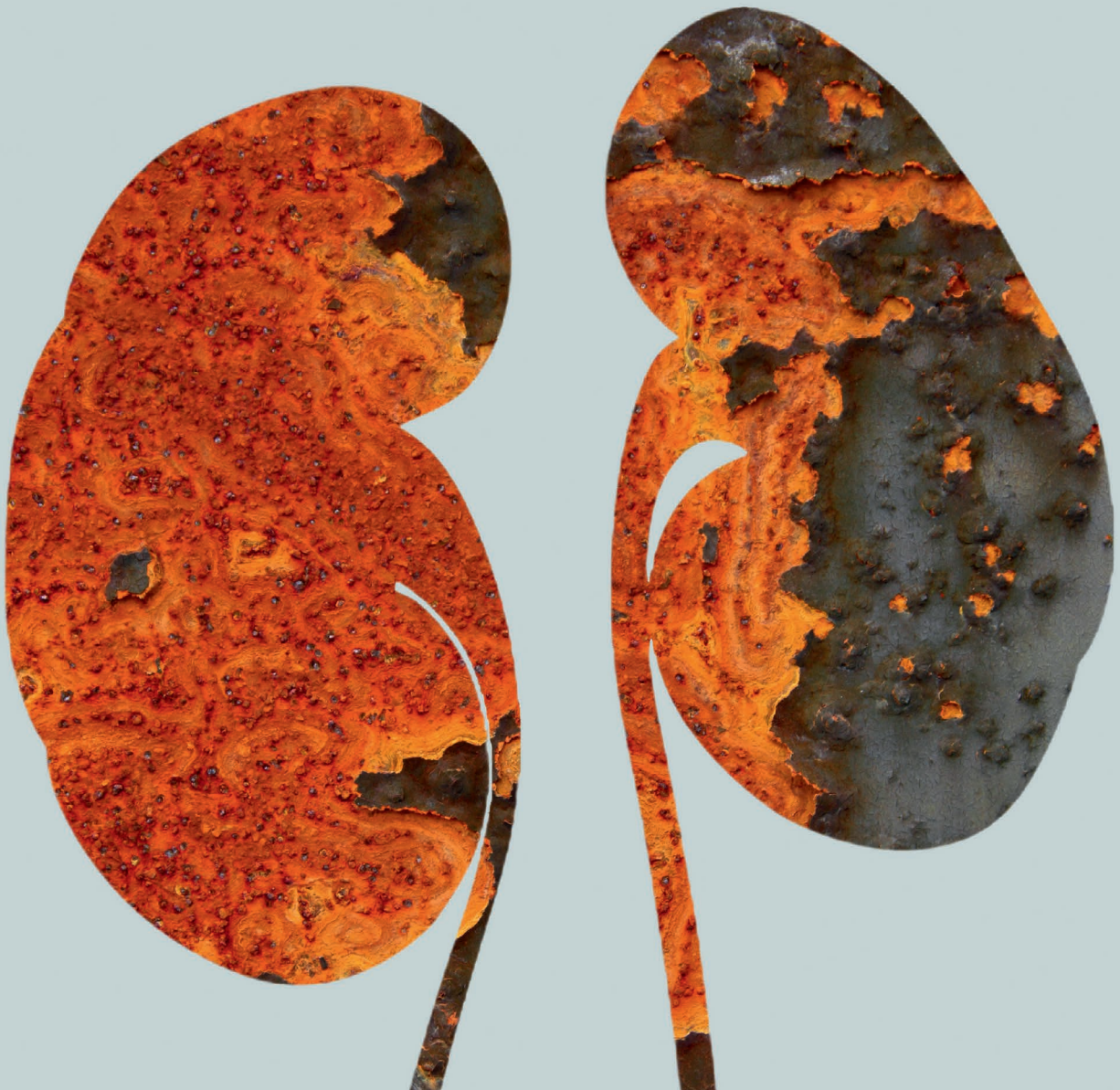

Chapter 5

Cellular Senescence as a Therapeutic Target to Improve Renal Transplantation Outcome

Hester van Willigenburg[1,2], Peter L.J. de Keizer[1,3], Ron W.F. de Bruin[1]
[1] Department of Surgery, Erasmus MC Transplant Institute Rotterdam, Rotterdam, The Netherlands, [2] Department of Molecular Genetics, Erasmus University Medical Center, Rotterdam, The Netherlands, [3] Department of Molecular Cancer Research, Center for Molecular Medicine, University Medical Center Utrecht, Utrecht University, The Netherlands

Pharmacological Research, 2018 Apr, PMID: 29471104

ABSTRACT

Kidney transplants from aged donors are more vulnerable to ischemic injury, suffer more from delayed graft function and have a lower graft survival compared to kidneys from younger donors. On a cellular level, aging results in an increase in cells that are in a permanent cell cycle arrest, termed senescence, which secrete a range of pro-inflammatory cytokines and growth factors. Consequently, these senescent cells negatively influence the local milieu by causing inflammaging, and by reducing the regenerative capacity of the kidney. Moreover, the oxidative damage that is inflicted by ischemia-reperfusion injury during transplantation can induce senescence and accelerate aging.

In this review, we describe recent developments in the understanding of the biology of aging that have led to the development of a new class of therapeutic agents aimed at eliminating senescent cells. These compounds have already shown to be able to restore tissue homeostasis in old mice, improve kidney function and general health- and lifespan. Use of these anti-senescence compounds holds great promise to improve the quality of marginal donor kidneys as well as to remove senescent cells induced by ischemia-reperfusion injury. Altogether, senescent cell removal may increase the donor pool, relieving the growing organ shortage and improve long-term transplantation outcome.

Abbreviations

CDK	cyclin-dependent kinase
CKD	chronic kidney disease
DR	dietary restriction
ESRD	end stage renal disease
FOXO4	Forkhead BOX O 4
HSP-90	heat shock protein 90
IF	interstitial fibrosis
IL-6	interleukin-6
IRI	ischemia reperfusion injury
NSAID	Nonsteroidal anti-inflammatory drug
PDGF-AA	platelet-derived growth factor-AA
ROS	reactive oxygen species
SASP	senescence associated secretory phenotype
TA	tubular atrophy
WT	wild type

INTRODUCTION

Aged kidneys perform worse after transplantation

Aging is the main risk factor for the development of age-related chronic diseases, which, in turn, pose a major burden for health care services and society [1–5]. This also holds true for kidney function. Age associated decline in kidney function can be accelerated by diabetes, hypertension and kidney diseases resulting in chronic kidney disease (CKD) [6,7]. With an estimated prevalence between 11 and 13% worldwide, CKD is a major age-related disease [6,8]. The treatment of CKD is mainly designed around targeting underlying causes such as inflammation, hypertension or obesity. Unfortunately, these only rarely restore primary kidney function [9].

The further decline of kidneys suffering from CKD can lead to end stage renal disease (ESRD), which is characterized by such loss of renal function that patients are in need of kidney replacement therapy such as dialysis or the more favorable kidney transplantation [7,10,11]. This has come at a cost, as due to the continuous increase in population age, not only the incidence of ESRD has increased, but consequently also the demand for donor kidneys, leading to a shortage of suitable donor kidneys. To meet the required demand, kidneys from extended criteria donors are now accepted, including those from old donors [10]. This in turn, has created a new layer of complications. Kidney transplants from aged (65+ years) donors are more vulnerable to ischemic injury, suffer more from delayed graft function and have a lower graft survival compared to kidneys from younger donors [12–15]. Also at the side of the recipient, old age is a complicating factor as aged patients are more vulnerable to dialysis-associated side effects and have a reduced survival rate after organ transplantation[16]. Finally, the transplantation procedure itself is a source of damage, which further accelerates the aging of the organ. This is delineated by the increased numbers of aged (senescent) cells, decreased function and increase of interstitial fibrosis (IF) and tubular atrophy (TA), as seen both in humans and model organisms such as mice following ischemia reperfusion injury (IRI) and transplantation [17,18]. Therefore, profit could be gained by tackling aging in old CKD patients and aged kidney donors as well as patients that have undergone kidney transplantation.

As aging is associated with poor kidney function, and IRI accelerates aging, advances in anti-aging research might provide new insights and treatment options to improve the outcome of kidney transplantation. To convert these findings to transplantation research, it is important to understand what drives aging on a cellular level.

Aging causes senescence and an associated pro-inflammatory phenotype

Aging can be described as the decline of physiological integrity due to an accumulation of damage and deterioration of protein and organelle function [3]. Whereas damaged proteins and organelles can be restored or replaced, cells only contain one copy of

their DNA and therefore unresolved DNA damage could have permanent deleterious consequences. Fortunately, most DNA damage can be repaired by specialized DNA damage repair mechanisms [19]. However, as these are not perfect, there is a chronic build-up of unresolved damage in time. This can accelerate cellular aging and in parallel lead to mutations that are potentially oncogenic [19]. To prevent the passage of DNA damage to daughter cells, the affected cells can undergo cell intrinsic cell death (apoptosis) or enter a state of permanent cell cycle arrest, called senescence [20,21]. Whereas critical levels of DNA damage are considered a major cause for senescence induction, several other stimuli have also been described, such as telomere shortening, high levels of reactive oxygen species (ROS), oncogenic mutation, chromatin remodeling and mitochondrial dysfunction [22]. Regardless of its cause, senescence is permanent and can independently be enforced by persistent upregulation of the cyclin-dependent kinase (CDK) inhibitors $p16^{Ink4a}$ or $p21^{Cip1}$, the latter in a p53 dependent manner (Fig.1). These force a permanent cell cycle arrest by impairing the activity of CDK's that are required for progression through the G1/S phase of the cell cycle [22–24]. The establishment of senescence is a multi-step process that can take several days to complete [25].

A permanent cell cycle arrest is not the only characteristic of senescent cells. In the majority of cases, senescent cells develop a phenotype in which they permanently secrete a plethora of factors such as proinflammatory cytokines and chemokines (i.e. interleukins-6 (IL-6), -8, -1α/β), matrix metalloproteinases (i.e. MMP-1, -3, -10) and growth factors [26,27]. The secretion of these factors by senescent cells is known as the senescence associated secretory phenotype (SASP). For a complete list of SASP factors and their function, we refer the readers to Coppé et al. (2010).

Through the SASP, senescent cells permanently impair tissue function during aging

Due to the secretory phenotype, senescent cells can have a diverse impact on their microenvironment. This can be beneficial, but only when present in a transient setting, e.g. during conditions of acute wound healing where some SASP factors such as platelet-derived growth factor-AA (PDGF-AA) aid in wound closure [28]. Similarly in models for cirrhosis-induced liver fibrosis or during certain stages of embryonic development the transient presence of senescent cells can be beneficial [22,29]. In contrast, senescent cells can cause severe problems when they exist permanently and their chronic secretion of SASP factors can have long term detrimental consequences. Fortunately, the secretion of cytokines and chemokines by senescent cells can attract immune cells and as such, the SASP primes senescent cells for degradation, especially by natural killer cells and other leukocytes [27,30]. However, during aging the efficiency of the immune system declines, impairing the eradication of SASP expressing senescent cells [22,31]. The gradual loss of senescent cell immune surveillance and the accumulation of damage with age, leads to increased numbers of senescent cells during aging. Importantly, immune surveillance in transplant recipients is also long-term suppressed with immune suppressive drugs to

prevent allograft rejection [32,33]. Thus, the ineffective clearance of senescent cells by the immune system leads to their increase in aged tissues and transplanted kidneys which can ultimately impair organ integrity.

Through SASP, accumulated senescent cells contribute to age associated low grade chronic inflammation (inflammaging) [34]. Inflammaging is a risk factor for age related diseases, as most of them have an inflammatory pathogenesis. Indeed, senescent cells are found at sites of age related pathologies such as glomerular disease, chronic allograft nephropathy, osteoarthritis, atherosclerosis and, ironically, cancer [20,22,35–37].

Furthermore, due to the inability of senescent cells to replace other damaged cells during wound healing, senescence reduces the regenerative capacity of tissues. This is particularly harmful in kidney tubules, as replacement of damaged tubular epithelial cells by surviving counterparts, is impaired when these are in a chronic cell cycle arrest [38]. Furthermore, senescent cells can invoke pluripotency in their neighboring cells [39]. As we reasoned before, senescent cells may thus impair tissue rejuvenation by enforcing a permanent state of stemness, which has been coined as the senescence stem-lock model for aging [40]. In this model, the persistent secretion of SASP factors as IL-6 invokes a state of pluripotency in neighboring cells. As the SASP is persistent, so is this remodeling event and at times of need, differentiation of these cells is impaired, hampering tissue rejuvenation. Taken together, the impact of senescent cells on tissue integrity depends on the moment and duration of their existence. By aiding in an acute manner during cutaneous wound repair and through the prevention of potential neoplastic cell proliferation, senescence can be regarded as beneficial. But, whenever our immune system fails to remove these cells, chronic SASP secretion impairs proper tissue function and regeneration, leading to a decline in organ function as seen with increasing age. How senescence affects tissue function at different stages of renal transplantation will be discussed next.

Senescent cells impair immediate and long-term transplant outcome

Natural aging causes senescence and reduces kidney function

The growing shortage of kidney donors has led to the utilization of marginal organs, such as aged donor kidneys. Besides reduced filtering capacity, aged donor kidneys show delayed graft function and reduced graft survival time [12,13]. This is, at least in part, caused by aged kidneys being more vulnerable to ischemia reperfusion injury (IRI) [12,14,15]. These processes cause a strong cellular oxidative stress response, resulting in impaired metabolism, inflammation and cell death [38]. In turn, these contribute to delayed graft function, graft rejection, fibrosis and acute or chronic kidney failure [41]. Senescent cells may be a prime culprit of these effects as they are known to reduce tissue regeneration, induce chronic inflammation and can enhance oxidative stress levels, stacked upon the

levels caused by IRI [27,38]. Indeed, elevated mRNA expression levels of several potent senescence markers such as $p21^{Cip1}$ and $p16^{Ink4a}$ in pre-transplant biopsies correlate with poor outcome of renal transplantation [42–44]. Therefore, aged donor kidneys might benefit from strategies that remove senescent cells to improve their resistance against IRI and improve transplant outcome.

Transplantation can amplify the senescence burden of grafted tissue

In addition to the natural build-up of senescence during aging, senescence can also be triggered actively when healthy cells are exposed to excessive amounts of damage, such as oxidative damage [22,36]. Thus, it could be that the oxidative stress caused by IRI can further elevate senescence burden of the already affected donor kidney. Deep biopsies of successfully transplanted organs are scarce, making it difficult to distinguish the levels of senescence after transplantation from those already present senescent cells in the donor organ, since superficial cortical biopsies do not reflect the level of senescence of the organ. Nonetheless, several studies show that transplantation induces senescence. For one, oxidative stress, as caused by IRI, was shown to be able to invoke senescence and lead to the accumulation of senescent cells in mice [41,45,46]. Moreover, renal IRI in mouse kidneys induced upregulation in protein or mRNA expression of senescence markers such as $p21^{Cip1}$ and $p16^{Ink4a}$ [17,47,48]. Also, hypertension, a common side-effect of transplantation can induce $p16^{Ink4a}$ driven senescence in both humans and rats [49]. A similar increase in protein expression of $p16^{Ink4a}$ was shown in post-transplant biopsies of rejected human kidneys [18], at least suggesting that this also holds true for humans. Whereas in healthy subjects senescent cells are removed by the immune system, this will be hampered in transplant recipients due to their long term follow-up with immunosuppressive drugs [30,32]. Thus, injuries associated with transplantation can induce senescence, which, on top of the already present levels of senescence in the donor tissue, cannot be removed by the immune system and may further contribute to the long-term damaging effects of transplantation.

Induction of temporary but not permanent senescence improves IRI outcome

Even though it is apparent that transplantation outcome can be improved by the removal of senescent cells before and after transplantation, the role of senescence during transplantation is more complicated. It is known that senescent cells have a beneficial role during cutaneous wound repair through the secretion of SASP factors [28,50]. However, it remains unclear whether senescent cells are also involved in renal repair [51,52]. To assess the role for senescence and SASP during IRI, diverse studies with senescence pathway knock out mice have been performed, with both beneficial and disadvantageous outcomes (Fig 1). There appears to be a discrepancy between which senescence pathway is interfered with versus disease outcome. For instance, mice carrying a homozygous deletion of the *cdkn2a* locus, which codes for the proteins $p16^{INK4a}$ and $p19^{ARF}$, have decreased levels of apoptosis and IF/TA, improved epithelial regeneration and improved creatinine clearance

after IRI, compared to wildtype (WT) littermates [17,53]. Transplantation of a *cdkn2a*$^{-/-}$ kidney to a WT mouse also improves survival and reduces IF/TA compared to transplantation of a WT kidney, suggesting a beneficial effect for the inhibition of senescence induction during IRI [17]. In contrast, depletion of p21^{Cip1}, which is also individually capable of inducing and maintaining senescence, aggravates ischemic injury compared to wild type mice, opposite to the effect of *cdkn2a*$^{-/-}$ mice [54,55]. Thus apparently, the mode of cell cycle arrest induction is of importance to the outcome of kidney injury.

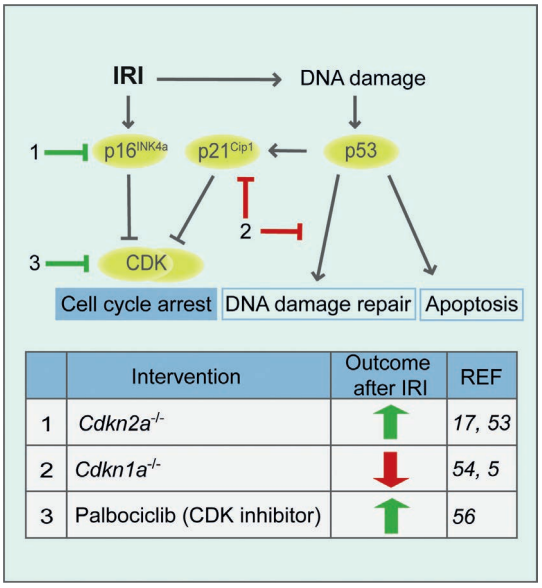

	Intervention	Outcome after IRI	REF
1	*Cdkn2a*$^{-/-}$	↑	*17, 53*
2	*Cdkn1a*$^{-/-}$	↓	*54, 5*
3	Palbociclib (CDK inhibitor)	↑	*56*

Figure 1. A temporary, but not permanent cell cycle arrest improves outcome after IRI.
Upon severe IRI induced DNA damage, p21^{Cip1} is activated to allow for DNA damage repair. This temporary cell cycle arrest can advance into senescence or apoptosis when DNA damage is irreparable. A knock out of the *Cdkn1a* locus, which codes for p21^{Cip1}, reduces DNA damage repair and worsens IRI outcome. In contrast, knock out of the *Cdkn2a* locus, coding for p16^{Ink4a}, which still allows DNA damage repair via p53 and p21^{Cip1}, improves IRI outcome. Therapeutic inhibition of CDK's using Palbociclib induces a temporary cell cycle arrest which improves outcomes after renal IRI. This might be caused by allowing DNA damage repair, without inducing senescence. Abbreviations: IRI; ischemia-reperfusion injury; CDK, cyclin-dependent kinase

This might be explained by differences in the mode of action through which p21^{Cip1} and p16^{Ink4a} regulate cell cycle arrest. Oxidative stress due to IRI causes DNA damage, which activates the DNA damage response and p53. To allow for acute DNA damage repair, p53 rapidly induces p21^{Cip1} transcription. P21^{Cip1} induces an initial temporary cell cycle arrest, which is reversed when repair is completed and only becomes a permanent senescence-mediated arrest when the DNA damage is irreparable. P16^{Ink4a}, on the other hand, is activated in a much slower fashion, taking up to 4 days after the damaging insult, and triggers a permanent senescence-arrest [22]. Activation of p53 due to IRI, cannot allow

for a temporary cell cycle arrest in *p21$^{Cip1\ -/-}$* mice, thus resulting in apoptosis or p16^{Ink4a} induced senescence, instead of DNA damage repair. The induction of a cell cycle arrest, without inducing senescence, which allows for DNA damage repair, might on the other hand improve IRI outcome. Excitingly, mimicking the mode of action of p16^{Ink4a}, only in a temporary fashion with the use of the CDK4/6 inhibitor Palbociclib, ameliorates the effects of IRI in mice by inducing a temporary cell cycle arrest [56]. Together, these data suggest that during transplantation-induced injury a temporary cell cycle arrest through p21^{Cip1} and the subsequent DNA damage repair response, is favored over the induction of a permanent cell cycle arrest via p16^{Ink4a}. Therefore, anti-senescence treatment should focus on the removal of established senescent cells but not on preventing the induction of cell cycle arrest via p21^{Cip1}.

Therapeutic interventions that prevent the induction of senescence and reduce SASP

Prevention of senescence induction after transplantation may improve outcome

To counteract the deleterious effects of senescence on transplantation success, an attractive solution would be to prevent accumulation of senescent cells in the first place. This is challenging for donor grafts in which the damage is already present, but it may be applicable to the recipient before and after transplantation (Fig 2). As senescence can both develop naturally over a prolonged period of time, or be actively induced by acute stress, different approaches may be necessary to prevent either. During IRI, any treatment that would prevent immediate oxidative stress and DNA damage might prevent the onset of senescence, whereas the prevention of aging associated senescence is closely related to a healthy lifestyle, such as regular exercise and a healthy diet [57,58]. It has been 80 years, since the life extending effects of caloric restriction were shown on rats by the group of McCay [59]. This simple intervention that restricts dietary intake without causing malnutrition, promotes a plethora of health benefits. Even though it is inconvenient to maintain dietary restriction (DR) regiments in practice, many studies testing the effects of DR in humans and animals collectively showed that DR lowers total cholesterol, improves insulin sensitivity, lowers DNA damage and oxidative stress and reduces levels of senescence markers p16^{Ink4a} and p21^{Cip1} [60–64]. The most profound features of DR on kidney function are improved filtration rates and reduced levels of fibrosis through a reduction in epithelial-to-mesenchymal-transition, which is recognized as a part of the kidney fibrosis mechanism during aging [60,63]. Therefore, dietary restriction might be considered as a means to prolong graft function after transplantation in recipients. There are indications that DR may be beneficial to acute transplantation-mediated injuries as well. For instance, 3 days of preoperative fasting protects against IRI, even in aged and overweight mice [65–68]. Dietary restriction increases expression of antioxidant defense markers and reduces expression of inflammatory markers through upregulation of the SIRT1, AMPK and downregulation of mTOR pathways [60,67]. These are all

interesting targets for lifespan extension and have exited researchers to pharmaceutically intervene with these processes to mimic the beneficial effects of dietary restriction, such as with Resveratrol, Metformin, Rapamycin and Nicotinamide mononucleotide [69–76]. Together, these data argue that healthy lifestyle factors, as reduced dietary intake, may improve graft function and are important determinants in the long-term outcome after renal transplantation.

Reducing SASP can improve organ function

DR interferes with many processes, but one pronounced beneficial consequence of DR is the systemic reduction in chronic inflammation. Therefore, DR might not only be used to prevent the development of senescent cells during aging, but also to reduce the negative effects of the SASP from pre-existing senescent cells. As such, anti-inflammatory compounds might give similar beneficial effects on health. The use of broad spectrum anti-inflammatory drugs, such as nonsteroidal anti-inflammatory drugs (NSAIDs) inhibit SASP and the production of prostaglandins, hormone-like lipids that are involved in inflammation [77,78]. Arguments that such drugs may be beneficial in counteracting SASP-mediated effects on aging, are for instance provided by studies showing that NSAIDs improve the lifespan and reduce the age-associated disease burden of fast aging *Lmna*$^{-/-}$ progeria mice that suffer from excessive senescence load and the associated inflammation [79]. A complication with NSAID treatment however, is that long term treatment can lead to severe adverse effects on stomach and intestinal integrity, and vascular and renal deterioration [77]. Inhibition of the JAK/STAT pathway, which is important for SASP expression, reduces organ dysfunction and insulin resistance and even frailty in old mice [77,80]. Unfortunately, also long term treatment with these compounds has deleterious effects as they can result in anemia and thrombocytopenia in humans [81]. Reduction of SASP might aid during and after renal transplantation. However, long periods of SASP reduction as accomplished by NSAID or use of JAK/STAT -inhibitors, are associated with complications on their own. Therefore, removing the root of the problem by eliminating senescent cells is preferred [73,82].

Therapeutic options to clear senescent cells

The discovery and development of anti-senescence compounds have been challenging researchers ever since the genetic removal of senescent cells was shown to improve healthspan and prolong lifespan [83,84]. Anti-senescence compounds, also referred to as senolytics or senotherapeutics, are food for imagination as animal studies show they can reverse aging phenotypes, including improvement of kidney function [40]. For example, the genetic removal of senescent cells in aged INK-ATTAC mice, lowered blood urea nitrogen levels and attenuated glomerulosclerosis [84].

As more and more anti-senescence drugs are being discovered or designed, it is important to optimize these to limit undesirable side effects. Senescence occurs throughout the body both diverse in cell types, mode of induction and maintenance and therefore

they are a heterogeneous cell population, which makes it difficult to distinguish them from healthy cells and specifically target them. Furthermore, it is crucial that an anti-senescence therapy eliminates the cells. Non-lethal damage could cause them to acquire mutations that force them back into a state of proliferation, adding to the potential of becoming tumorigenic. One potent area of therapy-development would thus be to develop drugs that selectively force senescent cells into apoptosis. Recently several anti-senescence drugs have been identified or prospectively designed of which few have proven to have anti-senescence abilities *in vivo* (table 1).

Regardless of the various reported anti-senescence compounds that may have more or less specific activity, two types of anti-senescence drugs have proven to be potent and consistent and we will highlight these here as such: the pan-BCL family inhibitor ABT-263 (Navitoclax) and the FOXO4 D-Retro-Inverso peptide (FOXO4-DRI).

Navitoclax

As the viability of senescent cells relies on their resistance to apoptosis, an anti-apoptotic approach might selectively target senescent cells. The pan-BCL inhibitor ABT-263 is a BH-3 mimetic that can overcome BCL-2 family regulated prevention of apoptosis [85]. ABT-263, with the commercial name Navitoclax, has been shown to remove senescent cells in aged mice and promote rejuvenation of stem cells of several tissues, allowing for tissue regeneration [86,87]. Unfortunately, apoptosis is not restricted to senescent cells, and interfering with this response may lead to adverse side-effects. Clinical trials with Navitoclax in cancer patients have revealed the dependence of platelets on BCL-2 and as a result ABT-263 reduces circulating platelet numbers and induces (severe) thrombocytopenia [88,89]. Other BCL-2 family inhibitors such as A1331852 and A1155463 also proved to be toxic and did not target all senescent cells [90]. However, these side effects might be overcome with the use of targeted delivery of these compounds [91].

FOXO4-DRI

Whereas the former drugs were discovered through multi-compound screening approaches, a different approach was used for the generation of the recently described anti-senescence compound FOXO4-DRI [92]. In contrast to the other members of the Forkhead BOX O family, FOXO1 and 3, FOXO4 inhibition is well tolerated in cells and *Foxo4*$^{-/-}$ mice show a relatively normal lifespan [93–95]. In senescent cells it was found that FOXO4 can serve as a binding partner of p53, preventing it from orchestrating its pro-apoptotic response [92,96]. This interaction formed the basis for an innovative approach; the disruption of the specific p53 and FOXO4 interaction with a peptide allowing p53 induced apoptosis of senescent cells[40,92,97].

Because p53 regulates many important processes in non-senescent cells, inhibition of complete protein function is undesirable. The small interfering peptide FOXO4-DRI was designed to overcome this off-target sensitivity [40,92]. FOXO4-p53 interacting foci

were found to be markedly elevated in senescent cells, arguing the interruption of this interaction would largely affect senescent cells. Indeed, no side-effects on liver, kidney and hematopoietic function were reported after administration of FOXO4-DRI in naturally aged mice and in the fast aging model *Xpd*$^{TTD/TTD}$. The removal of senescent cells with FOXO4-DRI in aged mice restored overall fitness and fur density. Importantly, a major restoration in renal function was observed in these aged mice as indicated by an average reduction in plasma urea concentration of over 50% and reduction of creatinine levels of almost 40%. This was accompanied by a reduction in senescence and inflammation markers in the kidney [92]. In line with the observations that genetic clearance of senescent cells in naturally aging mice can maintain renal filtering capacity, this study shows that renal function can be restored by senescent cell removal and that this is therapeutically feasible [84].

Anti-senescence compound	Observations	Ref
Navitoclax	*Animal studies:* **Effects:** Eliminates senescent cells and rejuvenates hematopoietic and muscle stem cells in aged mice. **Adverse effects:** induces thrombocytopenia	96, 97
	Clinical trials in cancer treatment: **Effects:** used as chemotherapeutic to overcome (chemotherapy induced) apoptosis resistance in solid and lymphoid tumors. **Adverse effects:** Induces thrombocytopenia	98, 109-111
FOXO4-DRI	*Animal studies:* **Effects:** Eliminates senescent cells and improves renal function, fur density and overall fitness of aged mice. **Adverse effects:** No reported liver, kidney and hematopoietic side-effects	86
Quercetin and Dasatinib	*Animal studies:* **Effects:** Extend healthspan aof aging mice and alleviate age-associated vasomotor dysfunction, osteoporosis and cardiac function in aged mice. **Adverse effects:** Target non-senescent cells, and are questioned to be truly anti-senescent or whether they prevent senescence induction.	85,88,89
	Clinical trials in cancer treatment: **Effects:** Quercetin reduces oxidative stress markers and lowers levels of IL-6 in healthy subjects and has anti-tumor activity in several cancer types. Dasatinib is used as a chemotherapeutic in chronic myeloid leukemia. **Adverse effects:** Quercetin induces renal toxicity in a dose dependent manner. Dasatinib can induce coronary artery disease, cardiac failure, and hypertension.	99, 107, 108
HSP-90 inhibitors (17-DMAG and Geldanamycin)	*Animal studies:* **Effects:** Delay onset of several age-related disorders upon long term treatment in fast aging mice. **Adverse effects:** none observed, are questioned to be truly anti-senescent or whether they prevent senescence induction.	90
	Clinical trials in cancer treatment: **Effects:**Have anti-proliferative effects on several cancer types. **Adverse effects:** HSP-90 inhibitors induce renal failure, cardiac arrest, diarrhea, nausea, and anorexia	91-94

Abbreviations: HSP-90, heat shock protein 90; IL-6, Interleukin-6

Table 1. Therapeutics with anti-senescence potency *in vivo*

Quercetin and Dasatinib

Though their efficacy has been challenged by several studies, Dasatinib and Quercetin were the first set of compounds described to have anti-senescence properties after a drug repurposing screen [92,98,99]. In combination, Quercetin and Dasatinib were reported to reduce senescent cell levels *in vivo*, improve cardiovascular function, pulmonary fibrosis, reduce frailty and extend healthspan [98,100,101]. Quercetin, a common flavonoid, appears most effective on senescent endothelial cells. Dasatinib, a chemotherapeutic, can eliminate senescent fat cell progenitors [98]. However, the combination of Quercetin and Dasatinib proved to be non-selective for senescent cells and also targeted healthy cells [98], making it less suitable for therapeutic use in patients. Furthermore, it has been questioned to what extent Quercetin and Dasatinib are truly anti-senescence compounds, or whether they slow down the accumulation of cellular damage, which, in turn, may reduce senescence induction [92,98].

HSP-90 inhibitors

A different drug screening method focused on the inhibition of heat shock protein 90 (HSP90), which reduces viability in senescent human fibroblasts and senescent mouse stem cells [102]. HSP90 plays an important role in protein stabilization and degradation and is upregulated in many cancers but also senescent cells [102,103]. HSP90 inhibitors, such as Geldanamycin and a more water-soluble successor 17-DMAG (Alvespimycin), have anti-proliferative effects on cancer, and were recently shown to have some anti-senescence activity as well [102–105]. Treatment of fast aging ERCCΔ/- mice with 17-DMAG delayed onset of several age-related disorders and improved overall healthspan [102]. However, it remains to be assessed whether HSP-90 inhibitors prevent the induction of senescent cells or truly eliminate them *in vivo* [102]. HSP-90 inhibitors can also target healthy cells and their use as cancer treatment in humans has been reported to give a side effect profile including renal failure, which has to be assessed when HSP90 inhibitors are considered as anti-senescence therapy [102,106].

The discovery and design of anti-senescence compounds has only just started. The use of designed, interaction modulating peptides will be a major opportunity to overcome the side-effects of non-specific anti-senescence agents, by interfering only with senescent cell specific interactions [92]. Although studies with anti-senescence compounds in models of renal disease and injury are lacking, the reversal of age-associated decrease in renal function with the use of anti-senescence compounds gives high hopes for overcoming senescence associated deterioration of aged donor kidneys. Moreover, their use after transplantation may counteract transplantation induced damage, improving long term graft function (Fig 2).

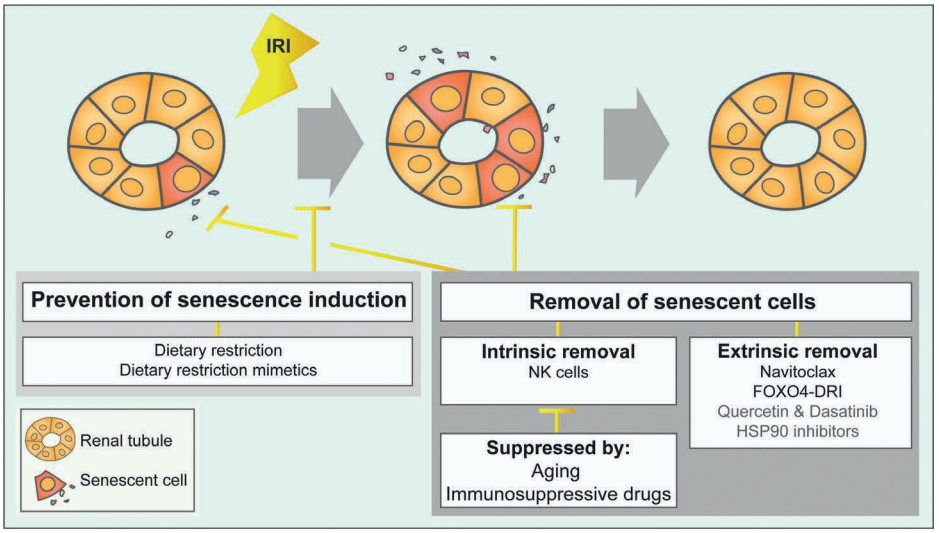

Figure 2. Hypothetical model with therapeutic interventions to prevent or overcome senescence during renal injury and aging.
Old renal tubules contain senescent cells (depicted in red color) that secrete SASP factors and therefore have poorer function compared to young renal tubules. Senescence induction upon acute damage, such as IRI, and upon aging can be prevented with dietary restriction and dietary restriction mimetics, reducing sensitivity to several types of damage. Senescent cells can be removed by immune cells or with the help of anti-senescence compounds, to improve organ function. Highlighted are the currently most potent anti-senescence drugs; Navitoclax and FOXO4-DRI. Abbreviations: IRI, ischemia reperfusion injury; NK cells, Natural killer cells; ROS, reactive oxygen species; SASP, senescence associated secretory phenotype,

Conclusions, discussion and future perspectives

As aged donor kidneys perform worse after transplantation and the transplantation associated injury accelerates aging of the graft, transplants might benefit from anti-aging therapies. The negative association between age and renal transplantation outcome has been explained here as a consequence of senescent cell abundance. Aging is caused by multiple deregulated processes, but it is clear that senescent cells are causal for aging due to their persistent secretory phenotype[84]. Through SASP, which mainly consists of pro-inflammatory factors, senescent cells negatively influence their environment and worsen transplantation outcome. Dietary restriction as well as several DR mimicking compounds prevent the onset of senescence and reduce inflammatory burden. These therapies might, in turn, improve graft survival if applied during initial periods after transplantation. As long-term interference with the SASP is impractical and leads to deleterious effects over time, a more realistic alternative would be to develop methods to eliminate senescent cells altogether before and after transplantation and, depending on the timing, during recovery from ischemia-reperfusion injury. By now, there are two drugs

that can potently eliminate senescent cells *in vivo*: Navitoclax and the less-toxic FOXO4-DRI. Their use in clinical studies for the purpose of targeting senescent cells to counteract age-related diseases still has to start. It will be exciting to see whether the promising findings on age related diseases in animal studies will hold true in human disease and in renal transplantation, and perhaps other organ transplants might benefit in the same manner. Several questions on anti-senescence therapies remain to be considered. The prospect of reversing signs of aging with anti-senescence compounds inspires people in search of everlasting youth, but it is important to recognize that senescent cells are not the sole cause of aging and side-effects of removing these cells have to be established [112]. So far, all anti-senescence compounds but FOXO4-DRI were repurposed from use in cancer treatment and have shown to cause side effects (table 1) [88,98,106]. Perhaps targeted delivery of anti-senescence compounds will overcome possible undesired effects in other organs [113]. Off-target effects of anti-senescence compounds on the function of the immune system are an important factor to take into account. With age, our immune-system declines in function and this influences immunosuppressive regimens in aged transplant recipients [15,31,114]. The anti-senescence compound Navitoclax was described to rejuvenate hematopoietic stem cells in mouse studies and it will be interesting to see what (other) anti-senescent compounds do with human immune system function. Perhaps these treatments boost rejuvenation of the aged immune system, which might demand altered immunosuppressive regimens in transplant recipients.

Anti-senescence compounds might also be applied in deceased kidney donors. Although it is not known at what time-interval anti-senescence compounds induce apoptosis *in vivo,* the use of anti-senescence compounds during machine reperfusion could allow for regeneration of the kidney during preservation.

It will be interesting to see whether interventions that reduce IRI, such as Sirolimus or machine reperfusion also prevent the induction of senescence [58]. And whether therapeutics that are nephrotoxic or worsen IRI outcome induce senescence. For example, the commonly used immunosuppressive agent Tacrolimus is known to be nephrotoxic, but it is not known whether Tacrolimus induces renal senescence *in vivo* [115]. Furthermore, immunosuppression with Tacrolimus might prevent clearance of senescent cells, which can accelerate aging in multiple tissues [33,116]. If so, anti-senescence compounds could counteract immunosuppressive-associated toxicity and improve overall health of patients receiving immunosuppressive therapy.

In conclusion, the advances within the anti-aging research facilitate treatments for multiple (age-related) diseases, and may improve renal transplantation outcome. With evidence mounting that senescent cells are responsible for the decrease in renal function during aging and a complicating factor in renal transplantation, the reduction of senescent cell levels and hopefully accompanying improvement in kidney function after transplantation should become subject of future research.

REFERENCES

1. Hazra, N. C., Rudisill, C. & Gulliford, M. C. Determinants of health care costs in the senior elderly: age, comorbidity, impairment, or proximity to death? Eur. J. Heal. Econ. (2017). doi:10.1007/s10198-017-0926-2
2. Kontis, V. et al. Future life expectancy in 35 industrialised countries: projections with a Bayesian model ensemble. Lancet (London, England) 389, 1323–1335 (2017).
3. López-Otín, C., Blasco, M. A., Partridge, L., Serrano, M. & Kroemer, G. The hallmarks of aging. Cell 153, (2013).
4. Marengoni, A. et al. Aging with multimorbidity: A systematic review of the literature. Ageing Res. Rev. 10, 430–439 (2011).
5. van Oostrom, S. H. et al. Multimorbidity of chronic diseases and health care utilization in general practice. BMC Fam. Pract. 15, 61 (2014).
6. Hill, N. R. et al. Global Prevalence of Chronic Kidney Disease - A Systematic Review and Meta-Analysis. PLoS One 11, e0158765 (2016).
7. Weinstein, J. R. & Anderson, S. The aging kidney: physiological changes. Adv. Chronic Kidney Dis. 17, 302–7 (2010).
8. Stevens, L. A., Viswanathan, G. & Weiner, D. E. Chronic kidney disease and end-stage renal disease in the elderly population: current prevalence, future projections, and clinical significance. Adv. Chronic Kidney Dis. 17, 293–301 (2010).
9. Heerspink, H. L. & de Zeeuw, D. Novel drugs and intervention strategies for the treatment of chronic kidney disease. Br. J. Clin. Pharmacol. 76, n/a-n/a (2013).
10. Thiruchelvam, P. T. R., Willicombe, M., Hakim, N., Taube, D. & Papalois, V. Renal transplantation. BMJ 343, d7300 (2011).
11. Agarwal, R. Defining end-stage renal disease in clinical trials: a framework for adjudication: Table 1. Nephrol. Dial. Transplant. 31, 864–867 (2016).
12. Lim, W. H. et al. Outcomes of Kidney Transplantation From Older Living Donors. Transplant. J. 95, 106–113 (2013).
13. Slegtenhorst, B. R. et al. Mechanisms and consequences of injury and repair in older organ transplants. Transplantation 97, 1091–9 (2014).
14. Tasaki, M. et al. Effect of donor–recipient age difference on long-term graft survival in living kidney transplantation. Int. Urol. Nephrol. 46, 1441–1446 (2014).
15. Oberhuber, R., Ge, X. & Tullius, S. G. Donor Age-Specific Injury and Immune Responses. Am. J. Transplant. 12, 38–42 (2012).
16. Kurschat, C. Nierentransplantation im Alter. Z. Gerontol. Geriatr. 49, 488–493 (2016).
17. Braun, H. et al. Cellular senescence limits regenerative capacity and allograft survival. J. Am. Soc. Nephrol. 23, 1467–73 (2012).
18. Melk, A., Schmidt, B. M. W., Vongwiwatana, A., Rayner, D. C. & Halloran, P. F. Increased expression of senescence-associated cell cycle inhibitor p16/INK4a in deteriorating renal transplants and diseased native kidney. Am. J. Transplant. 5, 1375–1382 (2005).
19. Hoeijmakers, J. H. J. DNA Damage, Aging, and Cancer. N. Engl. J. Med. 361, 1475–1485 (2009).
20. Campisi, J. & Robert, L. Cell senescence: role in aging and age-related diseases. Interdiscip. Top. Gerontol. 39, 45–61 (2014).
21. Campisi, J. Aging, Cellular Senescence, and Cancer. Annu. Rev. Physiol. 75, 685–705 (2013).
22. Muñoz-Espín, D. & Serrano, M. Cellular senescence: from physiology to pathology. Nat. Rev. Mol. Cell Biol. 15, 482–496 (2014).
23. Broude, E. V et al. p21Waf1/Cip1/Sdi1 mediates retinoblastoma protein degradation. Oncogene 26, 6954–6958 (2007).

24. Rayess, H., Wang, M. B. & Srivatsan, E. S. Cellular senescence and tumor suppressor gene p16. Int. J. cancer 130, 1715–25 (2012).
25. van Deursen, J. M. The role of senescent cells in ageing. Nature 509, 439–446 (2014).
26. Coppé, J.-P. et al. Senescence-Associated Secretory Phenotypes Reveal Cell-Nonautonomous Functions of Oncogenic RAS and the p53 Tumor Suppressor. PLoS Biol. 6, e301 (2008).
27. Coppé, J.-P., Desprez, P.-Y., Krtolica, A. & Campisi, J. The senescence-associated secretory phenotype: the dark side of tumor suppression. Annu. Rev. Pathol. 5, 99–118 (2010).
28. Demaria, M. et al. An essential role for senescent cells in optimal wound healing through secretion of PDGF-AA. Dev. Cell 31, (2014).
29. Muñoz-Espín, D. et al. Programmed Cell Senescence during Mammalian Embryonic Development. Cell 155, 1104–1118 (2013).
30. Sagiv, A. & Krizhanovsky, V. Immunosurveillance of senescent cells: the bright side of the senescence program. Biogerontology 14, 617–628 (2013).
31. Montecino-Rodriguez, E., Berent-Maoz, B. & Dorshkind, K. Causes, consequences, and reversal of immune system aging. J. Clin. Invest. 123, 958–65 (2013).
32. Hoffmann, U. et al. NK Cells of Kidney Transplant Recipients Display an Activated Phenotype that Is Influenced by Immunosuppression and Pathological Staging. PLoS One 10, e0132484 (2015).
33. Morteau, O. et al. Renal transplant immunosuppression impairs natural killer cell function in vitro and in vivo. PLoS One 5, e13294 (2010).
34. Franceschi, C. & Campisi, J. Chronic inflammation (Inflammaging) and its potential contribution to age-associated diseases. Journals of Gerontology - Series A Biological Sciences and Medical Sciences 69, (2014).
35. Campisi, J., Andersen, J. K., Kapahi, P. & Melov, S. Cellular senescence: A link between cancer and age-related degenerative disease? Semin. Cancer Biol. 21, 354–359 (2011).
36. Childs, B. G., Durik, M., Baker, D. J. & van Deursen, J. M. Cellular senescence in aging and age-related disease: from mechanisms to therapy. Nat. Med. 21, (2015).
37. Sturmlechner, I., Durik, M., Sieben, C. J., Baker, D. J. & van Deursen, J. M. Cellular senescence in renal ageing and disease. Nat. Rev. Nephrol. 13, 77–89 (2016).
38. Bonventre, J. V & Yang, L. Cellular pathophysiology of ischemic acute kidney injury. J. Clin. Invest. 121, 4210–21 (2011).
39. Mosteiro, L. et al. Tissue damage and senescence provide critical signals for cellular reprogramming in vivo. Science (80-.). 354, aaf4445 (2016).
40. de Keizer, P. L. J. The Fountain of Youth by Targeting Senescent Cells? Trends Mol. Med. 23, 6–17 (2017).
41. Salvadori, M., Rosso, G. & Bertoni, E. Update on ischemia-reperfusion injury in kidney transplantation: Pathogenesis and treatment. World J. Transplant. 5, 52–67 (2015).
42. Koppelstaetter, C. et al. Markers of cellular senescence in zero hour biopsies predict outcome in renal transplantation. Aging Cell 7, 491–497 (2008).
43. McGlynn, L. M. et al. Cellular senescence in pretransplant renal biopsies predicts postoperative organ function. Aging Cell 8, 45–51 (2009).
44. Melk, A. et al. Effects of Donor Age and Cell Senescence on Kidney Allograft Survival. Am. J. Transplant. 9, 114–123 (2008).
45. Boonstra, J. & Post, J. A. Molecular events associated with reactive oxygen species and cell cycle progression in mammalian cells. Gene 337, 1–13 (2004).
46. Zhang, Y. et al. A new role for oxidative stress in aging: The accelerated aging phenotype in Sod1–/ – mice is correlated to increased cellular senescence. Redox Biol. 11, 30–37 (2017).
47. Hochegger, K. et al. p21 and mTERT are novel markers for determining different ischemic time periods in renal ischemia-reperfusion injury. Am. J. Physiol. Renal Physiol. 292, F762-8 (2007).
48. Kailong, L. et al. P53-Rb signaling pathway is involved in tubular cell senescence in renal ischemia/reperfusion injury. Biocell 31, 213–23 (2007).

49. Westhoff, J. H. et al. Hypertension Induces Somatic Cellular Senescence in Rats and Humans by Induction of Cell Cycle Inhibitor p16INK4a. Hypertension 52, 123–129 (2008).
50. Jun, J.-I. & Lau, L. F. Cellular senescence controls fibrosis in wound healing. Aging (Albany. NY). 2, 627–31 (2010).
51. Seikrit, C. et al. Biological responses to PDGF-AA versus PDGF-CC in renal fibroblasts. Nephrol. Dial. Transplant. 28, 889–900 (2013).
52. Boor, P., Ostendorf, T. & Floege, J. PDGF and the progression of renal disease. Nephrol. Dial. Transplant. 29, i45–i54 (2014).
53. Lee, D. H., Wolstein, J. M., Pudasaini, B. & Plotkin, M. INK4a deletion results in improved kidney regeneration and decreased capillary rarefaction after ischemia-reperfusion injury. AJP Ren. Physiol. 302, F183–F191 (2012).
54. Megyesi, J., Andrade, L., Vieira, J. M., Safirstein, R. L. & Price, P. M. Positive effect of the induction of p21WAF1/CIP1 on the course of ischemic acute renal failure. Kidney Int. 60, 2164–2172 (2001).
55. Nishioka, S. et al. The cyclin-dependent kinase inhibitor p21 is essential for the beneficial effects of renal ischemic preconditioning on renal ischemia/reperfusion injury in mice. Kidney Int. 85, 871–879 (2014).
56. DiRocco, D. P. et al. CDK4/6 inhibition induces epithelial cell cycle arrest and ameliorates acute kidney injury. AJP Ren. Physiol. 306, F379–F388 (2014).
57. Baar, M. P., Van Willigenburg, H. & de Keizer, P. L. J. Maintenance and repair of an aging life cycle. Oncotarget 1–2 (2017). doi:10.18632/oncotarget.18046
58. Requião-Moura, L. R., De, M., Durão Junior, S., Carvalho De Matos, A. C. & Pacheco-Silva, A. Ischemia and reperfusion injury in renal transplantation: hemodynamic and immunological paradigms. einstein 13, 129–35 (2015).
59. McDonald, R. B. & Ramsey, J. J. Honoring Clive McCay and 75 years of calorie restriction research. J. Nutr. 140, 1205–10 (2010).
60. Dong, D. et al. Alleviation of senescence and epithelial-mesenchymal transition in aging kidney by short-term caloric restriction and caloric restriction mimetics via modulation of AMPK/mTOR signaling. Oncotarget 8, 16109–16121 (2017).
61. Krishnamurthy, J. et al. Ink4a/Arf expression is a biomarker of aging. J. Clin. Invest. 114, 1299–307 (2004).
62. Lanza, I. R. et al. Chronic Caloric Restriction Preserves Mitochondrial Function in Senescence without Increasing Mitochondrial Biogenesis. Cell Metab. 16, 777–788 (2012).
63. Ning, Y.-C. et al. Short-term calorie restriction protects against renal senescence of aged rats by increasing autophagic activity and reducing oxidative damage. Mech. Ageing Dev. 134, 570–579 (2013).
64. Trepanowski, J. F., Canale, R. E., Marshall, K. E., Kabir, M. M. & Bloomer, R. J. Impact of caloric and dietary restriction regimens on markers of health and longevity in humans and animals: a summary of available findings. Nutr. J. 10, 107 (2011).
65. van Ginhoven, T. M. et al. Preoperative fasting induced protection against renal ischemia/reperfusion injury is independent of ghrelin in mice. Nutr. Res. 30, 865–869 (2010).
66. Jongbloed, F. et al. Preoperative Fasting Protects against Renal Ischemia-Reperfusion Injury in Aged and Overweight Mice. PLoS One 9, e100853 (2014).
67. Mitchell, J. R. et al. Short-term dietary restriction and fasting precondition against ischemia reperfusion injury in mice. Aging Cell 9, 40–53 (2010).
68. Shushimita, S. et al. Protection against renal ischemia–reperfusion injury through hormesis? Dietary intervention versus cold exposure. Life Sci. 144, 69–79 (2016).
69. Tomé-Carneiro, J. et al. Resveratrol and clinical trials: the crossroad from in vitro studies to human evidence. Curr. Pharm. Des. 19, 6064–93 (2013).
70. An, H. & He, L. Current understanding of metformin effect on the control of hyperglycemia in diabetes. J. Endocrinol. 228, R97–R106 (2016).

71. Noren Hooten, N. et al. Metformin-mediated increase in DICER1 regulates microRNA expression and cellular senescence. Aging Cell 15, 572–581 (2016).
72. Wang, Z. et al. Metformin attenuated the inflammation after renal ischemia/reperfusion and suppressed apoptosis of renal tubular epithelial cell in rats. Acta Cir. Bras. 30, 617–23 (2015).
73. Arriola Apelo, S. I. & Lamming, D. W. Rapamycin: An InhibiTOR of Aging Emerges From the Soil of Easter Island. J. Gerontol. A. Biol. Sci. Med. Sci. 71, 841–9 (2016).
74. Yamamoto, T. et al. Nicotinamide mononucleotide, an intermediate of NAD+ synthesis, protects the heart from ischemia and reperfusion. PLoS One 9, e98972 (2014).
75. Li, J. et al. A conserved NAD + binding pocket that regulates protein-protein interactions during aging. Science (80-.). 355, 1312–1317 (2017).
76. Yamamoto, T. et al. Nicotinamide mononucleotide, an intermediate of NAD+ synthesis, protects the heart from ischemia and reperfusion. PLoS One 9, e98972 (2014).
77. Lasry, A. & Ben-Neriah, Y. Senescence-associated inflammatory responses: aging and cancer perspectives. Trends Immunol. 36, 217–28 (2015).
78. Pribluda, A. et al. A senescence-inflammatory switch from cancer-inhibitory to cancer-promoting mechanism. Cancer Cell 24, 242–56 (2013).
79. Osorio, F. G. et al. Nuclear lamina defects cause ATM-dependent NF- B activation and link accelerated aging to a systemic inflammatory response. Genes Dev. 26, 2311–2324 (2012).
80. Xu, M. et al. JAK inhibition alleviates the cellular senescence-associated secretory phenotype and frailty in old age. Proc. Natl. Acad. Sci. 112, E6301–E6310 (2015).
81. Xu, M., Tchkonia, T. & Kirkland, J. L. Perspective: Targeting the JAK/STAT pathway to fight age-related dysfunction. Pharmacol. Res. 111, 152–154 (2016).
82. Veroux, M. et al. Sirolimus in solid organ transplantation: current therapies and new frontiers. Immunotherapy 3, 1487–1497 (2011).
83. Baker, D. J. et al. Clearance of p16Ink4a-positive senescent cells delays ageing-associated disorders. Nature 479, 232–236 (2011).
84. Baker, D. J. et al. Naturally occurring p16Ink4a-positive cells shorten healthy lifespan. Nature 530, 184–189 (2016).
85. Tse, C. et al. ABT-263: A Potent and Orally Bioavailable Bcl-2 Family Inhibitor. Cancer Res 68, 3421–8 (2008).
86. Chang, J. et al. Clearance of senescent cells by ABT263 rejuvenates aged hematopoietic stem cells in mice. Nat. Med. 22, 78–83 (2015).
87. Yosef, R. et al. Directed elimination of senescent cells by inhibition of BCL-W and BCL-XL. Nat. Commun. 7, 11190 (2016).
88. Gandhi, L. et al. Phase I study of Navitoclax (ABT-263), a novel Bcl-2 family inhibitor, in patients with small-cell lung cancer and other solid tumors. J. Clin. Oncol. 29, 909–16 (2011).
89. Conchon, M., Freitas, C. M. B. de M., Rego, M. A. do C. & Braga Junior, J. W. R. Dasatinib - clinical trials and management of adverse events in imatinib resistant/intolerant chronic myeloid leukemia. Rev. Bras. Hematol. Hemoter. 33, 131–9 (2011).
90. Zhu, Y. et al. New agents that target senescent cells: the flavone, fisetin, and the BCL-X_L inhibitors, A1331852 and A1155463. Aging (Albany. NY). 9, 955–963 (2017).
91. Zhou, P., Sun, X. & Zhang, Z. Kidney-targeted drug delivery systems. Acta Pharm. Sin. B 4, 37–42 (2014).
92. Baar, M. P. et al. Targeted Apoptosis of Senescent Cells Restores Tissue Homeostasis in Response to Chemotoxicity and Aging. Cell 169, (2017).
93. van der Horst, A. et al. FOXO4 transcriptional activity is regulated by monoubiquitination and USP7/HAUSP. Nat. Cell Biol. 8, 1064–1073 (2006).
94. Hosaka, T. et al. Disruption of forkhead transcription factor (FOXO) family members in mice reveals their functional diversification. Proc. Natl. Acad. Sci. U. S. A. 101, 2975–80 (2004).

95. Martins, R., Lithgow, G. J. & Link, W. Long live FOXO: unraveling the role of FOXO proteins in aging and longevity. Aging Cell 15, 196–207 (2016).
96. Kruiswijk, F., Labuschagne, C. F. & Vousden, K. H. p53 in survival, death and metabolic health: a lifeguard with a licence to kill. Nat. Rev. Mol. Cell Biol. 16, 393–405 (2015).
97. Sawyer, N., Watkins, A. M. & Arora, P. S. Protein Domain Mimics as Modulators of Protein–Protein Interactions. Acc. Chem. Res. 50, 1313–1322 (2017).
98. Zhu, Y. et al. The Achilles' heel of senescent cells: from transcriptome to senolytic drugs. Aging Cell 14, 644–658 (2015).
99. Zhu, Y. et al. Identification of a novel senolytic agent, navitoclax, targeting the Bcl-2 family of anti-apoptotic factors. Aging Cell 15, (2016).
100. Roos, C. M. et al. Chronic senolytic treatment alleviates established vasomotor dysfunction in aged or atherosclerotic mice. Aging Cell 15, 973–977 (2016).
101. Schafer, M. J. et al. Cellular senescence mediates fibrotic pulmonary disease. Nat. Commun. 8, 14532 (2017).
102. Fuhrmann-Stroissnigg, H. et al. Identification of HSP90 inhibitors as a novel class of senolytics. Nat. Commun. 8, 422 (2017).
103. Workman, P. & Powers, M. V. Chaperoning cell death: a critical dual role for Hsp90 in small-cell lung cancer. Nat. Chem. Biol. 3, 455–457 (2007).
104. Bendell, J. C. et al. A Phase 2 Study of the Hsp90 Inhibitor AUY922 as Treatment for Patients with Refractory Gastrointestinal Stromal Tumors. Cancer Invest. 34, 265–270 (2016).
105. Seggewiss-Bernhardt, R. et al. Phase 1/1B trial of the heat shock protein 90 inhibitor NVP-AUY922 as monotherapy or in combination with bortezomib in patients with relapsed or refractory multiple myeloma. Cancer 121, 2185–2192 (2015).
106. Socinski, M. A. et al. A Multicenter Phase II Study of Ganetespib Monotherapy in Patients with Genotypically Defined Advanced Non-Small Cell Lung Cancer. Clin. Cancer Res. 19, 3068–3077 (2013).
107. Ferry, D. R. et al. Phase I clinical trial of the flavonoid quercetin: pharmacokinetics and evidence for in vivo tyrosine kinase inhibition. Clin. Cancer Res. 2, 659–68 (1996).
108. Askari, G., Ghiasvand, R., Feizi, A., Ghanadian, S. M. & Karimian, J. The effect of quercetin supplementation on selected markers of inflammation and oxidative stress. J. Res. Med. Sci. 17, 637–41 (2012).
109. Tolcher, A. W. et al. Safety, efficacy, and pharmacokinetics of navitoclax (ABT-263) in combination with erlotinib in patients with advanced solid tumors. Cancer Chemother. Pharmacol. 76, 1025–1032 (2015).
110. Vlahovic, G. et al. A phase I safety and pharmacokinetic study of ABT-263 in combination with carboplatin/paclitaxel in the treatment of patients with solid tumors. Invest. New Drugs 32, 976–984 (2014).
111. Wilson, W. H. et al. Navitoclax, a targeted high-affinity inhibitor of BCL-2, in lymphoid malignancies: a phase 1 dose-escalation study of safety, pharmacokinetics, pharmacodynamics, and antitumour activity. Lancet. Oncol. 11, 1149–59 (2010).
112. Homme, J., Fertita, D., Shuman, M. & van Leeuwen, T. Un-reborn again. QOTSA 6, (2017).
113. Valentijn, F. A., Falke, L. L., Nguyen, T. Q. & Goldschmeding, R. Cellular senescence in the aging and diseased kidney. J. Cell Commun. Signal. 1–14 (2017). doi:10.1007/s12079-017-0434-2
114. McKay, D. & Jameson, J. Kidney transplantation and the ageing immune system. Nat. Rev. Nephrol. 8, 700–708 (2012).
115. Tang, J. T. et al. Pharmacogenetic aspects of the use of tacrolimus in renal transplantation: recent developments and ethnic considerations. Expert Opin. Drug Metab. Toxicol. 12, 555–565 (2016).
116. Sagiv, A. & Krizhanovsky, V. Immunosurveillance of senescent cells: the bright side of the senescence program. Biogerontology 14, 617–628 (2013).

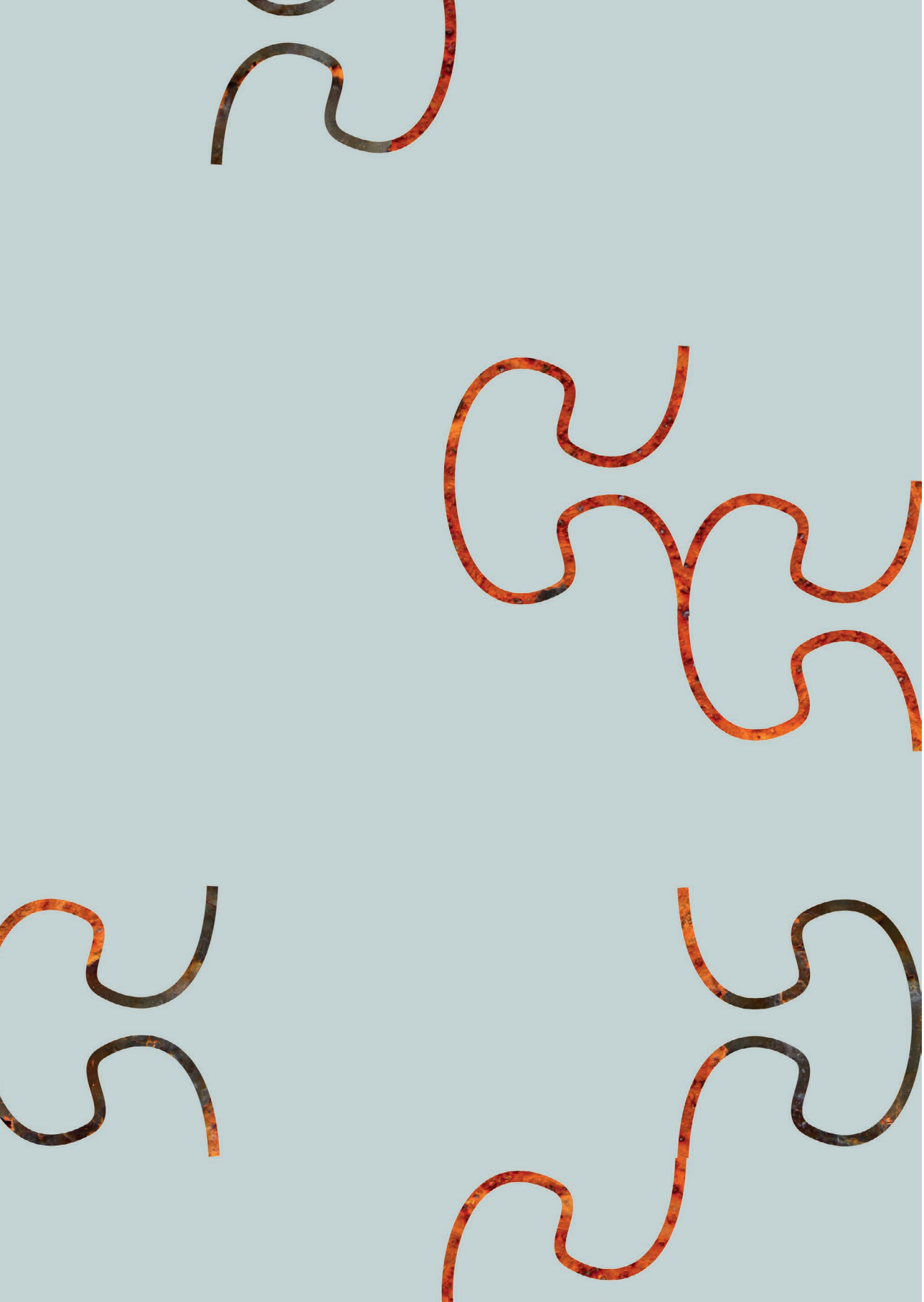

Chapter 6

Maintenance and Repair of an Aging Life Cycle

Marjolein P. Baar[1], Hester van Willigenburg[1] and Peter L.J. de Keizer[1]
[1] Department of Molecular Genetics, Erasmus University Medical Center, Wytemaweg, Rotterdam, The Netherlands

Oncotarget. 2017 May 21;8(50):86985-86986. doi: 10.18632

"Targeting signs of aging". It sounds more like a punch-line of a TV commercial, than a consequence of fundamental science. But as we observed recently, it might actually be possible to achieve just that, using a prospectively designed FOXO4-p53 interfering peptide that targets so-called "senescent" cells[1]. More research is needed to fully assess its true translational potential and whether it is even safe to remove such cells. However, these findings pose a very attractive starting point to develop ways to live out our final years in better health.

Aging has often been considered as an integral part of life; a form of "noise" that cannot be targeted or tampered with. This is in part because for long the underlying causes of organismal aging were simply too elusive to comprehend, let alone modify. The chronic build-up of DNA damage has now evidently been established as a major cause for aging, but to counteract the genomic damage that has occurred over a lifetime is an entirely different challenge altogether[2]. One approach to overcome this issue, is to eliminate those cells that are too damaged to faithfully perform their duty and to replace them by fresh and healthy counterparts. Senescent cells are exciting candidates for such an approach. Comparable to formation of rust on old equipment, like a bicycle (Fig. 1), they accumulate during aging and especially at sites of pathology. They develop a chronic secretory profile that is thought to impair tissue renewal and contribute to disease development, for instance by keeping neighboring cells "locked" in a permanent state of stemness[2]. Senescence can be beneficial in a transient setting, but the genetic removal of senescent cells over a prolonged period of time was found to be safe and to potently extended health- and lifespan of naturally aging mice[3]. Thus, senescence is an irrefutable cause for aging and targeting them is warranted. But can they also be eliminated therapeutically? And are such methods then safe on their own? And last, but not least, would such methods be applicable to not merely delay, but also to reverse aging?

Le tour de FOXO. A demanding journey, but one with great rewards

A first surprise when trying to address these questions was that senescent cells recruit a factor called FOXO4 to sites of persistent DNA damage, structures absent in normal healthy cells[1]. This is intriguing as FOXO4 is considered to be the ugly little sister of FOXO1 and FOXO3, which do play major roles in processes ranging from stem cell function, differentiation, tumor suppression, and, aging[4]. In senescence, however, FOXO4 appears to act as a brake on the apoptosis response by sequestering p53. Prospective design of a D-Retro-Inversed Cell Penetrating Peptide that perturbs this interaction, named FOXO4-DRI, allowed for nuclear release of active p53, followed by cell-intrinsic apoptosis and selective elimination of the senescent cells.

Recent work elegantly proved that senescent cells are a major cause for the toxic side effects caused by multiple independent forms of chemotherapy[5]. Excitingly, FOXO4-DRI counteracted senescence caused by Doxorubicin and reversed liver toxicity providing

evidence that therapeutic removal of senescent cells by FOXO4-DRI can counteract at least some aspects of chemotoxicity. Proceeding from this acute senescence-induction model, we then focused on fast aging *Xpd*$^{TTD/TTD}$ mice, which spontaneously develop senescence in an accelerated fashion, in parallel with organism-wide deterioration. FOXO4-DRI proved to significantly restore their health on multiple levels. Though not purposefully investigated, it was strikingly apparent that FOXO4-DRI treated mice regained fur and improved their voluntary exploratory behavior compared to PBS treated counterparts. In addition, kidney function markedly restored. Naturally aged mice showed more biological noise than the fast aging mice, making these features more difficult to address. But at least the effects on renal function were clearly prevalent in naturally aged mice. Thus, using FOXO4-DRI it indeed appears possible to not just delay aging but also reverse at least certain signs of it. So, what's next?

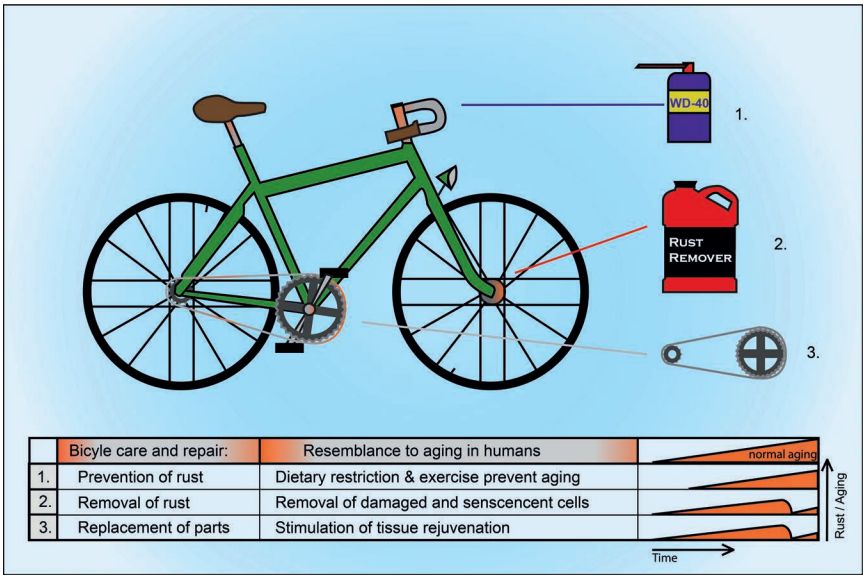

	Bicyle care and repair:	Resemblance to aging in humans
1.	Prevention of rust	Dietary restriction & exercise prevent aging
2.	Removal of rust	Removal of damaged and senscencent cells
3.	Replacement of parts	Stimulation of tissue rejuvenation

The aging cycle of life

The analogy compares senescent cells in an aged body to rust on a racing bicycle. Different strategies can be used to prevent, treat and remove rust and aging. WD-40, a corrosion inhibitor, resembles dietary restriction and regular exercise to delay rust or aging. When rust and aging have already settled, the FOXO4-DRI peptide can act as a rust remover by inducing cell death in senescent cells. Last, the stimulation of tissue rejuvenation can promote a healthy, revitalized tissue that can be compared with the replacement of bicycle parts. The combination of these strategies may be complimentary in fighting aging and age-related defects.

A combination of efforts to best the mountains ahead

Aging is ultimately still inevitable. But perhaps it can be strongly postponed, or even reversed, when independent anti-aging therapies are combined? It remains to be determined whether extension of lifespan is possible in humans[6], let alone whether this is desirable and then to what age? After all, life could at some point not simply "complete"? While this might be true for some, nobody likes being sick and frail. Imagine the possibilities if we would be able to enjoy our time with loved ones, exercise and travel more and simply just enjoy life in good health, instead of spending it in a retirement home.

Extending the healthy years of life is now closer than ever, but we are still not there yet. While mechanics can remove defective parts from an old bicycle, it is far more challenging to remove damaged parts from an old body (Fig. 1). Anti-aging strategies have therefore necessarily focused thus far on stalling the inevitable for as long as possible by eating less and exercising more. A multitude of new diets make it to the mainstream public each year, but ironically, people tend to exercise less and gain more and more weight. This argues that instead of focusing so much on dietary interventions, independent approaches deserve to be investigated. Here, we underscored the potential of therapeutic elimination of senescent cells, for instance by FOXO4-DRI. In addition, exciting developments were recently reported in the field of stem cell biology, where it was shown that transient expression of the Yamanaka stem cell factors can promote tissue rejuvenation[7]. This is not yet therapeutically applicable, but this will most likely only be a matter of time.

It is no longer merely science-fiction to restore healthspan with rationally designed approaches. To fully achieve the best possible outcome, it will therefore deserve special consideration to combine existing methods to delay aging with the recently developed therapies that counter senescence and promote tissue rejuvenation. With these, we finally have exciting tools to maintain and repair the aging cycle of life (Fig. 1). Time to gear up and head for the finish!

REFERENCES

1 Baar, M. P. et al. Targeted Apoptosis of Senescent Cells Restores Tissue Homeostasis in Response to Chemotoxicity and Aging. Cell 169, 132-147 e116, doi:10.1016/j.cell.2017.02.031 (2017).

2 de Keizer, P. L. The Fountain of Youth by Targeting Senescent Cells? Trends Mol Med 23, 6-17, doi:10.1016/j.molmed.2016.11.006 (2017).

3 Baker, D. J. et al. Naturally occurring p16(Ink4a)-positive cells shorten healthy lifespan. Nature 530, 184-189, doi:10.1038/nature16932 (2016).

4 Eijkelenboom, A. & Burgering, B. M. FOXOs: signalling integrators for homeostasis maintenance. Nat Rev Mol Cell Biol 14, 83-97, doi:10.1038/nrm3507 (2013).

5 Demaria, M. et al. Cellular Senescence Promotes Adverse Effects of Chemotherapy and Cancer Relapse. Cancer Discov 7, 165-176, doi:10.1158/2159-8290.CD-16-0241 (2017).

6 Dong, X., Milholland, B. & Vijg, J. Evidence for a limit to human lifespan. Nature 538, 257-259, doi:10.1038/nature19793 (2016).

7 Ocampo, A. et al. In Vivo Amelioration of Age-Associated Hallmarks by Partial Reprogramming. Cell 167, 1719-1733 e1712, doi:10.1016/j.cell.2016.11.052 (2016).


tion was prepared by dissolving the accurately weighted reference standard in ethanol. The samples
acrolimus (S5003, SelleckChem
were prepared by spiking blank mouse blood with the appropriate stock solution or an intermediate solution, resulting in samples of 250 µL with tacrolimus levels ranging between 4.5 ng/mL and 60 ng/mL. From these samples 50 µL was spotted on a DBS card for DBS measurements, and the other 200 µL was used for standard whole blood LC-MS/MS analysis. The DBS cards were dried for at least 10 minutes at room te
before being stored in zip bags
mice received 1 or 3 mg/kg tacroli
model 2004). The Alzet pumps were preloaded with tacrolimus (S5003, SelleckChem) dissolved in a 50%DMSO-50% EtOH solvent. After loading, the pumps were incubated in PBS at 37°C for 24 hours prior to subcutaneous intrascapular implantation. Blood samples were collected at the end of the mouse experiment. Blood was sampled in three manners; via tail-tip, cheek vein and heart puncture.
DBS samples were stored in a desiccator for at
months until they were measure
ner day for 28 days via Alzet osmotic mini-pumps (Alzet®,
pet + pipetpuntjes, Een bloedspotkaart,
bloedbuiz
nodigdheden: EDTA
bij de muis en vang op in EDTA buis, Vouw de bloedspot kaart open en raak hierbij het filterpapier niet aan. pipeteer direct 40-50 ul bloed in een van de cirkels op het whatmann papier (zie afbeelding). Zorg ervoor dat het rondje minimaal voor de helft gevuld is. Laat het eventuele resterende bloed in de buis staan voor 5 minuten en plaats daarna op ijs. Vouw het kaartje dicht nadat de laatste drupp
Een afsluitbaar plastic zakje met ontvochtiger, ijs. Uitvoering: Prik bloed
oroog (na
ongeveer 10 minuten

Chapter 7

Validation of a Dried Blood Spot Method to Measure Tacrolimus Concentrations in Small Volumes of Mouse Blood

Hester van Willigenburg[1,2,3*], Bart van Domburg[4], Gisela Ambagtsheer[1,2], Renata M. C. Brandt[3], Dennis A. Hesselink[1,5], Ron W. F. de Bruin[1,2], Brenda de Winter[4]

[1] Department of Surgery, Erasmus MC, University Medical Center Rotterdam, Rotterdam, The Netherlands, [2] Erasmus MC Transplant Institute, Rotterdam, The Netherlands, [3] Department of Molecular Genetics, Erasmus MC, University Medical Center Rotterdam, Rotterdam, The Netherlands, [4] Department of Hospital Pharmacy, Erasmus MC, University Medical Center Rotterdam, the Netherlands, [5] Department of Internal Medicine, Division of Nephrology and Transplantation, Erasmus MC, University Medical Center Rotterdam, the Netherlands, * Corresponding author, Doctor Molewaterplein 40, 3015 GD Rotterdam, +31107043455, h.vanwilligenburg@erasmusmc.nl

Bioanalysis, 2022 Apr, PMID: 35289217

Graphical Abstract

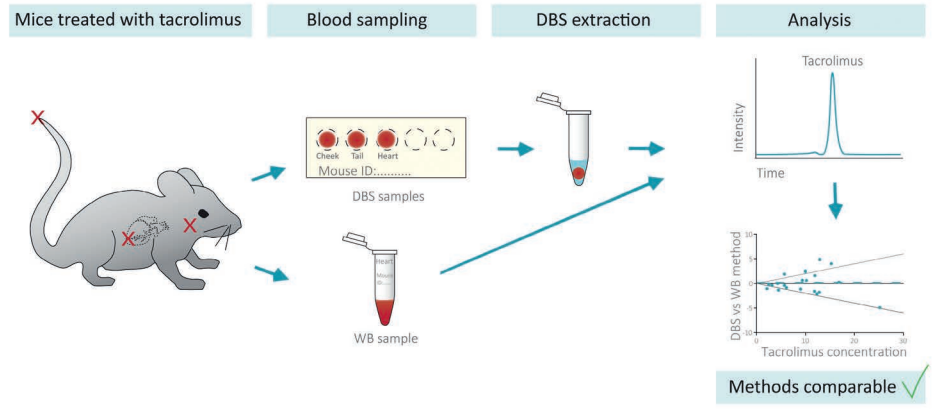

DBS cheek method can be used for serial monitoring of tacrolimus concentrations in mouse blood, offering an animal friendly method for tacrolimus pharmacokinetic studies in mice.

ABSTRACT

Background: The small blood volume of mice complicates tacrolimus pharmacokinetic studies in these animals. Here we explored dried blood spot (DBS) as a novel method to measure tacrolimus blood concentrations in mice. DBS samples were collected from three sampling sites, including cheek, tail and heart and compared with heart whole blood samples measured via LC-MS/MS method.

Results: Tacrolimus concentrations in the whole blood samples ranged from 2.56 to 27.64 µg/L. DBS of cheek vein blood was the most reliable sampling site with a mean bias of 0.15 µg/L (95% CI -4.20 - 4.50).

Conclusions: DBS cheek method can be used for serial monitoring of tacrolimus blood concentrations in mice, offering an animal friendly method for tacrolimus pharmacokinetic studies in mice.

Key terms: tacrolimus, dried blood spot, LC-MS/MS, mouse, method validation,

Article type: Research article**, subtype:** Methodology

INTRODUCTION

The immunosuppressive drug tacrolimus is a first-line treatment option to prevent organ and tissue rejection after transplantation[1]. Even at low dosages, tacrolimus can cause serious side-effects, including infections[2,3], nephrotoxicity[4], hypertension[5,6], diabetes mellitus[7] and neurotoxicity[8]. Mice are often used as a model organism to study these side effects of tacrolimus and its effects on transplant-immunology[9]. However, many tacrolimus studies using mice lack validation of tacrolimus blood concentration measurements[2,10,11], which makes it difficult to interpret the pharmacokinetic data and to compare studies.

Currently, the most common detection method for tacrolimus in human blood is liquid chromatography with tandem mass spectrometry (LC-MS/MS)[1,12]. However, it can be challenging to use LC-MS/MS for tacrolimus validation in mouse blood. For an average adult mouse weighing 25 g, the circulating blood volume approximates only 1.80 mL[13]. According to current guidelines, a maximum of 10% of the circulating blood volume can be sampled bi-weekly, which equals a maximal volume of 180 µL [13,14]. Exceeding this volume may induce hypovolemia and cardiovascular failure[13,14]. The required whole blood volume for LC-MS/MS analysis of the tacrolimus concentration is approximately 100-200 µL which limits the number of samples that can be obtained from a single mouse to a one-time or end-point measurement[14]. In addition, not every research facility is equipped with the possibility to measure tacrolimus with LC-MS/MS.

Advances in LC-MS/MS technology in combination with the dried blood spot (DBS) method have enabled the quantification of lower drug concentrations in smaller sample sizes. In DBS analyses, samples are blotted and dried on a filter paper which can be stored at ambient temperatures[15]. This method requires a whole blood volume of only 40-50 µL[16]. These DBS samples are then analyzed with LC-MS/MS[16]. The DBS method has been used before in pharmacokinetic mouse studies[17–20], showing that it can be used to reduce mouse sampling size and that DBS improves data quality[17]. An added benefit is the lowered cost of storing DBS samples compared to full blood samples[15], and the possibility to easily analyze tacrolimus blood concentrations in another research institute, by sending the DBS card by mail. However, so far, the DBS method has not been validated to measure tacrolimus concentrations in mouse blood.

Recently, a method for the analysis of tacrolimus in human DBS samples was developed and validated according to current guidelines in our hospital[16,21,22]. In this method, no correction for differences in hematocrit concentrations in the normal human range (0.25-0.50 L/L) was needed, which is in accordance with literature[23,24]. Mouse hematocrit concentrations range from 0.40-0.50 L/L[14]. For human DBS, blood samples are collected via finger prick. Capillary blood withdrawal via finger prick is not possible in mice and the site and manner of blood sampling might influence the blood quality

by, for example, tissue exudate. Therefore, we compared tacrolimus concentrations by means of DBS in whole blood of mice that was collected by three different blood withdrawal techniques: including tail tip bleeding, which resembles capillary bleeding; a cheek puncture, the recommended technique for venous blood sampling in mice in our institution; and lastly, heart blood derived via heart puncture during sacrifice. To validate whether DBS can be used as a method to measure tacrolimus concentrations in mouse blood, LC-MS/MS analysis of these samples are compared with standard LC-MS/MS on whole blood (WB).

MATERIALS AND METHODS

Tacrolimus Reference Samples

A tacrolimus (S5003, SelleckChem) stock solution was prepared by dissolving the accurately weighted reference standard in methanol. The samples were prepared by spiking blank mouse blood with the appropriate stock solution or an intermediate solution, resulting in samples of 250 µL with tacrolimus concentrations ranging between 4.50 ng/mL and 60 ng/mL. From these samples 50 µL was spotted on a DBS card (Whatman 903 Protein in Saver Cards, art. no. 10531018, GE Healthcare) for DBS measurements, and the other 200 µL was used for standard whole blood LC-MS/MS analysis. The DBS cards were dried for at least 10 minutes at room temperature before being stored in zip bags with desiccant. The remnants of the mouse whole blood samples spiked with tacrolimus were stored at -80^{o}C until both the DBS and whole blood (WB) samples were analyzed with LC-MS/MS.

Tacrolimus Administration in Mice

This study was performed in accordance with all applicable National and institutional policies. The protocol was approved by the Dutch Animal Ethics Committee (Protocol Number: AVD1010020197724). Certified biotechnicians carried out all experimental protocols under strict guidelines to ensure careful and consistent handling of the mice. The mice used in this study were 12 to 20 month old females and males of a C57BL/6J background. The mice were kept in individual cages from the start of the experiment with ad libitum access to food and water.

26 mice received 1 or 3 mg/kg tacrolimus per day for 28 days via Alzet osmotic mini-pumps (Alzet®, model 2004). The Alzet pumps were preloaded with Tacrolimus (S5003, SelleckChem) dissolved in a 50%DMSO-50% EtOH solvent. After loading, the pumps were incubated in PBS at 37°C for 24 hours prior to subcutaneous intrascapular implantation. Blood samples were collected at the end of the mouse experiment.

Blood Sampling for Tacrolimus Measurements

Blood was sampled in three manners: via tail-tip, cheek vein and heart puncture. Just before sacrificing the mice, 50 µL capillary mouse blood was sampled from the tail-tip

by removing the boneless tip of the tail with surgical scissors. Blood flow in the tail was supported by applying slight pressure on the tail vein from base to tip[25]. 50 µL per sample was spotted by use of a pipette on a DBS card. 50 µL venous blood was collected from the cheek, by a small needle puncture near the submandibular vein, which was spotted on a DBS card. After sacrifice, at least 250 µL venous blood was sampled via terminal cardiac puncture (under anesthesia) with a syringe, out of which 50 µL was spotted on a DBS card, and 200 µL surplus whole blood was transferred to an EDTA coated 1mL vial, which was frozen at -80^{o}C as LC-MS/MS sample until analysis. DBS samples were stored at room temperature in the dark in a desiccator for at most six months until they were measured. Tacrolimus DBS samples can be stored up to 6 months[26].

Sample Preparation

For sample preparation, a 6 mm punch was taken from the center of the DBS spot with an automatic puncher (Analytical Sales & Services Inc., USA). This 6 mm punch is the fully saturated part of the DBS spot and is used to prevent influence of inhomogeneous distribution of analytes near the edges of the DBS spot[27,28]. The punches were collected in vials to which 200 µL internal standard (5 µg/L tacrolimus-$^{13}C^{2}H_{4}$ (Alsa Chim, France)) working solution was added. The vials were vortexed and then sonicated for 15 min. The supernatant was transferred to a snap ring vial with insert (VWR, Netherlands). A volume of 10 µL was injected into the LC-system.

For whole blood sample preparation, 50 µl aliquots were spiked in a vial with 700 µl internal standard working solution (5 µg/L Tacrolimus-$^{13}C^{2}H_{4}$). The vials were vortex mixed for 10 s and then centrifuged at 13000 rpm for 10 min. The vials were placed in the auto-sampler of the LC-MS, where 10 µL of the supernatant was injected into the system.

Instrumentation and UPLC Conditions

Analyses were performed on a Waters Acquity UPLC-MS/MS system (Waters Corp., USA). The UPLC was connected to a Waters Xevo TQ-S micro triple quadrupole mass spectrometer. Chromatic separation was performed on a Waters Acquity UPLC BEH C_{18} column (1.7 µm; 50 x 2.1 mm) at a temperature of 60 °C. A multistep gradient elution was applied at a flow rate of 0.50 mL/min using 2 mM ammonium acetate an 0.1 % formic acid in water (eluent A) and 2 mM ammonium acetate and 0.10 % formic acid in methanol (eluent B). Initial gradient was set at 45:55 A:B. Eluent B increased to 70% in 0.6 min, then to 90% in 0.1 min, followed by 100% B in 0.1 min where it was kept for 1.0 min. Finally, the gradient was reset to the initial conditions for 0.20 min to equilibrate for the next injection adding up to a total runtime of 2.0 min.

Method Comparisons

Validation of the dried blood spot (DBS) method and whole blood (WB) method were based on the US Food and Drug Administration guidelines for bioanalytical validations

(US Department of Health and Human Services, 2001)guideline and the IATDMCT guideline[22]. The correlation coefficient (r) was > 0.99 over the concentration range of 1.00 – 35 µg/L for the WB method and 2.00 – 35 µg/L for the DBS method. For both methods, accuracy, intra-day precision and inter-day precision were within the requirements (RSD <15%). The results of these validation parameters are summarized in **Table 1**.

The analysis of tacrolimus in whole blood is based on an application note from Waters (Waters Corp., Wilmslow, UK)[29]. According to this application note, no matrix effects were reported. In human DBS tacrolimus samples, an average recovery of 0.92 (range 0.74 – 1.14) was found. No effect of hematocrit concentrations was seen.

Method	QC	Concentration (µg/L)	Accuracy RSD (%)	Intra-day precision RSD (%)	Inter-day precision RSD (%)
DBS	L	5.8	13.1	2.4	5.1
	M	17.2	14.6	2.4	9.4
	H	24.3	13.0	2.8	8.2
Whole Blood	L	4.0	8.0	2.2	5.1
	M	15.0	-1.3	2.5	3.7
	H	25.0	0.7	1.3	3.3

Table 1. results for accuracy, intra-day precision and inter-day precision for dried blood spot and whole blood methods. QC, quality control; L, low; M, medium; H, high; DBS, dried blood spot; RSD, relative standard deviation.

To compare tacrolimus measurement in mouse blood via DBS method with WB method, a method comparison was performed, based on Deming regression and a Bland–Altman plot. To do so, in 22 mice, 3x 22 DBS samples, and 22 WB samples were collected and compared. Deming regression was used to calculate a correction factor for every type of DBS sampling, to compensate for systematic differences between both methods. Corrected DBS values were compared with WB values in Bland-Altman plots. According to the guidelines of the European Medicines Agency (EMA), the difference between tacrolimus measurements with DBS and WB methods should be less than 20% of the mean of the concentrations for at least 66.67% of the samples[30].

RESULTS AND DISCUSSION

Quality control samples

In order to validate whether the DBS method can be applied to analyze tacrolimus concentrations in mouse blood, we first set out to analyze blank mouse blood spiked with tacrolimus. Simple linear regression analysis showed a highly significant relationship (r^2= 0.99, P < 0.0001) between WB tacrolimus concentrations and DBS tacrolimus

concentrations of the validation samples (**Figure 1**). This correlation analyses also showed that DBS tacrolimus concentrations tend to be higher than the WB tacrolimus concentrations (slope: 1.42).

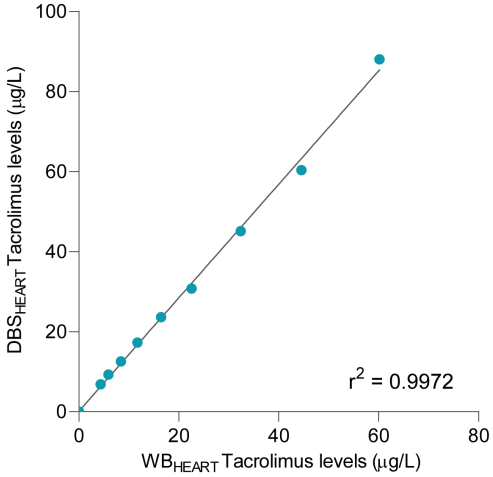

Figure 1. Linear regression analysis of DBSHEART spiked tacrolimus concentrations versus WBHEART spiked tacrolimus concentrations. DBS, dried blood spot; WB, whole blood.

Comparison of DBS LC-MS/MS tacrolimus concentrations with whole blood LC-MS/MS tacrolimus concentrations

Next, we analyzed the concentrations of tacrolimus in mice that had been treated with 1-3 mg/kg tacrolimus for over 2 weeks. A reference venous whole blood sample derived by heart puncture was compared with 3 techniques of blood withdrawal spotted on DBS, which were cheek puncture (DBS_{CHEEK}), heart puncture (DBS_{HEART}) and tail tip bleeding (DBS_{TAIL}) (**Figure 2A**). The tacrolimus concentrations in the WB samples ranged from 2.56 to 27.64 µg/L, and in all DBS samples from 3.39 to 30.97 µg/L.

Deming regression analysis showed a strong relationship between WB tacrolimus concentrations and DBS tacrolimus concentrations for all analyzed blood sampling methods (p>0.0001) (**Figure 2**) (n=22).

In accordance with the spiked blood samples, the DBS_{CHEEK} , DBS_{HEART} and DBS_{TAIL} tacrolimus concentrations tended to be higher than the whole blood tacrolimus concentrations. Therefore, a correction factor was calculated based on the DBS to WB tacrolimus concentration Deming regression fit slopes. DBS_{CHEEK} had a slope of 1.02 and a y-intercept of 1.74, DBS_{HEART} had a slope of 1.13, and an intercept of 1.06, DBS_{TAIL} had a slope of 1.30 and an intercept of 0.15 (**Figure 2**). A Bland-Altman plot with the corrected DBS_{CHEEK} values (**Figure 3A**), shows a very small mean bias (0.15), and 95% limits of agreement of -4.20 and 4.50. In total, 67% of the paired concentrations showed a difference

between methods ≤20%, thereby complying with the European Medicines Agency (EMA) predefined minimum of ≥66.67%[30].

The other assayed measurements had lower compliance; for DBS_{HEART} 64% of the measured samples fell within 20% of the ratio identity line (**Figure 3B**), and for DBS_{TAIL} this was only 54% (**Figure 3C**). No trends in deviations over the concentration range were observed. Taken together, these data indicate that DBS with mouse blood drawn via cheek puncture can be accurately used as a method to measure tacrolimus concentrations in mouse blood.

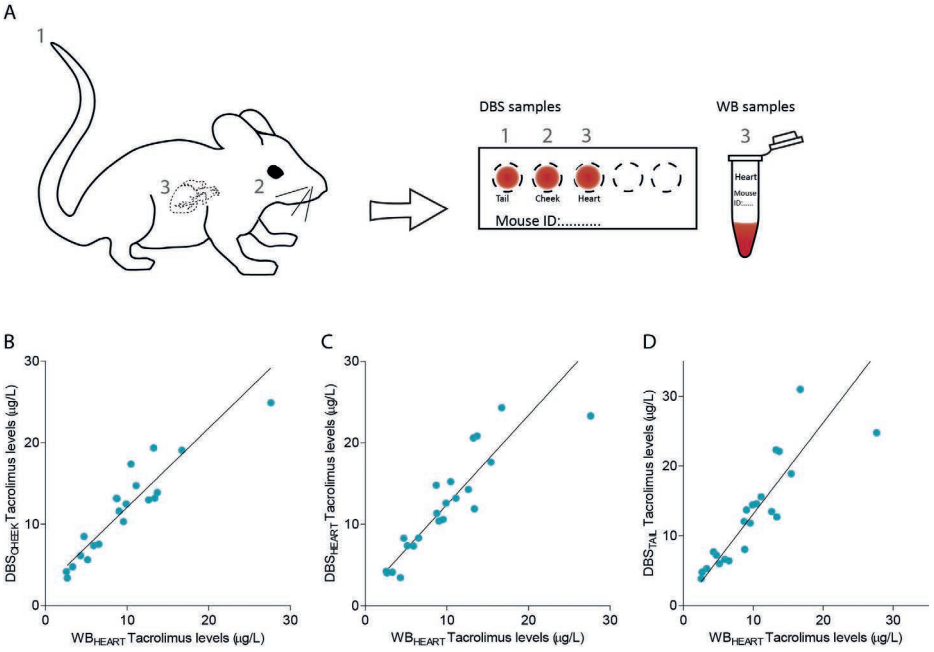

Figure 2. **(A)** Schematic overview of blood sampling. Blood was sampled from mice treated with tacrolimus at the tail tip (1), cheek (2) and, after sacrifice, heart (3). Tail tip, cheek and heart blood was spotted on a DBS card, heart blood was also stored as a whole blood (WB) sample and used as a reference. Deming regression analysis of DBS_{CHEEK} **(B)**, DBS_{HEART} **(C)**, and DBS_{TAIL} **(D)** tacrolimus concentrations versus heart blood tacrolimus concentrations measured with LC-MS/MS. Calculated correction factor formulas were Y = 1.02*X + 1.74 for DBS_{CHEEK}, Y = 1.13*X + 1.06 for DBS_{HEART} and Y = 1.30*X + 0.15 for DBS_{TAIL}. DBS, dried blood spot; WB, whole blood.

Interestingly, the DBS_{HEART} and WB_{HEART} method comparison of mice treated with tacrolimus has a lower agreement than the DBS_{HEART} and WB_{HEART} method comparison of heart blood spiked with tacrolimus (**Figure 1, Figure 3B**). This discrepancy suggests a role for varying pharmacokinetics of tacrolimus in mice or for example differences in wound exudate in the blood samples.

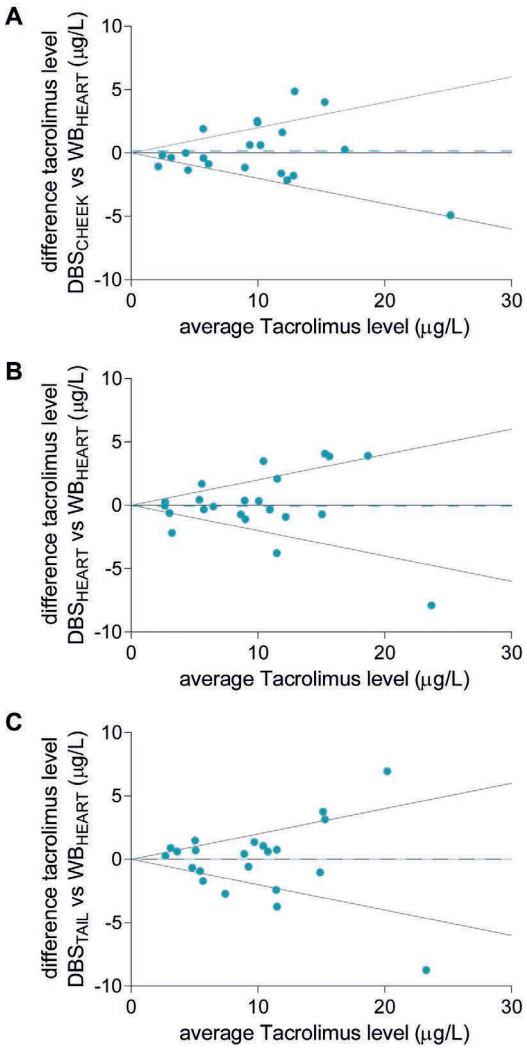

Figure 3. Bland–Altman absolute difference plot of tacrolimus WB concentrations vs DBS_{CHEEK} **(A)**, DBS_{HEART} **(B)**, and DBS_{TAIL} **(C)**. Upper and lower lines represent 20% and -20% difference from average, dotted blue line represents the bias. DBS, dried blood spot; WB, whole blood.

CONCLUSIONS

Our comparison between DBS and whole blood tacrolimus concentrations shows that DBS can be used to measure tacrolimus concentrations in a small volume of mouse blood. When comparing different blood sampling techniques, we discovered that the venous blood withdrawal by cheek puncture spotted on DBS cards gave the most reliable results. Heart DBS demonstrated almost equal agreements between DBS and

WB methods (64%compliance for DBS_{HEART} compared to 67% for DBS_{CHEEK}), however this method is not suitable for serial blood sampling as it can only be used as an end-point blood withdrawal technique. DBS_{TAIL} demonstrated poorer agreement between the DBS and WB methods, making this blood withdrawal spot also unsuitable for monitoring tacrolimus blood concentrations via DBS in mice. Differences in pharmacokinetic profiling between blood sampling sites have been observed before, attributing these differences to, amongst others, the distribution kinetics of therapeutics in the body[31,32]. Blood withdrawal from tail tip also promotes leakage of wound exudate, which might account for the lower agreement between DBS and WB methods for tail tip derived DBS samples. For cheek DBS, 67% of the samples scored a difference from the WB measurement within 20% of the mean, which just complies with the EMA guidelines for method agreement. For a specific pharmacokinetic study in mice it might be useful to optimize the DBS_{CHEEK} method to increase specificity, or to use the WB method, if a larger sample volume can be taken. We argue therefore that the DBS_{CHEEK} method can be used to obtain a solid estimate of tacrolimus blood concentration in mouse studies. For various compounds it has been shown that hematocrit levels can influence the extraction recovery from DBS. However, from dried blood spot assays developed for human samples we know that the hematocrit effect is not existing or at least very minimal for tacrolimus[23,33]. Especially in the hematocrit range between 0.25-0.50 L/L, there is no clinical relevance to correct for hematocrit in tacrolimus measurements. The average hematocrit levels for mice range between 0.40-0.50 L/L[14]. The authors have assumed that due to the comparable and even narrower range of hematocrit in mice, it is not necessary to correct for hematocrit in mice. It is important to consider hematocrit effects in advance when setting up DBS for other immunosuppressive compounds.

DBS is an advantageous method for monitoring mouse tacrolimus blood concentrations and has many benefits over whole blood sampling: lower blood volumes are necessary, which allows for serial sampling during the experiment; the DBS cards can be easily stored for longer times ay ambient temperature, offering a sustainable alternative to ultra-low freezer storage of whole blood samples; and lastly, the DBS cards can be sent via post to another laboratory for analyses, offering tacrolimus PK analysis to institutes that do not have the means to analyze this in house. Furthermore, using DBS_{CHEEK} improves animal welfare, as tacrolimus measurements are not restricted to an end-point sacrifice blood withdrawal and multiple blood samples can be taken from one mouse in a non-invasive manner. Only few publications containing data with mice treated with tacrolimus have actually measured tacrolimus blood concentrations, suggesting that there is a need for an assay measuring tacrolimus blood concentrations. Our results demonstrate that DBS of mouse cheek blood is a useful new method for measuring tacrolimus blood concentrations in mice.

Executive summary

- This is the first dried blood spot (DBS) bioanalytical method for determination of tacrolimus concentrations in mouse blood

- Out of the three tested blood sampling sites, DBS from cheek blood had the highest agreement with whole blood (WB) samples

- Mouse blood spiked with tacrolimus showed a high agreement between the DBS and WB methods for tacrolimus determination. These data suggest that the variation in the measured tacrolimus concentrations between the blood sampling sites in the same mice might be caused by pharmacokinetics or, for example, differences in wound exudate leakage.

Future perspective

Here we have developed a DBS method for the quantification of tacrolimus in mouse blood, which is useful for the quantification of tacrolimus in animal studies. However, the interlaboratory reproducibility of this method remains unclear. We hope that, in the future, the described method will be used as a template for DBS based analysis of tacrolimus in mouse blood, to improve the overall quality and interpretation of tacrolimus pharmacokinetic studies in mice.

REFERENCES

1. Brunet M, van Gelder T, Åsberg A, et al. Therapeutic Drug Monitoring of Tacrolimus-Personalized Therapy: Second Consensus Report. Therapeutic Drug Monitoring. 41(3), 261–307 (2019).
2. Emal D, Rampanelli E, Claessen N, et al. Calcineurin inhibitor Tacrolimus impairs host immune response against urinary tract infection. Scientific Reports. 9(1), 1–11 (2019).
3. Abidi MZ, Erlandson KM. A Comprehensive Review of Infections in Older Kidney Transplant Recipients. Current Transplantation Reports. 1–10 (2021).
4. Randhawa PS, Starzl TE, Demetris AJ. Tacrolimus (FK506)-Associated Renal Pathology. Advances in Anatomic Pathology. 4(4), 265 (1997).
5. Hošková L, Málek I, Kopkan L, Kautzner J. Pathophysiological mechanisms of calcineurin inhibitor-induced nephrotoxicity and arterial hypertension. Physiological Research. 66(2), 167–180 (2017).
6. Moes A, Hesselink D, van den Meiracker A, Zietse R, Hoorn E. Chlorthalidone Versus Amlodipine for Hypertension in Kidney Transplant Recipients Treated With Tacrolimus: A Randomized Crossover Trial. American journal of kidney diseases. 69(6), 796–804 (2017).
7. Shivaswamy V, Boerner B, Larsen J. Post-transplant diabetes mellitus: Causes, Treatment, and Impact on Outcomes. Endocrine Reviews. 37(1), 37–61 (2016).
8. Piotrowski PC, Lutkowska A, Tsibulski A, Karczewski M, Jagodziński PP. Neurologic complications in kidney transplant recipients. Folia Neuropathologica. 55(2), 86–109 (2017).
9. Diehl R, Ferrara F, Müller C, et al. Immunosuppression for in vivo research: state-of-the-art protocols and experimental approaches. Cellular & Molecular Immunology 2017 14:2. 14(2), 146–179 (2016).
10. Lee W-S, Jeong J-H, Lee E-G, et al. Tacrolimus regulates endoplasmic reticulum stress-mediated osteoclastogenesis and inflammation: In vitro and collagen-induced arthritis mouse model. Cell Biology International. 42(4), 393–402 (2018).
11. Vandenbussche C, Van der Hauwaert C, Dewaeles E, et al. Tacrolimus-induced nephrotoxicity in mice is associated with microRNA deregulation. Archives of Toxicology. 92(4), 1539–1550 (2018).
12. Kalt DA. Tacrolimus: A Review of Laboratory Detection Methods and Indications for Use. Laboratory Medicine. 48(4), e62–e65 (2017).
13. Diehl KH, Hull R, Morton D, et al. A good practice guide to the administration of substances and removal of blood, including routes and volumes. Journal of Applied Toxicology. 21(1), 15–23 (2001).
14. Zuthphen LFM van, Baumans V, Beynen AC. Principles of laboratory animal science revised edition. Elsevier.
15. Amsterdam P Van, Waldrop C. The application of dried blood spot sampling in global clinical trials. Bioanalysis2(11), 1783–1786 (2010).
16. Koster RA, Greijdanus B, Alffenaar JWC, Touw DJ. Dried blood spot analysis of creatinine with LC-MS/MS in addition to immunosuppressants analysis. Analytical and Bioanalytical Chemistry. 407(6), 1585–1594 (2014).

* **article of interest for the use of DBS to analyze creatinine and immunosuppressive compounds in human fingerprick blood**

17. Wickremsinhe ER, Perkins EJ. Using dried blood spot sampling to improve data quality and reduce animal use in mouse pharmacokinetic studies. Journal of the American Association for Laboratory Animal Science. 54(2), 139–144 (2015).

** **article of special interest for the advantages of the DBS method in mouse studies**

18. Clark GT, Haynes JJ, Bayliss MAJ, Burrows L. Utilization of DBS within drug discovery: Development of a serial microsampling pharmacokinetic study in mice. Bioanalysis. 2(8), 1477–1488 (2010).

19. Wong P, Pham R, Whitely C, et al. Application of automated serial blood sampling and dried blood spot technique with liquid chromatography-tandem mass spectrometry for pharmacokinetic studies in mice. Journal of Pharmaceutical and Biomedical Analysis. 56(3), 604–608 (2011).
20. Rahavendran S V., Vekich S, Skor H, et al. Discovery pharmacokinetic studies in mice using serial microsampling, dried blood spots and microbore LC-MS/MS. Bioanalysis4(9), 1077–1095 (2012).
21. van de Velde D, van der Graaf J, Boussaidi M, et al. Development and Validation of Hematocrit Level Measurement in Dried Blood Spots Using Near-Infrared Spectroscopy. Therapeutic drug monitoring. 43(3), 351–357 (2021).
22. Capiau S, Veenhof H, Koster RA, et al. Official International Association for Therapeutic Drug Monitoring and Clinical Toxicology Guideline: Development and Validation of Dried Blood Spot-Based Methods for Therapeutic Drug Monitoring. 41, 409–430 (2019). * Official International Association for Therapeutic Drug Monitoring and Clinical Toxicology Guidelines
23. Koster RA, Veenhof H, Botma R, et al. Dried blood spot validation of five immunosuppressants, without hematocrit correction, on two LC-MS/MS systems. Bioanalysis. 9(7), 553–563 (2017).
24. Martial LC, Hoogtanders KEJ, Schreuder MF, et al. Dried Blood Spot Sampling for Tacrolimus and Mycophenolic Acid in Children: Analytical and Clinical Validation. Therapeutic Drug Monitoring. 39(4), 412–421 (2017).
25. Buchanan J, Holiday S, Everhart R, Miley M. Pressure and Time. R.S. 2(3), 314 (2011).
26. den Burger JCG, Wilhelm AJ, Chahbouni A, Vos RM, Sinjewel A, Swart EL. Analysis of cyclosporin A, tacrolimus, sirolimus, and everolimus in dried blood spot samples using liquid chromatography tandem mass spectrometry. Analytical and bioanalytical chemistry. 404(6–7), 1803–1811 (2012).
27. Moretti M, Freni F, Tomaciello I, et al. Determination of benzodiazepines in blood and in dried blood spots collected from post-mortem samples and evaluation of the stability over a three-month period. Drug Testing and Analysis. 11(9), 1403–1411 (2019).
28. Ghareeb M, Akhlaghi F. Alternative matrices for therapeutic drug monitoring of immunosuppressive agents using LC–MS/MS. Bioanalysis. 7(8), 1037 (2015).
29. Balloch S, Calton LJ, Hammond G. Analysis of Cyclosporine, Everolimus, Sirolimus, and Tacrolimus in Whole Blood for Clinical Research. Waters, Application note
30. Medicines Agency E. 2 www.ema.europa.eu/en/bioanalytical-method-validation
** **Committee for Medicinal Products for Human Use (CHMP) Guideline on bioanalytical method validation.**
31. Rangaraj N, Vaghasiya K, Jaiswal S, Sharma A, Lal J. Do Blood Sampling Sites Affect Pharmacokinetics. Chemistry & Biology Interface. 4(3), 176-191. (2014).
32. Chiou WL. The Phenomenon and Rationale of Marked Dependence of Drug Concentration on Blood Sampling Site: Implications in Pharmacokinetics, Pharmacodynamics, Toxicology and Therapeutics (Part II). Clinical Pharmacokinetics17(4), 275–290 (1989).
** **article of special interest for the effects of blood sampling site on drug pharmacokinetics**
33. Koster RA, Alffenaar JWC, Greijdanus B, Uges DRA. Fast LC-MS/MS analysis of tacrolimus, sirolimus, everolimus and cyclosporin A in dried blood spots and the influence of the hematocrit and immunosuppressant concentration on recovery. Talanta. 115, 47–54 (2013).
** **article of special interest on the effect of hematocrit on tacrolimus measurements in human dried blood spot samples.**

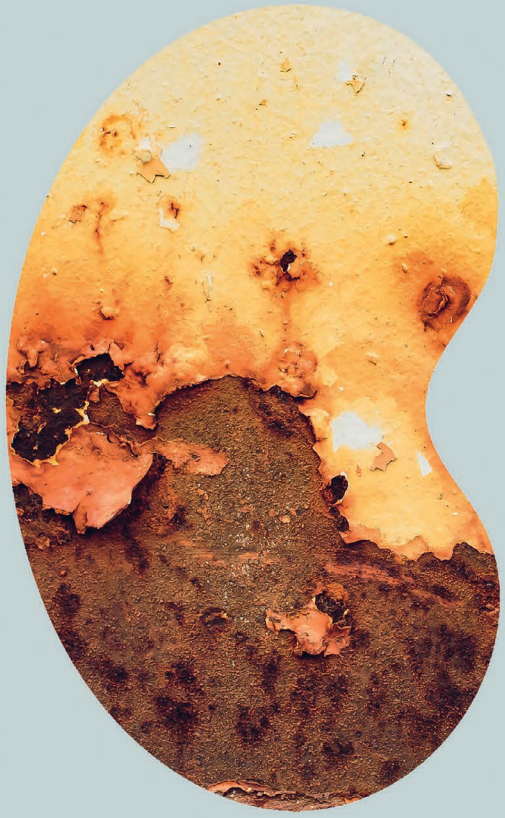

Chapter 8

The immunosuppressive compound tacrolimus inhibits NK cell mediated clearance of senescent cells *in vitro*

Hester van Willigenburg[1,2], Gisela Ambagtsheer[1], Renata Brandt[2], Sander Barnhoorn[2], Linda Cappetti[1], Jan N.M. IJzermans[2], Ron de Bruin[1]

[1] Department of Surgery, Erasmus MC Transplant Institute Rotterdam, Rotterdam, The Netherlands, [2] Department of Molecular Genetics, Erasmus MC, University Medical Centre Rotterdam, Rotterdam, The Netherlands

ABSTRACT

Patients that receive immunosuppressive therapies experience age-related diseases earlier than the average population. A common mechanism behind many age-related diseases is the accumulation of senescent cells, which are damaged cells that avoid replication by entering a permanent cell cycle arrest. These cells promote chronic inflammation and reduce the regenerative capacity of tissues. Senescent cells are subject to clearance by members of the immune system, especially NK-cells. We hypothesised that the suppression of immune cell function by immunosuppressive therapy might inhibit senescence clearance, and increases the chances of developing age-related diseases. Therefore, in this study, we investigated whether commonly used immunosuppressive compounds inhibit the NK-cell mediated clearance of senescent cells. We show that senescent fibroblasts upregulate NKG2D ligands and that NK-cells recognize senescent cells and kill them. Treatment with immunosuppressive compounds suppresses this NK-cell mediated senescence clearance *in vitro*. We have also tested whether tacrolimus administration inhibits senescence clearance in mice. Up to 56 days of continuous tacrolimus administration did not significantly change the number of senescent cells. Our results show that immunosuppressive agents inhibit NK cell mediated clearance of senescent cells *in vitro*. Since the natural occurrence of senescent cells might take longer than 2 months *in vivo*, the effects of tacrolimus on immune-cell mediated senescence remains elusive and requires further research.

INTRODUCTION

Advanced surgical techniques and the use of immunosuppressive compounds have led to considerable improvements in graft and patient survival after tissue and organ transplantation[1–3]. Without the use of immunosuppression, immune cells of the recipient patient can mark a transplanted graft as foreign, triggering transplant-rejection of the transplanted organ or tissue even years after transplantation[1]. Therefore, solid organ and tissue transplant patients are subjected to a life-long regiment of immunosuppressive therapies[1]. These immunosuppressive drugs are mainly directed against inflammation and T-cell activation, but cover suppression of NK-cells, dendritic cells, macrophages and other participants of the immune system as well[4]. The prevention of transplant-rejection by immunosuppressive therapies has become so successful that most transplant patients die with a functioning graft[5].

The leading causes of death in transplant patients with a functional graft are cardiovascular diseases, malignancies, diabetes and infections[2,5–7]. It is well established that immunosuppressive treatment correlates with increased risk for these diseases[8,9]. Cancer, diabetes and cardiovascular diseases are also common in the general population and their prevalence correlates with increasing age[10]. However, patients receiving immunosuppressive regiments typically experience these age-related diseases decades earlier than the average population[7,11], which is an indication of accelerated aging in this patient population. A common mechanism for these age-related diseases might be the presence of aged, or so called senescent cells[12,13]. These cells have been placed in a permanent cell cycle arrest as a result of excessive damage to cellular components[14]. Senescent cells accumulate with advanced age and promote a chronic pro-inflammatory state and malignant transformation, and reduce tissue integrity[14–18]. Accordingly, senescent cells have been found to play causative roles in several age-related diseases such as cardiovascular diseases[19,20], cancer[21–25] and obesity[14,26,27].

Senescent cells are under the control of immune-mediated clearance by several members of the immune system, mainly by NK-cells[28,29]. The upregulation of NKG2D ligands marks senescent cells for degradation by NK-cells[30]. However, impaired immune surveillance in mice, as a result of aging or as a result of a genetically compromised immune system, results in an accumulation of senescent cells and higher occurrence of age-related diseases[29,31]. The long-term use of immunosuppressive therapies in patients might also suppress the immune-cell mediated clearance of senescent cells, leading to increased numbers of senescent cells and increased risk for age-related diseases. Indeed, calcineurin inhibitors (CNIs) have been found to impair NK-cell function *ex vivo*[32]. Whether these types of immunosuppressive compounds also prevent NK-cell mediated senescence clearance, remains to be elucidated.

Here, we confirm that cultured senescent fibroblasts upregulate several NKG2D ligands and that NK-cells that are co-cultured with senescent cells recognize these cells and kill them. Treatment with immunosuppressive compounds suppresses NK-cell mediated senescence clearance *in vitro*. Of the tested immunosuppressive compounds, the calcineurin inhibitors tacrolimus and ciclosporin specifically inhibit T-cell and NK-cell activation. To test whether this type of immune-cell inhibition prevents immune-cell mediated senescence clearance and therefore leads to increases in the number of senescent cells, we treated mice with tacrolimus. Both 28 and 56 days of continuous tacrolimus administration did not result in a significant upregulation of senescence markers.

MATERIAL & METHODS

Cell culture

WI-38 cells (ATCC) were cultured in DMEM (Gibco) supplemented with 10% FCS (F7524 Sigma) and 1% penicillin/streptomycin. WI-38 cells were kept at 5% CO_2, 3% O_2 and used between 25-45 population doublings. NK-92 cells (ATCC) were cultured in RPMI 1640 culture medium (Gibco) supplemented with 10% FBS, 100 IU/ml IL-2 (202-IL-010, R&D systems), 2 mM L-glutamine (Gibco),

penicillin (100 UI/ml) and streptomycin (0.1 µg/ml) (Gibco). NK-92 cells were maintained in suspension at 5% CO_2 and ambient O_2. All cell lines were regularly tested for mycoplasma contamination. For senescence induction, cells were irradiated with 10GY X-ray at day 0 and 10GY X-ray at day 7. Unless otherwise indicated, all experiments with senescent cells were performed 14 days after the first X-ray irradiation.

NK-cell toxicity assays

WI-38 cells were seeded at such a density that at the start of treatment, both the proliferating and senescent cells were 90% confluent. 3 days after seeding, cells were co-cultured with NK-92 cells in a 1:1 ratio. In those experiments where immunosuppressive compounds were added, NK-92 cells were pre-incubated for 5 hours with tacrolimus (S5003, Selleck Chem), ciclosporin (S2286, Selleck Chem), rapamycin (Sirolimus) (S1039, Selleck Chem), mycophenolic acid (MPA) (S2487, Selleck Chem), prednisolone (S1737, Selleck Chem). After pre-incubation, the medium containing NK-92 cells and immunosuppressive compounds or vehicle control were added to washed and aspirated WI-38 cells. After the indicated amount of time, plates with WI-38 cells were staining for residual WI-38 cells with a Brilliant Blue staining. First, cells were washed with PBS, and then incubated for 30-120 min RT with Brilliant blue solution (50% methanol, 10% acetic acid and 0.1% G250 Coomassie Brilliant blue). Then, the solution was removed, the plates were washed under running water and dried overnight. The plates were scanned with a Gelcount and analysed with FIJI software.

NK-cell degranulation assay

Human NK cells were isolated from buffy-coats from healthy donors (NVT Sanquin) using an NK Cell Isolation Kit (Miltenyi Biotec), according to manufacturer's instructions. NK cells were resuspended in DMEM media (Lonza) supplemented with 10% human serum (Gibco), 1% Penicillin/Streptomycin (Gibco) and 200 U/mL IL-2 (202-IL-010, R&D systems) and left to acclimatize overnight. Then, NK cells were co-cultured with senescent WI-38 cells that were seeded 3 days earlier in a 1:1 ratio for 4h at 37 °C in the presence of 500 U/mL IL-2 and FITC conjugated anti-human CD107a (LAMP-1) antibody (Biolegend, 328606)[33] in the presence of a protein transport inhibitor cocktail (00-4980-93 Invitrogen). For the incubation with tacrolimus, a 1 mg tablet of Prograft (1E3375A, Astellas Pharma BV) was dissolved in DMSO, and filter sterilized, and added to the co-culture at the indicated concentrations. After 4 hours of co-culture, NK-cells were collected and washed with FACS buffer (PBS, 0.5% BSA), and subsequently stained with APC/Cy7 anti-human CD3 (Biolegend, 300318) and Pacific Blue anti-human CD56 (Biolegend, 328606) or their isotypes for 30 minutes at 4 °C in the dark. After washing, the samples were measured using a BD LSR Fortessa flow cytometer and the data was analysed using FlowJo software.

Immunofluorescence staining

WI-38 cells were triggered to senesce by 2x 10GY irradiation. 11 days after the first irradiation treatment, senescent and un-irradiated (proliferating) cells were seeded on glass coverslips in transwells plates. 3 days after seeding, all cells were fixated on the coverslips with 4% formaldehyde solution for 30'at RT and stored in TBS until further analyses.

Fixated cells were washed 2 x 5 minutes in TBS and incubate in TBS with 0.1% triton for 5 minutes. After two washes in TBS, cells were blocked in TBS-Gel (TBS with 0.2% Gelatin (04055, Sigma)) containing 50mM Glycine (50050, Sigma) and 5% horse serum (16050-122, Gibco) for 30 min to 1 hour at RT. Then cells were incubated with primary antibody (laminB1; ab16048 Abcam, γH2AX; 05-636 EMD Millipore, IL-6; ab6672 Abcam) diluted in TBS-Gel and incubated overnight at 4°C. The next day, the cells were washed 3x with TBS-gel and incubated with fluorescent conjugated secondary antibodies (1:1000) diluted in TBS-Gel with Hoechst (1:1000) for 42 min at room temperature. Next, slides were washed in TBS-gel, in TBS, rinsed in dH_2O and mounted with Vectashield. The stained cells were imaged on a LSM700 confocal microscope and those images were processed and analysed with FIJI software.

Click-it EdU reaction

For the Click-it EdU incorporation assays, senescent and un-irradiated (proliferating) cells were seeded on glass coverslips in transwells plates. 10µM EdU (A10044 Thermofischer) was added to the cells 2 days after seeding on the glass coverslips. 3 days after seeding, all cells were fixated on the coverslips with 4% formaldehyde solution for 15'at RT and stored in TBS until further analyses.

Fixated cells were permeabilized with 0.1% Triton X-100 in PBS for 10', washed with PBS and blocked with PBS containing 1.5% BSA for 10'. Cells were then washed and incubated for 1hr in the dark with a click-it solution (50 mM Tris buffer containing 60 µM Atto Azide (AD594-105; Atto Tech), 4 mM $CuSO_4 \cdot 5H_2O$ (209198-100G; Sigma-Aldrich) and 10 mM Ascorbic acid (A0278-100G; Sigma-Aldrich)). Then, cells were washed and incubated with Hoechst (1:1000) (565877 BD pharmingen), washed with 0.1% Triton-X100 in PBS, normal PBS and mounted with DAPI-Vectashield. The cells were imaged on a LSM700 confocal microscope and those images were processed and analysed with FIJI software.

RT-qPCR

Cells were disintegrated in Trizol (Sigma) for at least 5 minutes. Tissues were first sonicated to release cellular content, after which they were submerged in Trizol. After chloroform extraction, RNA was precipitated using isopropanol and washed with 75% ethanol. RNA was dissolved in DepC treated H_20 and then treated with 1U DNase (Thermo Fisher Scientific) for 30' at 37°C. DNAse was deactivated by a 10' incubation with EDTA (25 mM) at 65°C. 5 µM random hexamers (Thermo Fisher Scientific) and 10 mM dNTPs were added and the mixture was incubated at 65°C for 5 minutes. After denaturation, samples were placed on ice and RT-mix was added (5x first strand buffer, DTT (0.1 M) and RNase out (Thermo Fisher Scientific)). Samples were incubated at 25°C for 2'. Then cDNA was generated using 200 U Superscript II reverse transcriptase (Thermo Fisher Scientific) per sample, with an incubation of 10' at 25°C and 15' at 70°C. cDNA samples were stored at -20°C. Quantitative Real Time-Polymerase Chain Reaction (RT-qPCR) was performed using Platinum Taq DNA polymerase (Life Technologies) and Sybr Green (Sigma Aldrich) in a CFX 384 Real Time system (BioRad). Expression levels were normalized to YHWAZ/GAPDH for the WI-38 cells and HPRT1/GAPDH for mouse tissues, using the following primers:

Human primer sequences:

Gene	Forward primer	Reverse primer
YHWAZ	gatgaagccattgctgaacttg	ctatttgtgggacagcatgga
GAPDH	cggagtcaacggatttggtcgtat	agccttctccatggtggtgaagac
MICA	acttgacagggaacggaaagga	ccatcgtagtagaaatgctggga
MICB	atctgtgcagtcagggtttctc	tgaggtcttgcccattctctgt
ULBP1	tgggtatcatgcttactgtctggg	gggtttgggttcatagtgcagagtt
ULBP2	cagagcaactgcgtgacatt	gccagacagaagggcgagttt
p16INK4A	gtggacctggctgaggag	ctttcaatcggggatgtctg
p21	acagcagaggaagaccatgt	tcctcttggagaagatcagc

Mouse primers sequences:

Gene	Forward primer	Reverse primer
HPRT1	tgatagatccattcctatgactgtaga	caagacattctttccagttaaagttg
GAPDH	aaggtcatcccagagctgaa	ctgcttcaccaccttcttga
IL-6	ggagtcacagaaggagtggc	aacgcactaggtttgccgag
Kim1	agggaagccgcagaaaaacc	cggaaggcaaccacgcttag
tnf-α	gttgtaccttgtctactcccag	ggttgactttctcctggtatgag
IL-1b	cacagcagcacatcaacaag	gtgctcatgtcctcatcctg
p21	gagcaaagtgtgccgttgtc	ggtttggagactgggagagg

Mouse studies

The mice used in this study were either 12-month-old females, or 24 month old males and females of C57BL/6J background. The mice were kept in individual cages from the start of the experiment with ad libitum access to food and water. Certified biotechnicians carried out all experimental protocols under strict guidelines to ensure careful and consistent handling of the mice. In the first cohort, mice received 0, 1 or 3 mg/kg Tacrolimus per day for 28 days via Alzet osmotic mini-pumps (Alzet®, model 2004). The mice of the second cohort received 0 or 3 mg/kg tacrolimus per day for 56 days via Alzet osmotic mini-pumps. The Alzet pumps were filled with Tacrolimus (S5003, SelleckChem) dissolved in a 50%DMSO-50% EtOH solvent, and incubated in saline for 24 hours at 37°C prior to subcutaneous intrascapular implantation. Blood samples were collected at 1, 14 and 28 days after insertion of the Alzet pump for the first cohort and at 14, 42 and 56 days for the second cohort. At day 56 day blood tacrolimus levels measured via Dry Blood Spot (DBS) method combined with liquid chromatography tandem-mass spec (LC-MS/MS) analyses.

Tacrolimus blood level measurements

50 µL cheek blood was spotted on a DBS card and analysed with DBS methods, as described previously[34]. DBS samples were stored in a desiccator for at most six months until they were measured.

Serum creatinine measurements

Blood samples were derived via heart puncture at the end of the experiment, and centrifuged for serum collection. Serum creatinine levels were measured using creatinine assay kits (MAK080-1KT, Sigma) according to manufacturer's protocol.

Sirius red staining

5 µm paraffin sections of mouse kidney were emerged in Xylene and rehydrated in decreasing concentrations of ethanol. Then slides were incubated in Picro Sirius Red solution for 60 minutes, after which they were rinsed in 0.05% acetic acid, dehydrated in

increasing concentrations of ethanol and Xylene, and then mounted with Pertex. These sections were scanned with a Nanozoomer and subsequently analyzed with FIJI software.

Statistical analyses

All statistical analyses were performed with Graphpad (version 8.4.3), specific statistical tests are indicated in figure legends. All data are expressed as mean + SD, * $p < 0.05$, ** $p < 0.01$, *** $p<0.001$.

RESULTS

Human WI-38 fibroblasts express NK cell ligands upon induction of senescence.

In order to investigate the effects of immunosuppressive compounds on NK-cell mediated senescence clearance, we decided to first use an *in vitro* senescence model. Therefore, we have used the well-established method of ionizing radiation (IR) to induce senescence[35] in WI-38 fibroblast cells. To validate whether IR had caused senescence, protein expression of a combination of validated senescence markers was assessed via immunofluorescence (IF) staining. 14 days after irradiation, the number of γ-H2AX foci[36] is higher in irradiated cells than in non-irradiated cells (**Figure 1A**). Furthermore, as represented in **Figure 1A**, an accumulation of nuclear DNA in the cytosol is visible in some irradiated cells, which is a trigger of the senescence associated secretory phenotype (SASP)[37] (cytosolic DNA was not quantified). **Figure 1B** shows that IR treatment halts proliferation in WI-38 cells as indicated by an absence of EdU incorporation[38]. **Figure 1C** shows the loss of nuclear protein Lamin B1 in irradiated WI-38 cells, indicating the induction of senescence[39,40]. Lastly, expression of major SASP factor IL-6 was highly upregulated in irradiated cells (**Figure 1D**). Having established that IR causes senescence in WI-38 cells, NK-cell ligand expression was assessed 7 days and 14 days after irradiation (**Figure 1E**). All tested NK-cell ligands showed a modest upregulation in senescent cells, and particularly MicA and ULBP1 were highly expressed in senescent WI-38 fibroblasts. There was no significant difference in the upregulation of NK-cell ligands 7 days or 14 days after IR. Since gene expression of senescence marker *CDKN1A*, which encodes the $p21^{Cip1}$ protein, was significantly increased 14 days after IR (**Figure 1E**), we decided to continue our experiments with senescent cells 14 days after IR. Together, these data indicate that 14 days after ionizing radiation WI-38 cells have become senescent and highly express NK-cell ligands MicA and ULBP1.

The immunosuppressive compound Tacrolimus inhibits NK-cell mediated senescence clearance *in vitro.*

We then employed an *in vitro* cytotoxicity assay to assess the ability of NK cells to recognize and kill senescent WI-38 fibroblasts. Proliferating and senescent WI-38 cells were co-cultured up to 3 days with the human NK cell line NK-92 at a 1:1 ratio.

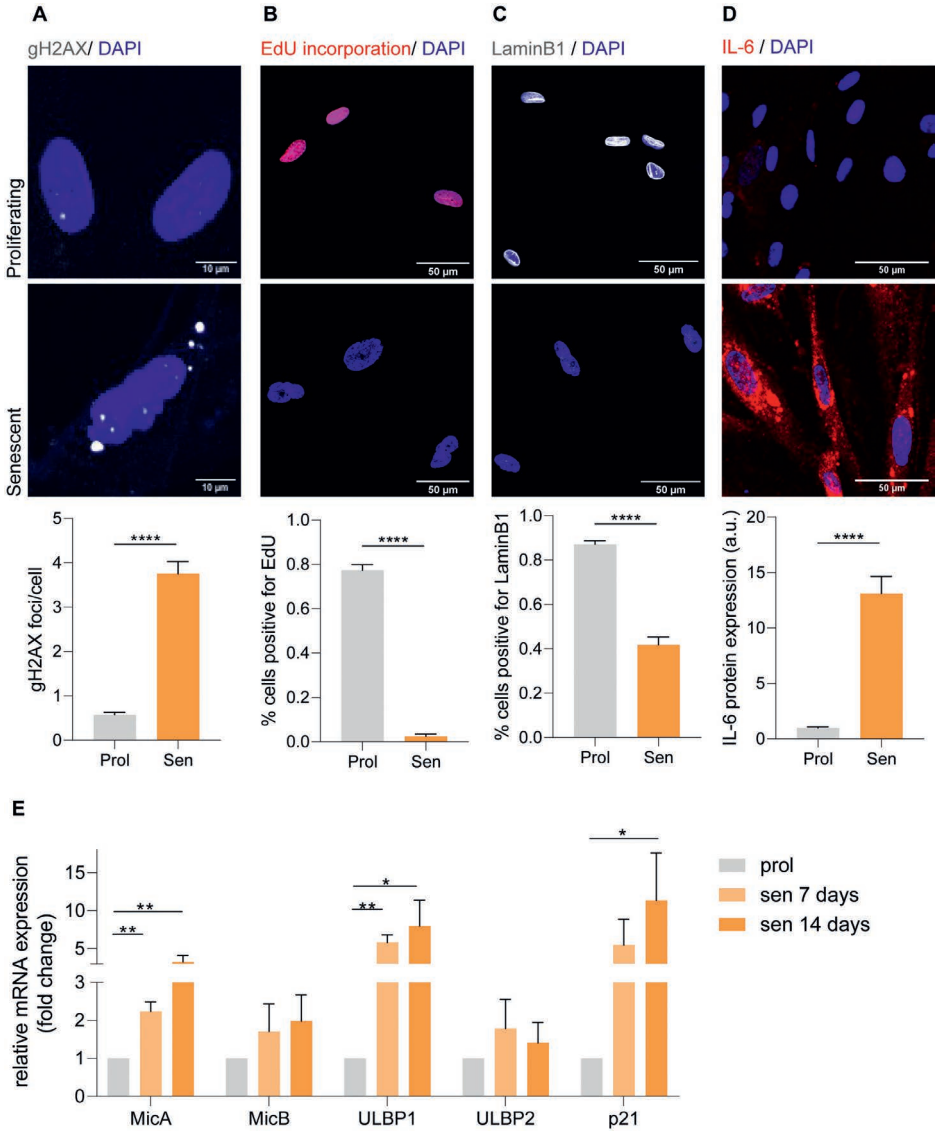

Figure 1. Irradiated WI-38 fibroblasts express senescence markers and upregulate NK-cell ligands

A-D. Representative images of immunofluorescence stainings for senescence markers γ-H2AX (A), EdU incorporation **(B)**, LaminB1 **(C)** and IL-6 **(D).** The top row represents proliferating WI-38 cells, the middle row represents senescent WI-38 cells 14 days post 2x10 GY irradiation. In the bottom row quantifications of the immunofluorescence analyses are presented. **E**. Gene expression analyses via RT-qPCR of NK-ligands MicA, MicB, ULBP1 and ULBP2, and of senescence marker p21. Data are expressed as mean +/- SD (combined data of n=3 independent assays). P -values were calculated with two-tailed student T-test, * $p < 0.05$, ** $p < 0.01$, *** $p<0.001$

Figure 2A shows the % of viable WI-38 cells after 1, 2 or 3 days of co-culture with NK-92 cells. This experiment shows that NK-92 cells kill both proliferating and senescent cells, but have a significant preference for targeting senescent cells ($p>0.0001$). Furthermore, 3 days of co-culture with NK cells had cleared all senescent cells, compared to 84% clearance after 1 day of co-culture, indicating that *in vitro* NK-cell mediated senescence clearance occurs in a time dependent fashion. To assess whether immunosuppressive compounds interfere with NK-cell mediated senescence clearance, NK-92 cells were treated with tacrolimus. Tacrolimus indeed prevents the NK-cell mediated cell death of senescent WI-38 cells in a dose-dependent manner (**Figure 2B**). Furthermore, preliminary assessment of other immunosuppressive compounds, including ciclosporin, prednisolone, rapamycin and mycophenolic acid (MPA) indicated that these agents can also inhibit NK-cell mediated senescence clearance (**supplemental figure 1**). The expression of CD107a on the outer cell membrane of NK cells marks NK-cell activation and cytotoxic degranulation. To test whether the clearance of senescent cells by NK-cells is due to activation and degranulation of NK-cells by senescent cells, we assessed CD107a expression by flow cytometry on NK cells co-cultured with senescent Wi-38 cells. These human NK cells were isolated from a buffy coat and gated as CD3-, CD56+ cells after 24 hours of co-culture with WI-38 cells. **Supplemental figure 2A** shows that a co-culture of isolated NK cells with senescent WI-38 cells upregulates the expression of surface marker CD107a on isolated NK cells. Next, we assessed the effect of low doses of tacrolimus on NK cell activation by senescent cells (**Supplemental figure 2B**). This preliminary experiment shows that tacrolimus might suppress NK cell degranulation, based on lower expression of CD107a on NK-cells co-cultured with senescent cells in the presence of tacrolimus. Together, these data indicate that the *in vitro* clearance of senescent cells by NK-cells can be inhibited by immunosuppressive therapies, and that this is probably caused by a repression of NK-cell degranulation.

28 days of continuous tacrolimus treatment does not increase the number of senescent cells in 1 year old WT mice.

Although NK-cells are attributed a prominent role in senescence clearance[30], senescent cells can be removed by other immune cell types[31,41,42]. Therefore, we decided to assess whether an immunosuppressive compound can prevent senescence clearance *in vivo*. As a result of reduced senescence clearance, we expected an increase in the number of senescent cells. To assess this, we first treated a pilot cohort of 12-month-old female Blck6 mice with 2 different doses of tacrolimus in groups of 4 mice. We made use of an Alzet mini osmotic pump for continuous stable tacrolimus delivery for 28 days. No mice died during treatment (data not shown), and no changes in body weight were observed (**Figure 3A**). We made use of our recently developed method to assess tacrolimus levels in mouse blood using DBS. Tacrolimus blood levels decreased during the 28 days of treatment, such that mice treated with 1 mg/kg tacrolimus ended with an average tacrolimus blood concentration of 1.4 ng/mL (ranges between 0.98 and 1.8 ng/mL), and the 3 mg/kg group had an average of 4.1 ng/mL (ranges between 2/29 and

8.16 ng/mL)(p=0.09). For human patients, the tacrolimus blood concentrations are generally maintained between 5.0 and 30.0 ng/mL to prevent organ rejection. Thus, although the mice treated with 3 mg/kg tacrolimus received appropriate levels of tacrolimus in the first two weeks of treatment, at day 28 of tacrolimus treatment, the tacrolimus blood levels of the 3mg/kg tac group were 1 ng/mL below recommended tacrolimus blood concentrations for humans. A previous study utilizing the Alzet mini pump to deliver 1 mg/kg tacrolimus in mice did not measure tacrolimus blood levels, but did show that this dose was sufficient to cause frequently observed side-effects of tacrolimus, such as renal fibrosis and inflammation[43]. Therefore, we assessed whether our tacrolimus treatment also induced renal fibrosis, by analysing a Sirius Red staining of the kidneys after 28 days of tacrolimus treatment. We did not observe any significant increase in fibrosis levels, but a slight trend (p=0.2) towards increased fibrosis in the mice treated with 3 mg/kg tacrolimus compared to controls that received no tacrolimus (**Figure 3C, right panel**). A marker for renal function, creatinine, also showed a slight trend towards reduced renal function in the 3mg/kg group, however no significant difference was found (**Figure 3D**). Lastly, we assessed whether tacrolimus treatment had increased the number of senescent cells, via RT-qPCR for senescence and renal injury markers (**Figure 3E**). No differences between the 0, 1 and 3 mg/kg groups were observed for any of the tested markers. Taken together, these data show that 28 days treatment with 1 or 3 mg/kg of tacrolimus does not induce renal injury, or senescence.

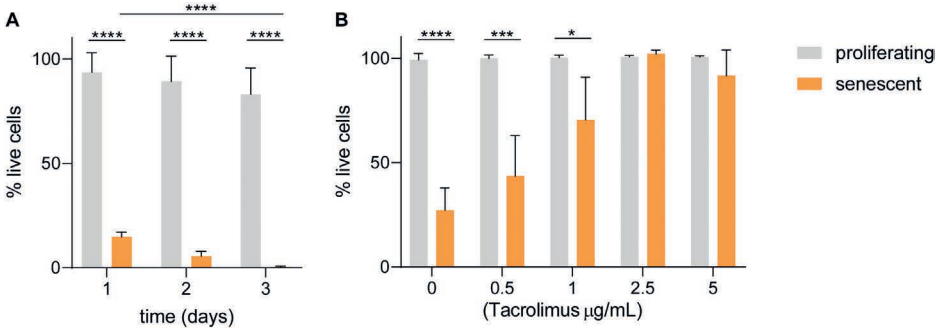

Figure 2. NK-92 cells preferentially kill senescent cells, which can be inhibited by the immunosuppressive compound Tacrolimus

A. Proliferating and senescent WI-38 cells were co-cultured for 1,2 and 3 days with NK-92 cells in a 1:1 ratio. Shown is the percentage (%) of viable cells after co-culture with NK-92 cells, compared to cells that were not co-cultured with NK-92 cells, based on a brilliant blue staining of the remnant WI-38 cells. **B.** Proliferating and senescent WI-38 cells were co-cultured for 1 day with NK-92 in a 1:1 ratio, with indicated concentrations of tacrolimus. Shown is the percentage of life WI-38 cells after co-culture with NK-92 cells, compared to cells that were not co-cultured with NK-92 cells, based on a brilliant blue staining of the remnant adherent WI-38 cells. Data are expressed as mean +/- SD (combined data of n=3 independent assays). P -values were calculated with two-tailed student T-test, * $p < 0.05$, ** $p < 0.01$, *** $p<0.001$

56 days of continuous tacrolimus treatment does not increase the number of senescent cells in two-year-old WT mice.

To allow more time for senescence accumulation upon tacrolimus treatment, we treated two-year-old WT mice for 12 weeks with 3mg/kg tacrolimus. However, because mice died of old age during the experiment, the experiment had to be terminated 4 weeks earlier than planned, leaving the two-year-old mice with 8 weeks of tacrolimus treatment. No differences in mortality between the tacrolimus or vehicle treated groups were observed (**Figure 4A**). The treatment with 3 mg/kg tacrolimus resulted in an average of 10ng/mL of tacrolimus blood levels at 28 days post the second insertion of the Alzet mini osmotic pumps (56 days after the start of the experiment) (**Figure 4B**). Yet, there was a large variation in tacrolimus blood levels (ranges between 3.8 and 17.3 ng/mL). To assess whether 8 weeks of 3mg/kg tacrolimus suppresses immune-cell mediated senescence clearance, and therefore leads to increases in the numbers of senescent cells, we assessed gene expression levels of several senescence markers in kidney, fat and liver tissue. No differences in expression of any senescence or renal injury markers were found based on RT-qPCR in kidney tissue (**Figure 4C**) or fat and liver tissue (**Supplemental figure 3**) of mice treated with 0 or 3 mg/kg tacrolimus . Assessments of renal function by serum creatinine levels showed that 2 months of tacrolimus treatment did not affect kidney function at 56 days after the start of the treatment (**Figure 4D**). These data show that 56 days of tacrolimus treatment had not caused renal injury or increased the number of senescent cells in 2-year-old WT mice.

DISCUSSION

The immune cell mediated clearance of senescent cells is necessary to maintain good health and to prevent age-related diseases[44]. However, little is known about the surveillance of senescent cells in patients undergoing immunosuppressive therapy. Here we show that senescent WI-38 fibroblasts express NK-cell ligands, which targets them for NK-92 mediated clearance. Furthermore, we show that the commonly used immunosuppressive compound tacrolimus inhibits this NK-cell mediated senescence clearance *in vitro.* Up to 8 weeks of 3 mg/kg tacrolimus treatment did not result in increased levels of senescent cells in WT mice. However, from the current *in vivo* experiments, we cannot elucidate whether tacrolimus does or does not inhibit immune cell mediated senescence clearance.

Our *in vitro* experiments show that immunosuppressive agents can block NK-cell mediated senescence clearance. In this study we could confirm that senescent WI-38 fibroblasts upregulate NK-cell activating ligands, as was shown in other cell lines after senescence induction as well[28,29,45]. A co-culture of senescent or proliferating WI-38 cells with NK-92 cells promotes degranulation of NK-cells, as marked by the expression of CD107a, which kills senescent cells. Several immunosuppressive compounds block this NK-cell mediated senescence clearance.

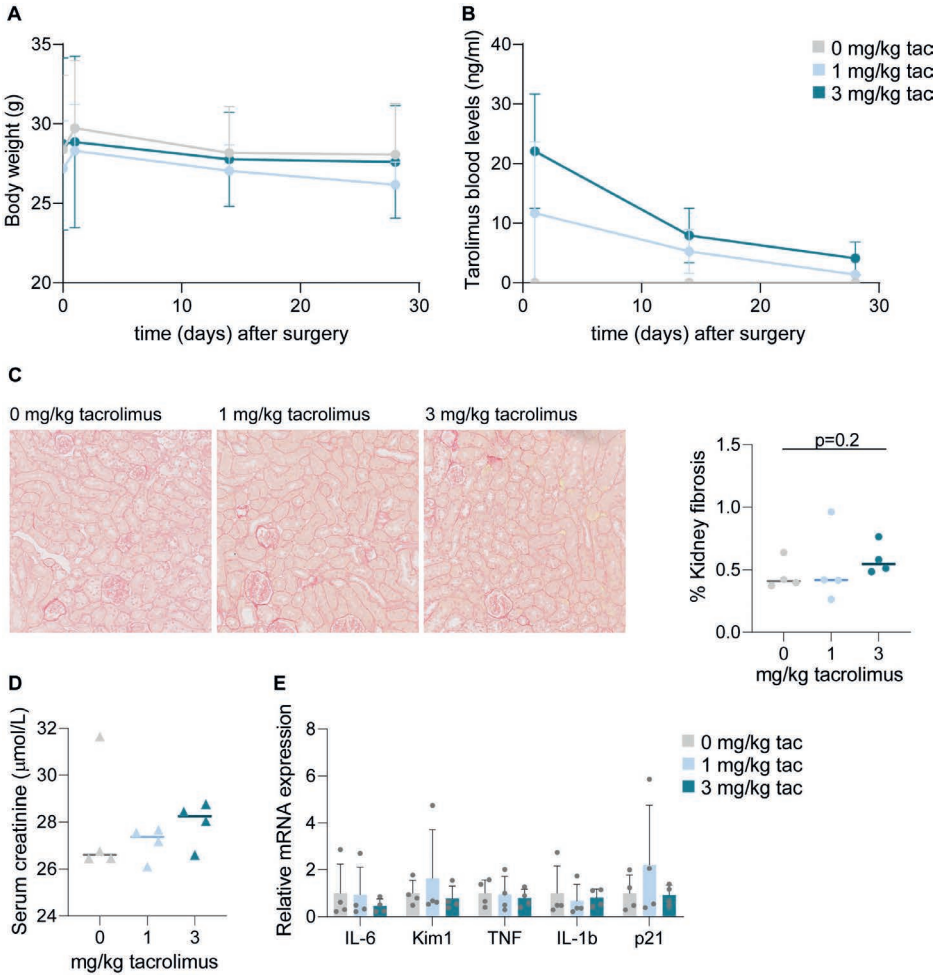

Figure 3. WT mice treated with tacrolimus for 28 days do not show signs of nephrotoxicity or senescence.

A. Average body weight during the treatment with tacrolimus of 12-month-old female C57BL/6J mice. **B.** Tacrolimus blood levels during treatment with tacrolimus for 28 days. **C.** Representative images of Sirius red staining for assessment of renal fibrosis. In the right panel, the % area positive for fibrosis is presented. **D**. Plasma creatinine levels after 28 days of tacrolimus treatment. **E.** Gene expression analyses via RT-qPCR of senescence and renal injury markers at 28 days after tacrolimus treatment. Tac; tacrolimus, IL-6; Interleukin-6, Kim1; Kidney injury molecule-1, TNF; tumor necrosis factor-alpha, IL-1b; Interleukin-1beta, p21; cyclin-dependent kinase inhibitor 1. Data are expressed as mean +/- SD (all assessments are based on n=4 mice per group). P-values were calculated with two-tailed student T-test, * $p < 0.05$, ** $p < 0.01$, *** $p<0.001$

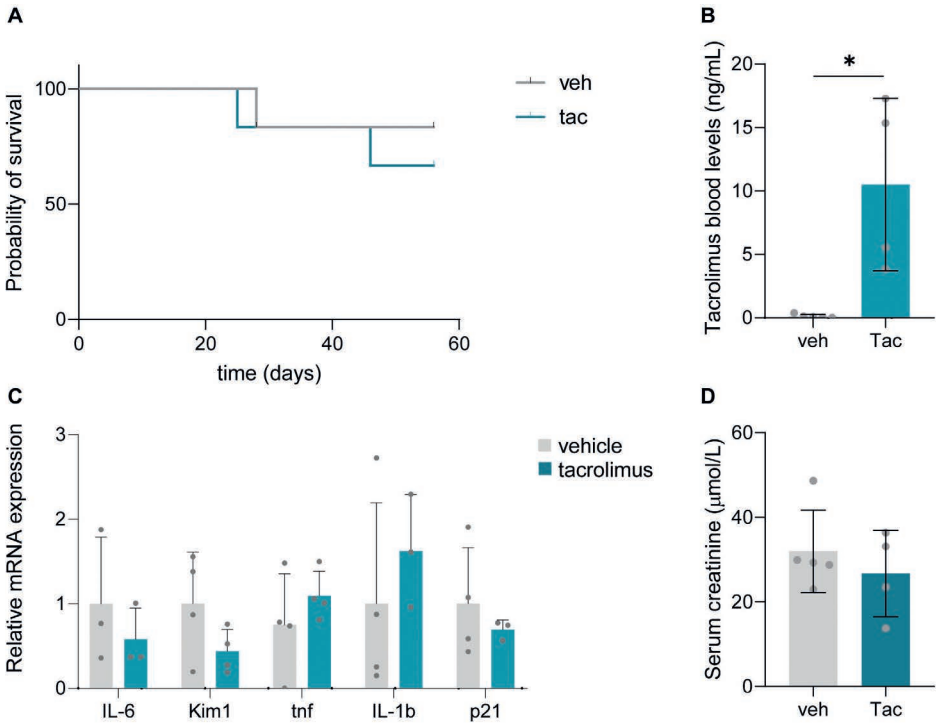

Figure 4. Two-year-old WT mice treated with tacrolimus for 56 days do not show increases in renal injury or senescence.

A. Survival of 2 year old C57BL/6J mice during treatment with 0 (veh) or 3 (tac) mg/kg tacrolimus for 56 days. **B.** Tacrolimus blood levels after 56 days of tacrolimus treatment. **C.** Gene expression analyses via RT-qPCR of renal injury and senescence markers. IL-6; Interleukin-6, Kim1; Kidney injury molecule-1, TNF; tumor necrosis factor-alpha, IL-1b; Interleukin-1beta, p21; cyclin-dependent kinase inhibitor 1. **D**. Plasma creatinine levels after 56 days of tacrolimus treatment. Data are expressed as mean + /- SD. P-values were calculated with two-tailed student T-test, * $p < 0.05$, ** $p < 0.01$, *** $p<0.001$

Our preliminary data suggest that this effect is the result of decreased degranulation of NK cells by at least tacrolimus treatment, urging for follow-up research[46]. Cytotoxic T-cells and natural killer cells both kill target cells by releasing the apoptosis-inducing contents of their granules. Intercellular, the recognition of a target cell activates calcineurin, which then activates nuclear factor of activated T-cell cytoplasmic (NFATc), which mediates T-cell or NK-cell proliferation, cytokine production and granule exocytosis[47]. In this study, we have focussed on the senescence clearance of NK-cells, however, senescent cells can be removed by degranulation of cytotoxic T-cells as well[31,41]. Therefore, the calcineurin inhibitor tacrolimus might not only suppress senescence clearance mediated by NK-cells, but also by T-cells.

To clarify whether immunosuppressive compounds inhibit immune cell mediated senescence clearance *in vivo*, we tested the effect of 4-8 week tacrolimus administration in WT mice. Assuming that senescent cells would be cleared by immune cells in untreated WT mice, we had expected to detect an increase in senescent cell markers within this timeframe. However, we did not observe even a trend towards increased expression of senescence markers.

It could be that the dose of tacrolimus used in our study was not sufficient to suppress immune cell activation by senescent cells. The absence of renal injury and fibrosis after tacrolimus administration indicate that our tacrolimus treatment dose may have been too low. Many studies using mice as a model organism, have used lower concentrations of tacrolimus, with alternative administration routes, solvents or sources of tacrolimus, but have observed increases in fibrosis or renal dysfunction due to tacrolimus. Unfortunately, few of these studies have measured tacrolimus blood levels, making it difficult to compare results. Although the Alzet pumps have delivered tacrolimus during the complete duration of our experiments, tacrolimus blood levels varied notably between mice and within the same mouse over time (**Figure 3B**). The decreased tacrolimus blood levels towards the end of the 28 days of use of the Alzet mini osmotic pump might have been too low to suppress activation of NK- or T-cells, leading to a restoration of senescence clearance. For future research, it should be assessed whether the observed reduction in blood tacrolimus levels can be contributed to tacrolimus stability over longer periods of time, or Alzet pump technicalities. In either case, other methods of tacrolimus delivery, for example by i.p. injection could be explored. Furthermore, we have not assessed whether the observed tacrolimus blood levels also suppressed NK-cell function in mice, which should be investigated[48].

Furthermore, waiting for cells to senescence due to aging, might take longer than the duration of our present studies. Naturally occurring senescence (as opposed to injury-induced senescence) can be a timely process. 2 year old WT mice have approximately 10% of senescent cells in several examined tissues[31], which would come down to an increase in the number of senescent cells of 0.4% per month, if natural senescence induction would occur in a linear fashion. However, there is evidence that the manifestation of senescent cells does not occur in a linear fashion. Mice harbouring a genetic defect in immune-cell activation, show an increased accumulation of senescent cells with increasing age[31]**.**Therefore, this study might be succeeded by even longer tacrolimus treatments, or kidney or liver injury models to induce senescence, such as cisplatin or ischemia-reperfusion models of acute injury[49,50], in combination with immunosuppressive therapy.

It must be noted that in our experiments other cells might have taken over the senescence-clearing role of the immunosuppressed NK-cells and T-cells. For example, Lujambio et al. have attributed some senescence clearing effects to liver resident and infiltrating macrophages *in vitro*[42]. However, a major increase in the number of senescent

cells has been found in mice that have a knock out in the PRF1 gene, which plays a key role in granule-dependent cell death[31]. PRF1 is only expressed in cytotoxic T-cells and NK-cells[31], suggesting that the therapeutic inhibition of NK-cells and T-cells only should be sufficient to suppress senescence clearance.

Interestingly, there have been some senescence inducing properties ascribed to the calcineurin inhibitor ciclosporin, but not to tacrolimus[51]. In our current study, we have not assessed whether tacrolimus itself induces senescence. If tacrolimus treatment indeed results in increased levels of senescent cells, it is in our current *in vivo* study setup impossible to determine whether these senescent cells are the result of increased senescence induction by tacrolimus, tacrolimus induced hypertension or nephrotoxicity or reduced senescence clearance by immune cell suppression. Therefore, an extra experiment would be needed, in which senescence induction by tacrolimus would be compared between WT and immune deficient mice.

The increasing success rate of organ and tissue transplantation has urged improvement of physiological patient care after transplantation. Still, transplant patients age faster and suffer from age-related diseases earlier than the general population and little is known about the effect of immunosuppressive compounds on the clearance of senescent cells. The here reported effects of immunosuppressive compounds on inhibiting senescence removal by NK-cells suggest that the accelerated aging of transplant patients might be attributed to increases in the number of senescent cells. This study is therefore also of interest to those patients receiving immunosuppressive therapies for other diseases as well, such as those with autoimmune diseases. These experiments have paved the way for future research on the effect of immunosuppression on senescence clearance. If tacrolimus indeed suppresses immune-clearance of senescent cells in humans, patients receiving immunosuppression could benefit from recently discovered anti-senescence treatments, to postpone age-related diseases and prolong a healthy life span.

Acknowledgements

The authors would like to thank Nicole Litjens for sharing her knowledge on NK-cell activation, Ingrid van der Pluijm for helping us to actualize the p16::3MR mouse experiments, and Yvette van Loon for genotyping the mice. HvW is supported by a grant from the Dutch Kidney Foundation (15OP11).

REFERENCES

1. Holt, C. D. Overview of Immunosuppressive Therapy in Solid Organ Transplantation. Anesthesiology Clinics vol. 35 365–380 (2017).
2. Ying, T. et al. Death after kidney transplantation: An analysis by era and time post-transplant. J. Am. Soc. Nephrol. 31, 2887–2899 (2020).
3. Black, C. K., Termanini, K. M., Aguirre, O., Hawksworth, J. S. & Sosin, M. Solid organ transplantation in the 21st century. Ann. Transl. Med. 6, 409–409 (2018).
4. Coelho, T., Tredger, M. & Dhawan, A. Current status of immunosuppressive agents for solid organ transplantation in children. Pediatr. Transplant. 16, 106–122 (2012).
5. Riella, L. V. Understanding the causes of mortality post-transplantation - there is more than meets the eye. Jornal brasileiro de nefrologia : 'orgao oficial de Sociedades Brasileira e Latino-Americana de Nefrologia vol. 40 102–104 (2018).
6. Shivaswamy, V., Boerner, B. & Larsen, J. Post-transplant diabetes mellitus: Causes, Treatment, and Impact on Outcomes. Endocrine Reviews vol. 37 37–61 (2016).
7. Webster, A. C., Craig, J. C., Simpson, J. M., Jones, M. P. & Chapman, J. R. Identifying high risk groups and quantifying absolute risk of cancer after kidney transplantation: A cohort study of 15 183 recipients. Am. J. Transplant. 7, 2140–2151 (2007).
8. Boerner, B. P., Swamy, V. S., Wolatz, E. & Larsen, J. Post-transplant diabetes: Diagnosis and management. Minerva Endocrinologica vol. 43 198–211 (2018).
9. Sprangers, B., Nair, V., Launay-Vacher, V., Riella, L. V. & Jhaveri, K. D. Risk factors associated with post-kidney transplant malignancies: An article from the Cancer-Kidney International Network. Clinical Kidney Journal vol. 11 315–329 (2018).
10. WHO. Preface Overview Humanity's Aging Living Longer New Disease Patterns Longer Lives and Disability New Data on Aging and Health Assessing the Cost of Aging and Health Care Changing Role of the Family Suggested Resources. Global Health and Aging.
11. Chapman, J. R., Webster, A. C. & Wong, G. Cancer in the transplant recipient. Cold Spring Harb. Perspect. Med. 3, (2013).
12. Childs, B. G., Durik, M., Baker, D. J. & van Deursen, J. M. Cellular senescence in aging and age-related disease: from mechanisms to therapy. Nat. Med. 21, (2015).
13. López-Otín, C., Blasco, M. A., Partridge, L., Serrano, M. & Kroemer, G. The hallmarks of aging. Cell vol. 153 (2013).
14. Hernandez-Segura, A., Nehme, J. & Demaria, M. Hallmarks of Cellular Senescence. Trends Cell Biol. 28, 436–453 (2018).
15. Franceschi, C. & Campisi, J. Chronic Inflammation (Inflammaging) and Its Potential Contribution to Age-Associated Diseases. vol. 69 4–9 (2014).
16. Coppé, J.-P., Desprez, P.-Y., Krtolica, A. & Campisi, J. The senescence-associated secretory phenotype: the dark side of tumor suppression. Annu. Rev. Pathol. 5, 99–118 (2010).
17. Baker, D. J. et al. Clearance of p16Ink4a-positive senescent cells delays ageing-associated disorders. Nature 479, 232–236 (2011).
18. Baker, D. J. et al. Naturally occurring p16Ink4a-positive cells shorten healthy lifespan. Nature 530, 184–189 (2016).
19. Gorenne, I., Kavurma, M., Scott, S. & Bennett, M. Vascular smooth muscle cell senescence in atherosclerosis. Cardiovascular Research vol. 72 9–17 (2006).
20. Shakeri, H., Lemmens, K., Gevaert, A. B., De Meyer, G. R. Y. & Segers, V. F. M. Cellular senescence links aging and diabetes in cardiovascular disease. American Journal of Physiology - Heart and Circulatory Physiology vol. 315 H448–H462 (2018).
21. Campisi, J. Aging, Cellular Senescence, and Cancer. Annu. Rev. Physiol. 75, 685–705 (2013).

22. Laberge, R.-M. et al. MTOR regulates the pro-tumorigenic senescence-associated secretory phenotype by promoting IL1A translation. Nat. Cell Biol. 17, (2015).
23. Pribluda, A. et al. A senescence-inflammatory switch from cancer-inhibitory to cancer-promoting mechanism. Cancer Cell 24, 242–56 (2013).
24. Jurk, D. et al. Chronic inflammation induces telomere dysfunction and accelerates ageing in mice. Nat. Commun. 2, (2014).
25. Coppé, J.-P. et al. Senescence-Associated Secretory Phenotypes Reveal Cell-Nonautonomous Functions of Oncogenic RAS and the p53 Tumor Suppressor. PLoS Biol. 6, e301 (2008).
26. Palmer, A. K. et al. Cellular senescence in type 2 diabetes: A therapeutic opportunity. Diabetes 64, 2289–2298 (2015).
27. Khosla, S., Farr, J. N., Tchkonia, T. & Kirkland, J. L. The role of cellular senescence in ageing and endocrine disease. Nature Reviews Endocrinology vol. 16 263–275 (2020).
28. Krizhanovsky, V. et al. Senescence of Activated Stellate Cells Limits Liver Fibrosis. Cell 134, 657–667 (2008).
29. Sagiv, A. et al. Granule exocytosis mediates immune surveillance of senescent cells. Oncogene 32, 1971–1977 (2013).
30. Sagiv, A. & Krizhanovsky, V. Immunosurveillance of senescent cells: the bright side of the senescence program. Biogerontology 14, 617–628 (2013).
31. Ovadya, Y. et al. Impaired immune surveillance accelerates accumulation of senescent cells and aging. Nat. Commun. 9, 1–15 (2018).
32. Morteau, O. et al. Renal transplant immunosuppression impairs natural killer cell function in vitro and in vivo. PLoS One 5, e13294 (2010).
33. Antonangeli, F. et al. Natural killer cell recognition of in vivo drug-induced senescent multiple myeloma cells. Oncoimmunology 5, (2016).
34. Koster, R. A., Greijdanus, B., Alffenaar, J. W. C. & Touw, D. J. Dried blood spot analysis of creatinine with LC-MS/MS in addition to immunosuppressants analysis. Anal. Bioanal. Chem. 407, 1585–1594 (2014).
35. Li, M., You, L., Xue, J. & Lu, Y. Ionizing radiation-induced cellular senescence in normal, non-transformed cells and the involved DNA damage response: A mini review. Frontiers in Pharmacology vol. 9 (2018).
36. Sedelnikova, O. A. et al. Senescing human cells and ageing mice accumulate DNA lesions with unrepairable double-strand breaks. Nat. Cell Biol. 6, 168–170 (2004).
37. Takahashi, A. et al. Downregulation of cytoplasmic DNases is implicated in cytoplasmic DNA accumulation and SASP in senescent cells. Nat. Commun. 9, 1–12 (2018).
38. Yu, Y., Arora, A., Min, W., Roifman, C. M. & Grunebaum, E. EdU incorporation is an alternative non-radioactive assay to [3H]thymidine uptake for in vitro measurement of mice T-cell proliferations. J. Immunol. Methods 350, 29–35 (2009).
39. Shah, P. P. et al. Lamin B1 depletion in senescent cells triggers large-scale changes in gene expression and the chromatin landscape. Genes Dev. 27, 1787–1799 (2013).
40. Freund, A., Laberge, R.-M., Demaria, M. & Campisi, J. Lamin B1 loss is a senescence-associated biomarker. Mol. Biol. Cell 23, 2066–2075 (2012).
41. Kang, T. W. et al. Senescence surveillance of pre-malignant hepatocytes limits liver cancer development. Nature 479, 547–551 (2011).
42. Lujambio, A. et al. Non-cell-autonomous tumor suppression by p53. Cell 153, 449–460 (2013).
43. Vandenbussche, C. et al. Tacrolimus-induced nephrotoxicity in mice is associated with microRNA deregulation. Arch. Toxicol. 92, 1539–1550 (2018).
44. Campisi, J. & Robert, L. Cell senescence: role in aging and age-related diseases. Interdiscip. Top. Gerontol. 39, 45–61 (2014).

45. Soriani, A. et al. ATM-ATR-dependent up-regulation of DNAM-1 and NKG2D ligands on multiple myeloma cells by therapeutic agents results in enhanced NK-cell susceptibility and is associated with a senescent phenotype. Blood 113, 3503–3511 (2009).
46. Parker, K. On track. T.I. 4, (2020).
47. Pores-Fernando, A. T., Gaur, S., Doyon, M. Y. & Zweifach, A. Calcineurin-dependent lytic granule exocytosis in NK-92 natural killer cells. Cell. Immunol. 254, 105–109 (2009).
48. Gong, J. H., Maki, G. & Klingemann, H. G. Characterization of a human cell line (NK-92) with phenotypical and functional characteristics of activated natural killer cells. Leukemia 8, 652–658 (1994).
49. Bao, Y. W., Yuan, Y., Chen, J. H. & Lin, W. Q. Kidney disease models: tools to identify mechanisms and potential therapeutic targets. Zoological research vol. 39 72–86 (2018).
50. van Willigenburg, H., de Keizer, P. L. J. & de Bruin, R. W. F. Cellular senescence as a therapeutic target to improve renal transplantation outcome. Pharmacological Research vol. 130 322–330 (2018).
51. Jennings, P. et al. Cyclosporine A induces senescence in renal tubular epithelial cells. Am. J. Physiol. - Ren. Physiol. 293, 831–838 (2007).

SUPPLEMENTAL FIGURES

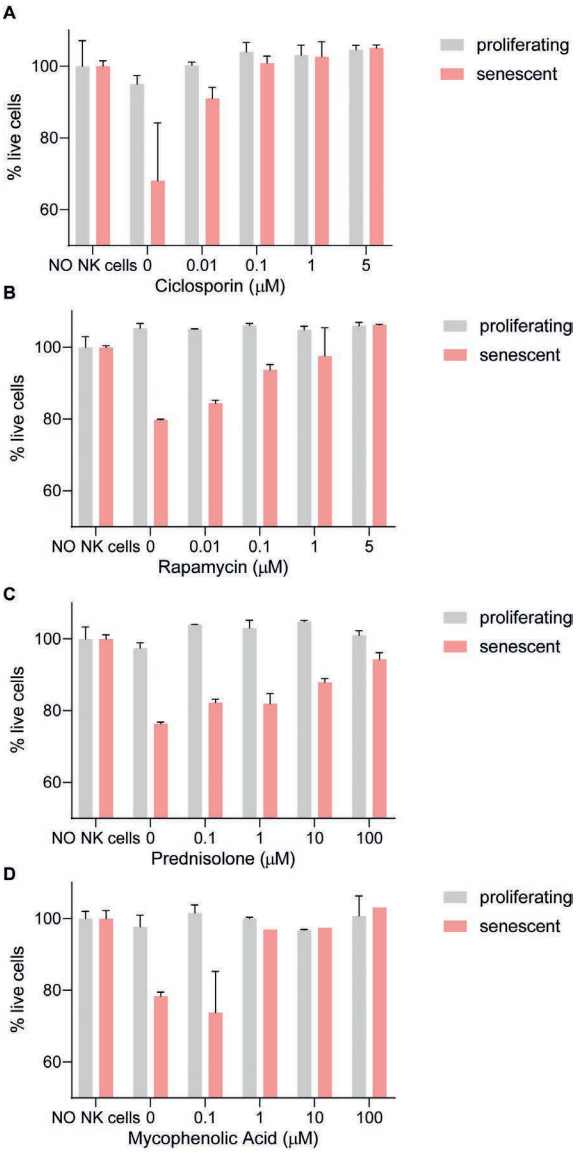

Supplemental figure 1. Immunosuppressive compounds inhibit NK-92 cell mediated senescence clearance *in vitro*

A-D. Proliferating and senescent WI-38 cells were co-cultured for 1 day with NK-92 in a 1:1 ratio, with indicated concentrations Ciclosporin **(A)**, Rapamycin **(B)**, Prednisolone **(C)** or Mycophenolic Acid **(D)**. Shown is the percentage of viable WI-38 cells after co-culture with NK-92 cells, compared to cells that were not co-cultured with NK-92 cells, based on a brilliant blue staining of the remnant adherent WI-38 cells. (n=1 independent assay).

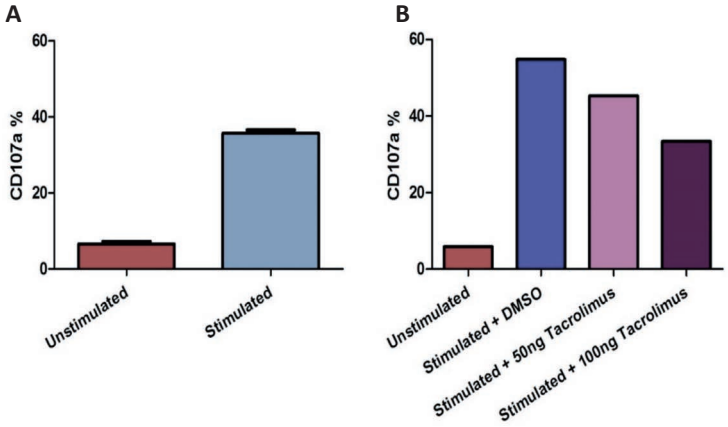

Supplemental figure 2. NK cell degranulation marker CD107a upregulates upon co-culture with senescent Wi-38, which can be suppressed by tacrolimus.
A. CD107a expression on isolated human NK cells after co-incubation with proliferating (unstimulated) or senescent WI-38 cells (stimulated), based on flow cytometry measurements (n=2). **B**. CD107a expression on isolated human NK cells after co-incubation with proliferating (unstimulated) or senescent WI-38 (stimulated) cells in the presence of 50 or 100 ng/ mL tacrolimus, based on flow cytometry measurements (n=1).

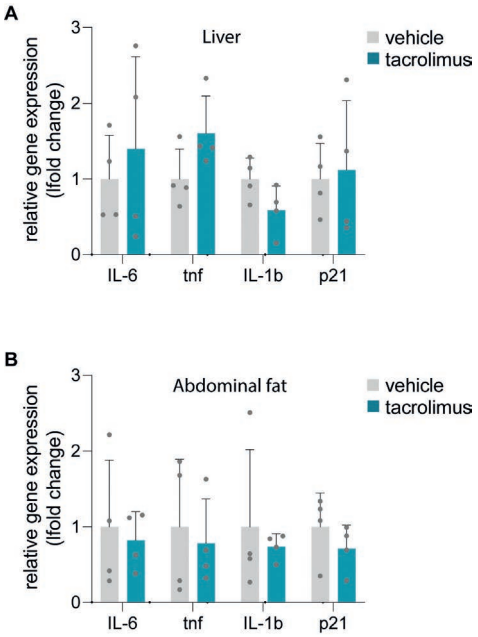

Supplemental Figure 3. 56 days of tacrolimus treatment does not alter gene expression levels of senescence-associated genes in liver and fat tissue A-B. Gene expression analyses via RT-qPCR of renal injury and senescence markers at 56 days after 0 or 3 mg/kg tacrolimus treatment in 2-year-old C57BL/6J mice, measured in liver **(A)** or fat **(B)** tissue. IL-6; Interleukin-6, TNF; tumor necrosis factor-alpha, IL-1b; Interleukin-1beta, p21; cyclin-dependent kinase inhibitor 1.


ng (2 µl) of the ligation mixture in a 1.5 ml microcentrifuge tube. Add 50 µl of competent cells to the DNA. Mix gently by pipetting up and down or flicking the tube 4–5 times to mix the cells and DNA. Do not vortex. Place the mixture on ice for 30 minutes. Do not mix. Heat shock at 42°C for 30 seconds*. Do not mix. Add 950 µl of room temperature media* to the tube. Place tube at 37°C for 60 minutes. Shake vigorously (250 rpm) or rotate. Warm selection plates to 37°C. Spread 50–100 µl of the cells and ligation mixture onto the plates. Incubate overnight at 37°C.. * Please note: Fo
w competent cells on ice. Chill app
n and tem
perature
f the heat sho
e phosphatase can be added directly into
gestion reaction during or after DNA digestion. Antarctic phosphatase is active in all NEB restriction enzyme buffers only when supplemented with Antarctic Phosphatase Reaction Buffer, which provides Zn2+ required for enzyme activity. The restriction enzyme should be heat inactivated at the same time as the phosphatase after digest and dephosphorylation. If restriction enzyme cannot be heat inactivated, DNA purification is required before ligation. The phosphatase can be added directly into the digestion reaction during or after DNA digestion. Antarctic Phosphatase is active in
B
estriction enzyme buffers only when su
on enzymes to produce a DNA fragment that can be
gest plasmid with the
appropria
cloned directly into a vector. Unidirectional cloning is achieved with restriction enzymes that produce non-compatible ends. Design primers with appropriate restriction sites to clone unidirectionally into a vector, Addition of 6 bases upstream of the restriction site is sufficient for digestion with most enzymes, If fidelity is a concern, choose a proofreading polymerase such as Q5 High-Fidelity DNA Polymerase. Purify PCR product by running the DNA on an agarose gel and
the band or by using a spin colun

Chapter 9

A Cumate-Responsive U6 Promoter for Controlled Knockdown of Target Gene Expression in Mammalian Cells

Hester van Willigenburg*[1,2], Joris J.P.G. Demmers*[2], Ziqin Tang[2], Duschka Klein[2], Wu Wei[2], Ron de Bruin[1], Joris Pothof[2]

[1] Department of Surgery, Erasmus MC Transplant Institute Rotterdam, Rotterdam, The Netherlands, [2] Department of Molecular Genetics, Erasmus MC, University Medical Centre Rotterdam, Rotterdam, The Netherlands, * These authors contributed equally

ABSTRACT

Controlled expression of short hairpin RNA (shRNA) levels to knock down target genes at a specific level is a useful tool to study gene function. To overcome the current limitations of controllable shRNA expression systems, we describe a novel cumate-responsive shRNA expression system. This system was created by adapting the human U6 promoter with operator CuO elements to which a cumate-responsive repressor protein (CymR) can bind. Treatment with increasing doses of cumate releases CymR from the adapted U6 promoters, resulting in an increased shRNA expression and a dose-dependent knock down of a target gene. Thus, by combining shRNA mediated gene silencing with the non-toxic and dose-responsive cumate–CymR system, we can now fine-tune target gene expression levels between 55% and 77% knockdown, a range we aim to improve with future adaptations. This new and versatile controllable non-coding RNA expression system will be especially useful in studies where partial and reversible down-regulation of gene expression levels are desired.

INTRODUCTION

Small differences in gene expression levels can have a crucial impact on complex genetic systems found in mammalian cells. To study the influence of altered gene expression *in vitro* or *in vivo,* gene expression regulation systems can be used, such as gene knockout, gene knock-in, and gene knockdown[1]. Unfortunately, these systems currently lack the ability to precisely tune the expression of a gene of interest (GOI). Although gene knock-out or knock-down can often answer general questions on gene function, for some genes, small variations in gene expression levels can lead to completely different cellular cell fates [2]. It is therefore of interest to develop new tools that can accurately regulate gene expression levels. Out of the currently available systems, gene knockdown has the most potency to achieve a specific partial knockdown by RNA interference (RNAi) via short hairpin RNA (shRNA). shRNA are small RNA molecules complementary to the mRNA of a GOI, which will trigger its degradation after binding[3]. The higher the ratio of shRNA to target mRNA, the higher the knockdown of the GOI. shRNA can be delivered in cells through transient oligonucleotide shRNA delivery, which is difficult to regulate and will result in decreasing knockdown over time when the shRNA is depleted[4]. shRNA can also be stably expressed by genomic integration of a vector containing a promoter driving shRNA expression[4]. However, regulating the amount of shRNA expression by such a promoter is challenging.

Tight control over promoter expression can be acquired by inserting a transcription regulatory element in or around a promoter[5]. Such adaptations have been made in promoters that drive shRNA before[6], however, so far, these systems experience leakiness or a level of toxicity[6,7]. The well-known tet-on/tet-off system for example, does not allow a dose-dependent control over gene expression[5] and depends on the toxic compound doxycycline[7]. Tight and safe regulation of shRNA expression might be possible by utilizing the recently introduced CymR-cumate inducible system[8]. In this system, the transcription regulator protein CymR represses transcription after binding to the cumate operator sequence (CuO sequence)[8,9]. Binding of CymR to CuO can be dose-dependently reversed with the non-toxic compound cumate[8,9]. So far, this transcription regulator has only been applied to protein-coding RNA polymerase II-dependent promoters, but not yet to RNA polymerase III-dependent promoters necessary for shRNA expression.

In this study, we describe a gene expression regulation system that has a reversible and fine-tunable regulation, which is easy to use and non-toxic. This system is based on shRNA interference driven by an RNA polymerase III dependent U6 promoter[10] and is combined with the CymR transcription regulator. Several adaptations of the U6 promoter were constructed, with careful placement of CuO elements within the promoter, to make the U6 promoter cumate–CymR responsive. We validated whether this system results in tight control of shRNA in a fluorescent-based reporter cell line. Two adapted U6 promoters could be partially repressed by CymR, which could be dose-dependently

reversed by addition of cumate. This study has resulted in an easy to use system to tightly down-regulate gene expression of any gene of interest at a biologically-relevant dose.

MATERIAL AND METHODS

Vector design

All constructed plasmids were cloned using standard molecular cloning strategies. The mScarlet-fluorescent reporter construct was based on the psB700 plasmid (Addgene plasmid # 64046[11]), and generated in two steps: first the U6 promoter sequence was removed; second, the mCerulean sequence, driven by the CAG promoter, was replaced for the sequence of mScarlet (Addgene plasmid #85044[12]) which was fused at the 3'end to a nucleoplasmin nuclear-localization sequence (KRPAATKKAGQAKKKK). This resulted in a lentiviral plasmid with a CAG promoter driving expression of the nuclear-localizing mScarlet-fluorescent protein.

The mammalian-codon modified CymR gene (Addgene plasmid #119907) was placed in a pLCKO plasmid (Addgene Plasmid # 73311) via BamHI, MluI mediated restriction and ligation. Next, the Puromycin gene was replaced by the Hygromycin gene . Lastly, in order to make a plasmid containing both the CymR gene and the ultimate adapted U6 promoter driving shRNA, we removed the restriction sites EcoRI and AgeI from CymR. These restriction sites are universally used for the insertion of shRNA behind the U6 promoter, and to make these two restriction sites unique for shRNA insertion, two base pairs in the CymR sequence were changed via site-directed mutagenesis to remove these restriction sites in the CymR gene. These base pair changes resulted in silent mutations: the removal of the EcoRI restriction site was accomplished by a GAA(Glu) to GAG(Glu) mutation; and the removal of the AgeI restriction site was achieved by a ACC(Thr) to ACG(Thr) mutation. This resulted in a plasmid containing an ef1a promoter driving CymR and Hygromycin (Addgene # 17454), which were separated by a P2A self-cleaving peptide, without EcoRI and AgeI restriction sites in the CymR gene.

The plasmids containing the CuO-adapted U6 promoters were based on the pLCKO plasmid (Addgene Plasmid # 733116). Heaps of adaptations were made to the U6 promoter[13] with CuO elements by replacing the 3'end of the U6 promoter with annealed oligonucleotides (IDT, oligonucleotides) via NdeI, KpnI mediated digestion and ligation for modifications around the PSE and TATA box. For alterations around the DSE, specifically designed and synthesized dsDNA fragments (Eurofins) were inserted via AleI, NdeI mediated digestion and ligation. The sequences of the adapted U6 promoter with CuO elements are listed in **Supplementary table 1**. Finally, shRNAs directed against target genes were inserted behind the adapted U6 promoters. The sequences for the used shRNAs are listed in the **Supplementary table 2**.

Mammalian cell culture and establishment of U6-CymR cell lines

MRC-5 cells (ATCC CCL-171) were maintained in high-glucose Dulbecco's Modified Eagle's Medium (Gibco), supplemented with 10% FBS (Capricorn Scientific) and 1% penicillin/streptomycin (Sigma). Cells were maintained at 37 °C and 5% CO2 in a humidified incubator, and tested for mycoplasma bimonthly. The MRC5-mScarlet reporter cell line was created by transducing MRC-5 cells with the mScarlet-fluorescent reporter construct. To do so, HEK293t cells grown in a 6-wells plate to a confluency of 70% were transfected with 1µg viral plasmids (Addgene #12259, #12251, #12253) using JetPEI (Westburg) according to manufacturer's instructions. After 24 hours of transfection, the transfection medium was replaced with fresh medium in which viral particles were allowed to accumulate for 1-2 days. Harvested medium was filtered with a 0.45µm pore size filter and added to the medium of target cells for another 2 days to transduce them. mScarlet positive cells were sorted by Fluorescence-activated Cell Sorting (FACS), after which an mScarlet positive single cell colony was created, with which the experiments were continued. Then, MRC5-mScarlet reporter cells were transduced with CymR and/or with a CuO-adapted U6 promoter plasmid, as described for the transduction with the mSarlet-fluorescence reporter. Afterwards, cells were cultured as normal and placed on 10µg/ml Puromycin (Invivogen) antibiotic selection if a plasmid containing the U6 promoter was transduced, or 100µg/ml Hygromycin B gold (Invivogen) antibiotic selection if a plasmid containing CymR was transduced. Cells were allowed to recover from antibiotic selection for at least one week before the mixed population was used in assays. Cumate (QM150A-1-SBI, System Biosciences), was diluted in medium and used at indicated concentrations.

Flow cytometry

The mScarlet-fluorescence reporter expression was quantified using flow cytometry. After treatment, cells were harvested through trypsinization in PBS with 10% FBS), before measuring mScarlet fluorescence intensity levels on a BD LSR Fortessa Analyzer. Data were analyzed using FlowJo software (version 10.7).

Statistical analysis

Statistical analysis were performed with GraphPad Prism 8, statistical tests, including one way ANOVA, are indicated in the corresponding legend. Data are presented as mean ± SD . All p-values <0.05 were considered significant.

RESULTS

Design of CuO-adapted U6 promoters

To regulate shRNA expression levels, we inserted CymR operator sequences (CuO) elements around several regulatory elements of the U6 promoter. The U6 promoter drives RNA polymerase III-dependent expression of small non-coding RNAs (ncRNA)[14], and consists of three highly conserved promoter elements: a distal sequence element

(DSE), a proximal sequence element (PSE), and a TATA box [15–17]. The DSE is located 150 base pairs (bp) upstream of the PSE, and consists of various binding sites, including an SPH motif and an octamer sequence (OCT)[18,19] (**Figure 1A.1**). The binding of multiple transcription-initiation complex proteins to each of these promoter elements triggers ncRNA transcription by RNA Polymerase III[17]. By placing CuO sequences near these essential promoter elements, we aimed to interfere with the assembly of the transcription initiation complex due to the physical obstruction of CymR proteins bound to CuO. The CymR protein consists of a dimerization domain and a DNA binding domain, which recognizes the CuO element[20]. The CuO element has a palindromic nature (**Figure 1B**), which allows binding of CymR-dimers. Full-length CuO sequences (28 base pairs) were placed directly behind the OCT element and before the PSE element (**Figure 1A**). The position and distance between other U6 elements are conserved and essential for U6 function. In particular, the distance of 15 bp between the PSE element and the TATA should not be interfered with[21]. Because the CuO sequence is too long to fit between these elements, we hypothesized that by (1) splitting the palindromic sequence into two partial CuO elements (pCuO), and by (2) stripping base pairs between the palindromic sequence forming a stripped CuO element (sCuO), we could construct smaller functional CuO sequences to place around these conserved elements (**Figure 1B**). We also theorized that combinations of given designs would allow for an even tighter control of expression (**Figure 1A, Supplemental table 1**).

The adaptations of the U6 promoter reduce its basic activity slightly

To test whether our CuO adaptations affected U6 promoter function, we transduced plasmids containing our adapted U6 promoters driving expression of a shRNA against mScarlet in our MRC5-mScarlet reporter cell line (**Figure 2A**). Mixed populations of transduced cells were analysed for mScarlet expression (**Figure 2B-C**). As negative controls, both mScarlet cells without a U6 transduction and mScarlet cells transduced with an unadapted U6 promoter driving a scramble-shRNA were analysed. These cells had equal mScarlet fluorescence intensity (**Figure 2B-C**), indicating that the transduction and insertion of plasmids with a U6 promoter itself does not affect mScarlet fluorescence intensity. mScarlet knockdown (K.D.) efficiency of the unadapted U6 promoter driving shRNA against mScarlet was 91.8% (**Figure 2C**), and although all U6 adaptations had significantly lowered mScarlet expression, none were as efficient as the unadapted U6 promoter. The OCT-CuO—CuO-PSE and 2xCuO-PSE adaptations had the lowest K.D. efficiency of 83.1 and 78.8% respectively, indicating that CuO adaptations to the U6 promoter lower the efficiency of U6 promoter expression.

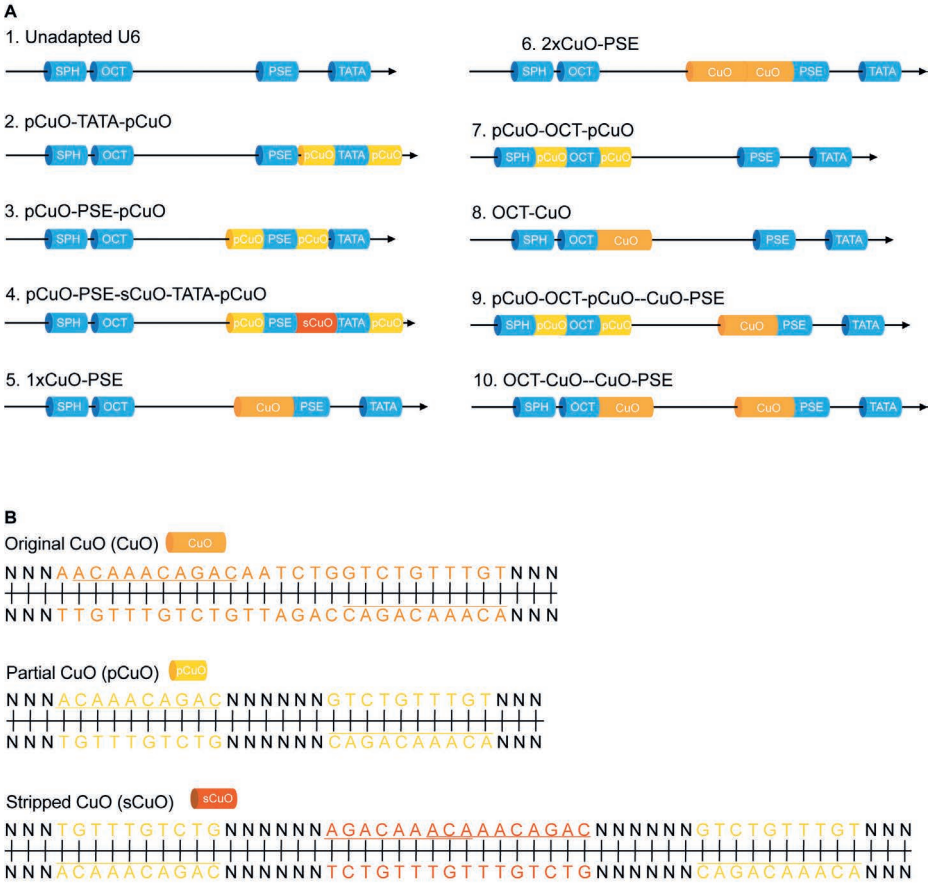

Figure 1. Graphical overview of U6 adaptations with CuO elements
A. Schematic representation of the conserved elements of the U6 promoter (blue) and the insertion of 3 types of CuO elements in the U6 promoter (orange shades). **B.** Sequences of three CuO elements including the original CuO (CuO), 2 partial CuO elements (pCuO), and a stripped CuO element (sCuO). The palindromic CymR binding elements are underlined.

CymR inhibits shRNA transcription in two U6 adaptations

We next assessed whether binding of the CymR protein to CuO elements in the U6 promoter inhibits its expression. To do so, MRC5-mScarlet cells were transduced with a plasmid containing the mammalian codon modified CymR gene and/or with a plasmid with unadapted or adapted U6 promoters. These cell lines were analysed for mScarlet expression by flow cytometry (**Figure 3**). Again, all cell lines were compared to those transduced with the unadapted U6 promoter driving a shRNA against mScarlet, or an unspecific shRNA (scramble) (**Figure 3A**). The unadapted U6 promoters driving mScarlet or scrambled shRNA show no difference in K.D. efficiency in the presence of CymR (**Figure 3B&C**), indicating that CymR expression itself does not interfere with

U6 promoter shRNA transcription. Of all tested U6 adaptations (**Figure 3D-L**), two adaptations showed an increase in mScarlet expression in presence of CymR : the 2x CuO-PSE and the OCT-CuO—CuO-PSE cell lines (**Figure 3H, L)**, indicating that CymR successfully inhibits U6-driven shRNA transcription in these cell lines. With CymR binding these U6 promoters, a knockdown range was obtained between approximately 53 and 77% (OCT-CuO—CuO PSE) and 53 and 75% K.D. for the 2xCuO-PSE adaptation.

Cumate treatment prevents CymR promoter repression in a dose dependent manner

The small compound cumate has been found to be non-toxic in its host, *Bacillus*[22]. To validate the toxicity of cumate in mammalian cells, four commonly used human cell lines, Hek293t (embryonic kidney derived), MRC5 (lung fibroblasts), MCF7 (breast cancer) and U-2 OS (bone osteosarcoma) were treated with a range of cumate concentrations (**Supplemental Figure 1**). Only the MCF7 cell line showed mitigated proliferation at the excessive concentration of 70 µg/mL. This concentration far exceeded the maximum cumate dose of 10 µg/mL that was further used in this study, indicating that cumate is non-toxic to these cells within its working range.

Having established two U6 adaptations that interact with CymR, we determined whether we could reverse this CymR repression with cumate treatment. To do so, the cell lines expressing either the unadapted U6 or the 2xCuO-PSE or the OCT-CuO—CuO-PSE adapted U6 promoters driving shRNA against mScarlet were cultured with a range of cumate concentrations. After 4 days of treatment, single-cell mScarlet fluorescence intensity was measured with flow cytometry (**Figure 4A, C**). Both cell lines with adapted U6 promoters show a dose-dependent decrease in mScarlet signal (**Figure 4B, D**) in the presence of CymR, but not in the absence of CymR, indicating that CymR repression is indeed dose-dependently relieved by cumate. Increasing doses of cumate did not alter mScarlet expression in cell lines with unadapted U6 promoters (**Figure 4E-F**), showing that cumate itself does not lower mScarlet intensity. Taken together, these results show that we have successfully generated two new U6 promoters that are able to be repressed by binding of CymR, and that this binding can be reversed in a dose-dependent manner by cumate, resulting in a dose dependent knock-down of a target gene. Our controllable U6 promoter driving shRNA will be a noteworthy addition to current gene regulation systems.

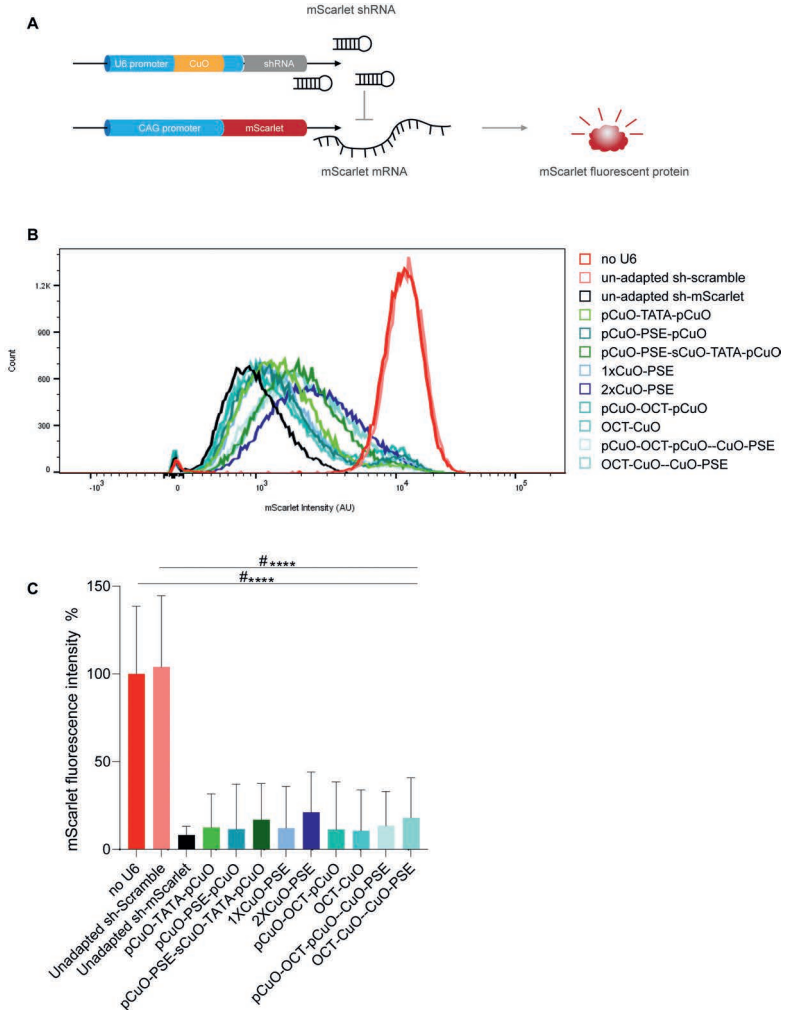

Figure 2. Basic activity of U6 promoters adapted with CuO elements in an mScarlet reporter cell line

A Schematic representation of the mScarlet reporter cell system, wherein adapted U6 promoters driving an mScarlet shRNA target mScarlet mRNA will lower mScarlet fluorescent protein levels. **B-C** Flow cytometry analyses of mScarlet fluorescence intensity in MRC5-mScarlet cells transduced with un-adapted and adapted U6 promoters driving expression of shRNA against mScarlet. **A** Representative graph of n=3 experiments, **B** Quantification of flow cytometry analyses. P-values were calculated using one-way ANOVA, **** $p<0.0001$, data are expressed as mean ± SD.

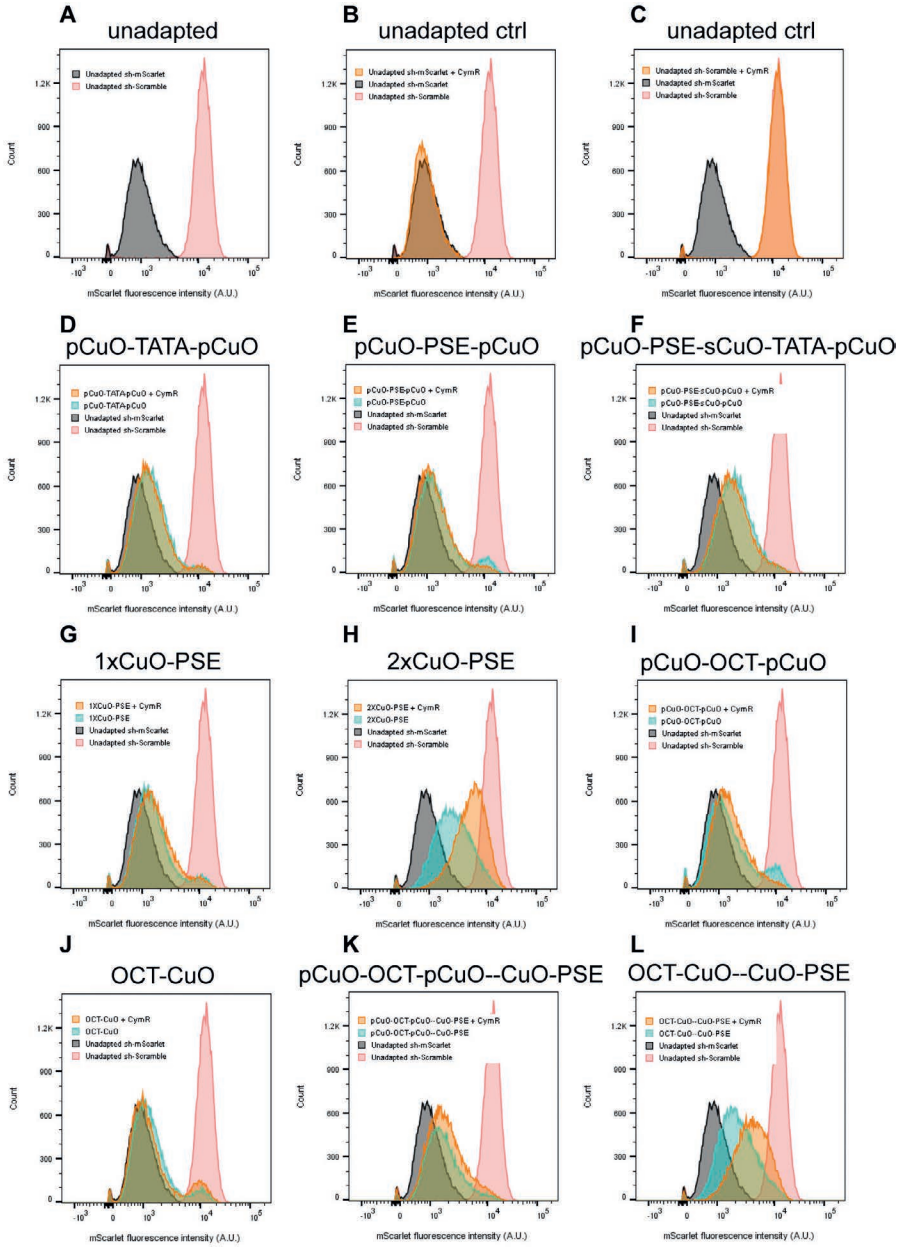

Figure 3. Effect of CymR on CuO adapted U6 promoters shRNA transcription

A-L Flow cytometry analyses of mScarlet fluorescence intensity in MRC5-mScarlet cells transduced with CymR and with un-adapted or adapted U6 promoters driving expression of shRNA against mScarlet. The black and pink plots represent un-adapted U6 promoters driving shRNA against mScarlet (Black) or nothing (scrambled) (pink). The blue plots are cells transduced with only the adapted U6 promoter. The orange plots are cells transduced with the adapted U6 promoters and CymR. Representative graphs of n=3 experiments.

DISCUSSION

The study of gene function benefits from systems that allow tight control over gene expression of a gene of interest (GOI). Here we describe a novel gene regulation system, which offers a quick and cheap tool to downregulate the expression of any gene of interest in a controlled manner, without having to genetically edit the gene of interest. In this study we created two controllable U6 promoters that drive expression of shRNA to downregulate expression of a GOI. These U6 promoters were adapted with cumate operator (CuO) elements, which can be recognized and subsequently bound by the CymR protein, leading to U6 promoter repression. The small molecule cumate can release CymR from the CuO element in a dose-dependent manner, restoring U6 promoter function, promoting shRNA transcription and lowering the expression of a target gene.

With our system, gene expression can be downregulated between approximately 55 and 77% in a cumate-dose dependent manner. Increasing this knockdown range of the adapted U6 promoters is desirable and has two areas of focus.

The first area of improvement is increasing the basal U6 activity to increase the maximal K.D. percentage. Assessing basic activity of the adapted U6 promoters showed that all adaptations reduced

U6 promoter effectivity in some degree compared to the unadapted U6 promoter (**Figure 2**). The lowest K.D. efficiency was observed in the U6 adaptations with most CuO inserts between the OCT and PSE elements of the U6 promoter, which extended the distance between these elements from 150 bp to 206 bp. The U6 promoter organizes itself around a nucleosome, bringing the DSE and PSE/TATA elements in close proximity and allowing the transcription initiation complex to trigger RNA polymerase III to transcribe a ncRNA[23], thus the increase in distance between these two elements might partially inhibit promoter activation. The removal of these excess base pairs between DSE and PSE, bringing the number of bp back to 150, might improve the spatial arrangement of the transcription initiation complex and therefore improve the basal U6 promoter activity of these adapted U6 promoters.

The second area of enhancement is directed at increasing the repressive effect of CymR. Complete repression of shRNA transcription allows study of normal gene expression of the gene of interest. At this moment, the maximal repression of shRNA transcription by CymR in our adapted U6 promoters is about 47%. To extend the tuneable knockdown range, we have to further repress U6 expression without affecting the basal efficiency of the U6 promoter. In earlier studies of the cumate CymR system, 6 tandem CuO elements before or after a CMV promoter were used to regulate its expression[8]. We observed that increasing the number of CuO sequences before the PSE element, from 1 to 2 CuO sequences was critical for CymR to repress U6 function.

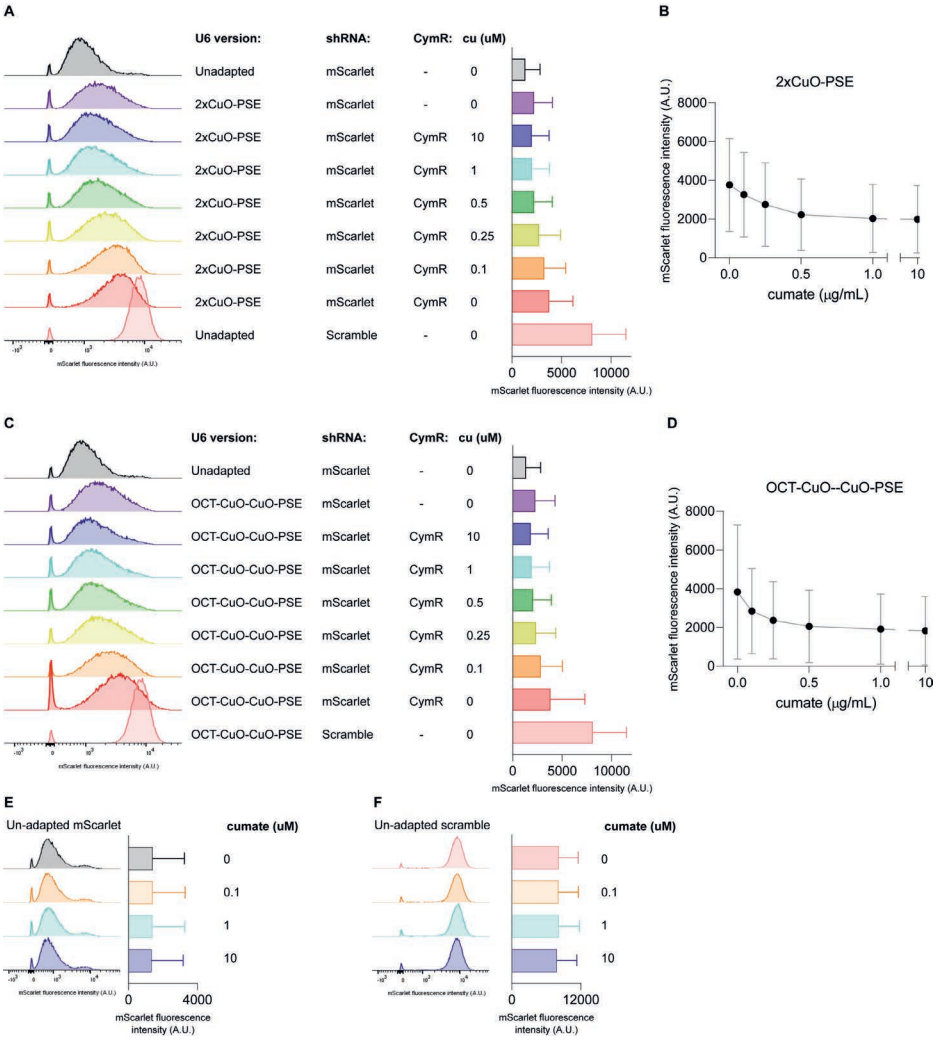

Figure 4. Cumate treatment dose-dependently reduces target gene expression by CymR binding adapted U6 promoters

A, C Flow cytometry analyses of mScarlet fluorescence intensity in MRC5-mScarlet cells transduced with CymR and with un-adapted or the 2x CuO-PSE **(A)** or the OCT-CuO—CuO-PSE (**C**) adapted U6 promoters driving expression of shRNA against mScarlet. The top and bottom plots represent un-adapted U6 promoters driving shRNA against mScarlet (Black) or nothing (scrambled) (pink). Indicated is the concentration of cumate (cu) in µg/mL. **C,D** Quantification of the flow cytometry analyses for dose response to cumate of the 2x CuO-PSE **(B)** or the OCT-CuO—CuO-PSE **(D)** U6 adaptations. All measured concentrations differ significantly from each other ($p<0.0001$). **E-F** Flow cytometry analyses of mScarlet fluorescence intensity in MRC5-mScarlet cells transduced with CymR and with un-adapted U6 promoters driving expression of shRNA against mScarlet **(E)** or scramble **(F)**. Representative graphs of n=3 experiments. P-values were calculated using one-way ANOVA, data are expressed as mean ± SD.

The same was true for the insertion of a CuO element after the OCT element—while the single insertion of CuO behind the OCT element did not offer CymR-mediated repression. Combining OCT–CuO with the non-functional 1XCuO–PSE (OCT–CuO—1XCuO-PSE) did show functional repression. Thus, both of the CymR-sensitive U6 promoters contain two CymR binding spots, indicating that multiple CuO elements are necessary to block transcription. Interestingly, given the distance between the OCT and PSE elements, these CuO elements do not have to be in close proximity to be functional. Therefore increasing the number of CuO elements between OCT and PSE may increase CymR binding and improve repression of the U6 promoter.

So by (1) improving basal expression levels and (2) improving CymR-repression levels, we hope to gain full control of U6 expression.

None of the U6 promoters adapted with the smaller CuO elements pCuO and sCuO were repressed by CymR (**Figure 3**). Importantly, the OCT-CuO—CuO-PSE adaptation was suppressed by CymR, but the pCuO-OCT-pCuO—CuO-PSE was not. Indicating that the splitting of the palindromic CuO element into two partial CuO elements is not effective in binding CymR. The original palindromic CuO element has 6 bps between the palindromic sequences (**Figure 1B**). These palindromic sequences were placed around the OCT element, which is 8 bp long, and therefore 2 bp longer than the sequence that divides the palindromic CuO elements in CuO. It could be that the length between the palindromic sequences is essential for proper CymR dimer binding, and that therefore the palindromic CuO elements will only work when they bridge maximally 6bp.

Interestingly, the small molecule cumate has been shown to relieve CymR binding to CuO elements between concentrations of 10-200µg/mL *in vitro*[8,24]. In our study, cumate doses between 0.1 and 1 µg/mL offered a suitable working range. This discrepancy could be explained by a crucial difference between our method setup and these previous studies. In the two studies using the CymR cumate system, CymR is introduced in cells via transfection[8,24], whereas in our study CymR was introduced via lentiviral transduction. And where a transduction introduces on average 1 or 2 plasmid copies into the cell[25], transfection may introduce thousands of plasmids into a single cell[26]. Increased CymR gene copies results in increased CymR protein levels, which might explain why more cumate was needed to release CymR from CuO elements. Furthermore, these studies have inserted six tandem CuO elements to control gene expression, whereas in the current study maximally two CuO elements were used. Future research will clarify whether increased binding spots for CymR will increase the necessary cumate dosage of for CymR release.

Taken together, we described the development of CuO-adapted CymR-responsive human U6 promoters of which activity can be regulated with the non-toxic small molecule cumate. We used this system to control shRNA transcription in a reversible and fine-

tuneable fashion, resulting in regulated knockdown of target gene expression. The U6 promoter can drive other ncRNA as well, such as miRNA, or sgRNA, which might be used to control dCas9-mediated gene-regulation[11]. Our system will especially be useful in studies where partial and reversible down-regulation of gene expression levels are desired.

Acknowledgements

The authors would like to thank Maaike M.P. Kuijten for her PiggyBac construct to generate the mScarlet reporter cell line.

REFERENCES

1. AM Z, YK P, T C, RWM K, SF P. Loss-of-function approaches in comparative physiology: is there a future for knockdown experiments in the era of genome editing? J Exp Biol. 2019;222(Pt 7). doi:10.1242/JEB.175737
2. CH H, SJ A, LF W. Patterns of Early p21 Dynamics Determine Proliferation-Senescence Cell Fate after Chemotherapy. Cell. 2019;178(2):361-373.e12. doi:10.1016/J.CELL.2019.05.041
3. PJ P, AA C, E B, GJ H, DS C. Short hairpin RNAs (shRNAs) induce sequence-specific silencing in mammalian cells. Genes Dev. 2002;16(8):948-958. doi:10.1101/GAD.981002
4. Moore CB, Guthrie EH, Huang MT-H, Taxman DJ. Short Hairpin RNA (shRNA): Design, Delivery, and Assessment of Gene Knockdown. Methods Mol Biol. 2010;629:141. doi:10.1007/978-1-60761-657-3_10
5. Gossen M, Bujard H. Tight control of gene expression in mammalian cells by tetracycline-responsive promoters. Proc Natl Acad Sci. 1992;89(12):5547-5551. doi:10.1073/PNAS.89.12.5547
6. Henriksen JR, Løkke C, Hammerø M, et al. Comparison of RNAi efficiency mediated by tetracycline-responsive H1 and U6 promoter variants in mammalian cell lines. Nucleic Acids Res. 2007;35(9). doi:10.1093/nar/gkm193
7. Ermak G, Cancasci VJ, Davies KJA. Cytotoxic effect of doxycycline and its implications for tet-on gene expression systems. Anal Biochem. 2003;318(1):152-154. doi:10.1016/S0003-2697(03)00166-0
8. Mullick A, Xu Y, Warren R, et al. The cumate gene-switch: a system for regulated expression in mammalian cells. BMC Biotechnol 2006 61. 2006;6(1):1-18. doi:10.1186/1472-6750-6-43
9. Eaton RW. p-cymene catabolic pathway in Pseudomonas putida F1: Cloning and characterization of DNA encoding conversion of p-cymene to p-cumate. J Bacteriol. 1997;179(10):3171-3180. doi:10.1128/JB.179.10.3171-3180.1997
10. Mäkinen PI, Koponen JK, Kärkkäinen AM, et al. Stable RNA interference: comparison of U6 and H1 promoters in endothelial cells and in mouse brain. J Gene Med. 2006;8(4):433-441. doi:10.1002/JGM.860
11. Chavez A, Scheiman J, Vora S, et al. Highly efficient Cas9-mediated transcriptional programming. Nat Methods. 2015;12(4):326-328. doi:10.1038/nmeth.3312
12. Bindels DS, Haarbosch L, Van Weeren L, et al. MScarlet: A bright monomeric red fluorescent protein for cellular imaging. Nat Methods. 2016;14(1):53-56. doi:10.1038/nmeth.4074
13. Staebler JR, McLeod B, Parks CM. Workhorse. ATW. 2018;2(5).
14. Kwak Y-D, Koike H, Sugaya K. RNA Interference With Small Hairpin RNAs Transcribed From a Human U6 Promoter-Driven DNA Vector. J Pharmacol Sci. 2003;93:214-217.
15. Carbon P, Murgo S, Ebel J-P, Krol A, Tebb G, Mattaj IW. A common octamer motif binding protein is involved in the transcription of U6 snRNA by RNA polymerase III and U2 snRNA by RNA polymerase II. Cell. 1987;51(1):71-79. doi:10.1016/0092-8674(87)90011-0
16. Goomer R, Kunkel G. The transcriptional start site for a human U6 small nuclear RNA gene is dictated by a compound promoter element consisting of the PSE and the TATA box. Nucleic Acids Res. 1992;20(18):4903-4912. doi:10.1093/NAR/20.18.4903
17. Kunkel GR, Maser RL, Calvet JP, Pederson T. U6 small nuclear RNA is transcribed by RNA polymerase III. Proc Natl Acad Sci U S A. 1986;83(22):8575. doi:10.1073/PNAS.83.22.8575
18. Kunkel GR, Cheung TC, Miyake JH, Urso O, Mcnamara-Schroeder KJ, Stumph WE. Identification of a SPH Element in the Distal Region of a Human U6 Small Nuclear RNA Gene Promoter and Characterization of the SPH Binding Factor in HeLa Cell Extracts. Gene Expr. 1996;6(2):59. Accessed July 7, 2021. /pmc/articles/PMC6148301/

19. Kunkel GR, Hixson JD. The distal elements, OCT and SPH, stimulate the formation of preinitiation complexes on a human U6 snRNA gene promoter in vitro. Nucleic Acids Res. 1998;26(6):1536-1543. doi:10.1093/NAR/26.6.1536
20. Shepard W, Soutourina O, Courtois E, England P, Haouz A, Martin-Verstraete I. Insights into the Rrf2 repressor family – the structure of CymR, the global cysteine regulator of Bacillus subtilis. FEBS J. 2011;278(15):2689-2701. doi:10.1111/J.1742-4658.2011.08195.X
21. Schramm L, Pendergrast PS, Sun Y, Hernandez N. Different human TFIIIB activities direct RNA polymerase III transcription from TATA-containing and TATA-less promoters. Genes Dev. 2000;14(20):2650. doi:10.1101/GAD.836400
22. Seo S-O, Schmidt-Dannert C. Development of a synthetic cumate-inducible gene expression system for Bacillus. Appl Microbiol Biotechnol 2018 1031. 2018;103(1):303-313. doi:10.1007/S00253-018-9485-4
23. X Z, PS P, N H. A positioned nucleosome on the human U6 promoter allows recruitment of SNAPc by the Oct-1 POU domain. Mol Cell. 2001;7(3):539-549. doi:10.1016/S1097-2765(01)00201-5
24. Sato S, Kikuchi T, Nishimura Y, et al. Generation of mouse iPS cells using an inducible expression of transgenes via the cumate gene-switch. Anal Biochem. 2020;599:113748. doi:10.1016/J.AB.2020.113748
25. Santeramo I, Bagnati M, Harvey EJ, et al. Vector Copy Distribution at a Single-Cell Level Enhances Analytical Characterization of Gene-Modified Cell Therapies. Mol Ther - Methods Clin Dev. 2020;17:944-956. doi:10.1016/J.OMTM.2020.04.016
26. Cohen RN, Aa MAEM van der, Macaraeg N, Lee AP, Szoka FC, Jr. Quantification of Plasmid DNA Copies in the Nucleus after Lipoplex and Polyplex Transfection. J Control Release. 2009;135(2):166. doi:10.1016/J.JCONREL.2008.12.016

SUPPLEMENTARY DATA

	Name	sequence
1.	Original U6	gagggcct**atttcccatgattccttcatatttgcat**atacgatacaag gctgttagagagataattagaattaatttgactgtaaacacaaagatatt agtacaaaatacgtgacgtagaaagtaataatttcttgggtagtttgca gttttaaaattatgttttaaaatggactatcatatg**cttaccgtaacttga aagta**tttcgatttcttggc**tttatatat**cttgtggaaaggac
2.	pCuO-TATA-pCuO	gagggcct**atttcccatgattccttcatatttgcat**atacgatacaag gctgttagagagataattagaattaatttgactgtaaacacaaagatatt agtacaaaatacgtgacgtagaaagtaataatttcttgggtagtttgca gttttaaaattatgttttaaaatggactatcatatg**cttaccgtaacttga aagta**tttcgacaaacagac**tttatatat**gtctgtttgtggac
3.	pCuO-PSE-pCuO	gagggcct**atttcccatgattccttcatatttgcat**atacgatacaag gctgttagagagataattagaattaatttgactgtaaacacaaagatatt agtacaaaatacgtgacgtagaaagtaataatttcttgggtagtttgcag ttttaaaattatgttttaaaatggactatcatatgacaaacagac**cttacc gtaacttgaaagta**gtctgtttgtttggc**tttatatat**cttgtggaaag gac
4.	pCuO-PSE-sCuO-TATA-pCuO	gagggcct**atttcccatgattccttcatatttgcat**atacgatacaag gctgttagagagataattagaattaatttgactgtaaacacaaagatatt agtacaaaatacgtgacgtagaaagtaataatttcttgggtagtttgcag ttttaaaattatgttttaaaatggactatcatatgttgtttgtctg**cttaccg taacttgaaagta**gacaaacaaacagac**tttatatat**gtctgtttgtg gac
5.	1xCuO-PSE	gagggcct**atttcccatgattccttcatatttgcat**atacgatacaag gctgttagagagataattagaattaatttgactgtaaacacaaagatatt agtacaaaatacgtgacgtagaaagtaataatttcttgggtagtttgcag ttttaaaattatgttttaaaatggactatcatatgaacaaacagacaatct ggtctgtttgta**cttaccgtaacttgaaagta**tttcgatttcttggc**ttt atatat**cttgtggaaaggac
6.	2x CuO-PSE	gagggcct**atttcccatgattccttcatatttgcat**atacgatacaag gctgttagagagataattagaattaatttgactgtaaacacaaagatatt agtacaaaatacgtgacgtagaaagtaataatttcttgggtagtttgcag ttttaaaattatgttttaaaatggactatcatatgaacaaacagacaatct ggtctgtttgtatatgaacaaacagacaatctggtctgtttgta**cttaccg taacttgaaagta**tttcgatttcttggc**tttatatat**cttgtggaaagg ac
7.	pCuO-OCT-pCuO	gagggcct**atttcccatgattccttcat**acaaacagac**atttgcat**gt ctgtttgtatacgatacaaggctgttagagagataattagaattaatttga ctgtaaacacaaagatattagtacaaaatacgtgacgtagaaagtaata atttcttgggtagtttgcagttttaaaattatgttttaaaatggactatcat atg**cttaccgtaacttgaaagta**tttcgatttcttggc**tttatatat**ctt gtggaaaggac

Supplementary table 1 *[Continued]*

	Name	sequence
8.	OCT-CuO	gagggcct**atttcccatgattccttcatatttgcat**aacaaacagaca atctggtctgtttgtaatacgatacaaggctgttagagagataattagaa ttaatttgactgtaaacacaaagatattagtacaaaatacgtgacgtag aaagtaataatttcttgggtagtttgcagttttaaaattatgttttaaaat ggactatcatatg**cttaccgtaacttgaaagta**tttcgatttcttggc**t ttatatat**cttgtggaaaggac
9.	pCuO-OCT-pCuO—CuO-PSE	gagggcct**atttcccatgattccttcat**acaaacagac**atttgcat**gt ctgtttgtatacgatacaaggctgttagagagataattagaattaatttg actgtaaacacaaagatattagtacaaaatacgtgacgtagaaagtaat aatttcttgggtagtttgcagttttaaaattatgttttaaaatggactatca tatgaacaaacagacaatctggtctgtttgta**cttaccgtaacttgaaa gta**tttcgatttcttggc**tttatatat**cttgtggaaaggac
10.	OCT-CuO—CuO-PSE	gagggcct**atttcccatgattccttcatatttgcat**aacaaacagaca atctggtctgtttgtaatacgatacaaggctgttagagagataattagaa ttaatttgactgtaaacacaaagatattagtacaaaatacgtgacgtaga aagtaataatttcttgggtagtttgcagttttaaaattatgttttaaaatgg actatcatatgaacaaacagacaatctggtctgtttgta**cttaccgtaac ttgaaagta**tttcgatttcttggc**tttatat**atcttgtggaaaggac

Supplementary table 1 CuO adaptations in the U6 promoter
Essential elements in the U6 promoter are accentuated in bold, from left to right: **SPH**, **OCT** (which is also underlined to distinguish from SPH), **PSE** and **TATA**. In yellow the pCuO elements, in orange the CuO elements and in red the sCuO element.

shRNA target	5'to 3' target sequence
Scramble	CCTAAGGTTAAGTCGCCCTCG
mScarlet	CGTGCTGAAGGGCGACATTAA

Supplementary table 2. shRNA sequences

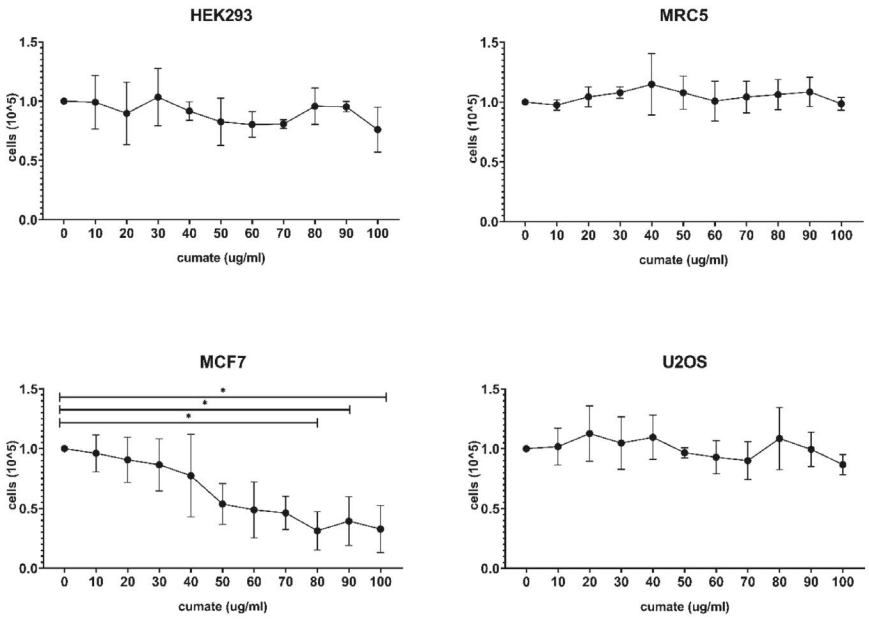

Figure S.1. cumate halts cell proliferation in MCF7 cells at excessive concentrations
Human cells of different origin (HEK293, MRC5, MCF7 and U2OS) were treated for seven days with increasing doses of cumate (0 to 100 µg/ml), after which cell numbers were counted. Representative graphs of n=3 experiments. P-values were calculated using Tukey's test, data are expressed as mean ± SD. (* $P < 0.05$).

Chapter 10

Summary, general discussion and future perspectives

Summary and general discussion

The increasing age of our population brings new challenges to our healthcare system. The incidence in age-related kidney disease and kidney failure is increasing and only limited treatment options are available, most of which have high costs or poor outcomes. Senescent cells are an important driver of aging, and have been causatively linked to several age related diseases. However, much remains to be elucidated on the role of senescent cells in kidney diseases. In this thesis we set out to increase our knowledge on the causes and consequences of senescence in several kidney pathologies, including autosomal dominant polycystic kidney disease (ADPKD), acute kidney injury (AKI), and as a consequence of immunosuppression after (renal) transplantation.

Autosomal dominant polycystic kidney disease (ADPKD) is the most common inherited kidney disease. Almost all cases of ADPKD are caused by a mutation in the *PKD1* (85% cases) or the *PKD2* genes (15% cases). However there are several indications that there is an important role for biological context in driving cyst formation. For example, there is a great variety in disease progression between family members that carry the same PKD mutation[1]. Moreover, kidney injury can trigger cystogenesis[2,3], which suggest the involvement of additional factors other than a PKD mutation in disease progression. So far, the exact molecular mechanisms behind cyst formation have not yet been elucidated. In **chapter 2** we describe a novel ADPKD organoid model system using adult human kidney stem cells derived from healthy and ADPKD kidney tissue. In this model we discovered a senescent gene expression profile in the ADPKD patient derived organoids. Subsequently, we show that both gene and protein expression of several senescence markers are upregulated in a mouse model of ADPKD and in kidney biopsies of ADPKD patients. We also show that cystic fluid contains SASP factors. Several of these SASP factors detected in cystic fluid were tested for their cystogenic potential. Indeed, some of these SASP factors can stimulate proliferation of renal epithelial cells *in vitro*, suggesting that senescent cells present in the kidney might trigger cystogenesis in neighbouring epithelial cells.

On a molecular level, we have also made some discoveries regarding the kidney injury response. In healthy cells, DNA damage activates p53[4], which in turn upregulates expression of the cyclin-dependent kinase inhibitor p21[5] (**Figure1**). Upregulation of p21 induces a cell cycle arrest in G0/G1, and stimulates the DNA damage repair response[6]. Even though there are elevated levels of DNA damage in ADPKD[7], we confirm in this study that p21 expression remains low in ADPKD tissue[8,9]. Mutations in the *PKD1* or *PKD2* genes, as found in ADPKD patients, stimulate c-Myc expression[10], which is an active repressor of the p21 promoter[11], offering an explanation for the lack of p21 activation upon DNA-damage in ADPKD. Furthermore, c-Myc overexpression stimulates proliferation and mediates cystogenesis (**Figure 1, right panel**)[9,10,12].

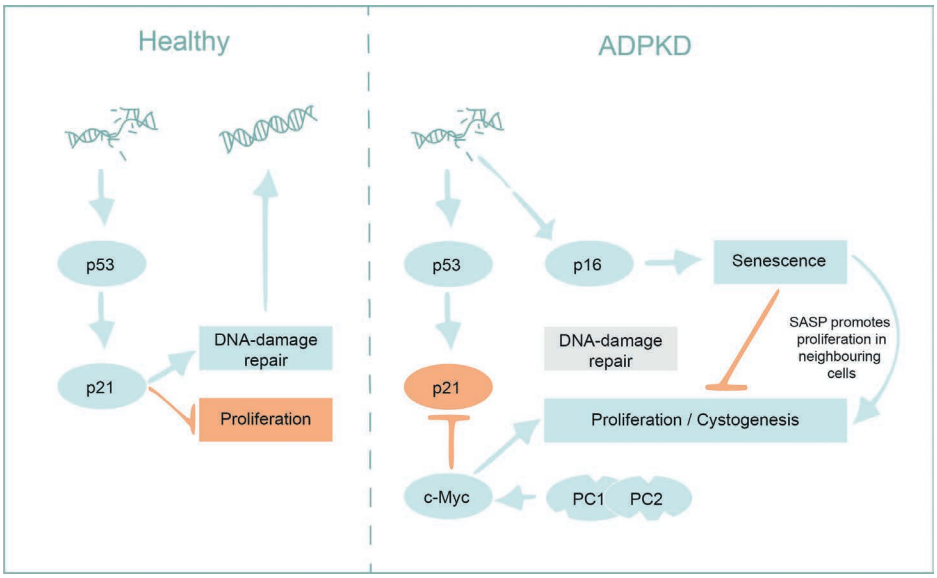

Figure 1. Impaired DNA damage response in ADPKD patients results in cystogenesis and senescence
Hypothesised molecular model for the induction and consequences of senescence in healthy and *PKD1* or *PKD2* mutated cells. ADPKD, autosomal dominant polycystic kidney disease; PC1, polycystin 1; PC2, polycystin 2,

In this study we also show that ADPKD derived organoids, and ADPKD mouse and human tissues have elevated numbers of senescent cells, and high expression of the senescence gene *CDKN2A*, which codes for the p16 protein. Although cystogenesis starts with uncontrolled growth, proliferation eventually stops, which distinguishes ADPKD from cancer. These observations indicate that a cell cycle arrest response, such as senescence, is still in place in ADPKD. The trigger for this delayed arrest might be shortening of telomeres with every somatic cell division in cystic epithelial cells. Such delayed cell cycle arrests are also observed in nevi, where after uncontrolled melanocytic cell growth, senescence is induced and nevus size is maintained[13]. Indeed, there is a strong correlation between telomere length and nevus size[14]. The idea of telomere-shortening induced senescence in ADPKD cysts is supported by our observation that senescence in cystic epithelial cells correlates with increasing cyst size, and could be confirmed by a telomere length measurement in cystic epithelial cells.

Importantly, we show that several SASP factors can trigger renal tubular cell proliferation *in vitro*. Suggesting that although the senescent cell-cycle arrest might halt cystic growth, through the secretion of SASP factors, senescent cells might trigger cystogenesis in neighbouring cells (**Figure 1, right panel**). This important notion may have an effect on the treatment of senescence in ADPKD. Whereas senescence induction is important for

the halt of cyst growth, SASP-mediated cystogenesis in neighbouring cells should be prevented. To determine the effect of senescent cells on ADPKD disease progression, the use of senolytics or a genetic model for senescence removal could be combined with an ADPKD mouse model. Whether senescent cells are a cause or a mere consequence ADPKD pathology remains to be elucidated. Yet, these findings link ADPKD for the first time to senescence and provide new insights in ADPKD pathology.

Most ADPKD patients will suffer from progressive decline of kidney function, eventually resulting in end stage renal disease (ESRD). ADPKD patients account for up to 9% of all ESRD cases[15]. ESRD is fatal if left untreated, and therefore most ESRD patients will need to undergo renal replacement therapy such as kidney transplantation. The increasing shortage of suitable kidney donors, urges the use of extended criteria donors, including those from aged (65+ years) donors[16]. However, kidney transplants from aged donors suffer from worse recovery from transplantation than those from younger donors[17–19]. To validate whether senescent cells are the cause of the impaired recovery from transplantation, we investigate in **chapter 3 and 4** the role of senescent cells in aged kidneys on the recovery from acute kidney injury (AKI), which is a transplantation associated injury. In **chapter 3** we removed senescent cells using the p16::3MR mouse model, that allowed us to remove p16-positive cells by injecting ganciclovir[20]. The p16::3MR transgene was combined with a *Xpd*^{TTD} mouse model, which is a mouse model of accelerated aging that at 26 weeks of age resembles a 2-year old wild-type mouse[21]. Senescent cells were removed in 26 weeks old *Xpd*^{TTD} mice before subjecting these mice to AKI via induction of bilateral ischemia reperfusion injury. In **chapter 4** we have removed senescent cells with senolytics in 19 month old wild type (WT) mice, before subjecting these mice to AKI.

Together, these studies show that the presence of senescent cells in aged kidneys makes aged kidneys susceptible to the adverse effects of AKI, including mortality. The removal of senescent cells in aged mice prior to AKI alleviates these effects, demonstrated by reduced plasma urea levels after AKI.

These studies did have some limitations. The group size of the final experiments in **chapter 3** was quite small. The mice used in **chapter 4**, were surprisingly youthful and senescence free for their age of 19 months, which made it more difficult to assess the effects of senescence removal in these mice. However, both studies show a strong trend towards improved recovery from AKI in aged kidneys after senescence removal. How senescent cells impair kidney recovery from AKI, remains to be elucidated. Proximal tubular repair is mainly regulated through dedifferentiation and self-renewal of proximal tubular epithelial cells[22]. The senescence-associated growth arrest may impair self-renewal of senescent proximal tubular epithelial cells, thereby reducing tissue regeneration after AKI. It is also possible that senescent cells impair kidney recovery from AKI through the senescence

associated secretory phenotype (SASP). The secretion of SASP factors, such as TGF-β, promotes fibrosis and impairs regeneration of muscle and bone tissue[23,24].

However, it appears that senescent cells can also function as a regenerative niche for nearby stem cells. Through the transient secretion of IL-6, senescent cells that are in close proximity to stem cells provide essential signals for the regeneration of heart[25,26], skin[27] and pancreas[28]. Although transient SASP secretion promotes regeneration, the prolonged exposure to SASP has been shown to reduce the regenerative capacity of stem cells. For example, prolonged SASP exposure results in a subsequent senescence arrest in skin stem cells[27], or differentiation with loss of self-renewal in hematopoietic and salivary gland stem cells[29,30].

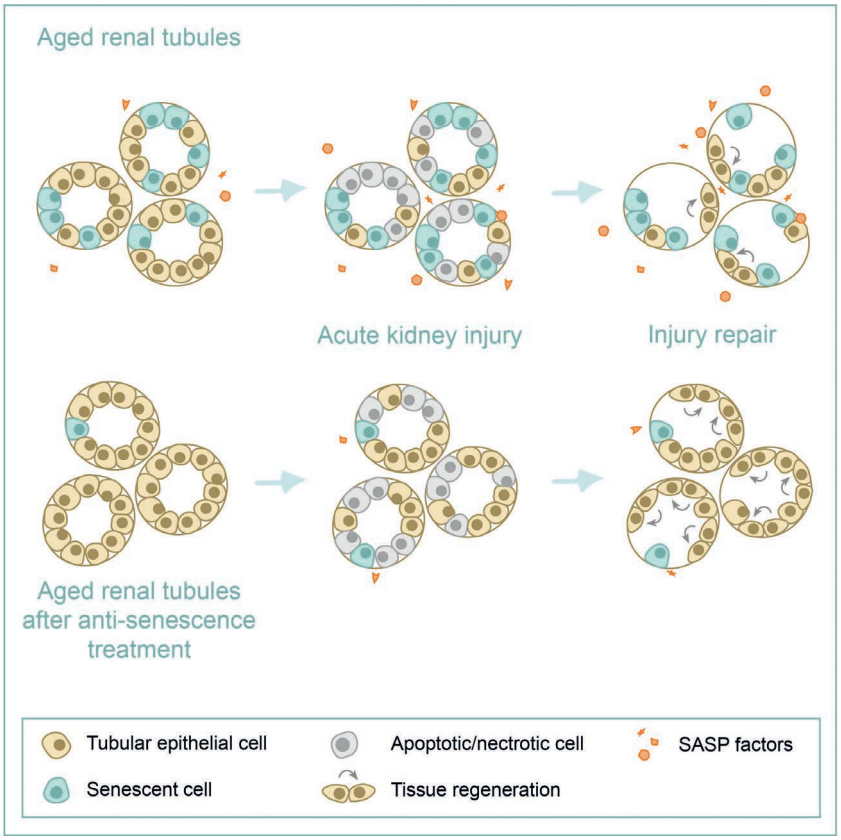

Figure 2. The removal of senescent cells with anti-senescence therapies improves the recovery of aged kidneys upon acute injury
Senescent cells impair tissue regeneration of the aged injured kidney, resulting in unresolved injury and reduced kidney function. The removal of senescent cells before the induction of AKI improves regeneration of the kidney, which results in improved kidney function. SASP: senescence associated secretory phenotype.

This implies that transient or acute senescent cells that arise at sites of injury promote the regenerative capacity of stem cells, but that chronic SASP secretion of senescent cells reduces this. If chronic senescent cells reduce the regenerative capacity of stem cells in the kidney as well, we expect increased markers of injury in untreated aged mice after AKI. Indeed, we have observed a trend towards increased expression of repair markers NGAL and SOX9 four weeks after AKI in the untreated *Xpd*^{TTD} mice (**chapter 3**), indicating impaired repair. These mice also showed a reduced recovery of kidney function after AKI compared to those where senescent cells had been removed.

A similar trend in improved recovery from AKI was observed in aged WT mice treated with the senolytic compound FOXO4-DRI before being subjected to AKI. Mice treated with FOXO4-DRI have better kidney function after AKI than those treated with vehicle. Moreover, the FOXO4-DRI treated mice show a trend towards lower incidence of interstitial fibrosis and tubular atrophy and lowered expression of kidney injury marker Kim1 (**chapter 4**). Whether senescent cells indeed reduce the regenerative potential of renal cells, remains to be confirmed in larger mouse cohorts.

Taken together, these results provide new insights on the role of senescent cells in kidney injury and repair and provide a starting point for the exploration of senolytic treatment in aged kidneys that might be subjected to AKI. Indeed, a recent study using the senolytic compound navitoclax in aged mice, shows that this senolytic treatment protects mice from AKI[31]. Together, these results offer a rationale for the use of senolytics to optimize aged kidneys and increase donor organ quality for organ transplantation.

To prevent the rejection of transplanted kidneys by immune cells, transplant patients receive immunosuppressive therapy throughout their lives. Immune cells have the important task of senescent cell clearance[32]. This raised the question whether, as a side effect, immunosuppressive therapies would impair the elimination of senescent cells by immune cells. Therefore, we examined the effect of immunosuppressive compounds on immune-mediated senescence clearance which is described in **chapter 8**. To this end, we first present a new method for measuring the concentration of the immunosuppressive drug tacrolimus in mouse blood in **chapter 7**. The current detection method for tacrolimus, LC-MS/MS, is optimized for human blood and requires a sample size that limits the number of samples that can be obtained from a single mouse[33–35]. In **chapter 7** we describe the use of the dried blood spot (DBS) method[36] to measure tacrolimus concentrations in mouse blood. This method has been used before to validate drug concentrations in small blood samples[37–39], and offers an animal friendly tacrolimus measurement method in mice. In **chapter 7** we not only show that DBS can be used for tacrolimus concentration measurements in mouse blood, but we also compare three different blood sampling sites, including the cheek, tail tip and heart. Of these blood sampling sites, venous blood sampled from the cheek proved to be the most reliable for tacrolimus blood concentration measurements. Taken together, this method can be used

to analyse tacrolimus in mouse blood, and can be used to improve the interpretation of tacrolimus pharmacokinetic studies in mice.

The novel method described in chapter 7 is used in **chapter** 8, where the effect of tacrolimus on immune-cell mediated senescence clearance is investigated *in vitro* and *in vivo*. The removal of senescent cells by immune cells is essential to maintain good health and prevent age-related diseases[40]. However, so far it is largely unknown what the effects of immunosuppressive therapies are on senescent cell surveillance. Here we confirm that upon senescence induction, WI-38 fibroblasts express NK-cell stimulatory NKG2D ligands. Co-culturing proliferating or senescent WI-38 fibroblasts with NK-92 cells promotes the selective elimination of senescent cells by NK-92 cells, and only to a minimal extent proliferating WI-38 cells. Treatment of NK-92 cells with the immunosuppressive compound tacrolimus suppresses this elimination of senescent cells *in vitro*, in a dose dependent manner. To test whether tacrolimus treatment also inhibits senescence clearance *in vivo*, mice were continuously treated with tacrolimus for 4-8 weeks. However, no differences in senescence marker expression between the tacrolimus treated mice or control group were observed.

This study has two limitations: the tacrolimus dosage and the short time frame of tacrolimus treatment in mice. Regarding the dose, tacrolimus blood concentrations were validated after the study with our DBS technique described in chapter 7. Tacrolimus was administered via subcutaneously inserted Alzet mini pumps that delivered tacrolimus for 28 consecutive days. However, we observed that tacrolimus blood concentrations decreased over time. We have not assessed whether the lowest tacrolimus concentrations suppressed NK-cell function in mice. Therefore, future studies should focus on finding the lowest tacrolimus blood concentration that suppresses immune cell function, for example with an NK-cell stimulation assay. Secondly, natural aging (rather than damage from injury) is a timely process. Approximately 10% of the cells in different tissues of two-year-old WT mice are senescent[41]. Assuming a linear senescence accumulation with age, an increase of 0.4% senescent cell accumulation can be expected per month. However, there is evidence that senescent cell accumulation increases with increasing age[42]. Treating 2 year old mice with tacrolimus for 56 days did however not result in detectable differences in senescent cell numbers. These results might however be influenced by a deterioration of the immune system with increasing age. The accumulation of senescent cells due to natural aging might also be too slow to detect in our model. Therefore, the effects of immunosuppression on senescent cell clearance might in the future be studied in a tissue injury model where senescent cells are induced, such as acute kidney injury models.

Patients receiving immunosuppressive treatment are afflicted with age-related diseases at a younger than average age[43–45]. Still, little is known on the effect of immunosuppressive treatment on the clearance of senescent cells. Our *in vitro* data suggest that the

accelerated aging of patients that receive immunosuppressive therapy is caused by a suppression of immune-cell mediated senescence clearance, resulting in increases in senescent cell numbers. Therefore, this patient group could potentially benefit from senolytic treatment to postpone the onset of age-related diseases and improve quality of life.

Lastly, in **chapter 9**, we present a novel tool to down regulate gene expression levels using a controllable U6 promoter. Today's methods to regulate gene expression are unfortunately unable to tightly control gene expression, are not-dose responsive, or induce toxicity[46–48]. To overcome the limitations of controlled RNA expression systems, we here describe a novel cumate-responsive controllable U6 promoter driving expression of short-hairpin RNA (shRNA). ShRNA can be used to knockdown the expression of a target gene. To regulate the levels of shRNA, and thereby regulating the level of target gene knockdown, we have modified the human U6 promoter with CuO fragments that can bind the cumate-responsive repressor protein (CymR). We show that treatment with increasing doses of cumate releases CymR from the adapted U6 promoters in a dose-dependent manner. This results in a dose-responsive knock-down of a target gene, which we can now fine-tune between 55% and 77% knockdown.

This novel knockdown system can be improved in two areas. Firstly, the basal U6 activity of the adapted promoters might be improved to increase the maximal knockdown level. The current adaptations to the U6 promoter have reduced the U6 promoter effectivity. The U6 promoter consists of highly conserved promoter elements and their spatial arrangement is essential for U6 function. By inserting CuO elements between these conserved promoter elements, the distance between some promoter elements increased, which might have negatively influenced their function. The removal of excess base pairs between the promoter elements might therefore improve the basal U6 promoter activity.

Secondly, leakage of the adapted U6 promoter should be countered, to completely repress shRNA expression. "Leakage" of the promoter results in shRNA transcription in the presence of CymR and absence of cumate. It indicates that CymR binding to the promoter is not sufficient to completely block transcription of the shRNA. So far, we have only tested U6 promoters with one or two CuO elements inserted. Other studies have used the CymR-cumate system with up to 6-tandem CuO elements, resulting in strong repression of gene expression[49]. Therefore, increasing the number of CuO elements in the U6 promoter, might improve the repressive effect of CymR to decrease promoter leakage.

This new and versatile system of controlled shRNA expression will be particularly useful in studies requiring partial and reversible control of gene expression. This tool offers a low-cost and easy to use method to tightly regulate endogenous gene levels, circumventing the time-consuming and expensive process of inserting gene-regulatory elements in

endogenous promoters of target genes. This tool will enable us to mimic decreased gene expression as observed in disease, and broadens our toolbox for gene function analyses. This tool might for example be applied to study ADPKD, where most patients have a mutation in the *PKD1* gene, which codes for polycystin 1. Both the lowering and the overexpression of polycystin 1 levels have been found to trigger cystogenesis in mice[50,51]. Our tool could be used to further investigate these dose-dependent effects of *PKD1* mutations on cystogenesis.

Future perspectives

Taken together, this thesis provides new insights in the role of senescent cells in renal aging and disease. Once more is known about the role of senescence in certain kidney diseases, future studies on renal aging will benefit from focussing on three areas of research: the detection, the treatment and the prevention of senescence and aging in kidney disease.

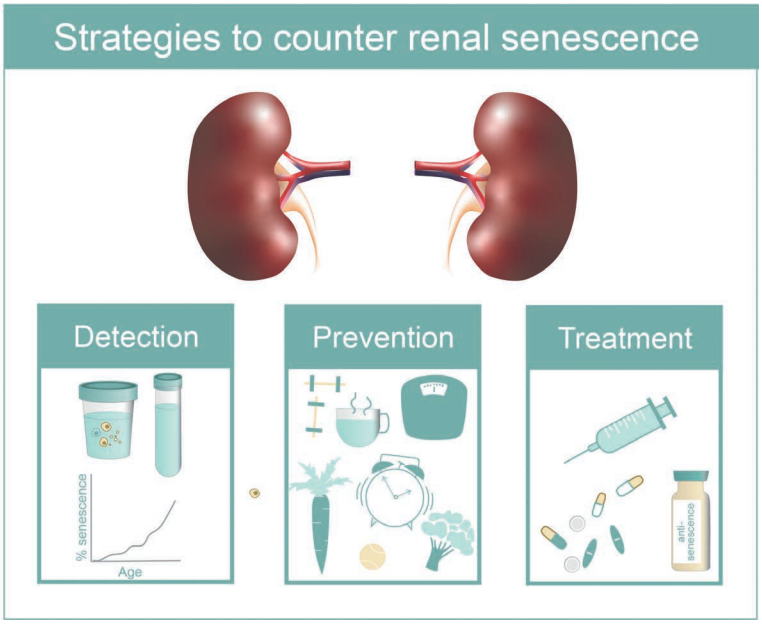

Figure 3. Strategies to counter renal senescence include detection, prevention and treatment of senescence.

Detection

Senescence is a heterogeneous and dynamic process that expresses itself differently in different organs and diseases. By improving our knowledge on senescence and aging in kidney disease, we can establish biomarkers of senescence and aging that can be used to provide personalized medicine. These biomarkers are preferably measured in a non-

invasive procedure. Kidney biopsies have certain risks and provide only a small snapshot of kidney tissue[52]. Extracellular vesicles are cell-derived lipid particles that are filled with proteins, RNA and even DNA that reflect the physiological state of the cell. Extracting renal extracellular vesicles from urine (uEVs) and analysing their content is a non-invasive and low-cost procedure that can provide a general insight in kidney function[53]. Moreover, renal epithelial cells that are shedded into urine might be used as a method to determine senescence status and the epigenetic clock of the kidney. The epigenetic clock is based on the methylation status of DNA and provides a highly accurate measurement of biological age[54]. This method can be used to provide a more general idea of renal aging. Creating a senescence signature in uEVs, and optimizing measurement of biological age in urine derived renal cells will improve our toolbox for detecting renal senescence and aging in patients and could provide rationale for personalized anti-aging treatments.

Prevention

The Dutch philosopher Desiderius Erasmus, figurehead of our medical institute, once said: "prevention is better than cure". This fundamental principle of healthcare offers a possibility for self-care by maintaining a healthy lifestyle. A healthy lifestyle includes physical exercise, maintaining a healthy weight, a vegetable rich diet, moderate alcohol consumption and a regular and adequate sleeping pattern. Such healthy lifestyles have been shown to prevent or delay aging and age-related diseases[56–62]. Unfortunately, adherence to a healthy lifestyle is declining[63–66], and was worsened by the corona-pandemic[67]. Major factors for non-adherence include lack of time, low socioeconomic status, low education level, high frequency of social gatherings, cost of medication, abundance of fast food outlets, depression, stress and insufficient information on the benefits of a healthy lifestyle[68–70]. These data imply that, to counter non-adherence to a healthy lifestyle, population-based, multifactorial interventions are required. These include educational campaigns, improved consumer information and governmental regulation on food costs, such as subsidies on healthy food or taxes on unhealthy products. Challenging as this may be, the multitude of benefits to be gained from a healthy lifestyle are worth the investment, as the economic costs of preventable diseases are staggering.

Treatment

The data presented in this thesis provides evidence for the removal of senescent cells to improve kidney function in ADPKD and in aged kidneys to recover from AKI. These data contribute to the growing body of studies pinpointing senescence as a culprit for age-related kidney diseases, urging for therapies to counteract senescence. Several anti-senescence (senolytic) and SASP-reducing (senomorphic) agents are being developed for use in humans. These enticing developments in drug development have so far resulted in the start of a few clinical trials, including treatment of patients with diabetic kidney disease with the senolytics quercetin and dasatinib[55]. Hopefully, these and other senolytic treatments will in the future be able to prevent, halt or even reverse age-related pathologies.

REFERENCES

1. Leonhard, W. N., Happe, H. & Peters, D. J. M. Variable Cyst Development in Autosomal Dominant Polycystic Kidney Disease : The Biologic Context. jasn 3530–3538 (2016) doi:10.1681/ASN.2016040425.
2. Formica, C. & Peters, D. J. M. Molecular pathways involved in injury-repair and ADPKD progression. Cell. Signal. 72, 109648 (2020).
3. H, H. et al. Toxic tubular injury in kidneys from Pkd1-deletion mice accelerates cystogenesis accompanied by dysregulated planar cell polarity and canonical Wnt signaling pathways. Hum. Mol. Genet. 18, 2532–2542 (2009).
4. Kruiswijk, F., Labuschagne, C. F. & Vousden, K. H. p53 in survival, death and metabolic health: a lifeguard with a licence to kill. Nat. Rev. Mol. Cell Biol. 16, 393–405 (2015).
5. Huang, R. & Zhou, P.-K. DNA damage repair: historical perspectives, mechanistic pathways and clinical translation for targeted cancer therapy. Signal Transduct. Target. Ther. 2021 61 6, 1–35 (2021).
6. Cazzalini, O., Scovassi, A. I., Savio, M., Stivala, L. A. & Prosperi, E. Multiple roles of the cell cycle inhibitor p21CDKN1A in the DNA damage response. Mutat. Res. Mutat. Res. 704, 12–20 (2010).
7. Zhang, J. Q. J. et al. Up-Regulation of DNA Damage Response Signaling in Autosomal Dominant Polycystic Kidney Disease. Am. J. Pathol. 191, 902–920 (2021).
8. Park, J.-Y. et al. p21 is decreased in polycystic kidney disease and leads to increased epithelial cell cycle progression: roscovitine augments p21 levels. BMC Nephrol. 2007 81 8, 1–11 (2007).
9. Zhou, X. et al. Therapeutic targeting of BET bromodomain protein, Brd4, delays cyst growth in ADPKD. Hum. Mol. Genet. 24, 3982 (2015).
10. Trudel, M. c-Myc Signalling in the Genetic Mechanism of Polycystic Kidney Disease. Polycystic Kidney Dis. 231–257 (2015) doi:10.15586/CODON.PKD.2015.CH10.
11. Gartel, A. L. et al. Myc represses the p21(WAF1/CIP1) promoter andinteracts with Sp1/Sp3. Proc. Natl. Acad. Sci. U. S. A. 98, 4510 (2001).
12. García-Gutiérrez, L. et al. Myc stimulates cell cycle progression through the activation of Cdk1 and phosphorylation of p27. Sci. Reports 2019 91 9, 1–17 (2019).
13. Ross, A. L., Sanchez, M. I. & Grichnik, J. M. Nevus Senescence. ISRN Dermatol. 2011, 1–8 (2011).
14. V, B. et al. Nevus size and number are associated with telomere length and represent potential markers of a decreased senescence in vivo. Cancer Epidemiol. Biomarkers Prev. 16, 1499–1502 (2007).
15. Perrone, R. D., Ruthazer, R. & Terrin, N. C. Survival after end-stage renal disease in autosomal dominant polycystic kidney disease: contribution of extrarenal complications to mortality. Am. J. Kidney Dis. 38, 777–784 (2001).
16. McCormick, F., Held, P. J. & Chertow, G. M. The Terrible Toll of the Kidney Shortage. J. Am. Soc. Nephrol. 29, 2775–2776 (2018).
17. Lim, W. H. et al. Outcomes of Kidney Transplantation From Older Living Donors. Transplant. J. 95, 106–113 (2013).
18. Tasaki, M. et al. Effect of donor–recipient age difference on long-term graft survival in living kidney transplantation. Int. Urol. Nephrol. 46, 1441–1446 (2014).
19. Oberhuber, R., Ge, X. & Tullius, S. G. Donor Age-Specific Injury and Immune Responses. Am. J. Transplant. 12, 38–42 (2012).
20. Demaria, M. et al. An essential role for senescent cells in optimal wound healing through secretion of PDGF-AA. Dev. Cell 31, 722–33 (2014).
21. De Boer, J. et al. A mouse model for the basal transcription/DNA repair syndrome trichothiodystrophy. Mol. Cell 1, 981–990 (1998).

22. Kumar, S. et al. Sox9 Activation Highlights a Cellular Pathway of Renal Repair in the Acutely Injured Mammalian Kidney. Cell Rep. 12, 1325–1338 (2015).
23. Tominaga, K. & Suzuki, H. I. TGF-β signaling in cellular senescence and aging-related pathology. International Journal of Molecular Sciences vol. 20 (2019).
24. Saito, Y. & Chikenji, T. S. Diverse Roles of Cellular Senescence in Skeletal Muscle Inflammation, Regeneration, and Therapeutics. Frontiers in Pharmacology vol. 12 2372 (2021).
25. Feng, T. et al. CCN1-Induced Cellular Senescence Promotes Heart Regeneration. Circulation vol. 139 2495–2498 (2019).
26. Sarig, R. et al. Transient p53-Mediated Regenerative Senescence in the Injured Heart. Circulation vol. 139 2491–2494 (2019).
27. Ritschka, B. et al. The senescence-associated secretory phenotype induces cellular plasticity and tissue regeneration. Genes Dev. 31, (2017).
28. Mosteiro, L. et al. Tissue damage and senescence provide critical signals for cellular reprogramming in vivo. Science (80-.). 354, aaf4445 (2016).
29. Pietras, E. M. et al. Chronic interleukin-1 exposure drives haematopoietic stem cells towards precocious myeloid differentiation at the expense of self-renewal. Nat. Cell Biol. 18, 607–618 (2016).
30. Peng, X. et al. Cellular senescence contributes to radiation-induced hyposalivation by affecting the stem/progenitor cell niche. Cell Death Dis. 11, 1–11 (2020).
31. Mylonas, K. J. et al. Cellular senescence inhibits renal regeneration after injury in mice, with senolytic treatment promoting repair. Sci. Transl. Med. 13, eabb0203 (2021).
32. Krizhanovsky, V. et al. Senescence of Activated Stellate Cells Limits Liver Fibrosis. Cell 134, 657–667 (2008).
33. Kalt, D. A. Tacrolimus: A Review of Laboratory Detection Methods and Indications for Use. Lab. Med. 48, e62–e65 (2017).
34. Brunet, M. et al. Therapeutic Drug Monitoring of Tacrolimus-Personalized Therapy: Second Consensus Report. Ther. Drug Monit. 41, 261–307 (2019).
35. Diehl, K. H. et al. A good practice guide to the administration of substances and removal of blood, including routes and volumes. J. Appl. Toxicol. 21, 15–23 (2001).
36. D, van de V. et al. Development and Validation of Hematocrit Level Measurement in Dried Blood Spots Using Near-Infrared Spectroscopy. Ther. Drug Monit. 43, 351–357 (2021).
37. Wickremsinhe, E. R. & Perkins, E. J. Using dried blood spot sampling to improve data quality and reduce animal use in mouse pharmacokinetic studies. J. Am. Assoc. Lab. Anim. Sci. 54, 139–144 (2015).
38. Clark, G. T., Haynes, J. J., Bayliss, M. A. J. & Burrows, L. Utilization of DBS within drug discovery: Development of a serial microsampling pharmacokinetic study in mice. Bioanalysis 2, 1477–1488 (2010).
39. Wong, P. et al. Application of automated serial blood sampling and dried blood spot technique with liquid chromatography-tandem mass spectrometry for pharmacokinetic studies in mice. J. Pharm. Biomed. Anal. 56, 604–608 (2011).
40. Campisi, J. & Robert, L. Cell senescence: role in aging and age-related diseases. Interdiscip. Top. Gerontol. 39, 45–61 (2014).
41. Yousefzadeh, M. J. et al. Tissue specificity of senescent cell accumulation during physiologic and accelerated aging of mice. Aging Cell 19, (2020).
42. Ovadya, Y. et al. Impaired immune surveillance accelerates accumulation of senescent cells and aging. Nat. Commun. 9, 1–15 (2018).
43. Chapman, J. R., Webster, A. C. & Wong, G. Cancer in the transplant recipient. Cold Spring Harb. Perspect. Med. 3, (2013).

44. Webster, A. C., Craig, J. C., Simpson, J. M., Jones, M. P. & Chapman, J. R. Identifying high risk groups and quantifying absolute risk of cancer after kidney transplantation: A cohort study of 15 183 recipients. Am. J. Transplant. 7, 2140–2151 (2007).
45. NN, R. & PT, C. Cardiovascular Disease After Kidney Transplant. Semin. Nephrol. 38, 291–297 (2018).
46. Gossen, M. & Bujard, H. Tight control of gene expression in mammalian cells by tetracycline-responsive promoters. Proc. Natl. Acad. Sci. 89, 5547–5551 (1992).
47. Henriksen, J. R. et al. Comparison of RNAi efficiency mediated by tetracycline-responsive H1 and U6 promoter variants in mammalian cell lines. Nucleic Acids Res. 35, (2007).
48. Ermak, G., Cancasci, V. J. & Davies, K. J. A. Cytotoxic effect of doxycycline and its implications for tet-on gene expression systems. Anal. Biochem. 318, 152–154 (2003).
49. Mullick, A. et al. The cumate gene-switch: a system for regulated expression in mammalian cells. BMC Biotechnol. 2006 61 6, 1–18 (2006).
50. Lantinga-van Leeuwen, I. S. et al. Lowering of Pkd1 expression is sufficient to cause polycystic kidney disease. Hum. Mol. Genet. 13, 3069–3077 (2004).
51. Thivierge, C. et al. Overexpression of PKD1 Causes Polycystic Kidney Disease. Mol. Cell. Biol. 26, 1538 (2006).
52. Bakdash, K. et al. Management of Complications in IR: Complications of Percutaneous Renal Biopsy. Semin. Intervent. Radiol. 36, 97 (2019).
53. Salih, M., Zietse, R. & Hoorn, E. J. Urinary extracellular vesicles and the kidney: biomarkers and beyond. https://doi.org/10.1152/ajprenal.00128.2014 306, 1251–1259 (2014).
54. Horvath, S. DNA methylation age of human tissues and cell types. Genome Biol. 14, R115 (2013).
55. Hickson, L. T. J. et al. Senolytics decrease senescent cells in humans: Preliminary report from a clinical trial of Dasatinib plus Quercetin in individuals with diabetic kidney disease. EBioMedicine 47, 446–456 (2019).
56. Trepanowski, J. F., Canale, R. E., Marshall, K. E., Kabir, M. M. & Bloomer, R. J. Impact of caloric and dietary restriction regimens on markers of health and longevity in humans and animals: a summary of available findings. Nutr. J. 10, 107 (2011).
57. Mazzotti, D. R. et al. Human longevity is associated with regular sleep patterns, maintenance of slow wave sleep, and favorable lipid profile. Front. Aging Neurosci. 6, (2014).
58. Shield, K. D., Parry, C. & Rehm, J. Chronic Diseases and Conditions Related to Alcohol Use. Alcohol Res. 35, 155 (2014).
59. Ciolac, E. G. & Guimarães, G. V. Physical exercise and metabolic syndrome. Rev. Bras. Med. do Esporte 10, 319–324 (2004).
60. EF, B. et al. Effects of exercise training on frailty in community-dwelling older adults: results of a randomized, controlled trial. J. Am. Geriatr. Soc. 50, 1921–1928 (2002).
61. K, D. et al. Genetic risk, adherence to a healthy lifestyle, and cognitive decline in African Americans and European Americans. Alzheimers. Dement. (2021) doi:10.1002/ALZ.12435.
62. Zhu, N. et al. Adherence to a healthy lifestyle and all-cause and cause-specific mortality in Chinese adults: a 10-year prospective study of 0.5 million people. Int. J. Behav. Nutr. Phys. Act. 2019 161 16, 1–13 (2019).
63. DE, K., AG, M., M, C. & CJ, E. Adherence to healthy lifestyle habits in US adults, 1988-2006. Am. J. Med. 122, 528–534 (2009).
64. AM, W., IP, C., RW, H. & PA, P. Using Death Certificates to Explore Changes in Alcohol-Related Mortality in the United States, 1999 to 2017. Alcohol. Clin. Exp. Res. 44, 178–187 (2020).
65. Hruby, A. & Hu, F. B. The Epidemiology of Obesity: A Big Picture. Pharmacoeconomics 33, 673 (2015).
66. Agha, M. & Agha, R. The rising prevalence of obesity: part A: impact on public health. Int. J. Surgery. Oncol. 2, e17 (2017).

67. Sevilla, G. G. P. de et al. Adherence to a Lifestyle Exercise and Nutrition Intervention in University Employees during the COVID-19 Pandemic: A Randomized Controlled Trial. Int. J. Environ. Res. Public Heal. 2021, Vol. 18, Page 7510 18, 7510 (2021).
68. Sharma, B. & Agrawal, M. Factors Affecting Adherence to Healthy Lifestyle. Int. J. Pure App. Biosci 5, 105–116 (2017).
69. Serour, M., Alqhenaei, H., Al-Saqabi, S., Mustafa, A.-R. & Ben-Nakhi, A. Cultural factors and patients' adherence to lifestyle measures. Br. J. Gen. Pract. 57, 291 (2007).
70. Chaabane, S., Chaabna, K., Doraiswamy, S., Mamtani, R. & Cheema, S. Barriers and Facilitators Associated with Physical Activity in the Middle East and North Africa Region: A Systematic Overview. Int. J. Environ. Res. Public Health 18, 1–21 (2021).

$C_{43}H_{66}N_{12}O_{12}S_2$
P<0.01
9780345453747

Chapter 11

Nederlandse samenvatting

De toenemende leeftijd van onze bevolking brengt nieuwe uitdagingen voor ons gezondheidszorgsysteem. De incidentie van leeftijdsgebonden nierziekten en nierfalen neemt toe en er zijn slechts beperkte behandelingsopties beschikbaar, waarvan de meeste hoge kosten meebrengen of niet curatief zijn. Senescente cellen zijn een belangrijke karakteristiek van veroudering en zijn oorzakelijk in verband gebracht met verschillende leeftijd gerelateerde ziekten. Er moet echter nog veel worden opgehelderd over de rol van senescente cellen bij nierziekten. In dit proefschrift wilden we onze kennis vergroten over de oorzaken en gevolgen van senescence bij verschillende nierpathologieën, waaronder autosomaal dominante polycystische nierziekte (ADPKD), acuut nierletsel (AKI), en als gevolg van immunosuppressie na (nier)transplantatie.

Autosomaal dominante polycystische nierziekte (ADPKD) is de meest voorkomende erfelijke nierziekte. Tot nu toe is het exacte moleculaire mechanisme achter cystevorming echter nog niet opgehelderd. Er zijn verschillende aanwijzingen dat er een belangrijke rol is weggelegd voor biologische context bij het aansturen van cystevorming. Zo is er een grote variëteit in ziekteprogressie tussen familieleden die dezelfde PKD-mutatie dragen. Bovendien kan nierbeschadiging cystogenese (vorming van een cyste) stimuleren, wat wijst op de betrokkenheid van andere factoren dan alleen een PKD-mutatie bij ADPKD-ziekteprogressie. In **Hoofdstuk 2** beschrijven we een nieuw ADPKD organoïde modelsysteem dat gebruik maakt van volwassen menselijke nier stamcellen afkomstig van gezond en ADPKD-nier weefsel. In dit model ontdekten we een senescent genexpressieprofiel in de ADPKD-organoïden. Om te valideren of senescence een kenmerk is van ADPKD *in vivo*, hebben we getest of senescente cellen aanwezig waren in een muismodel van ADPKD en in nier biopten van gezonde en ADPKD-patiënten. Inderdaad, zowel gen- als eiwitexpressie van verschillende senescentie markers werden verhoogd tot expressie gebracht in ADPKD-nieren. Bovendien werden er verschillende SASP-factoren gevonden in biopten van cyste vloeistof. Vervolgens hebben we laten zien dat verschillende van de SASP-factoren die werden uitgescheiden in cyste vloeistof de proliferatie van nier epitheelcellen kunnen stimuleren *in vitro*, wat suggereert dat senescente cellen in de nier cystogenese kunnen stimuleren.

Belangrijk is dat we laten zien dat hoewel het senescence gen p16 sterk tot expressie komt in ADPKD-weefsel, het senescence gen p21 dat niet doet. Het ontbreken van p21-activering in deze beschadigde weefsels suggereert dat de schade respons in cystische cellen is aangetast. Deze bevindingen koppelen ADPKD voor het eerst aan senescentie, wat nieuwe inzichten oplevert in ziektepathologie en een potentieel nieuw mikpunt vormt voor ADPKD-therapieën.

ADPKD is een progressieve ziekte, en de meeste patiënten zullen in de loop van hun leven nierfalen ontwikkelen. ADPKD-patiënten vertegenwoordigen ongeveer 9% van alle patiënten met eindstadium nierfalen, of 'end-stage renal disease' (ESRD). ESRD is dodelijk als het niet wordt behandeld, en daarom zullen de meeste ESRD-patiënten een nierfunctie

vervangende therapie moeten ondergaan, zoals een niertransplantatie. Het toenemende tekort aan geschikte nierdonoren spoort aan tot het gebruik van 'niet-optimale' donoren, zoals van donoren met een hogere leeftijd (65+ jaar). Niertransplantaties van oudere donoren hebben een slechter herstel van transplantatie dan die van jongere donoren.

Om te valideren of senescente cellen de oorzaak zijn van het verminderde herstel van oude nieren na transplantatie, onderzoeken we in **hoofdstuk 3 en 4** de rol van senescente cellen in verouderde nieren op het herstel van acuut nierletsel, of 'acute kidney injury' (AKI), een transplantatie-geassocieerd letsel. In **hoofdstuk 3** hebben we verouderde cellen verwijderd met behulp van het p16::3MR muismodel, waarmee we p16-positieve senescente cellen konden verwijderen door ganciclovir te injecteren. In **hoofdstuk 4** verwijderen we senescente cellen met behulp van zogenoemde senolytische middelen. Dit is een groep geneesmiddelen die senescente cellen elimineren. In deze hoofdstukken laten we zien dat senescente cellen het herstel van AKI belemmeren en dat het gebruik van het senolytische geneesmiddel FOXO4-DRI dit kan tegengaan. Gezamenlijk geven deze data reden voor het gebruik van senolytica om verouderde nieren te optimaliseren en de donorpool te vergroten.

Hoofdstuk 5 en 6 geven literatuuroverzichten van senescentie en senolytica, met een focus op niertransplantatie (hoofdstuk 5).

Om immuuncel-gemedieerde afstoting van getransplanteerde nieren te voorkomen, krijgen transplantatiepatiënten een levenslange behandeling met immunosuppressieve therapie. We vragen ons af of deze therapieën, als bijwerking, de immuun gemedieerde senescentieklaring kunnen verminderen. Daarom onderzoeken we in **Hoofdstuk 8** het effect van immunosuppressieve geneesmiddelen op de immuun gemedieerde senescentieklaring.

Om dit te kunnen doen, presenteren we eerst in **hoofdstuk 7** een nieuwe methode om de bloedconcentratie van het immunosuppressieve medicijn tacrolimus in muizenbloed te analyseren. De huidige detectiemethode voor tacrolimus in bloed, LC-MS/MS, is geoptimaliseerd voor menselijk bloed en vereist een relatief groot bloedvolume die het aantal monsters beperkt dat kan worden verkregen van een enkele muis. In **hoofdstuk 7** beschrijven we het gebruik van de 'dried blood spot' (DBS) methode om tacrolimus concentraties in muizenbloed te meten. Deze methode is al eerder gebruikt om geneesmiddelconcentraties in kleine bloedmonsters te valideren, maar was nog niet eerder toegepast op tacrolimus. In dit hoofdstuk tonen we aan dat deze methode goed gebruikt kan worden om tacrolimus in muizenbloed te analyseren, wat een diervriendelijke methode biedt voor farmacokinetische studies van tacrolimus bij muizen.

De nieuwe methode beschreven in hoofdstuk 7 wordt gebruikt in **hoofdstuk 8**, waar het effect van tacrolimus op immuuncel gemedieerde senescentieklaring *in vitro* en *in vivo* wordt onderzocht. Het verwijderen van senescente cellen door immuuncellen is essentieel om een goede gezondheid te behouden en ouderdomsziekten te voorkomen. Tot nu toe is het echter grotendeels onbekend wat de effecten van immunosuppressieve therapieën zijn op de surveillance van senescente cellen. In dit hoofdstuk bevestigen we dat senescente fibroblasten NK-cel stimulerende NKG2D-liganden tot expressie brengen. Dit stimuleert NK-cellen tot het selectief elimineren van senescente fibroblasten en in mindere mate gezonde, prolifererende fibroblasten. Behandeling van NK-cellen met het immunosuppressieve geneesmiddel tacrolimus onderdrukt deze eliminatie van senescente cellen *in vitro*, op een dosisafhankelijke manier. Om te testen of behandeling met tacrolimus ook de senescentieklaring *in vivo* remt, werden muizen gedurende 4-8 weken continu met tacrolimus behandeld. Er werden echter geen verschillen waargenomen in de expressie van senescentiemarkers tussen de met tacrolimus behandelde muizen of de controlegroep. Deze observatie kan verklaard worden doordat het langer kan duren voor natuurlijke senescentie om detecteerbaar te ontwikkelen, dan de 8 weken van onze behandeling. Hoewel de effecten van immunosuppressieve behandeling op de klaring van senescentie *in vivo* nog moeten worden bevestigd, impliceren de *in vitro* gegevens dat patiënten die immunosuppressieve therapie krijgen, senescente cellen accumuleren. Daarom zou deze patiëntengroep baat kunnen hebben bij senolytische behandeling om het ontstaan van ouderdomsziekten uit te stellen en de kwaliteit van leven te verbeteren.

Ten slotte presenteren we in **hoofdstuk 9** een nieuw hulpmiddel om genexpressieniveaus gecontroleerd te reguleren met behulp van een induceerbare U6-promotor. Deze tool zal ons in staat stellen om verminderde genexpressie na te bootsen zoals waargenomen bij ziekte, en onze toolbox voor genfunctieanalyses te verbreden.

Samen genomen biedt dit proefschrift nieuwe inzichten in de rol van senescente cellen bij nierziekte, van patiënten met ADPKD tot patiënten die een transplantatie ondergaan en immunosuppressieve therapie krijgen. Deze bevindingen dragen bij aan het algemene begrip van nierveroudering en bieden een startpunt voor de verkenning van senolytische behandeling bij ADPKD, AKI en immunosuppressieve therapie. Verder worden twee nieuwe methoden gepresenteerd die zullen helpen bij toekomstig onderzoek naar immunosuppressieve studies bij muizen en de studie van genfunctie in zoogdieren.

Appendices

PhD Portfolio
List of publications
Curriculum vitae
Dankwoord

PHD PORTFOLIO

PhD student: Hester van Willigenburg

Erasmus MC Departments: Surgery and Molecular Genetics

Research School: MGC

PhD period: April 11th 2016 - December 11th 2020

Promotor: Dr. Ing. Ron W.F. de Bruin

Copromotors: Dr. Peter L.J. de Keizer

Summary of PhD training and teaching activities

Courses and Workshops	**Year**	**workload (ECTS)**
Supervising students	2019	0.15
Biomedical English Writing and Communication	2019	3.00
Personal Leadership	2019	2.00
Microscopic Image Analysis: From Theory to Practice	2018	0.80
Safely working in the Laboratory	2018	0.30
Animated Science	2017	2.00
Scientific Integrity	2017	0.30
Genetics PhD course	2017	3.00
Special topics course on CRISPR-Cas	2017	2.00
Systematic Literature Retrieval	2016	0.30
Functional Imaging and Super resolution	2016	2.00
		15.85
Conferences, seminars and presentations		
Dutch Transplantation Society conference - oral presentation	2020	1.00
Surgery Science day EMC - oral presentation	2020	0.30
Nature Conference on Ageing, Health and Rejuvenation - poster presentation	2019	1.00
International Meeting on Ischemia Reperfusion Injury in Transplantation - oral presentation	2018	1.00
Dutch Transplantation Society conference - poster presentation	2018	1.00
Conference on Molecular Biology of Aging	2017	0.30

Conference of the European Society for Organ Transplantation (ESOT)	2017	0.30
MGC PhD workshop - oral presentation	2019	1.00
MGC PhD Workshop - poster presentation	2017	1.00
MGC PhD Workshop	2016	1.00
Winter school Nephrology from Dutch Kidney Foundation	2020	2.00
Molecular Genetics work discussion – oral presentations	2016-2020	2.00
		11.90

Teaching

Supervising Bachelor student Duschka Kleijn	2020	0.90
Supervising Master student Feiko Nuijten	2020	1.30
Supervising Master student Wu Wei	2019	0.70
Supervising Master student Linda Cappetti	2019	0.90
Supervising Master student Ziqin Tang	2018	1.60
Supervising Bachelor student Finette Paardekoper	2018	1.50
Supervising Bachelor student Tim van Tienhoven	2017	1.00
Supervising Master student Dian Kortleve	2016	1.20
Assisting various Molecular Biology courses (Bsc Nanobiology)	2012-2016	1.00
		10.10

Grant

Chiesi award for best idea in transplantation research 2020 €5000,-

total ECTS: 37.85

LIST OF PUBLICATIONS

Validation of a dried blood spot method to measure tacrolimus concentrations in small volumes of mouse blood.
H van Willigenburg, Domburg BV, Ambagtsheer G, Brandt RM, Hesselink DA, de Bruin RW, de Winter BC.
Bioanalysis. 2022 Apr, PMID: 35289217

Cellular senescence as a therapeutic target to improve renal transplantation outcome
H van Willigenburg, PLJ de Keizer, RWF de Bruin
Pharmacological research, 2018 Apr, PMID: 29471104

Maintenance and repair of an aging life cycle
MP Baar, **H. van Willigenburg**, PLJ de Keizer
Oncotarget, 2017 May, PMID: 29152057

Targeted apoptosis of senescent cells restores tissue homeostasis in response to chemotoxicity and aging
Marjolein P. Baar, Renata M.C.Brandt, Diana A. Putavet, Julian D.D. Klein, Kasper W.J. Derks, Benjamin R.M. Bourgeois, Sarah Stryeck, Yvonne Rijksen, **Hester van Willigenburg**, Danny A. Feijtel, Ingrid van der Pluijm, Jeroen Essers, Wiggert A. van Cappellen, Wilfred F. van IJcken, Adriaan B.Houtsmuller, Joris Pothof, Ron W.F.de Bruin, Tobias Madl, Jan H.J. Hoeijmakers, Judith Campisi, Peter L.J. de Keizer
Cell, 2017 Mar, PMID: 28340339

Submitted manuscripts

Senescence is a hallmark of polycystic kidney disease
Hester van Willigenburg*, Annegien T. Kenter*, Frans Schutgens*, Eveline Rentmeester, Job van Riet, Beatrice Tan, Harmen J.G. van de Werken, Anusha S. Shankar, Martin J. Hoogduijn, Geert J.L.H. van Leenders, Paul C.M.S. Verhagen, Ron W.F. de Bruin, Peter L.J. de Keizer, Wilfred F.J. van IJcken, Jeroen A.A. Demmers, Marianne C. Verhaar, Gert Jansen, Robert Zietse, Maarten B. Rookmaaker, Dorien J.M. Peters, Ewout J. Hoorn, Joost H. Gribnau
EMBO reports

Elimination of senescent cells improves the recovery of aged kidneys upon acute injury in mice
Hester van Willigenburg, Gisela Ambagtsheer, Jan N.M. IJzermans, Peter L.J. de Keizer, Ron W.F. de Bruin
LIFE

Manuscripts in preparation

A cumate-responsive U6 promoter for controlled knockdown of target gene expression in mammalian cells
Hester van Willigenburg*, Joris J.P.G. Demmers*, Ziqin Tang, Duschka Klein, Wu Wei, Ron de Bruin, Joris Pothof

The immunosuppressive compound tacrolimus inhibits NK cell mediated clearance of senescent cells *in vitro*
Hester van Willigenburg, Gisela Ambagtsheer, Renata Brandt, Sander Barnhoorn, Linda Cappetti, Jan N.M. IJzermans, Ron de Bruin

CURRICULUM VITAE

Hester van Willigenburg is geboren op de herfstige zondagochtend van 20 oktober 1991 te Haarlem, dochter van Karin Gouverneur en Bert van Willigenburg, zusje van Luuk en Job en zus van Boaz van Willigenburg. Na haar gymnasium opleiding op het Mendelcollege te Haarlem werd zij september 2009 toegelaten tot de Bachelor Biologie aan de Universiteit van Leiden. De Bachelor heeft zij afgerond in 2012, waarna zij een jaar deelgenomen heeft aan het bestuur van de studievereniging de Leidse Biologen Club waarin ze gedurende haar hele studie Biologie actief was in diverse commissies. In 2013 vervolgde zij haar opleiding met een Master Biologie aan de Universiteit Leiden, met een focus op moleculaire celbiologie. Haar master afstudeerstage volgde zij in het laboratorium van dr. P.L.J. de Keizer aan het Erasmus MC bij de afdeling Moleculaire Genetica, op het onderwerp therapieresistentie geassocieerde senescence-eigenschappen in borstkanker.

In 2016 startte zij met haar promotie onderzoek naar de invloed van senescente cellen op nier ziekten en veroudering aan het Erasmus MC Rotterdam bij de afdelingen Chirurgie en Moleculaire Genetica onder begeleiding van Prof. dr. J.N.M. IJzermans, dr. R.W.F. de Bruin en dr. P.L.J. de Keizer. Gedurende haar promotieonderzoek is zij twee maanden op werkbezoek geweest aan de Harvard University, Department of public health, Boston, MA, U.S.A. onder begeleiding van Prof. dr. J.R. Mitchell. Tevens is zij geselecteerd voor de Chiesi prijs voor beste idee in transplantatie onderzoek 2020. Tijdens haar promotietraject heeft zij deelgenomen aan de activiteiten commissie van de afdeling moleculaire Genetica. Tevens is zij actief betrokken geweest met het PhD beleid in het Erasmus MC, als lid van de Erasmus MC PhD commissie.

Sinds 2021 is zij werkzaam bij de afdeling Interne Geneeskunde, sectie Nefrologie van het Erasmus MC onder begeleiding van Prof. dr. E.J. Hoorn. Hester woont in het levendige centrum van Delft, met haar man Tim.

From the song 'Praise you', by Norman Cook, aka Fatboy Slim

DANKWOORD

Dit proefschrift is mede mogelijk gemaakt dankzij de financiële support van de Nierstichting en dankzij de hulp van de mensen die ik al kende, of die ik ontmoet heb tijdens mijn PhD. Met veel plezier neem ik hier de ruimte om jullie te bedanken.

Allereerst wil ik professor Jan IJzermans van de afdeling Heelkunde bedanken voor de mogelijkheid om mijn PhD in zijn onderzoeksgroep te mogen doen. Ook professor Jan Hoeijmakers wil ik bedanken, niet alleen voor zijn adviezen tijdens de woensdag werkbesprekingen, maar ook voor het deelnemen in mijn promotiecommissie. Graag wil ik ook de rest van mijn promotiecommissie bedanken voor de bereidheid zitting te nemen in de commissie en voor het beoordelen van mijn proefschrift. Ik kijk uit naar de discussie.

Ron, ook jou wil ik graag bedanken. Van jou mocht altijd alles! Elk idee was de moeite waard te bestuderen, elke samenwerking welkom, en zeker ook alle vakantieaanvragen werden van harte goedgekeurd. Deze mindset gaf me het vertrouwen om mijn instincten in het onderzoek te volgen, maar me ook hierbuiten te ontwikkelen. De hieruit volgende onderzoeksprojecten ook daadwerkelijk tot een finale brengen zit nog in mijn leercurve, maar, zoals Frank Zappa zou zeggen: “Without deviation from the norm, progress is not possible.” En zo promoveer ik, zonder die gouden standaard van 4 publicaties, met jou als mijn promoter. Bedankt.

Peter, je enthousiasme voor onderzoek, welke ik heb mogen meemaken bij mijn afstudeerstage en in de eerste anderhalf jaar van mijn PhD, heeft mij veel geleerd en geïnspireerd. Na je vertrek naar Utrecht werd het zoeken naar een nieuwe vorm van patentloos-contact. Door de grote afstand in ruimte en tijd tussen onze meetings, werden onze werkbesprekingen meer beschouwend en vooruitziend. Precies waar ik het laatste jaar van mijn PhD behoefte aan had. Dank je wel voor je tijd en enthousiasme. Appelflap, proxofimski, awesome!

Beste Joris (sr.), bedankt voor het openstellen van de Aging groep na Peters verhuizing naar Utrecht. Ik heb me echt thuis gevoeld in die vrolijke ruimte, waar alles mocht, elke grap gemaakt kon worden, axolotls welkom waren en jij altijd tijd had voor een overleg, een idee, of een goed gesprek.

I would also like to thank all my former colleagues and friends in the Molecular Genetics and experimental Surgery departments. The scientific staff with whom it was a pleasure to discuss life and science and whom have assisted me in the lab. I would also like to thank the non-scientific staff in the kitchen, the secretary office, from IT and the purchasing department on the 7th floor. Together you’ve made these departments great places to work and to enjoy life as a PhD student.

Lieve Marjolein, niet lang na jouw en Diana's vertrek naar Utrecht was ik opeens de eerstvolgende PhD student in de groep die zou gaan promoveren, terwijl ik nog zoveel moest leren! Gedurende de 3.5 jaar PhD die nog zouden volgen en dat extra jaar thesis schrijven hebben we gelukkig regelmatig contact gehouden om over het PhD zijn te sparren. Jouw wijze uitspraken als: 'oh, het is heel normaal dat je thesis voelt als een heel groot master eindverslag vol onafgemaakt onderzoek', hebben me door het schrijven heen geholpen. En voilà, nu staat je naam in het dankwoord! Ook in de colofon, want je bent mijn paranimf. Muchos, muchos gracias voor je hulp en je luisterende oor! Ik denk met plezier terug aan al onze spelletjesavonden, het spuien over onze begeleiders, samen koken met de andere PhD studenten, het lab-uitje organiseren, 1 april grappen bedenken en samen met Diana hamburgers keuren om die vervolgens weg te spoelen met een cocktail in een random bar waar Diana weer een voucher voor had gevonden. Ach ja, zo kom je nog eens ergens.

Diana, I miss your hard jokes (that's what she said!) and your evil laugh. We should still go to that kunstavond on Friday night and now I've mentioned it here, it's official. (You may use this page as a voucher). You're a kind, hardworking and bright scientist and I hope you'll continue to kick some ass in science! P.s. I will always think of you and Marjolein whenever I order mango ice cream.

Dear office mates, let me start with a thank you, which seems appropriate in this section of my thesis. Thank you for being so warmly distracted by the undersigned! I know I'm not the most silent coworker, but I hope that my good days eclipsed all bad ones. You all, together with a beer or two, have made my PhD more bearable.

Astrid, de eerste keer dat ik je zag was ik verliefd. Nee, maar ik dacht wel, daar zou ik wel eens vriendinnen mee kunnen worden. En voilà! Nu sta ook jij in mijn thesis als paranimf! Wat zijn we samen gegroeid (al zeg ik het zelf). Het was fijn om iemand te hebben om cursussen mee te volgen en eens iets te doen aan dat zogeheten "zelfreflectie". Het was, en is, waardevol om iemand in de buurt te hebben die mijn passie voor onderzoek deelt en ook kan toegeven dat de wetenschappelijke wereld je niet altijd blij maakt. We hebben gelukkig ook leuke dingen gedaan. Je was fotograaf op mijn bruiloft (echt, je go-to vangnet mocht het niets worden bij de MDL stichting), we hebben geborreld, gevierd, geluncht, gedeeld, geprotesteerd en gefeest! Ik zeg, niets meer aan doen, behalve nog heel vaak herhalen.

Joris (jr.), het lijkt misschien gek, maar het eerste waar ik aan moet denken is Ethiopische jazz. Man, ik ben echt fan nu! Ik had natuurlijk moeten beginnen met project C (en Q, T, Z, B, H, J, …), met jouw fantastische label kunsten (def.def.final), met jouw super harde werken en mega veel kloneren en optimisme en het gezellig samen bijkletsen in het ML-II. "Ok, maar nu even stil, want dit moet in een keer goed gaan". Wat het natuurlijk NOOIT gaat. "Ik voel het, dit wordt 'em", en dat was 'em niet. Ik ben voor geen van

mijn projecten tegen zoveel mysteries aangelopen als bij dit project. En toch staat ons hoofdstuk nu echt in mijn boekje te shinen. Het is er nog niet helemaal, maar we zijn er nu toch echt bijna. Ik heb genoten en geleerd van jouw soms andere kijk op de wereld en ook van je super harde lach. Ik heb iets minder genoten van jouw gebrek aan aldehyde dehydrogenase en hoe je daar toch keer op keer weer niet van lijkt te leren, al heb je zo wel menig feestje op gang gebracht (en het einde niet meegemaakt). Hahaha, wat een feest. Bedankt voor de mooie jaren en ik kijk uit naar jouw boekje! (Met hopelijk een nog mooier hoofdstuk dan het mijne).

Dear Chang, Xièxiè nǐ suǒyǒu dì měihǎo shíguāng, Nǐ hěn bàng! (Ok, so this is copy pasted from google translate, and if it doesn't make any sense, just give yourself the best compliment you can think of). I have loved those afternoons where work just didn't work and instead we learned about our cultural differences. You have accepted the Dutchman in you, and I have started to embrace Chinese qualities and nature. I love how we have brainstormed of feng-shuing the shit out of our office (so sad that water fountain never made it), and how you have introduced Tim and me to Cixin Liu. I will never forget your kindness and jokes. All the best to you Chang!

Gisela, de afgelopen jaren zijn we steeds meer naar elkaar gegroeid en op elkaar ingespeeld. Ik heb je leren kennen als een warm en zorgzaam iemand met een goede dosis humor. Ik ben blij dat ik nog steeds langs kan wippen om bij te kletsen en voor wetenschap. Het is jammer dat we het labuitje nooit van de grond hebben gekregen. Toen er eindelijk een plan was, kwam daar helaas een pandemie tussen. Maar we hebben het er gelukkig met z'n tweeën van genomen in Boston! Burgers, country muziek, Red Sox en geshopt tot onze koffers niet meer dicht konden. Yeah baby!

Aan al mijn oud-mede-PhD studenten in de kelder, oftewel in het Hugh Hefner hol (wat iets heel anders is dan Hugh Hefners ..). Franny, Jeroen, Daniël, Cloë, Leonard, Stefan en later ook Yagmur, ik wil jullie allemaal bedanken voor de inkijk die jullie me geboden hebben in de wereld van de chirurgie, de hechtingsvormen en statistische trucjes. Over de moeite die het kost om in opleiding te komen, zelfs nog na een PhD die je soms net zo graag had overgeslagen. Ook erg leerzaam waren jullie belastingtips en jullie verregaande pogingen om digitaal meer te leren over een voorbijlopende knappe vrouw (heb maar mooi mijn digitale profiel aangescherpt na deze inzichten).

Kristel, ze zeggen wel eens: 'beter goed gejat, dan slecht bedacht' en hoewel dat een discutabele stelling is voor een proefschrift, doet hij hier meer dan dienst.. Ik wil je bij deze danken voor het delen van jouw onbegrijpelijke statistiek, je verhalen over 'dikkerdjes', en onze kletspraatjes tijdens het laboverleg op dinsdagochtend. Ik wens je heel veel succes met je opleiding tot huisarts!

Renata, bedankt voor je gezelligheid en voor je hulp. Streng doch rechtvaardig organiseer je het lab en heb je me met regelmaat bijgestaan door te lachen om mijn kansloze grappen of door te helpen met mijn suboptimale experimenten. Ik heb het fantastisch gevonden om met jou de straten van Boston te ontdekken en ons te verbazen over de Amerikaanse gastvrijheid. Pancakes, sushi, Cheers!

Sander, ik hou van je onafgemaakte…

verhalen. Jij weet met iedereen een kletspraatje te houden, een grap te maken en iets moois in ze te zien. Ik moet, sorry daarvoor, een beetje lachen om mijn herinneringen aan jouw gevloek tegen je computerscherm bij de zoveelste kleuring die niet werkte of als deze iets anders liet zien dan de kleuring daarvoor. Ze stelden mijn eigen teleurstellingen in het lab altijd weer in perspectief. Gelukkig is er dan altijd nog muziek. Muziek! Bedankt voor de goede tijden en voor het met regelmaat onderbreken van de top40 op het lab.

To the rest of the aging/clock group: Inez, Bert, Shanon, Yvette, Txema, Ping, and all former members, thank you for the nice lunches, drinks, dinners, train rides, movie nights, Sinterklaaslunches and lab outings we have shared. Together, you all make your part of the 7th floor the best part of the 7th floor! Oh and thanks for taking care of Axl, Lotte & Timmy (say Blubblublub blub blubber blub to them from me if you see them).

To the party committee! OMG that was fun. Who would have thought so many people would appreciate an Irish tribute to the Glomax, wear a mustache to our snorrel, come glitter and shine at the Christmas party and just.. Elevator party. I've always felt that a party was a success when Thom decided to place his hands on the floor, plant his feet against a freshly painted wall to shake that fine ass of his. Or when Danny started talking in "Irish", when Marjolijn started to show of her beer bottle opening skills and Diana started giggling about all above. Marjolijn, Danny, Thom, Diana, Giulia, Astrid, Joris and Chang, thank you all for the fun times.

Bij deze een shout-out naar Ingrid van der Pluijm, die me heeft bijgestaan in mijn queeste om mijn muizen in leven te houden tussen de regelgeving bij de IVD door. En uiteraard ook voor de roze koeken.

To all my students: Dian, Tim, Finette, Linda, Ziqin, Wei, Feiko and Duschka. You have bled, cried and sweat under my supervision, but I have always made sure that you never choked (still can't perform a Heimlich, but will find someone who can). All jokes aside, I'm glad that we all have learned from these bursts of body fluids. Thank you all for keeping me company in the lab and for supporting my research.

Ik wil ook graag Ewout Hoorn bedanken, voor de kans om mijn proefschrift af te ronden als postdoc in zijn lab. Wat een onwijs leuk team heb je samengesteld in het 'Water en

Zout lab', vol intelligente en enthousiaste collega's. Ik ben blij dat ik hier mag bijdragen aan het lopende en nieuwe onderzoek en ondertussen zoveel ruimte krijg om me verder te ontwikkelen. I also want to thank all my new colleagues of the cardiovascular pharmacology department on the 14th floor who have welcomed me with open arms.

Ik wil hier ook graag mijn lieve vrienden en familie bedanken. Max, Janine, al die broers en zussen van mij, casa Amor, de Biobitches en ons Binkie natuurlijk, (bestuurs) Biologen, de Harem, Myrthe, Marloes, (aangetrouwde) neven, nichten, ooms en tantes, teamgenoten, festivalgangers. Planning is nooit mijn sterkste punt geweest en met mijn PhD moest ik opeens opzoek naar een werk-privé balans. Minder vrije tijd dus en ook veel moeten bijkomen op die vrije dagen. Maar wat waren die momenten die wel doorgingen waardevol. Bijkletsen, spuien, of even helamaaal je hoofd leeg. De concerten (Shaggy! The DON!), Rock Werchter (HeeHee) (dat was Michael Jackson), Bruiloften, Taizé (Halleluja!), hockeytoernooien, bestuursweekenden, kerstdiners, goede gesprekken, kaasplankjes, verjaardagsfeesten, de Pandemic-, Mahjong-, Justinianus-, Andor-, of klaverjas- spelletjesavonden, escaperooms, fotoshoots, strandwandelingen, familieweekenden, (Goh, als je het zo allemaal achter elkaar zet, had ik eigenlijk best veel vrije tijd!) vakanties, bierproeverijen, stapavonden, of gewoon gezellig koken en bijkletsen waren memorabele momenten om er weer volle bak tegenaan te kunnen. Ik zeg het denk ik niet vaak genoeg, dus hier staat het dan maar zwart op wit: wat ben ik dankbaar dat ik jullie allemaal in mijn leven heb.

Lieve Karin en Bert, graag wil ik jullie hier nog noemen. Ik mag eigenlijk van jullie je telefoonnummer niet labelen onder thuis, 'want mijn thuis is bij Tim' en dat is het ook. Toch belt mijn telefoon naar jullie als ik op thuis druk. Niet alleen omdat Tim en ik geen huistelefoon hebben, maar ook omdat jullie voor mij nog steeds een thuis zijn. Wat er ook gebeurt, bij jullie vind ik altijd een luisterend oor. Gewoon even mijn hart luchten, of samen nadenken over een oplossing die bij me past. Maar ook: samen kletsen, kaarten, lachen, dankbaar zijn. Bedankt dat jullie me altijd met in ieder geval een voet op de grond houden en er voor me zijn als dat nodig is.

Tim, na zoveel woorden geschreven te hebben, valt mijn hand nu stil. Welke woorden zijn voldoende? Jij was er aan het begin, en hier zijn we nu, samen, aan het einde van dit verhaal. Sterker, wijzer, getrouwd en vol vertrouwen, vol plannen en ideeën. Op naar het volgende avontuur!

Liefs,

Hester

"YOU MISS 100% OF THE SHOTS YOU DON'T TAKE. - WAYNE GRETZKY"

- MICHAEL SCOTT